0084013

C4104 (T-106)

GEOLOGICAL DESCRIPTION OF CORE OBTAINED DURING OPENING IN LAB

DATA PACKAGE

SECTION

2 OF 2

Table 4.50. (contd)

Sample No.	Units		µg/L	mg/L	µg/L	µg/L	mg/L	mg/L	mg/L
	Depth (ft bgs)	Stratigraphic Unit	Al	Si	Fe	Mn	Zn	PO_4 (ICP)	SO_4 (ICP)
17A	110.0	CCU_l	ND	2.32E+02	(3.80E+02)	(1.28E+03)	(4.74E-01)	(1.58E+00)	2.37E+03
17A DUP	110.0	CCU_l	ND	1.79E+02	(1.16E+02)	(5.31E+02)	(3.26E-01)	(1.13E+00)	1.63E+03
18A	116.0	R_{tf}	ND	7.30E+01	(2.33E+01)	1.45E+03	(1.06E-01)	(1.90E-01)	1.60E+02
19A UFA	120.9	R_{tf}	**ND**	**2.49E+01**	**(3.4E+01)**	**1.0E+03**	**8.90E-02**	**(5.13E-01)**	**1.54E+02**
19A	120.9	R_{tf}	ND	8.47E+01	(2.03E+01)	ND	(9.08E-02)	(3.57E-01)	2.09E+02
20A UFA	123.9	R_{wi}	**ND**	**(2.8E+01)**	**(2.2E+02)**	**(9.4E+01)**	**1.03E-01**	**(9.27E-01)**	**3.00E+02**
20A	123.9	R_{wi}	ND	4.89E+02	(1.68E+02)	(1.82E+02)	(5.33E-01)	(1.23E+00)	7.84E+02
21A	129.8	R_{wi}	ND	2.18E+02	(1.31E+02)	(1.86E+02)	(3.79E-01)	(7.59E-01)	2.90E+02

(a) Parentheses signify values below level of quantitation but considered valid.
(b) ND = not determined.
(c) Bold values designate the actual porewater data obtained by ultracentrifugation of the sediments.

008401 3
Section 2 of 2

Table 4.51. Derived and Actual Porewater Concentrations of Potentially Mobile Constituents in C4105 Vadose Sediments

Units		pCi/L	µg/L	µg/L	µg/L	µg/L	µg/L	µg/L	µg/L	µg/L	µg/L	µg/L
Sample	Depth (ft bgs)	Tc-99[a] (ICP-MS)	U-238 (ICP-MS)	Cr ICP-OES	Cr (ICP-MS)	Mo ICP-OES	Mo 95 (ICP-MS)	Mo 98 (ICP-MS)	Mo 100 (ICP-MS)	Ru 101 (ICP-MS)	Ru 102 (ICP-MS)	Ru 104 (ICP-MS)
1A	15.3	(0.00)[a]	6.01E+01	(4.55E+01)	(4.59E+00)	(3.92E+02)	3.56E+02	3.28E+02	1.53E+02	(9.05E-02)	(6.34E-01)	(9.96E-01)
2A	22.7	(0.00)	3.13E+01	(2.70E+01)	(3.87E+00)	4.94E+02	4.93E+02	4.56E+02	2.16E+02	<2.38E+01	<1.19E+01	<2.38E+01
3A	36.8	(316.49)	5.39E+01	(3.06E+01)	2.32E+01	1.38E+03	1.39E+03	1.29E+03	6.08E+02	<1.87E+01	<9.33E+00	<1.87E+01
4A	40.2	(667.29)	5.27E+01	(2.84E+01)	1.35E+01	4.60E+02	4.49E+02	4.15E+02	2.01E+02	<1.31E+01	<6.56E+00	(2.75E-01)
5A	48.4	<4551.4	1.40E+01	(2.90E+01)	(2.87E+00)	(2.68E+02)	2.41E+02	2.24E+02	1.08E+02	<2.68E+01	<1.34E+01	<2.68E+01
6A	56.1	(2351.69)	9.78E+00	(2.64E+02)	2.11E+02	(3.99E+02)	5.27E+02	3.89E+02	3.54E+02	(2.51E+00)	(1.07E+00)	(1.52E+00)
7A UFA	70.1	**3.07E+05[c]**	**5.72E+00**	**(5.3E+02)**	**5.53E+02**	**(1.7E+03)**	**2.70E+03**	**1.65E+03**	**1.96E+03**	**9.08E+01**	**(3.83E+01)**	**(3.91E+01)**
7A	70.1	1.98E+05	3.01E+01	2.77E+03	2.38E+03	2.41E+03	3.32E+03	2.07E+03	2.52E+03	7.95E+01	3.77E+01	3.86E+01
8A	81.2	1.24E+05	2.68E+01	1.63E+03	1.47E+03	(1.67E+02)	1.77E+02	1.60E+02	7.97E+01	7.00E+01	3.31E+01	3.58E+01
9A	86.7	7.30E+06	8.96E+00	3.26E+04	2.87E+04	ND[b]	4.49E+01	4.28E+01	3.86E+01	2.05E+03	9.91E+02	9.93E+02
10A UFA	88.2	**8.68E+06**	**3.99E+00**	**1.4E+04**	**1.46E+04**	**(4.8E+01)**	**(1.19E+01)**	**(9.60E+00)**	**2.85E+01**	**2.71E+03**	**1.29E+03**	**1.27E+03**
10A	88.2	8.29E+06	6.15E+00	2.30E+04	2.13E+04	ND	3.97E+01	3.67E+01	4.03E+01	2.56E+03	1.22E+03	1.21E+03
10A DUP	88.2	7.47E+06	6.49E+00	1.94E+04	1.80E+04	ND	4.20E+01	3.91E+01	3.87E+01	2.20E+03	1.07E+03	1.05E+03
11A UFA	93.3	**4.37E+06**	**3.89E+00**	**5.0E+03**	**4.95E+03**	**(9.6E+01)**	**4.77E+01**	**4.21E+01**	**3.64E+01**	**1.50E+03**	**7.14E+02**	**6.97E+02**
11A	93.3	6.11E+06	2.46E+01	1.20E+04	9.65E+03	1.48E+02	2.43E+02	2.27E+02	1.28E+02	2.24E+03	1.07E+03	1.08E+03
12A	97.1	4.10E+06	1.38E+01	3.55E+02	3.10E+02	2.07E+02	3.48E+02	3.20E+02	1.61E+02	1.06E+03	5.11E+02	5.05E+02
13A	100.3	5.48E+06	2.72E+01	2.09E+02	2.00E+02	(1.03E+02)	2.78E+02	2.58E+02	1.29E+02	7.29E+02	3.52E+02	3.51E+02
14A	102.0	8.61E+06	4.01E+01	3.04E+04	2.25E+04	1.34E+03	1.86E+03	1.21E+03	1.41E+03	1.67E+03	8.14E+02	8.21E+02
15A	103.2	8.15E+06	4.15E+01	3.25E+04	2.62E+04	4.85E+03	6.93E+03	3.82E+03	4.68E+03	2.11E+03	1.03E+03	1.03E+03
16A UFA	106.9	**4.49E+06**	**1.10E+01**	**4.3E+04**	**4.37E+04**	**1.0E+04**	**1.55E+04**	**9.51E+03**	**1.15E+04**	**3.15E+03**	**1.52E+03**	**1.49E+03**
16A	106.9	1.55E+06	1.34E+01	2.19E+04	1.68E+04	7.29E+03	1.01E+04	6.35E+03	7.90E+03	1.88E+03	9.17E+02	9.07E+02

Table 4.51. (contd)

Units		pCi/L	µg/L	µg/L	µg/L	µg/L	µg/L	µg/L	µg/L	µg/L	µg/L	µg/L
Sample	Depth (ft bgs)	Tc-99[a] (ICP-MS)	U-238 (ICP-MS)	Cr ICP-OES	Cr (ICP-MS)	Mo ICP-OES	Mo 95 (ICP-MS)	Mo 98 (ICP-MS)	Mo 100 (ICP-MS)	Ru 101 (ICP-MS)	Ru 102 (ICP-MS)	Ru 104 (ICP-MS)
17A	110.0	7.67E+06	1.25E+01	6.89E+03	5.38E+03	2.97E+03	4.26E+03	2.86E+03	3.10E+03	1.58E+03	7.60E+02	7.59E+02
17A DUP	110.0	6.91E+06	1.05E+01	2.44E+03	1.19E+03	7.26E+02	9.59E+02	6.70E+02	7.33E+02	1.12E+03	5.52E+02	5.53E+02
18A	116.0	8.85E+05	5.73E+00	(1.04E+01)	(2.34E+00)	(4.39E+01)	8.66E+01	7.93E+01	4.03E+01	8.33E+01	4.06E+01	4.30E+01
19A UFA	120.9	**2.18E+06**	**2.06E+00**	**(3.8E+01)**	**1.47E+01**	**(4.7E+01)**	**1.67E+01**	**(1.15E+01)**	**1.29E+01**	**2.80E+02**	**1.32E+02**	**1.32E+02**
19A	120.9	2.49E+06	2.94E+00	(3.92E+01)	3.32E+01	ND	3.53E+01	3.29E+01	1.81E+01	2.76E+02	1.31E+02	1.33E+02
20A UFA	123.9	**2.57E+06**	**1.90E+00**	**(1.2E+02)**	**(3.96E+01)**	**(1.4E+02)**	**(5.04E+01)**	**(4.30E+01)**	**(2.48E+01)**	**3.22E+02**	**1.51E+02**	**1.50E+02**
20A	123.9	6.25E+06	1.11E+01	(6.04E+01)	(2.05E+01)	(0.00E+00)	2.45E+02	2.25E+02	1.12E+02	6.45E+02	3.11E+02	3.17E+02
21A	129.8	2.40E+06	2.00E+00	(4.46E+01)	(1.55E+01)	(2.11E+02)	2.84E+02	2.66E+02	1.30E+02	2.28E+02	1.11E+02	1.13E+02

(a) Parentheses signify values below level of quantitation, but considered valid.
(b) ND = not determined.
(c) Bold values designate the actual porewater data obtained by ultracentrifugation of the sediments.

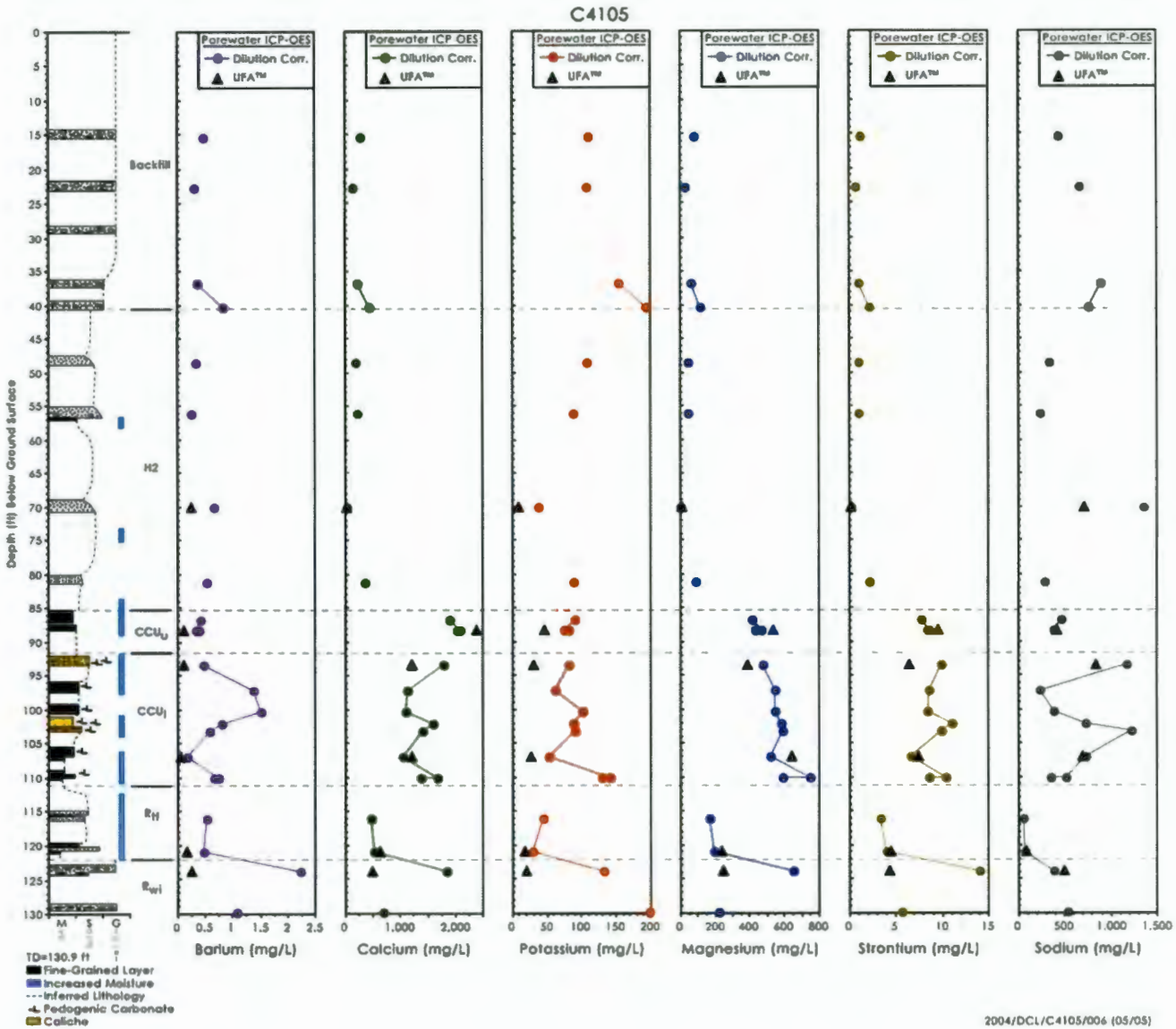

Figure 4.46. Porewater Composition of Major Cations in C4105 Vadose Zone Sediments

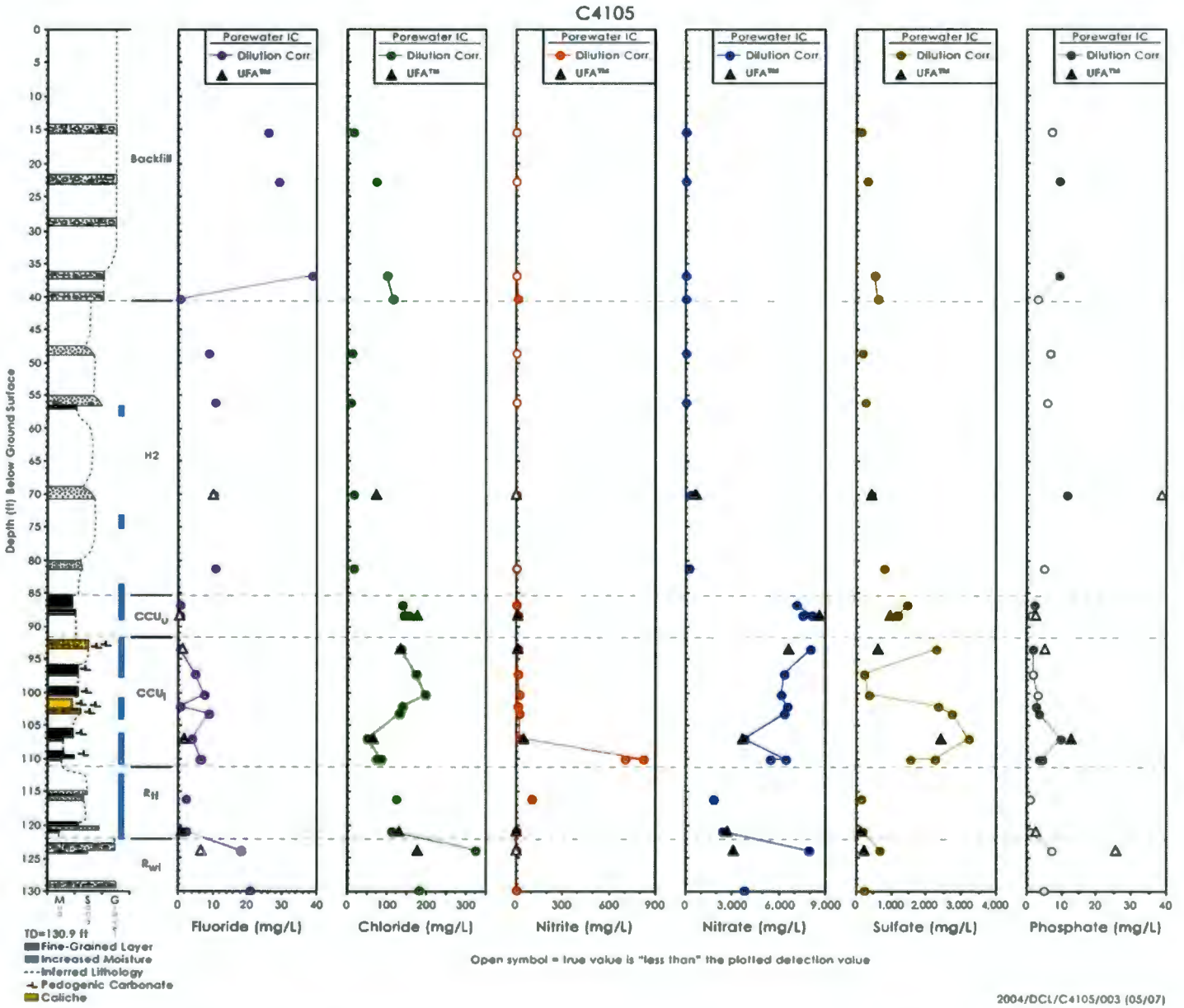

Figure 4.47. Porewater Anion Composition in C4105 Vadose Zone Sediments

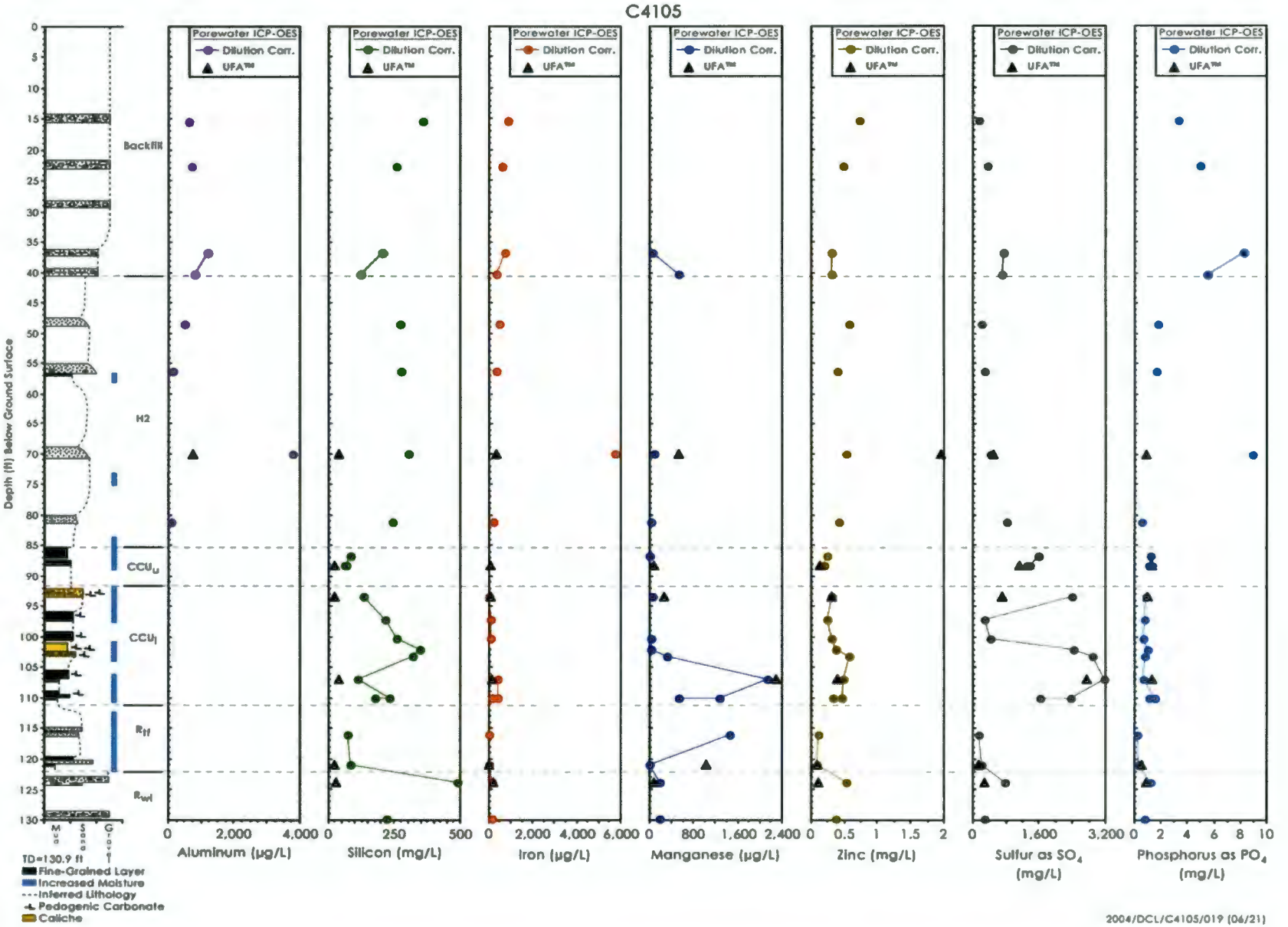

Figure 4.48. Porewater Composition for Selected Metals in C4105 Vadose Zone Sediments

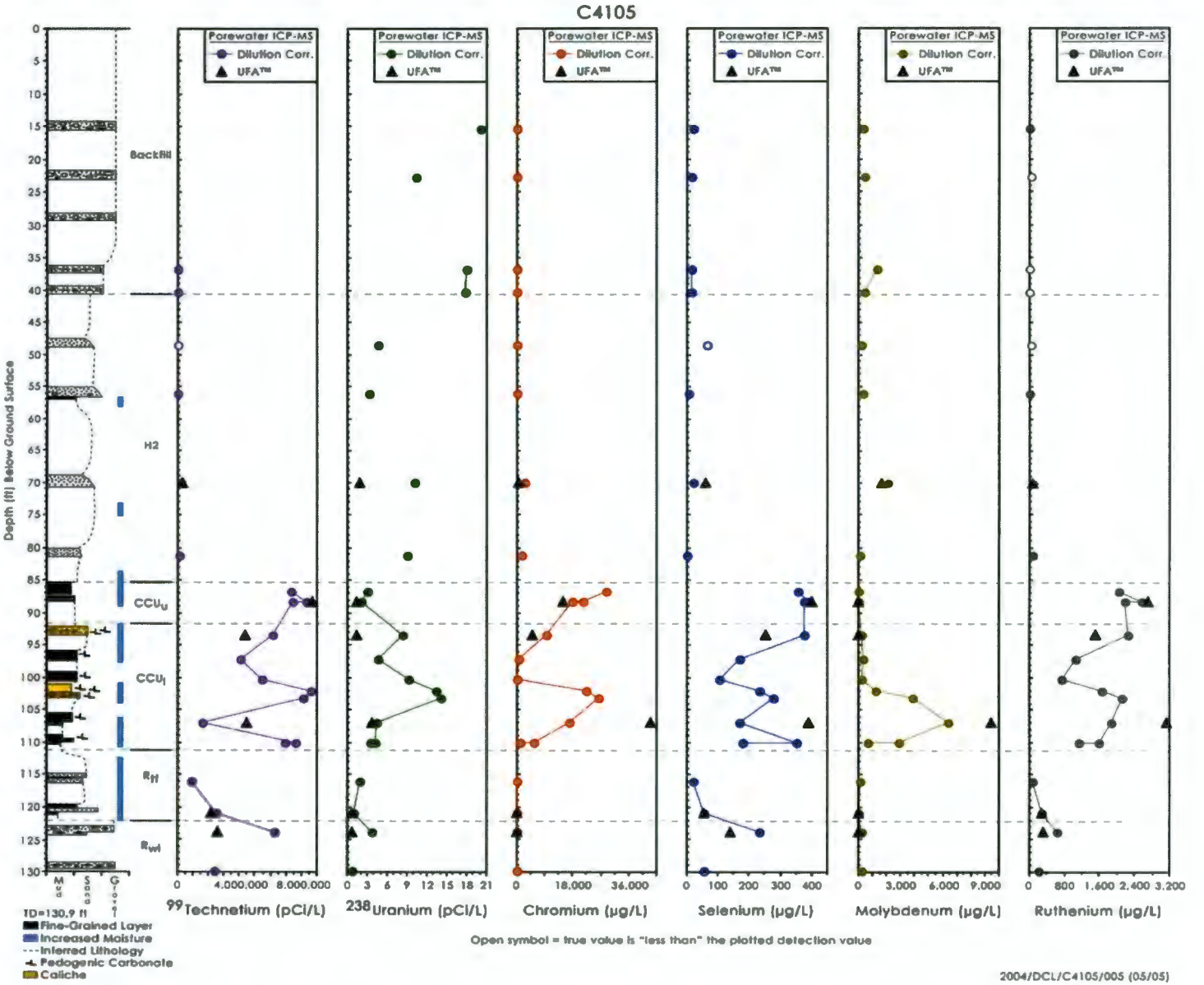

Figure 4.49. Porewater Composition of Mobile Metals in C4105 Vadose Zone Sediments

4.4.4 8 M Nitric Acid-Extractable Amounts of Selected Elements in C4105 Sediments

The same cores that were characterized for water-extractable constituents were also characterized to see how much of various constituents could be leached with hot 8 M nitric acid. A comparison between the quantities that are acid extractable with those that are water extractable often indicates the relative mobility of a given constituent and can sometimes differentiate man-disposed from naturally occurring constituents. Finally, a comparison of the acid-extractable quantities in suspected contaminated sediments with acid-extractable amounts in uncontaminated sediments can be used to delineate the presence of less mobile contaminants.

The quantities of various constituents in the C4105 vadose zone sediments that were acid extractable are shown in Tables 4.52 to 4.55 and Figures 4.50 through 4.53. Upon comparing the acid extract data for borehole C4105 with similar lithologies in the uncontaminated borehole 299-W10-27, most of the variation in mass leached per gram of sediment versus depth in found to be lithology related. That is, for most major constituents there are no signs of elevated values of acid-leachable constituents in borehole C4105 sediments, excepting acid-extractable sodium in the backfill, one elevated acid-extractable calcium value at 81.2 ft bgs near the bottom of the Hanford H2 unit, and sulfate throughout the profile. The high acid-extractable sodium in the shallow background sediments suggests some waste was released on the sediment surface or from pipelines. The elevated calcium near the bottom of the Hanford H2 unit may indicate that the ion exchange front from the tank waste plume has reached this borehole at this depth. The high sulfate throughout the sediment profile is confusing although the tank leak did contain sulfate. However, elevated concentrations should not be seen in the entire sediment profile. Elevated sulfate was also observed throughout the C4104 sediment profile so perhaps some of the high sulfate may be a localized natural phenomenon.

For the mobile fission products technetium-99, molybdenum, and ruthenium, the acid extracts show elevated concentrations at C4105 borehole from 86.7 to ~130 ft bgs (the bottom of the borehole), 93.3 to 110, and 86.7 to 110 ft bgs, respectively.

Figure 4.54 shows that the vast majority of the sediment phosphate content is not water extractable in comparison with the amounts that are acid extractable. The same trend was observed for the uncontaminated sediments from boreholes 299-W10-27 and from contaminated C4104 sediments. Alternatively, some of the acid-extractable phosphorous may be present in a form other than phosphate such that when we convert the acid-extractable phosphorous number to phosphate (essentially multiplying by 3), we are inflating the acid-extractable value. Some of the sulfate that is acid extractable is also water extractable.

As mentioned, the ratio of water-extractable to acid-extractable quantities of constituents can identify samples that may contain leaked fluids from Hanford waste disposals. The comparison of the water to acid-extractable quantities of each constituent was performed by taking the data in Tables 4.45 through 4.47 and dividing by the data in Tables 4.52 through 4.55. The data are not presented herein but show distinct regions where the water to acid extractable percentages are much larger than found for uncontaminated borehole (299-W10-27) sediments. For the uncontaminated sediments, less than 0.1% of the acid-extractable quantities of the following elements are water leachable: aluminum, barium, iron, manganese, chromium, and P as phosphate. Less than 0.5% of the acid-extractable quantities of the following elements are water leachable: calcium, potassium, magnesium, strontium, zinc, and uranium. Less than 20% of the acid-extractable sodium, sulfur, and molybdenum are water extractable in uncontaminated sediments.

The comparison of water to acid extracts for borehole C4105 sediments suggests that there are unnaturally high percentages [i.e., Tc-99: 60 to 100%; Mo: 3 to 50%; Ru: 30 to 85%] of water-leachable technetium-99, molybdenum, and ruthenium at depths of between ~70 to 121, 70 to 110, and 87 to 121 ft bgs ft bgs, respectively.

There is also high water-extractable sodium, sulfate, and chromium in the Cold Creek upper subunit and the bottom of the Cold Creek lower subunit. In both depth zones the percentage of water- to acid-leachable concentrations for these species ranges from 15 to 30% while in most other depth regions less than a few percent of these species is water leachable. The water- to acid-extractable uranium percentages for the C4105 sediments do not show any high values (all are <1%) such that we do not believe there is measurable quantities of tank derived uranium in the C4105 sediments.

The acid-extractable concentrations of major cations in the sediments at C4105 show significantly less sodium than the sediments at C4104 as would be expected if the tank leak fluids were interacting with the sediments and sodium were to get incorporated into or onto the sediments in a form that readily dissolves in strong acid. Both ion exchangeable and secondary mineral sodium would dissolve in the strong acid. There also appears to be slightly less acid soluble phosphate in the C4105 sediments than the C4104 sediments, suggesting that phosphate present in the T-106 tank fluid that leaked deposited measurable amounts in the vicinity of C4104. With the exception of the acid extract for C4104 sediments at 63.4 ft bgs in the Hanford formation H2 unit, which has significantly higher values for zinc, copper and vanadium, there are no significant differences between the acid-extractable concentrations of most other metals between the two boreholes' sediments. A comparison of the acid-extractable, potentially mobile fission products technetium-99, chromium, molybdenum, ruthenium, and uranium shows that there is elevated technetium-99 values shallow in the Hanford formation H2 unit at C4104 that do not occur at C4105. There is higher acid-extractable uranium and chromium in sediments at C4104 than at C4105. There are also larger concentrations of acid extractable molybdenum between 58 and 64 ft bgs in the C4104 sediments than found in the C4105 sediments. These comparisons suggest that a portion of the truly mobile constituents such as technetium-99 descended deeper from the tank bottom near C4104 while another portion spread out horizontally towards C4105 sediments. Other water extract data suggests that the Cold Creek upper subunit was the stratum that promoted most of the horizontal migration. Uranium must be interacting quite significantly with the sediments because it is not observed at elevated concentrations at C4105. Some interaction is also indicated for chromium and molybdenum because acid-extractable concentrations are less at C4105, which is farther from the leak source.

Table 4.52. Acid-Extractable Cations from C4105 Vadose Zone Sediments (µg/g dry sediment)

Sample No.	Depth (ft bgs)	Stratigraphic Unit	Mg	Ca	Sr	Ba	Na	K
1A	15.3	Bkfl	3.73E+03	7.03E+03	2.88E+01	6.86E+01	5.63E+02	7.27E+02
2A	22.7	Bkfl	4.25E+03	8.04E+03	3.61E+01	1.20E+02	8.96E+02	9.93E+02
3A	36.8	Bkfl	4.32E+03	9.09E+03	3.94E+01	1.21E+02	1.38E+03	1.03E+03
4A	40.2	Bkfl	4.95E+03	1.03E+04	4.01E+01	1.53E+02	1.04E+03	1.30E+03
5A	48.4	H2	4.67E+03	8.66E+03	3.27E+01	7.06E+01	3.23E+02	1.09E+03
6A	56.1	H2	3.94E+03	8.16E+03	2.89E+01	6.16E+01	3.90E+02	8.03E+02
7A	70.1	H2	4.65E+03	9.35E+03	3.67E+01	5.74E+01	5.44E+02	1.10E+03
8A	81.2	H2	5.52E+03	2.22E+04	6.20E+01	7.11E+01	3.55E+02	1.23E+03
9A	86.7	CCU_u	7.37E+03	1.42E+04	4.13E+01	1.28E+02	3.02E+02	2.09E+03
10A	88.2	CCU_u	9.02E+03	1.70E+04	5.08E+01	1.61E+02	3.64E+02	2.51E+03
10A DUP	88.2	CCU_u	8.59E+03	1.53E+04	4.69E+01	1.54E+02	3.27E+02	2.31E+03
11A	93.3	CCU_l	8.14E+03	1.97E+05	2.89E+02	1.32E+02	6.06E+02	7.11E+02
12A	97.1	CCU_l	9.58E+03	6.81E+04	2.13E+02	1.00E+02	5.84E+02	9.19E+02
13A	100.3	CCU_l	5.40E+03	3.22E+04	1.05E+02	8.42E+01	6.03E+02	1.06E+03
14A	102.0	CCU_l	1.38E+04	2.50E+05	3.55E+02	1.31E+02	5.78E+02	6.62E+02
15A	103.2	CCU_l	1.32E+04	2.10E+05	3.68E+02	1.33E+02	6.60E+02	8.58E+02
16A	106.9	CCU_l	1.32E+04	2.47E+04	7.34E+01	1.16E+02	5.93E+02	1.84E+03
17A	110.0	CCU_l	6.26E+03	6.70E+03	3.65E+01	7.96E+01	2.99E+02	1.20E+03
17A DUP	110.0	CCU_l	6.27E+03	5.19E+03	3.32E+01	8.02E+01	2.68E+02	1.10E+03
18A	116.0	R_{tf}	9.76E+03	1.52E+04	4.58E+01	1.10E+02	2.29E+02	1.92E+03
19A	120.9	R_{tf}	9.83E+03	1.52E+04	5.29E+01	1.13E+02	2.46E+02	2.07E+03
20A	123.9	R_{wi}	8.29E+03	2.61E+04	5.92E+01	1.07E+02	4.77E+02	1.82E+03
21A	129.8	R_{wi}	5.05E+03	6.14E+03	3.47E+01	8.52E+01	8.86E+02	1.74E+03

Table 4.53. Acid-Extractable Constituents in C4105 Vadose Zone Sediments (µg/g dry sediment)

Sample No.	Depth (ft bgs)	Stratigraphic Unit	Al	Fe	Mn	P as PO_4	S as SO_4
1A	15.3	Bkfl	6.42E+03	1.79E+04	2.68E+02	3.13E+03	6.57E+02
2A	22.7	Bkfl	8.26E+03	2.24E+04	2.68E+02	3.19E+03	7.53E+02
3A	36.8	Bkfl	9.52E+03	2.29E+04	2.88E+02	2.87E+03	8.20E+02
4A	40.2	Bkfl	8.77E+03	2.38E+04	3.34E+02	3.16E+03	1.01E+03
5A	48.4	H2	7.37E+03	1.63E+04	2.57E+02	2.25E+03	6.91E+02
6A	56.1	H2	6.17E+03	1.68E+04	2.28E+02	2.81E+03	6.82E+02
7A	70.1	H2	7.48E+03	1.55E+04	2.82E+02	1.77E+03	6.91E+02
8A	81.2	H2	8.06E+03	1.59E+04	2.68E+02	1.79E+03	1.62E+03
9A	86.7	CCU_u	1.42E+04	1.94E+04	4.32E+02	1.85E+03	1.20E+03
10A	88.2	CCU_u	1.76E+04	2.30E+04	5.09E+02	1.81E+03	1.39E+03
10A DUP	88.2	CCU_u	1.49E+04	2.12E+04	4.81E+02	1.92E+03	1.30E+03
11A	93.3	CCU_l	8.06E+03	1.11E+04	1.58E+02	1.25E+03	1.28E+04
12A	97.1	CCU_l	9.97E+03	1.53E+04	2.40E+02	1.48E+03	4.48E+03
13A	100.3	CCU_l	1.03E+04	1.42E+04	2.19E+02	1.28E+03	2.22E+03
14A	102.0	CCU_l	6.09E+03	7.19E+03	8.08E+01	8.61E+02	1.56E+04
15A	103.2	CCU_l	7.14E+03	9.27E+03	1.31E+02	9.97E+02	1.40E+04
16A	106.9	CCU_l	1.72E+04	2.35E+04	5.29E+02	1.98E+03	2.53E+03
17A	110.0	CCU_l	1.03E+04	1.68E+04	3.29E+02	1.35E+03	5.96E+02
17A DUP	110.0	CCU_l	9.67E+03	1.67E+04	3.36E+02	1.34E+03	5.13E+02
18A	116.0	R_{tf}	1.63E+04	2.43E+04	6.07E+02	1.89E+03	1.00E+03
19A	120.9	R_{tf}	1.70E+04	2.58E+04	5.72E+02	2.13E+03	1.03E+03
20A	123.9	R_{wi}	1.64E+04	2.20E+04	4.41E+02	2.57E+03	1.74E+03
21A	129.8	R_{wi}	9.89E+03	1.64E+04	2.54E+02	1.77E+03	4.69E+02

Table 4.54. Acid-Extractable Trace Metals in C4105 Vadose Zone Sediments

Sample No.	Depth (ft bgs)	Stratigraphic Unit	ICP-OES Ni	ICP-OES Zn	ICP-OES Cu	ICP-OES V	ICP-MS Ag-109	ICP-MS Cd-114	ICP-MS Pb-208
1A	15.3	Bkfl	7.92E+00	3.40E+01	(2.02E+01)[a]	(3.03E+01)	2.55E-02	8.75E-02	2.57E+00
2A	22.7	Bkfl	9.29E+00	3.62E+01	(2.61E+01)	(3.35E+01)	2.52E-02	8.14E-02	2.27E+00
3A	36.8	Bkfl	1.01E+01	4.70E+01	(2.75E+01)	(4.99E+01)	1.07E-01	1.17E-01	2.46E+01
4A	40.2	Bkfl	1.21E+01	4.69E+01	(2.85E+01)	(4.67E+01)	4.53E-01	1.04E-01	1.77E+01
5A	48.4	H2	1.10E+01	3.49E+01	(1.84E+01)	(2.52E+01)	3.05E-02	6.87E-02	3.11E+00
6A	56.1	H2	8.60E+00	3.32E+01	(2.00E+01)	(2.72E+01)	2.48E-02	7.28E-02	2.86E+00
7A	70.1	H2	1.05E+01	3.35E+01	(1.77E+01)	(2.49E+01)	2.54E-02	5.91E-02	3.00E+00
8A	81.2	H2	1.08E+01	3.64E+01	(1.96E+01)	(2.54E+01)	2.45E-02	6.71E-02	3.06E+00
9A	86.7	CCU_u	1.70E+01	5.37E+01	(2.84E+01)	(1.78E+01)	5.20E-02	1.47E-01	8.76E+00
10A	88.2	CCU_u	1.82E+01	6.30E+01	3.33E+01	(2.08E+01)	5.73E-02	1.43E-01	1.04E+01
10A DUP	88.2	CCU_u	1.87E+01	6.00E+01	3.09E+01	(1.86E+01)	5.63E-02	1.37E-01	9.69E+00
11A	93.3	CCU_l	1.11E+01	2.46E+01	(1.90E+01)	(2.17E+01)	1.85E-02	1.03E-01	3.09E+00
12A	97.1	CCU_l	1.30E+01	3.50E+01	(1.80E+01)	(2.58E+01)	1.15E-02	9.03E-02	3.68E+00
13A	100.3	CCU_l	1.14E+01	3.00E+01	(1.70E+01)	(2.76E+01)	1.11E-02	7.70E-02	3.58E+00
14A	102.0	CCU_l	8.18E+00	1.76E+01	(1.59E+01)	(2.51E+00)	3.94E-01	1.11E-01	1.79E+00
15A	103.2	CCU_l	1.05E+01	2.30E+01	(1.66E+01)	(1.72E+00)	1.31E-02	1.31E-01	2.58E+00
16A	106.9	CCU_l	2.39E+01	7.26E+01	3.64E+01	(2.12E+01)	1.94E-02	1.53E-01	1.42E+01
17A	110.0	CCU_l	1.40E+01	4.59E+01	(2.11E+01)	(2.45E+01)	1.27E-02	7.45E-02	6.21E+00
17A DUP	110.0	CCU_l	1.40E+01	4.58E+01	(2.12E+01)	(2.35E+01)	1.37E-02	7.00E-02	6.40E+00
18A	116.0	R_{tf}	1.95E+01	7.04E+01	3.42E+01	(3.78E+01)	1.00E-02	1.83E-01	1.31E+01
19A	120.9	R_{tf}	2.17E+01	7.21E+01	3.65E+01	(4.39E+01)	1.32E-02	1.17E-01	1.42E+01
20A	123.9	R_{wi}	2.39E+01	5.98E+01	3.57E+01	(3.46E+01)	1.05E-02	1.16E-01	8.01E+00
21A	129.8	R_{wi}	9.75E+00	3.81E+01	(1.84E+01)	(3.25E+01)	2.42E-02	8.29E-02	3.28E+00

(a) Parentheses signify values below level of quantitation, but considered valid.

Table 4.55. Acid-Extractable Mobile Trace Metals in C4105 Vadose Zone Sediments

Sample No.	Depth (ft bgs)	Stratigraphic Unit	ICP-MS	ICP-MS	ICP-MS	ICP-OES	ICP-MS	ICP-MS	ICP-MS	ICP-OES	ICP-MS	ICP-MS	ICP-MS
			Tc 99	U 238	Cr 52	Cr	Mo 95	Mo 98	Mo 100	Mo	Ru 101	Ru 102	Ru 104
1A	15.3	Bkfl	(0.00E+00)[a]	4.76E-01	1.18E+01	1.08E+01	1.19E+00	1.09E+00	5.01E-01	ND[b]	<5.67E-02	(5.39E-03)	(1.19E-02)
2A	22.7	Bkfl	<4.68E+01	4.16E-01	3.39E+01	3.22E+01	4.20E+00	3.86E+00	1.82E+00	1.62E+00	<5.52E-02	(1.44E-03)	(1.03E-02)
3A	36.8	Bkfl	(0.00E+00)	4.21E-01	2.54E+01	2.27E+01	6.09E+00	5.60E+00	2.61E+00	3.57E+00	<6.04E-02	(3.14E-03)	1.53E-02
4A	40.2	Bkfl	(0.00E+00)	4.46E-01	2.67E+01	2.30E+01	7.08E+00	6.48E+00	3.02E+00	4.20E+00	<6.01E-02	(2.89E-03)	(1.50E-02)
5A	48.4	H2	<4.28E+01	4.38E-01	1.14E+01	1.05E+01	4.23E-01	3.79E-01	1.76E-01	ND	(0.00E+00)	(5.55E-03)	1.32E-02
6A	56.1	H2	(9.00E-01)	4.04E-01	8.34E+00	7.07E+00	2.90E-01	2.53E-01	1.29E-01	ND	(5.89E-03)	(9.29E-03)	1.57E-02
7A	70.1	H2	(1.10E+01)	3.68E-01	1.27E+01	1.15E+01	5.82E-01	4.11E-01	3.52E-01	ND	(1.72E-02)	(1.60E-02)	2.48E-02
8A	81.2	H2	(8.56E+00)	5.14E-01	1.26E+01	1.18E+01	2.79E-01	2.44E-01	1.19E-01	ND	(1.45E-02)	(1.88E-02)	3.35E-02
9A	86.7	CCU_u	1.06E+03	6.79E-01	2.45E+01	2.23E+01	2.58E-01	2.25E-01	1.04E-01	ND	3.41E-01	1.63E-01	1.69E-01
10A	88.2	CCU_u	7.34E+02	7.17E-01	2.34E+01	2.18E+01	2.40E-01	2.04E-01	9.20E-02	ND	3.59E-01	1.73E-01	1.83E-01
10A DUP	88.2	CCU_u	1.87E+03	6.60E-01	2.52E+01	2.39E+01	2.29E-01	2.00E-01	9.12E-02	ND	4.84E-01	2.29E-01	2.40E-01
11A	93.3	CCU_l	1.38E+03	8.49E-01	1.50E+01	1.35E+01	4.18E-01	3.77E-01	1.80E-01	ND	4.47E-01	3.24E-01	3.52E-01
12A	97.1	CCU_l	5.41E+02	8.42E-01	1.56E+01	1.39E+01	4.30E-01	3.91E-01	1.77E-01	ND	1.14E-01	(7.74E-02)	1.34E-01
13A	100.3	CCU_l	6.13E+02	7.04E-01	1.28E+01	1.16E+01	3.47E-01	3.15E-01	1.45E-01	ND	6.36E-02	(3.90E-02)	6.37E-02
14A	102.0	CCU_l	5.57E+02	1.93E+00	1.07E+01	9.62E+00	6.55E-01	4.65E-01	4.02E-01	ND	2.01E-01	2.66E-01	2.71E-01
15A	103.2	CCU_l	7.64E+02	1.69E+00	1.40E+01	1.32E+01	1.59E+00	1.15E+00	9.74E-01	ND	2.99E-01	2.69E-01	3.25E-01
16A	106.9	CCU_l	8.17E+02	1.02E+00	3.20E+01	3.16E+01	3.67E+00	2.38E+00	2.46E+00	ND	7.62E-01	3.76E-01	3.85E-01
17A	110.0	CCU_l	5.75E+02	4.93E-01	1.55E+01	1.55E+01	4.79E-01	3.90E-01	2.45E-01	ND	1.32E-01	(6.13E-02)	7.16E-02
17A DUP	110.0	CCU_l	4.48E+02	3.78E-01	1.63E+01	1.52E+01	5.43E-01	4.29E-01	2.83E-01	ND	1.33E-01	(5.81E-02)	7.11E-02
18A	116.0	R_{tf}	9.59E+01	8.16E-01	1.65E+01	1.50E+01	3.83E-01	3.37E-01	1.51E-01	ND	(1.05E-02)	(4.35E-03)	1.74E-02
19A	120.9	R_{tf}	5.73E+02	8.76E-01	1.89E+01	1.76E+01	3.89E-01	3.45E-01	1.54E-01	ND	7.47E-02	(3.55E-02)	5.18E-02
20A	123.9	R_{wi}	5.44E+02	7.51E-01	2.14E+01	2.20E+01	2.58E-01	2.25E-01	1.03E-01	ND	(5.27E-02)	(2.57E-02)	3.94E-02
21A	129.8	R_{wi}	4.44E+02	3.56E-01	1.09E+01	1.03E+01	4.72E-01	4.22E-01	1.89E-01	ND	(3.06E-02)	(1.07E-02)	2.45E-02

(a) Parentheses signify values below level of quantitation, but considered valid.
(b) ND = Not determined.

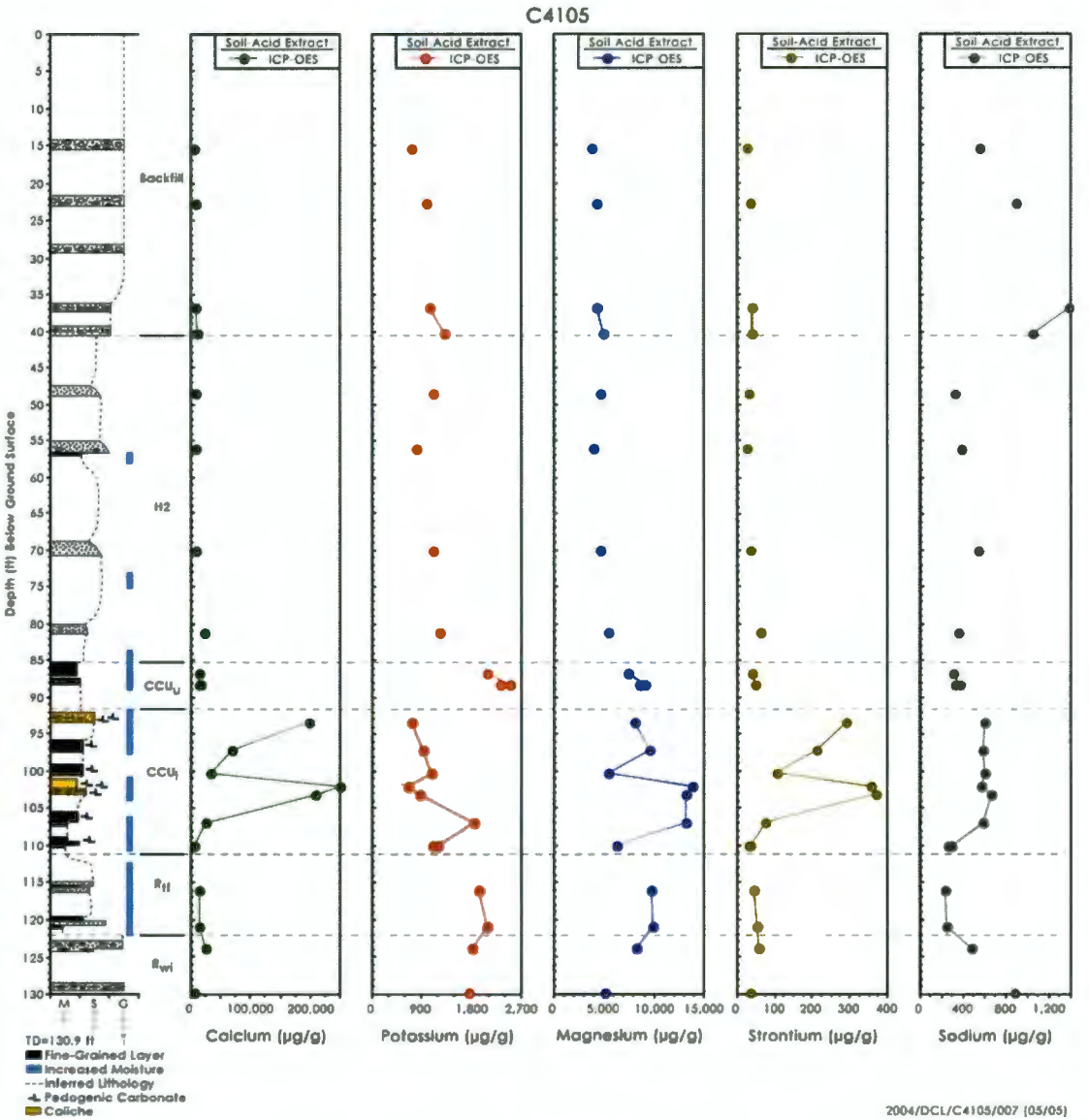

Figure 4.50. Acid-Extractable Cations in C4105 Vadose Zone Sediments (µg/g dry sediment)

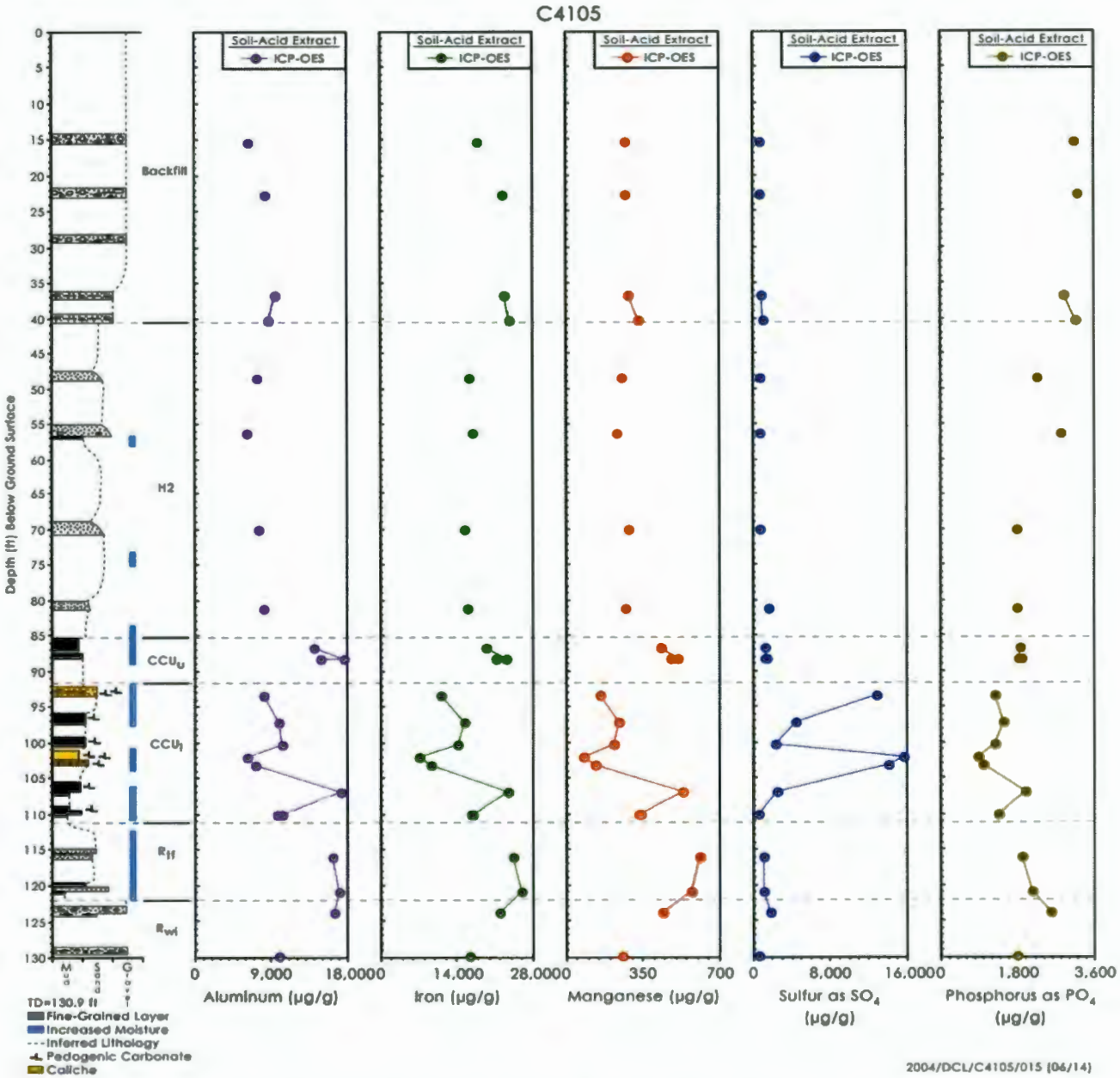

Figure 4.51. Acid-Extractable Metals in C3832 Vadose Zone Sediments (µg/g dry sediment)

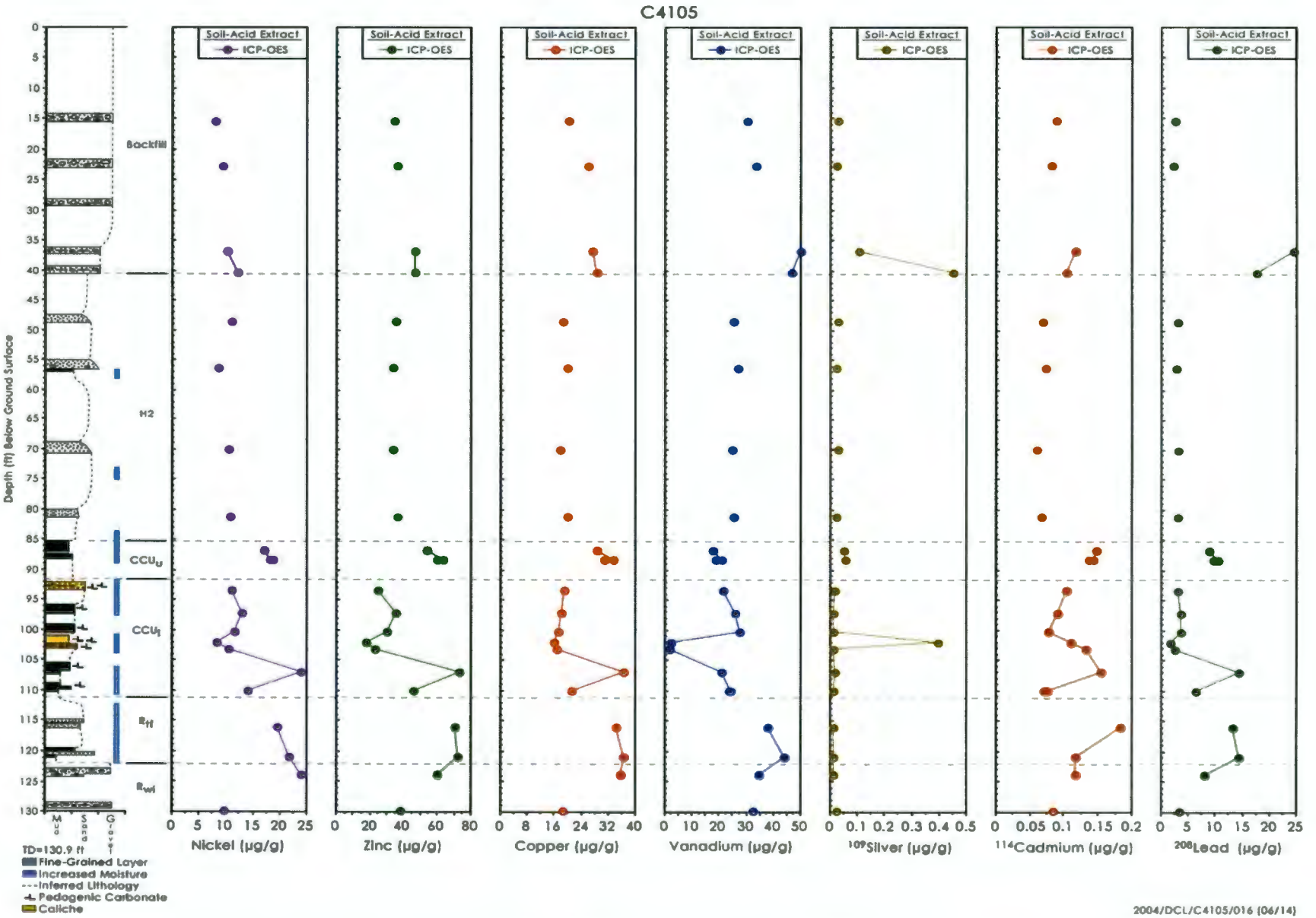

Figure 4.52. Acid-Extractable Trace Metals in C4105 Vadose Zone Sediments (µg/g)

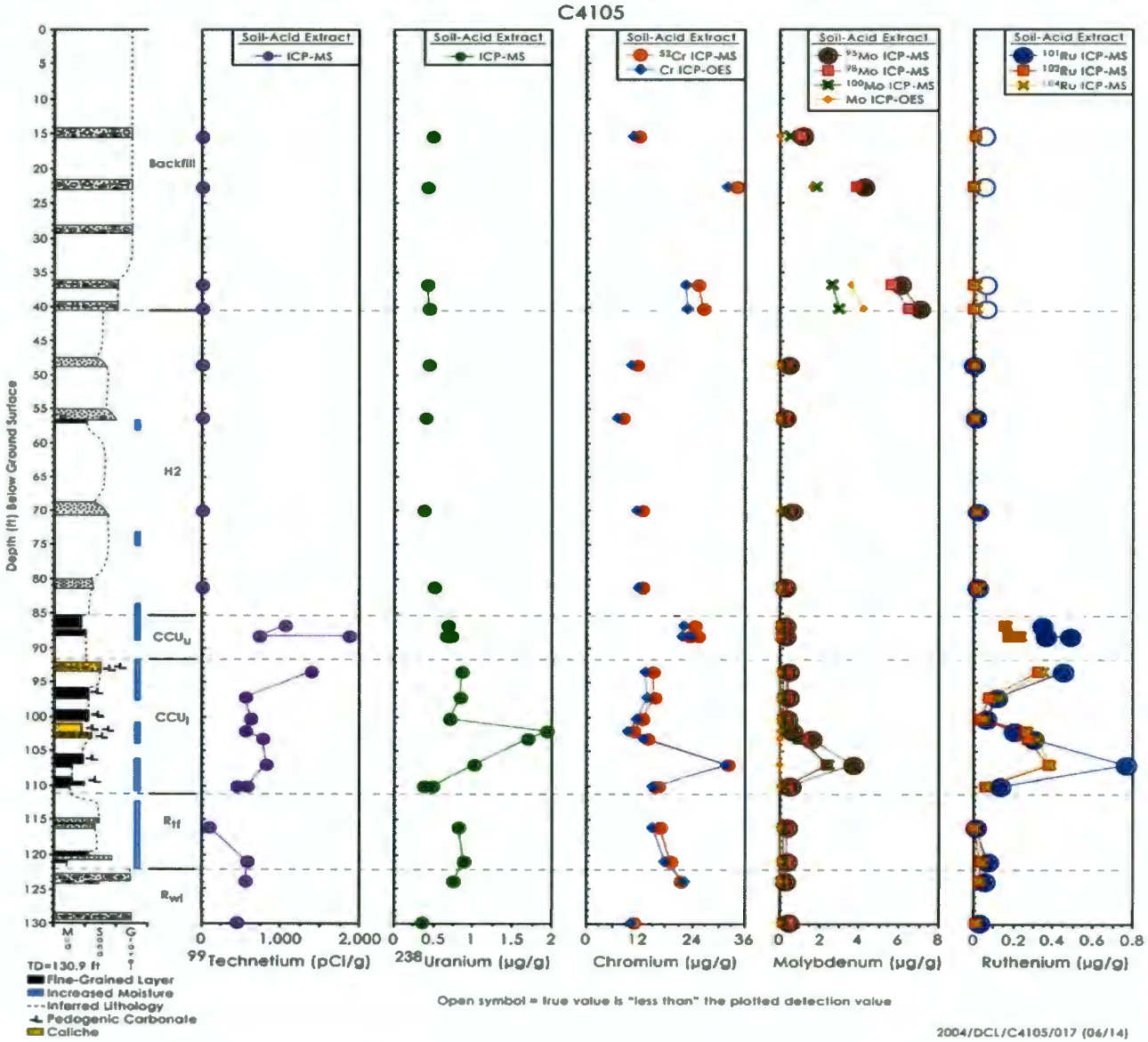

Figure 4.53. Acid-Extractable Mobile Trace Metals in C4105 Vadose Zone Sediments (units vary)

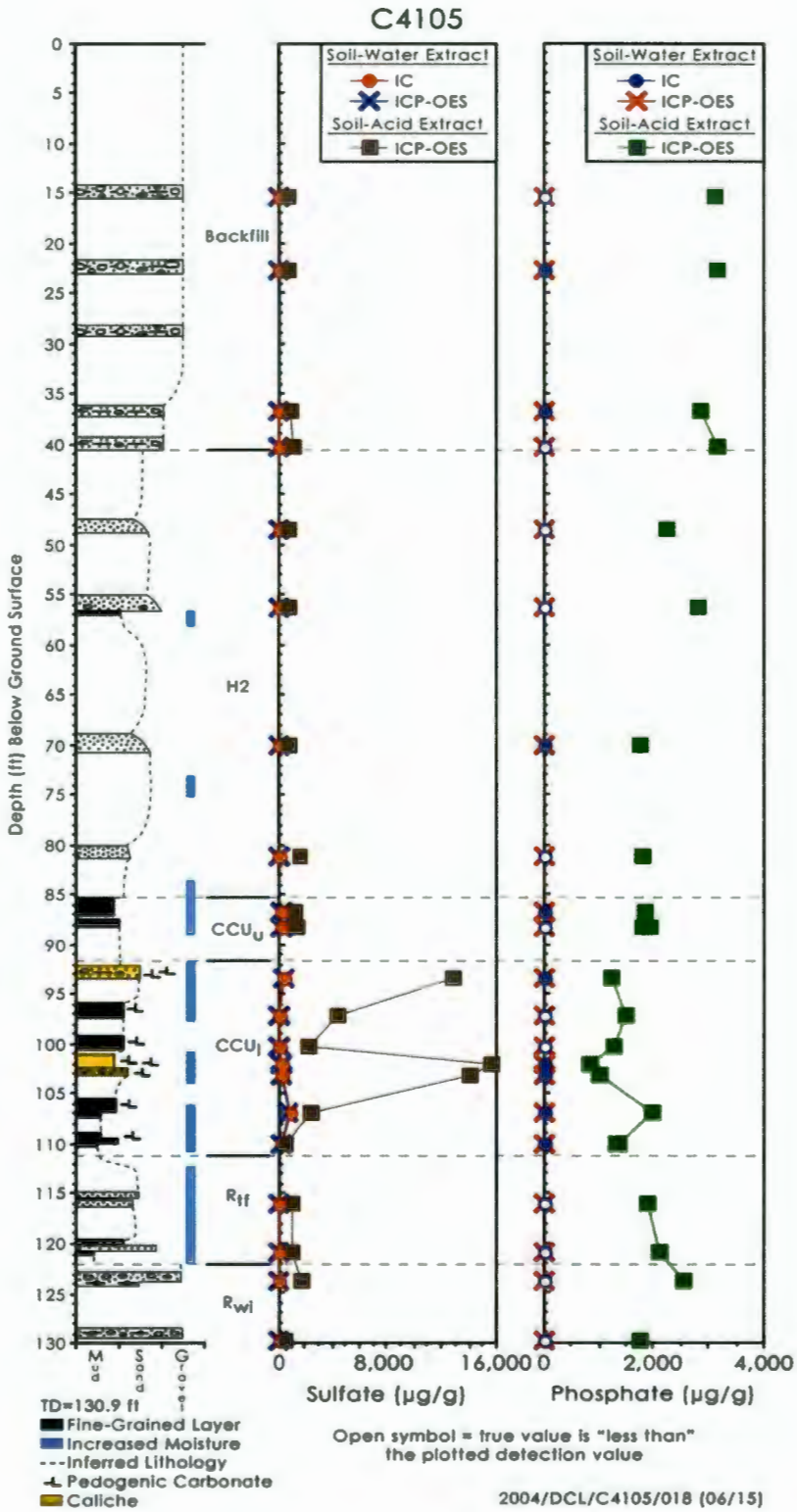

Figure 4.54. Water- versus Acid-Extractable Sulfates and Phosphate in C4105 Vadose Zone Sediments

4.4.5 Radionuclide Content in Vadose Zone Sediment from C4105

Aside from the technetium-99 and uranium-238 data already presented, our gamma energy analyses of sediment from the C4105 "B core liners" found low concentrations of cobalt-60, cesium-137, and europium-155 (one value above detection limit) as tabulated in Table 4.56 and shown in Figure 4.55. Only the cobalt is present at concentrations high enough above background to identify a vertical distribution. Based on the field gamma log, cobalt-60 is present from 57 to 112 ft bgs. The vertical extent of the cobalt-60 is defined by the contact between the Cold Creek lower subunit and the Ringold Formation Taylor Flat member. The field spectral gamma data suggests that our sparse sampling in the lower Hanford formation H2 unit (only three cores were obtained between 57 and 87 ft bgs) may cause us to underestimate horizontal migration of tank leak fluids in the Hanford formation H2 unit and over-emphasize the horizontal migration in the Cold Creek subunit. The cobalt-60 activities found in the C4105 sediments is ~ 10 times lower than in the sediments from C4104 suggesting either some dilution occurs in the porewater or some adsorption occurs in the sediments as the plume travels between these boreholes. More discussion on cobalt-60 mobility is found in Section 6.6.

Aside from a small amount of surface cesium-137 contamination in the first 5 feet of backfill there are only three "random" places in the vertical profile where the field spectral gamma tool registered cesium-137 signal above background. The lab detector was able to measure cesium-137 with greater sensitivity but as shown in Figure 4.55 there is no trend to the lab data and all values are <0.2 pCi/g. The field logging and lab results for potassium-40 and uranium-238 show excellent agreement and the uranium data suggests that there is insignificant activities of Hanford tank leak uranium in C4105 sediments as suggested with the water and acid extract data.

Gross alpha and beta measurement were made on both the 1:1 sediment:water and sediment:acid extracts. With knowledge of the mass of dry sediment to extraction fluid used the data were converted to activity of gross beta and alpha leached per gram of dry sediment. None of the water or acid extracts of the C4105 showed gross alpha activities significantly greater than the detection limits for the procedure. For the total alpha analyses the detection limit for both extracts was 5 to 10 pCi/g dry sediment.

The total beta data for the acid and water extracts were significantly greater than the detection limit for samples from 86.7 ft bgs to the bottom of the borehole, which is what was observed for the technetium-99 data. The comparison of the values in Table 4.57 show that the two independent measurement techniques track each other but the total beta values for the water extracts are somewhat higher than the direct measurement of technetium-99. Conversely, the acid extract total beta values are in general slightly lower than the ICP-MS direct measurement of technetium-99.

No detectable (above background values) strontium-90 was found in the acid extracts from the "A liner" samples from borehole C4105 sediments.

4.4.6 Total Carbon, Calcium Carbonate, and Organic Carbon Content of Vadose Zone Sediment from Borehole C4105

The total, inorganic, and organic carbon contents of the C4105 sediments are reported in Table 4.58. The lower Cold Creek subunit (caliche) samples obtained between 93.3 to 97.1 and 102 to 103 ft bgs contain significant amounts of calcium-carbonate equivalent material with 16 to 60% by weight. The sediment from the upper Cold Creek subunit and the deepest sample of Hanford H2 sediment at 81.2 ft bgs also contain about 3% by weight calcium-carbonate content. As found in most vadose sediments from the Hanford Reservation, there is very little (<0.1% by weight) organic carbon in the vadose zone sediments, excepting the sediments with the highest calcium carbonate content. These samples are difficult to measure for organic carbon so that values as high as 0.3% by weight are likely not accurate.

The caliche at borehole C4105 corresponds quite well to the high values (quantity) and depth of occurrence as the data from borehole C4104. This suggests that the caliche lenses are fairly continuous between these two boreholes.

Table 4.56. Gamma Emitter Concentrations in Vadose Zone Sediments in Borehole C4105 (pCi/g)

Sample No.	Depth (ft bgs)	Stratigraphic Unit	K-40	Co-60	Cs-137	Eu-155	U-238
1B	14.5	Bkfl	9.65	**<0.0374**	0.078	**<0.149**	**<0.78**
2B	22.0	Bkfl	10.24	**<0.0316**	**<0.0373**	**<0.15**	2.33
5B	47.7	H2	18.11	**<0.0354**	**<0.0429**	**<0.142**	**<1.05**
6B	55.4	H2	11.26	0.283	0.033	**<0.15**	**<0.69**
7B	69.3	H2	18.25	3.989	0.039	**<0.158**	**<1.10**
8B	80.5	H2	16.48	1.071	0.095	**<0.166**	2.05
9B	85.8	CCU_u	22.26	0.453	0.028	0.265	**<1.06**
10B	87.5	CCU_u	18.89	0.659	**<0.0467**	**<0.167**	2.18
11B	92.6	CCU_l	12.80	2.707	0.121	**<0.199**	2.20
12B	96.4	CCU_l	11.48	0.555	0.039	**<0.184**	6.58
13B	99.7	CCU_l	12.95	0.171	0.064	**<0.194**	**<1.09**
13B DUP	99.7	CCU_l	12.95	0.164	0.041	**<0.171**	1.66
14B	101.4	CCU_l	4.41	1.307	0.044	**<0.162**	**<1.31**
15B	102.5	CCU_l	6.58	1.646	0.044	**<0.205**	**<1.42**
16B	106.2	CCU_l	12.03	6.910	0.061	**<0.23**	3.01
17B	109.4	CCU_l	19.23	5.452	**<0.0668**	**<0.242**	2.39
17B DUP	109.4	CCU_l	18.83	5.279	0.114	**<0.19**	**<1.20**
18B	115.3	CCU_l	18.05	0.743	0.067	**<0.179**	2.45
19B	120.2	R_{tf}	13.17	**<0.0344**	0.028	**<0.139**	**<1.01**
20B	123.2	R_{tf}	7.72	0.077	0.035	**<0.154**	**<0.87**
21B	129.2	R_{wi}	30.26	**<0.06**	0.071	**<0.217**	2.72

Values in bold are less than values (below stated detection limit).

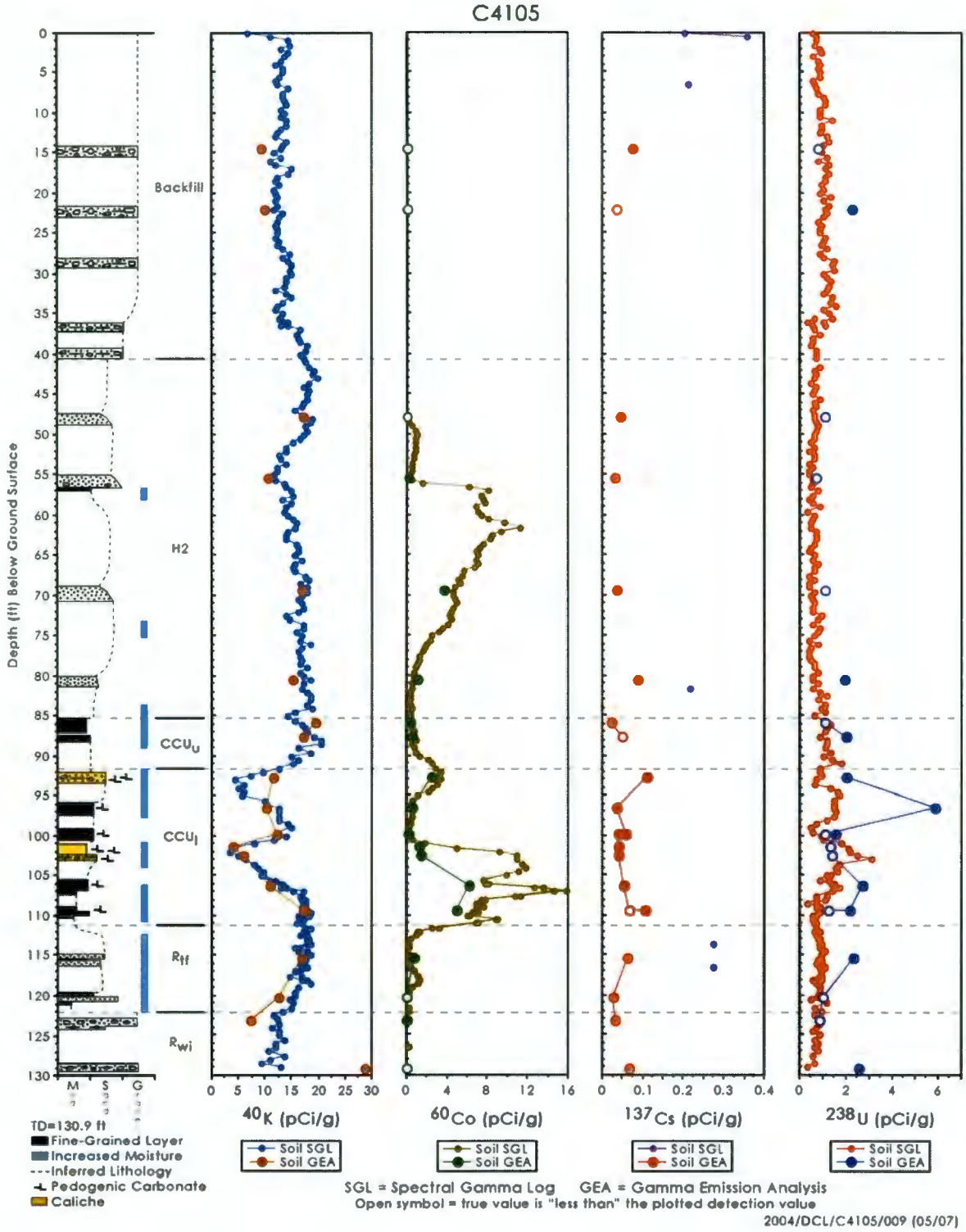

Figure 4.55. Comparison of Lab Gamma Energy Analysis (GEA) and Field Log for Natural Gamma Emitters

Table 4.57. Total Beta Comparison to Technetium-99 Measurements in Water and Acid Extracts in Vadose Zone Sediments in Borehole C4105 (pCi/g)

Sample No.	Depth (ft bgs)	Stratigraphic Unit	Water Extract		Acid Extract	
			Tc-99	Tot β	Tc-99	Tot β
1A	15.3	Bkfl	0.00E+00	3.34E+00	0.00E+00	1.46E+01
2A	22.7	Bkfl	0.00E+00	4.03E+00	4.68E+01	1.05E+01
3A	36.8	Bkfl	1.70E-02	4.51E+00	0.00E+00	9.88E+00
4A	40.2	Bkfl	5.09E-02	3.89E+00	0.00E+00	1.73E+01
5A	48.4	H2	1.70E-01	5.99E+00	4.28E+01	9.24E+00
6A	56.1	H2	1.02E-01	4.26E+00	9.00E-01	9.12E+00
7A	70.1	H2	9.04E+00	1.88E+01	1.10E+01	3.78E+01
8A	81.2	H2	6.04E+00	2.88E+01	8.56E+00	1.94E+01
9A	86.7	CCU_u	1.05E+03	1.21E+03	1.06E+03	7.26E+02
10A	88.2	CCU_u	1.65E+03	1.79E+03	7.34E+02	5.35E+02
10A DUP	88.2	CCU_u	1.41E+03	1.56E+03	1.87E+03	1.27E+03
11A	93.3	CCU_l	8.12E+02	9.96E+02	1.38E+03	7.99E+02
12A	97.1	CCU_l	4.97E+02	5.02E+02	5.41E+02	4.85E+02
13A	100.3	CCU_l	4.07E+02	4.10E+02	6.13E+02	4.97E+02
14A	102.0	CCU_l	8.21E+02	1.07E+03	5.57E+02	2.92E+02
15A	103.2	CCU_l	7.83E+02	1.32E+03	7.64E+02	4.42E+02
16A	106.9	CCU_l	3.94E+02	1.43E+03	8.17E+02	7.53E+02
17A	110.0	CCU_l	5.12E+02	6.60E+02	5.75E+02	4.52E+02
17A DUP	110.0	CCU_l	5.44E+02	6.47E+02	4.48E+02	4.28E+02
18A	116.0	R_{tf}	1.94E+02	2.02E+02	9.59E+01	5.95E+01
19A	120.9	R_{tf}	6.34E+02	6.33E+02	5.73E+02	3.23E+02
20A	123.9	R_{wi}	2.07E+02	2.06E+02	5.44E+02	3.29E+02
21A	129.8	R_{wi}	1.23E+02	1.22E+02	4.44E+02	3.18E+02

Table 4.58. Carbon Contents of Vadose Zone Sediments in Borehole C4105

Sample No.	Depth (ft bgs)	Stratigraphic Unit	Total Carbon %	Inorganic Carbon %	IC as $CaCO_3$ %	Organic Carbon (by difference)
1A	15.3	Bkfl	0.12	0.08	0.67	0.04
2A	22.7	Bkfl	0.15	0.07	0.58	0.08
3A	36.8	Bkfl	0.16	0.06	0.50	0.10
4A	40.2	Bkfl	0.29	0.10	0.83	0.19
5A	48.4	H2	0.18	0.12	1.00	0.06
6A	56.1	H2	0.16	0.10	0.83	0.06
7A	70.1	H2	0.19	0.13	1.08	0.06
8A	81.2	H2	0.38	0.32	2.66	0.06
9A	86.7	CCU_u	0.49	0.37	3.10	0.12
10A	88.2	CCU_u	0.53	0.47	3.91	0.06
10A DUP	88.2	CCU_u	0.51	0.40	3.29	0.11
11A	93.3	CCU_l	5.41	5.22	**43.47**	0.19
12A	97.1	CCU_l	2.15	1.96	**16.30**	0.19
13A	100.3	CCU_l	0.86	0.81	6.76	0.05
14A	102.0	CCU_l	7.33	7.02	**58.50**	0.31
15A	103.2	CCU_l	5.80	5.68	**47.34**	0.12
16A	106.9	CCU_l	0.82	0.71	5.95	0.11
17A	110.0	CCU_l	0.13	0.12	1.00	0.01
17A DUP	110.0	CCU_l	0.10	0.07	0.56	0.03
18A	116.0	R_{tf}	0.24	0.20	1.70	0.04
19A	120.9	R_{tf}	0.45	0.37	3.07	0.08
20A	123.9	R_{wi}	0.21	0.18	1.50	0.03
21A	129.8	R_{wi}	0.05	0.03	0.22	0.02

Samples with values in bold type contain significant amounts of caliche.

4.4.7 Particle Size Analyses

Six of the samples from borehole C4105 were characterized for particle size distribution using the hydrometer method described in Section 3.3.8. One sample from each of the major lithologies was characterized as shown in Table 4.59 and plotted in Figure 4.56. The sample of the Hanford unit H2 has the least silt and clay and is predominately sand and gravel. The sample from the Ringold Formation Wooden Island member is also coarse with little silt and clay. The two samples from the Cold Creek lower subunit are fairly coarse also, especially at the top of the subunit where less than 35% of the mass is <60 microns. At the bottom of the Cold Creek lower unit 60% of the mass is <60 microns. The Ringold Formation Taylor Flats member sample is fine grained with 75% of the mass being <60 microns in size. The Cold Creek upper subunit is the finest grained material characterized and had more than 80% of the mass <60 microns in size.

Table 4.59. Particle Size Data for One Sample from Each Major Stratigraphic Unit in Borehole C4105 Sediments

Sample	7A	10A		11A		16A		19A		20A	
Depth (ft bgs)	Strat Unit	Depth (ft bgs)	Strat Unit	Depth (ft bgs)	Strat Unit	Depth (ft bgs)	Strat Unit	Depth (ft bgs)	Strat Unit	Depth (ft bgs)	Strat Unit
70.1	H2	88.2	CCU_u	93.3	CCU_l	106.9	CCU_l	120.9	R_{tf}	123.9	R_{wi}
µm	% finer than	µm	% finer than	µm	% finer than	µm	% finer than	µm	% finer than	µm	% finer than
80.93	9.85	96.32	92.44	89.06	41.64	94.56	71.64	97.18	84.73	83.76	22.70
56.71	7.22	67.02	83.96	61.79	35.03	64.95	58.96	67.63	77.23	58.72	19.77
32.66	6.57	38.18	77.18	35.19	30.41	36.57	48.51	38.02	65.23	33.76	18.31
17.85	5.91	20.30	62.76	19.00	25.78	19.12	30.60	20.03	48.74	18.21	13.18
10.26	4.60	11.32	46.65	10.93	24.46	10.72	20.15	11.17	35.24	10.39	9.52
7.22	3.28	7.83	38.16	7.66	22.47	7.45	14.18	7.73	26.99	7.30	7.32
5.91	3.94	6.30	30.53	6.26	21.15	6.06	12.69	6.24	23.24	5.95	6.59
5.09	2.63	5.44	29.68	5.38	19.83	5.20	9.70	5.37	20.99	5.14	5.86
1.47	3.28	1.52	16.11	1.54	16.52	1.49	6.72	1.50	9.75	1.49	6.59

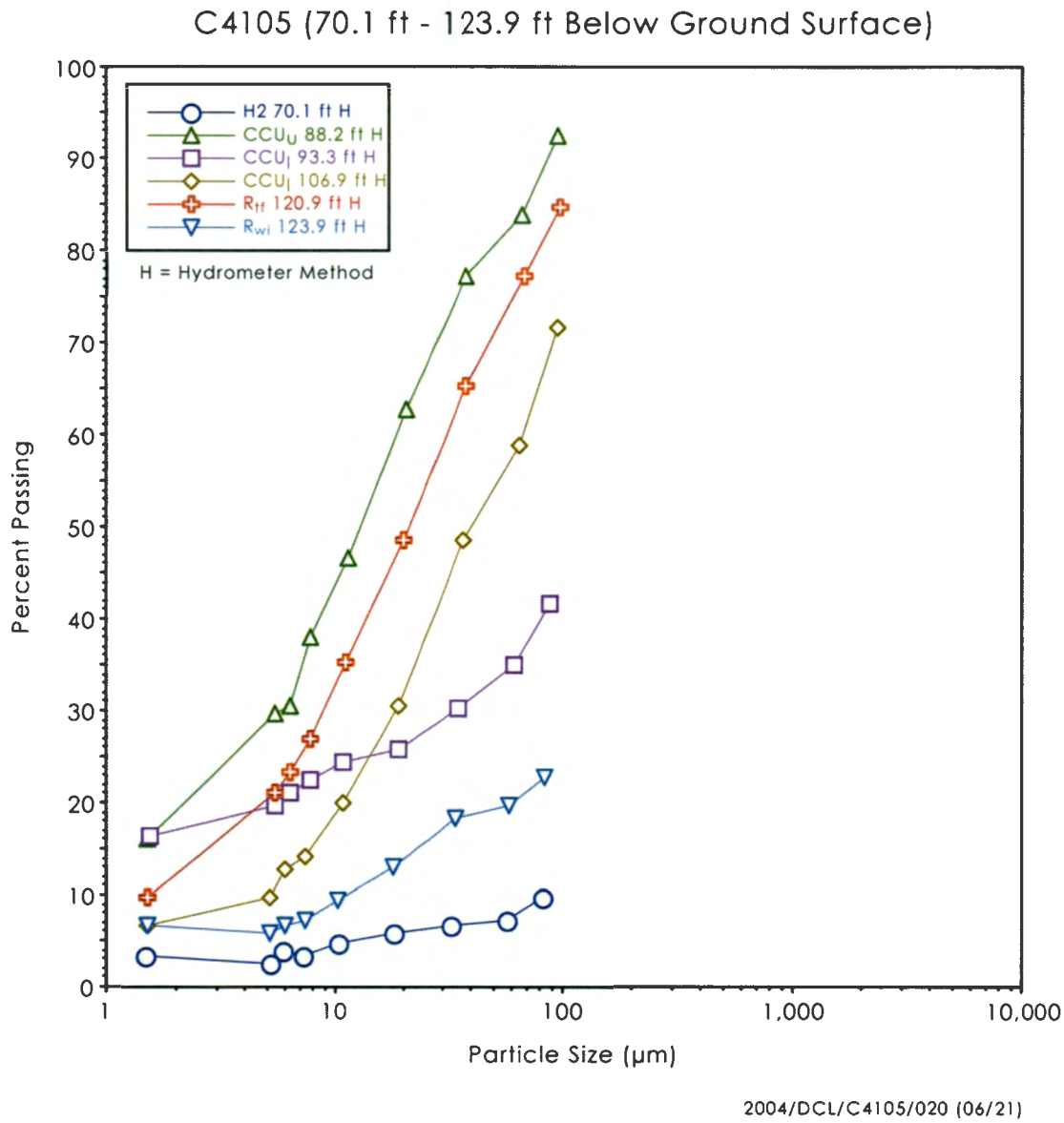

Figure 4.56. Particle Size Distribution for Selected Borehole C4105 Sediments

4.4.8 Mineralogy of C4105 Sediments

This section discusses the minerals identified in XRD patterns for vadose zone samples collected from borehole C4105. Phase identification was based on a comparison of the peak reflections and intensities observed in each pattern to the mineral Powder Diffraction Files (PDF™) published by the Joint Committee on Powder Diffraction Standards (JCPDS) International Center for Diffraction Data (ICDD).

Each pattern is shown as a function of degrees 2θ based on CuKα radiation (λ=1.5406 Å). The vertical axis represents the intensity or relative intensity of the XRD peaks. The XRD patterns show for

comparison purposes one or more schematic database (PDF™) patterns considered for phase identification. The height of each line in the schematic PDF™ patterns represents the relative intensity of an XRD peak [i.e., the most intense (the highest) peak has a relative intensity (I/Io) of 100%]. A crystalline phase typically must be present at greater than 5 wt% of the total sample mass (greater than 1 wt% under optimum conditions) to be readily detected by XRD.

XRD analysis of C4105 borehole samples 7A, 10A, 16A, 19A, and 20A show the sediments are mineralogically similar. The samples are dominated by quartz and feldspar (both plagioclase and alkali-feldspar), with lesser amounts of clay, calcite, and amphibole. Figure 4.57 is an example background subtracted XRD pattern of sample 10A (88.2 ft bgs). Intensity for the primary quartz reflection (26.6° 2θ) was truncated to increase the pattern detail. All XRD patterns are shown in Appendix C. The main reflection for quartz is at 26.63° 2θ, followed by less intense reflections at 20.86, 36.53, 39.46, 42.43, 50.12, and 59.92° 2θ. The main reflections associated with feldspar minerals are between 27.34° 2θ and 27.92° 2θ, with the higher 2θ values belonging to the plagioclase series. Clay minerals were identified on the X-ray tracings by the reflections at 6.3° 2θ and 8.8° 2θ and will be described in detail later in this section. The presence of an amphibole was established by the characteristic 100% reflection at 10.5° 2θ. In addition, minor amounts of calcite were identified in these samples by a diffraction peak positioned at 29.45° 2θ.

In contrast, XRD results from sample 11A indicate the sediment is dominated by calcite. The major reflection for calcite (29.40° 2θ) dominates the pattern as shown in Figure 4.58. Lesser amounts of quartz, feldspar, amphibole, and clays were also identified by XRD, but at much lower concentrations than in the previously described sediments. The calcite domination is corroborated by the data shown in Table 4.58 for sample 11A.

Results from the semi quantification of the minerals in the bulk samples are provided in Table 4.60.

Quartz concentrations range from 27 to 54 wt%, (excluding 11A) with an average quartz concentration of 38 ± 10 wt%. Plagioclase feldspar is present at concentrations between 12 to 43 wt% and potassium feldspar concentrations are between 4 to 15 wt%. Plagioclase feldspar was more abundant than potassium feldspar in all C4105 samples. The amphibole phase comprised <5 wt%. Calcite concentrations measured 55 wt% in sample 11A, with all other samples having <4 wt%. Clay minerals, consisting primarily of a 6.3 ° 2θ reflection (chlorite and smectite) as well as the 8.8° 2θ reflection (mica), make up between 8 and 32 wt% of the sediment samples.

Table 4.60. Whole Rock Quantitative XRD Results Determined by JADE Whole Pattern Fitting on Sediment Samples Collected From Borehole C4105. Results are given in wt%.

Sample ID	Depth (ft bgs)	Quartz	Plagioclase	Microcline	Amphibole	Calcite	Clay Minerals
7A	70.1	34	39	15	2	1	8
10A	88.2	41	17	6	4	2	29
11A	93.3	11	18	7	<1	55	10
16A	106.9	35	19	6	5	3	33
19A	120.9	54	12	4	<1	2	28
20A	123.9	27	43	12	4	4	11

Detailed XRD examination of the clay fraction from each sediment sample (except 11A) was conducted and the results are presented below. XRD tracings of the Mg-saturated air dried and Mg-saturated ethylene glycol solvated <2.0 μm fractions are shown in Appendix C. The clay fraction is dominated by four clay minerals: smectite, chlorite, illite, and kaolinite with minor amounts of quartz and feldspar.

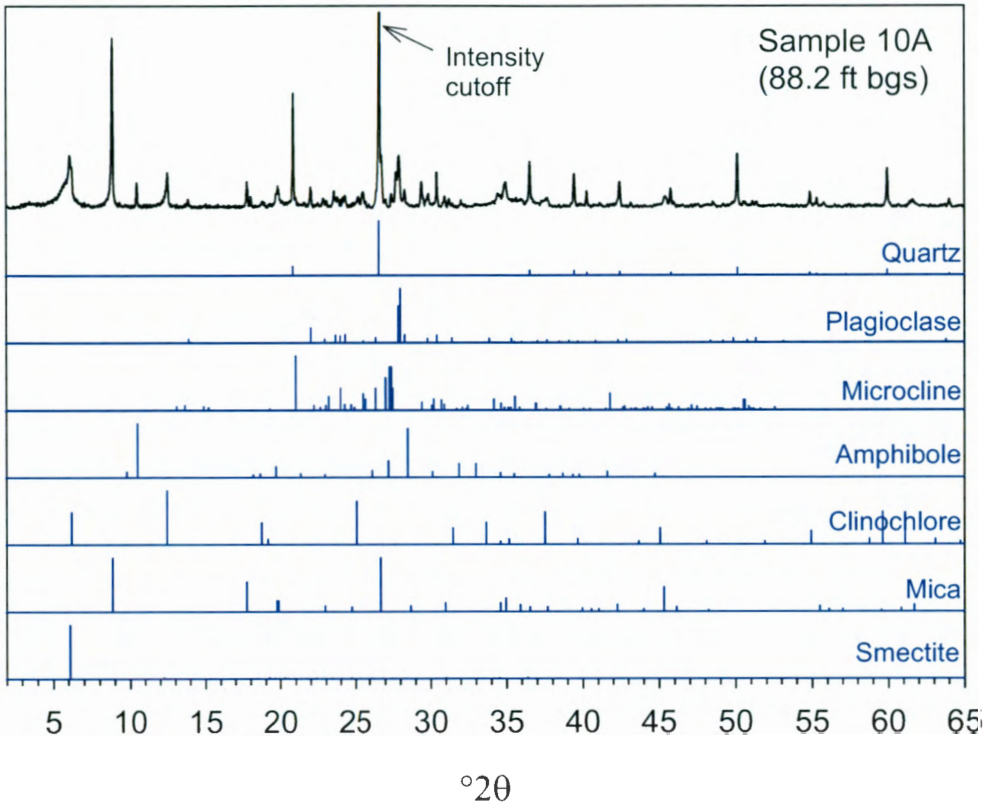

Figure 4.57. XRD Tracing for Sediment Sample 10A (88.2 ft bgs) Collected From Borehole C4105, With Matching PDF™ Files

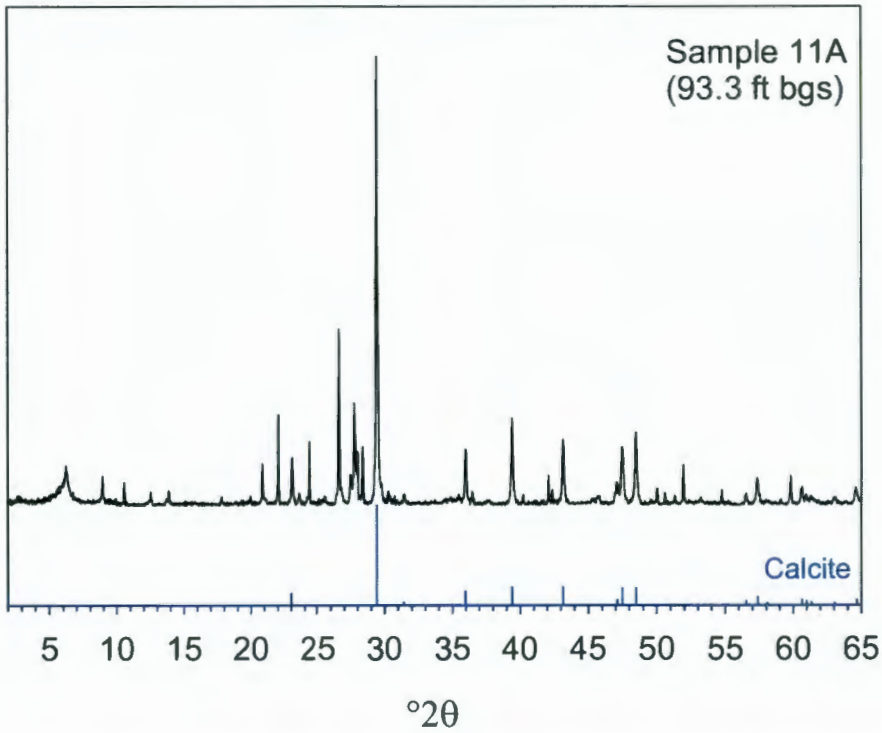

Figure 4.58. XRD Tracing for Sediment Sample 11A (93.3 ft bgs) Collected From Borehole C4105, With Calcite PDF™ File

Figure 4.59 provides an example XRD pattern of a typical clay assemblage (sample 19A) following two different treatments. Smectite is the fraction of the Mg-saturated sub-sample that gives a basal reflection at 5.85° 2θ and expands to 5.28° 2θ after solvation with ethylene glycol. Glycerol solvation treatments on two Mg-saturated clay slides (10A and 19A) were used to confirm the absence of vermiculite in the clay fraction. Vermiculite clay produces a basal reflection at 5.00° 2θ in the presence of glycol; however, in the presence of glycerol, vermiculite retains a basal reflection of 6.10° 2θ. A significant change in intensity of the basal reflection at 6.10° 2θ between the two treatments would indicate the presence of vermiculite. No observable intensity changes occurred on the basal reflection positioned at 6.10° 2θ in either of the two clay samples examined.

Illite is the easiest of the four clay minerals to identify in these sediments. The basal reflections for illite are at 8.88, 17.8, and 26.7° 2θ. The various treatments, including cation saturation and solvation with ethylene glycol, do not affect the position of these reflections. Chlorite is identified by a basal series of diffraction peaks at 6.24, 12.5, 18.8, and 25.2° 2θ, which are unaffected by cation saturation or ethylene glycol solvation . Kaolinite is difficult to identify in the presence of chlorite. Basal reflections characteristic of kaolinite are at 12.5 and 24.9° 2θ and are superimposed on the even-ordered chlorite reflections. Kaolinite reflections are unaffected by cation saturation and ethylene glycol solvation. Positive identification of kaolinite in the presence of chlorite can be determined by differentiating kaolinite basal reflection at 24.9° 2θ from the chlorite reflection at 25.2° 2θ (Figure 4.59). Published reports characterizing clay fractions of Hanford formation sand-dominated sediment from other studies

(Serne et al. 2002a, b, c, d, e, f and Lindenmeier et al. 2002) identified kaolinite using electron microscopy.

Trace amounts of quartz in the <2.0 μm fractions are evident by the diffraction peak located at 20.85° 2θ. The 100% reflection for quartz (26.6° 2θ) is hidden by the third-order basal reflection of illite located at 26.6° 2θ. Plagioclase feldspar is also identified in the clay fractions by the minor diffraction peak at 27.8° 2θ. Semi-quantification results of clay minerals in the <2.0 μm fractions are presented in Table 4.61. Total recoveries were normalized to 100%. Smectite concentrations range from 26 to 56 wt% with an average of 41 wt%. Illite concentration varies from 33 to 50 wt% with an average concentration of 42 wt%. Chlorite and kaolinite are the least abundant of the clay minerals identified in the samples with concentrations equal to or less than 20 and 7 wt%, respectively. Quartz and feldspar minerals were present as trace amounts in the clay fraction and therefore were not included in totals presented in Table 4.61.

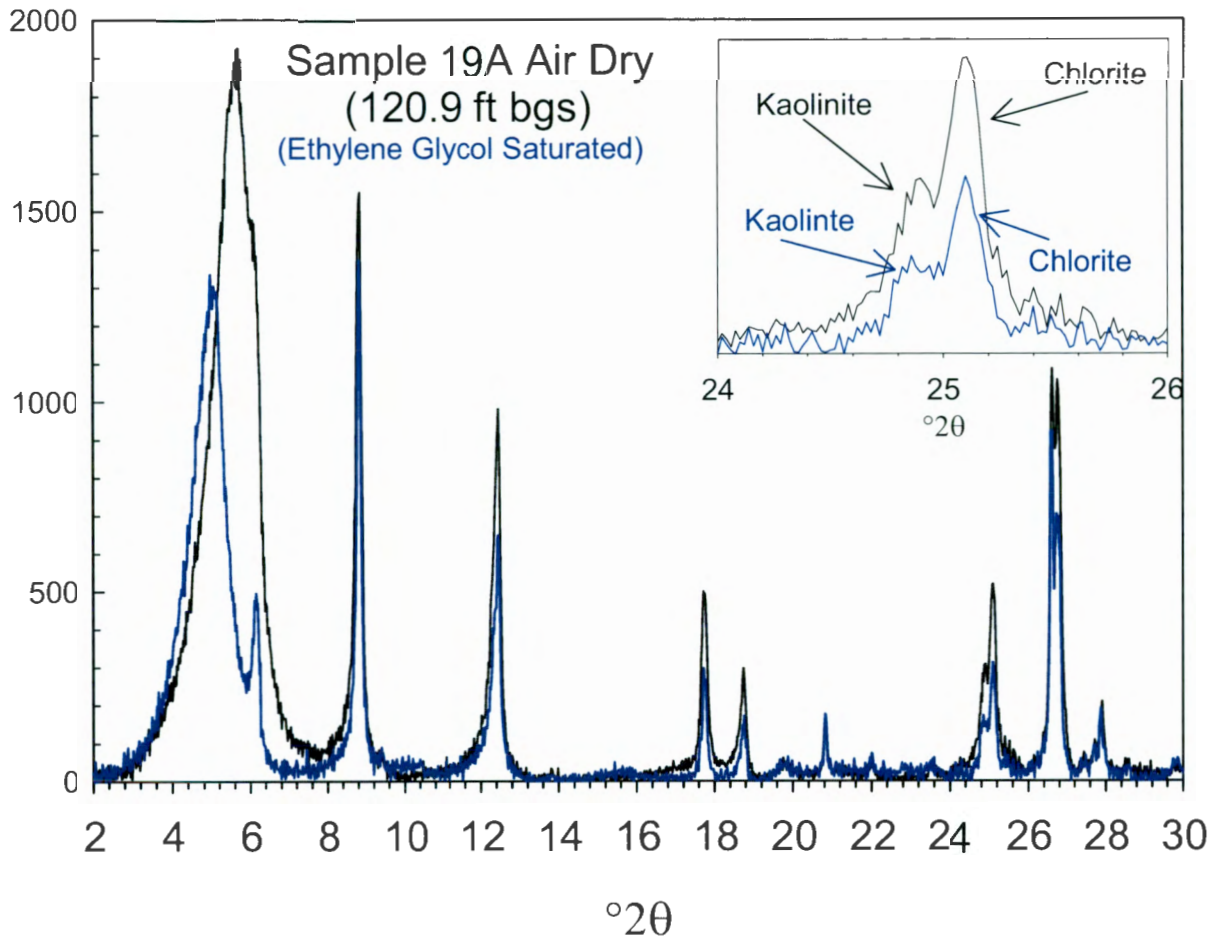

Figure 4.59. XRD Tracing of Clay Fraction from Sediment Sample 19A (120.9 ft bgs) Collected From Borehole C4105, With Matching PDF™ Files

Table 4.61. Semi Quantitative XRD Results of Clay Minerals in <2 um Fraction of Sediment Samples Collected From Borehole C4105. Results are given in wt%.

Sample ID	Depth (ft bgs)	Smectite	Illite	Chlorite	Kaolinite
7A	70.1	26	47	20	7
10A	88.2	35	50	10	5
16A	106.9	48	42	6	5
19A	120.9	56	33	7	5
20A	123.9	40	40	13	7

5.0 Groundwater Status Below the T Tank Farm

This section summarizes historical as well as recent groundwater data from the uppermost, unconfined aquifer in the vicinity of WMA T. The data then are used to describe the nature and extent of contamination in the area. The primary focus is on relating ambient groundwater contamination to releases from waste storage and disposal facilities within or near the WMA. Accordingly, historical water levels and flow directions, and contaminant histories in key wells near the WMA are reviewed as background for understanding current groundwater contaminant distribution patterns and their relationship to possible waste management area sources.

Selected ratios of mobile contaminants in 1) the vadose zone sediments sampled by the two boreholes, C4104 and C4105 (see Section 4), 2) the groundwater, and 3) specific single-shell tanks at the time of suspected leaks are used to assess whether there are indications that the groundwater contamination is related to the current vadose zone contamination and to the tank leaks.

5.1 Aquifer Properties

This section provides information on the properties of the uppermost, unconfined aquifer in the immediate region of WMA T. Aquifer properties were determined from stratigraphic interpretations, current water level elevations, and aquifer testing.

Beneath the 200 West Area, the suprabasalt aquifer system contains the uppermost unconfined aquifer and the underlying Ringold confined aquifer. Deeper confined and semi-confined aquifer systems also exist beneath these sedimentary aquifers in the basalt flow tops, flow bottom zones, and sedimentary interbeds (DOE 1998). Groundwater flow, both vertically and horizontally, in the suprabasalt aquifers is less constrained than in the deeper basalt aquifers.

The suprabasalt aquifers below the Hanford Reservation have been impacted by past practice, liquid waste disposal operations and unplanned releases, in some instances from single-shell tank leaks. In the area of WMA T, large volumes of waste water disposed to ground between the 1940s and 1997 created large artificial groundwater mounds particularly beneath the 216-T pond system, north of WMA T, and beneath the 216-U pond, southwest of WMA T. The disposed liquids contained many of the contaminants that now move through the upper unconfined aquifer. Water mounding has declined significantly since the 1997 cessation of non-permitted liquid waste disposal.

The following discussion focuses on the uppermost, suprabasalt aquifer system within the Ringold and Hanford formations. The suprabasalt aquifers are the uppermost regionally extensive aquifers beneath the WMA T. Groundwater within this aquifer system is contained within the fluvial-lacustrine sediments of the Ringold Formation. Figure 5.1 shows a map of WMA T with the location of all wells discussed in this section.

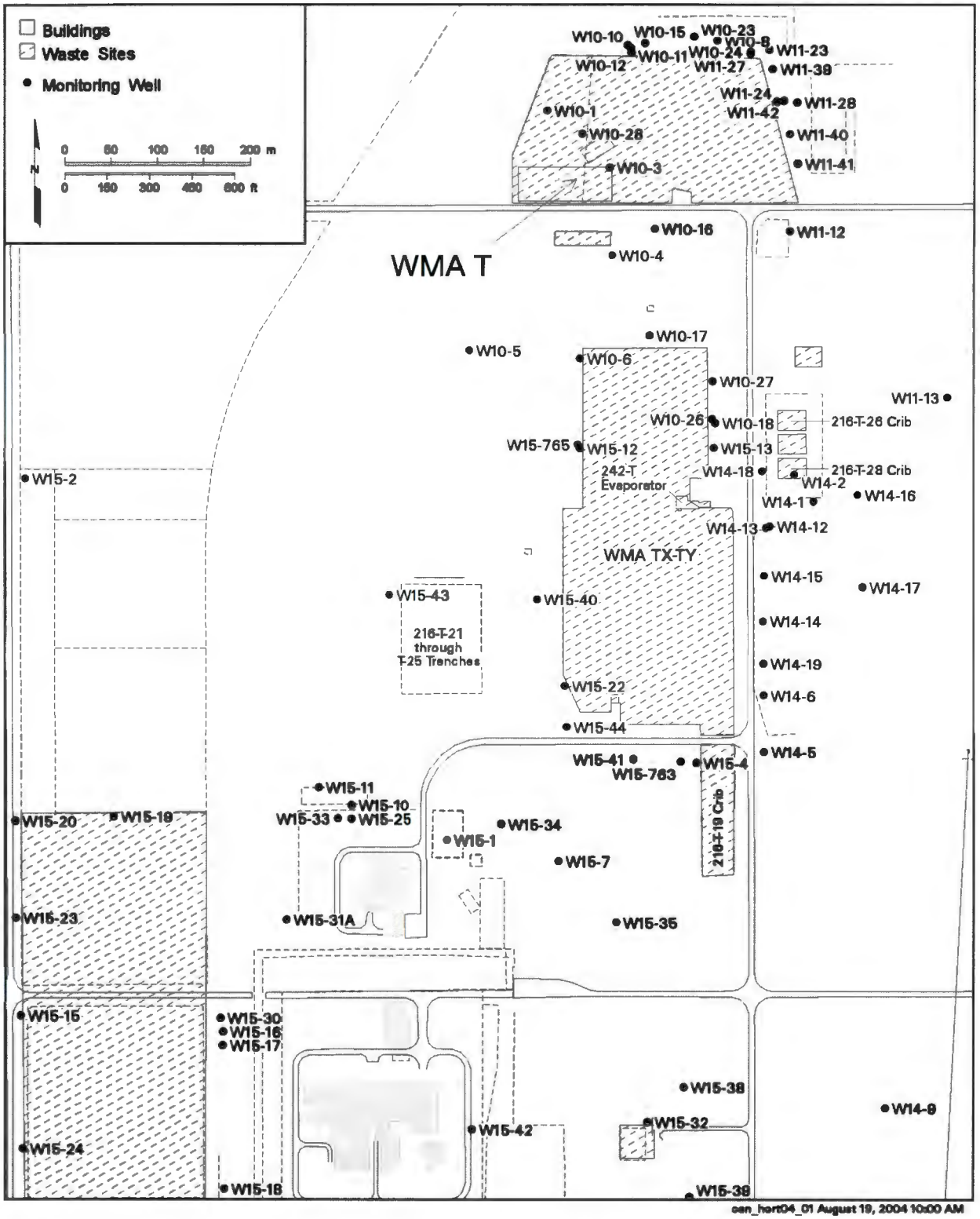

Figure 5.1. Well Location Map for Waste Management Area T

Only one well, 299-W11-13, near WMA T extends to the top of basalt and has recent water level data. (Well 299-W11-13 is located about 270 meters southeast of the southeast corner of WMA T.) Based on the March 2003 water table elevation, the suprabasalt aquifer system is approximately 73 meters thick at this well.

The base of the uppermost, unconfined aquifer generally is regarded as the basalt surface and, where this is the case, the entire suprabasalt aquifer is unconfined. However, beneath WMA T (and beneath the entire 200 West Area), the silt and clay deposits of the Ringold Formation lower mud unit (hydrogeologic unit 8 of Williams et al. 2002) form a confining layer that separates the suprabasalt aquifer into the uppermost unconfined aquifer and the underlying Ringold confined aquifer (Williams et al. 2002). Thus, the uppermost, unconfined aquifer in the area of interest extends from the water table down to the top of the lower mud unit. The unconfined aquifer is about 50 meters thick at well 299-W10-24 (located at the northeast corner of WMA T), based on the August 2003 water level. The unconfined aquifer consists of sandy gravels and gravelly sands of the Ringold Formation member of Wooded Island unit E (hydrogeologic unit 5 of Williams et al. 2002). All wells in the WMA T monitoring networks are screened in hydrogeologic unit 5. Currently, the water table at WMA T is 136 to 137 meters above sea level.

Water levels in the uppermost unconfined aquifer raised as much as 13.5 meters (above the pre-Hanford natural water table) beneath WMA T because of artificial recharge from liquid waste disposal operations that were active since the mid 1940s and continued for 30-40 years. The largest volumes of discharge were to the 216-T pond system and the 216-U-10 pond. Figure 5.2 shows the liquid discharge history for the two ponds. The 216-T pond system is estimated to have received approximately 424 billion liters of effluent (Alexander et al. 1995); the 216-U pond received about 158 billion liters of effluent (Last 1994). The large-volume disposals to the ponds (and, lesser volumes to cribs and ditches) artificially recharged the uppermost unconfined aquifer, creating large water-table mounds.

Figure 5.3 shows the groundwater elevations in the area of WMA T since the late 1940s. The figure shows that the increase in water-table elevation was most rapid from 1949 to 1956 and was somewhat stabilized between the late 1960s and the late 1980s. Water levels began to decline in the late 1980s beneath WMA T when wastewater discharges in the 200 West Area were reduced. The decline in water levels may have implications for the groundwater monitoring network at the WMA T as discussed later.

Accompanying the changes in water level were changes in groundwater flow direction. Histograms (rose diagrams) showing groundwater flow directions beneath the T tank farm during different time periods are shown in Figure 5.4. The rose diagrams plot the solutions to numerous three-point analyses using water level information from various well triplets in the north central part of the 200 West Area. The petals of the rose diagrams point in the direction of groundwater flow and the length of the petals represents the percentage of measurements showing that groundwater flowed in the indicated direction.

Pre-Hanford Site groundwater flow direction was toward the east (Kipp and Mudd 1974). The rose diagram in Figure 5.4A shows that groundwater flow had changed toward the south in the area by the early 1950s. This shift resulted from disposal of large volumes of liquid to the 216-T pond system.

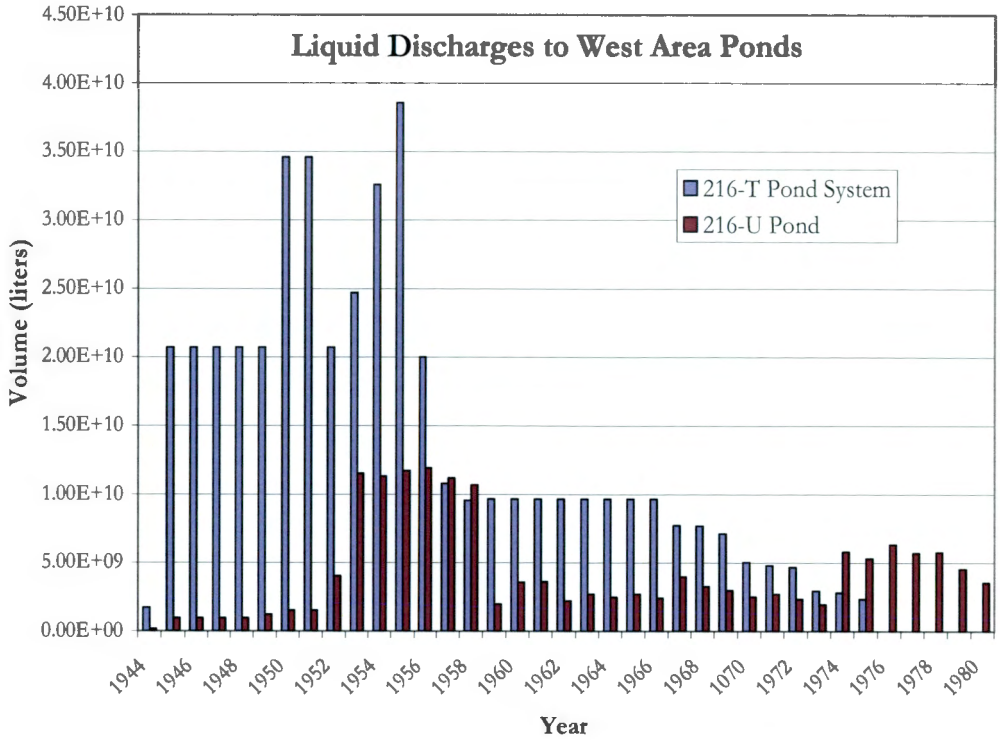

Figure 5.2. Discharge History for the 216-T Pond and the 216-U Pond. *Data for the 216-T Pond are from Alexander et al. 1995; data for the 216-U pond are from Last 1994.*

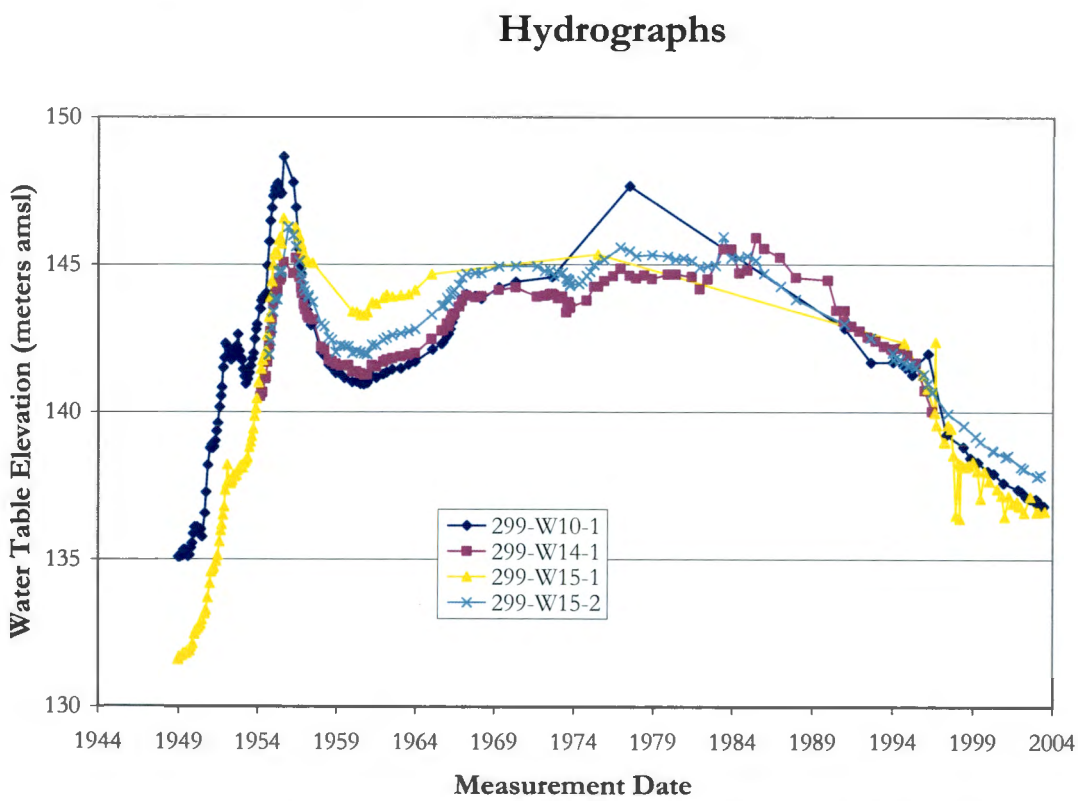

Figure 5.3. Hydrographs of Selected Wells in the North 200 West Area

In 1956, groundwater flow direction changed again and started flowing towards the northeast due to the increasing influence of the groundwater mound under 216-U pond and a decreasing influence of the mound under 216-T pond (Figure 5.4B). Discharges to 216-T pond ended in 1976 but continued at 216-U pond until 1984. As discharges to the 216-U pond declined in the early 1980s, groundwater flow shifted to a more northerly direction as the groundwater mound began to decrease and discharges to the 216-U-14 ditch continued. The slight westerly component to the groundwater flow direction between early 1980s and mid 1990s (Figure 5.4C) is probably a result of the discharges to the 216-U-14 ditch, located southwest of WMA T. All non-permitted discharges to the ground ceased and the influence of the 216-U pond mound on the groundwater beneath the T tank farm diminished in 1995. Consequently, the flow direction changed again in about 1996 and began to return toward an easterly direction (Figure 5.4D).

These large shifts in groundwater flow direction have broad implications for contaminant distribution in the uppermost aquifer beneath WMA T. In the late 1940s and early 1950s, contamination was spread south in the aquifer. Then, in the late 1950s and until the mid-1990s, that same contamination returned to the north along with any new contamination that entered the aquifer after the 1950s. Today, groundwater contamination beneath the WMA and surrounding area is generally migrating east.

Recently, two trend-surface analyses, using August and September 2002 data, yielded groundwater flow directions of 98° to 96° (azimuth) and a water table gradient between of 0.00114 and 0.00132 (Spane et al. 2002). An earlier trend-surface analysis yielded a flow direction of 85° and a water table gradient of 0.00172 (Spane et al. 2001a,b). All trend-surface analysis data are shown in Table 5.1. Although the flow direction may differ from well to well due to heterogeneous aquifer sediments, the groundwater flow direction at WMA T, as determined by the trend surface analyses, is consistent with the data shown in Figure 5.4D and the current regional groundwater map (Figure 5.5).

Borehole tracer dilution and tracer pumpback tests were conducted in three new RCRA monitoring wells at the T tank farm between fiscal years 1999 and 2001. These tests permitted some inferences about flow rate and aquifer homogeneity. The tests allowed direct observation of the effect of lateral groundwater flow through the screened interval of the wells and, thus, provided an indication of the variability of flow through the screened intervals. Details of the test methods, computations, and the results are included in Spane et al. (2001a,b and 2002).

A significant feature of the tracer dilution test results is evidence for downward, vertical hydraulic gradients within the upper portion of the aquifer in wells 299-W11-39 and 299-W11-40. Table 5.2 summarizes the test results for these wells. Vertical flow within 200 West Area wells was first indicated by tracer-dilution studies and later confirmed (for two wells at WMA TX-TY) by vertical tracer tests specifically designed to detect vertical flow within a borehole (Spane et al. 2001a, b). Downward vertical flow was subsequently confirmed by electromagnetic flowmeter surveys (Waldrop and Pearson 2000).

A

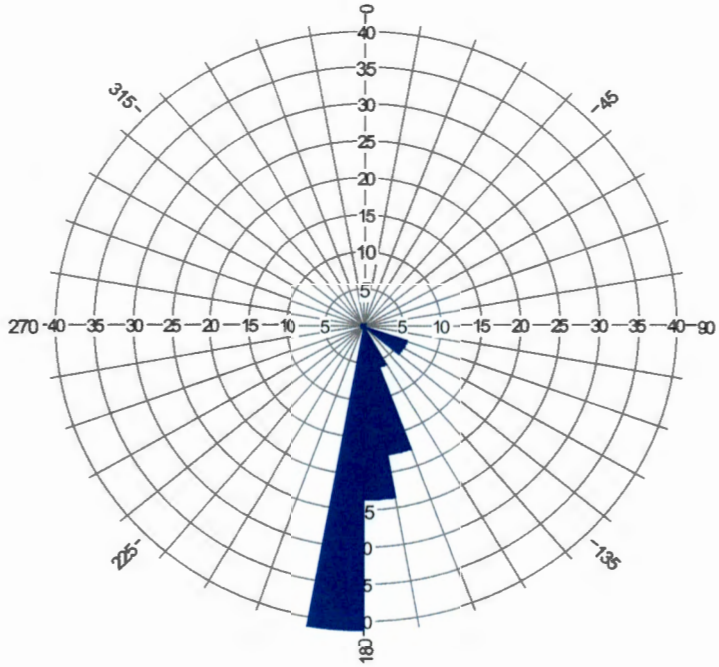

B

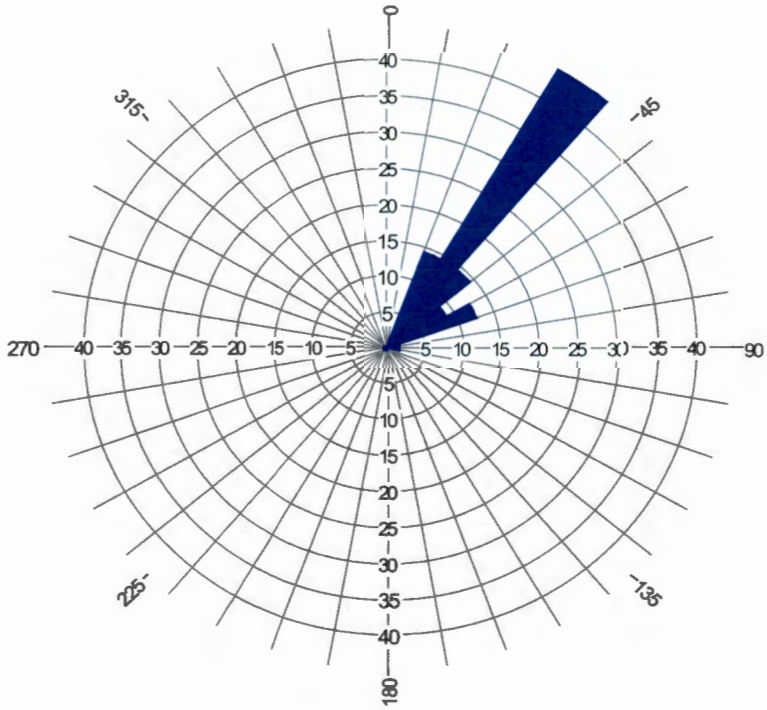

Figure 5.4. Groundwater Flow Directions in the North Part of 200 West Area. A. 1954 to 1956, 1 Well Triplet, 17 Measurements; B. 1957 to 1982, 2 Well Triplets, 56 Measurements.

C

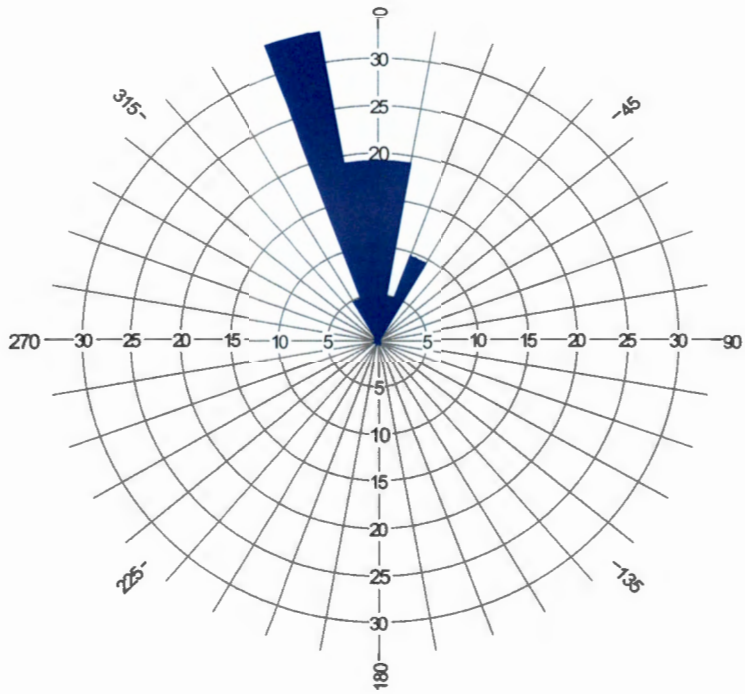

D

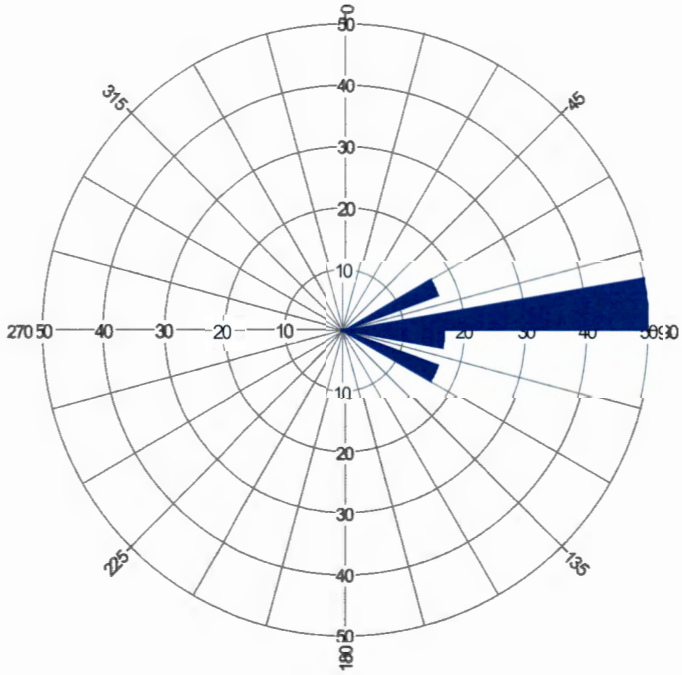

Figure 5.4. Groundwater Flow Directions in the North Part of 200 West Area. C. 1983 to 1995, 4 Well Triplets, 21 Measurements; D. 1997 to 2003, 3 Well Triplets, 6 Measurements.

Table 5.1. Groundwater Flow Characterization Results Based on Trend Surface Analyses. (Data are from Spane et al. 2001a, 2001b, 2002.)

Well	Measurement Date	Groundwater Flow Direction	Hydraulic Gradient	Wells Used in Analyses
299-W10-24	4/21/99	N 85° E	0.00172	299-W10-8 299-W10-12 299-W10-22 299-W10-24 299-W11-23 299-W11-27
299-W11-39	9/4/01 9/18/01	N 98° E N 96° E	0.00115 0.00114	299-W10-1 299-W10-4 299-W10-24 299-W11-40 299-W11-41 299-W11-42
299-W11-40	8/9/01	N 96° E	0.00132	299-W10-1 299-W10-4 299-W10-24 299-W11-39 299-W11-41 299-W11-42

The existence of vertical flow in a well does not necessarily reflect actual groundwater flow conditions within the surrounding aquifer, but its presence implies a vertical flow gradient and has implications pertaining to the representativeness of groundwater samples collected from the wells. Thus, the vertical gradient detected in some wells, especially along the current downgradient edge of WMA T (eastern edge) may have an impact on contaminant distribution patterns in the area.

A second feature of the hydrologic test data is the suggestion of higher or lower hydraulic conductivity at certain depths within the screened interval of some wells relative to other depths. For example, tracer tests indicate that the upper 3 to 4 meters of the screened interval of well 299-W10-24 is less permeable than the lower part of the screened interval. However, a tracer test in nearby well 299-W11-39 indicated that the lower 3 meters of the screened interval are relatively impermeable compared to the rest of the interval. (Flow in the lower interval was described as stagnant in Spane et al. [2002].) Thus, apparent differences in permeability do not appear to correlate from well to well.

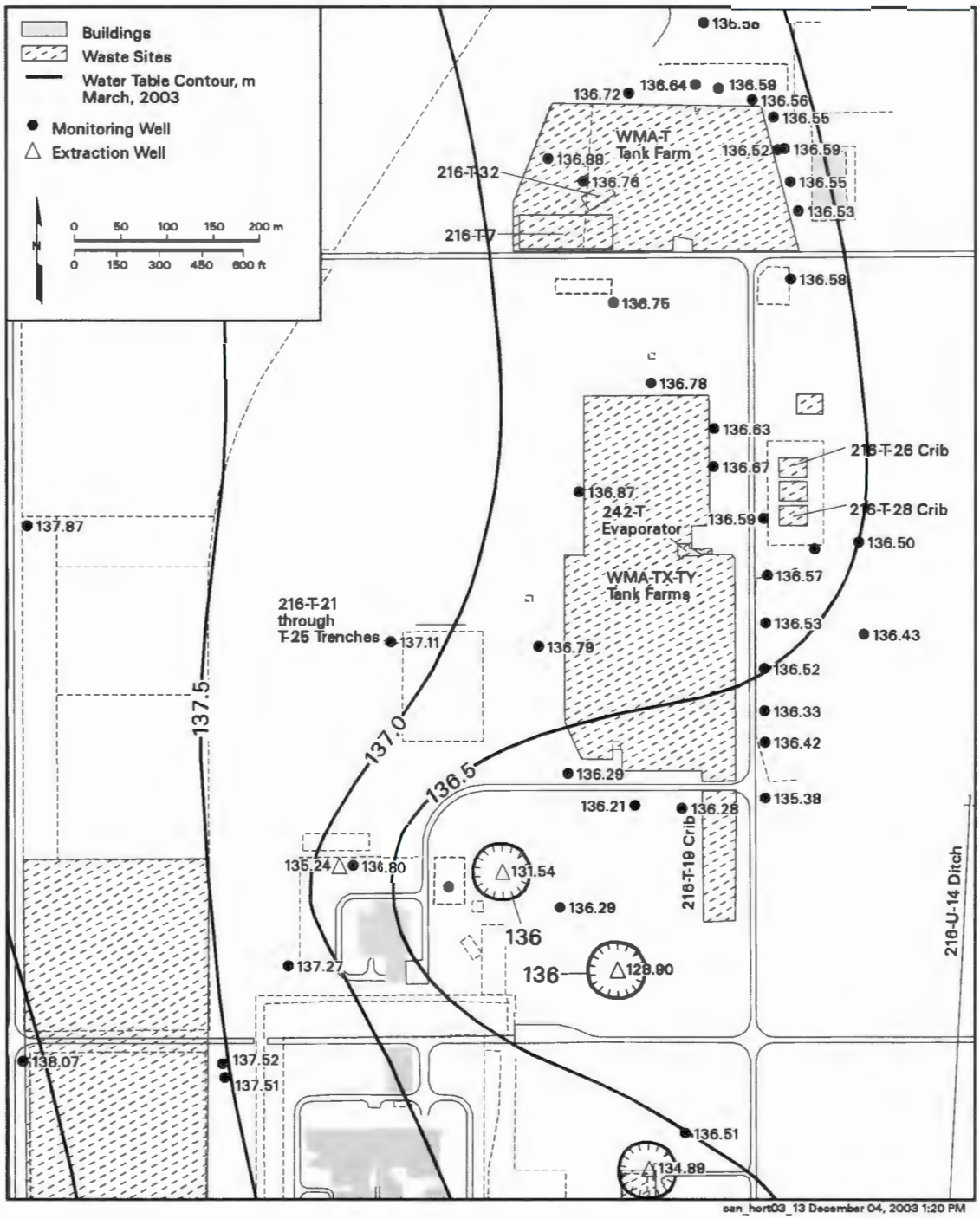

Figure 5.5. March 2003 Water Table Map for the Area Around Waste Management Area T

Table 5.2. In-Well, Downward Vertical, Flow-Velocity Summary for Wells 299-W11-39 and 299-W11-40 at Waste Management Area T (Spane et al. 2002)

Test Well	Tracer Dilution Profile	
	Range (m/min)	Average (m/min)
299-W11-39	0.0003 – 0.002	0.001
299-W11-40	0.011 – 0.020	0.017

For the WMA T groundwater assessment, new hydraulic conductivity data were obtained from slug tests and drawdown tests conducted in 9 new wells drilled since 1999. Effective porosities were determined from tracer drift and tracer pumpback tests. Hydraulic properties are discussed in detail by Spane et al. (2001a, b), Spane (2002), and Spane et al. (2003) and are presented in Tables 5.3 and 5.4.

Table 5.3 shows horizontal groundwater flow velocities determined from tracer pump back tests. These horizontal velocities are greater than the calculated velocities in Table 5.4 for well 299-W11-40, which has downward vertical flow in the well. The vertical flow in the well probably resulted in overestimation of the measured flow velocity. Both the measured and calculated velocities are about the same for wells 299-W10-24, which has no vertical flow.

Overall, there is about an order of magnitude difference in the horizontal flow velocities in Table 5.4. The horizontal velocity in wells 299-W10-28 and 299-W11-42 are substantially greater than the velocities calculated for the other wells (Table 5.4). Very rapid recoveries during slug testing were noted (90% recovery within 4 seconds for both wells), which suggests fairly permeable formations (Spane et al. 2002 and 2003). However, there is nothing in the geologist's logs or the geophysical logs to suggest that the formation in the screened interval of these wells is significantly different than the formation at nearby wells.

Table 5.3. Results from Tracer-Dilution and Tracer-Pumpback Tests in Wells at Waste Management Area T (Spane et al. 2001a, b and 2002)

Well	Effective Porosity[(a)]	Groundwater[(a)] Flow Velocity (m/d)	Average In-Well Flow Velocity[(b)] (m/d)
299-W10-24	0.072	0.029	0.012
299-W11-39[(c)]	0.045	0.022	0.014
299-W11-40[(d)]	1.1	0.002	0.176

(a) Data from tracer pump back tests.
(b) Data from tracer dilution tests.
(c) Slight downward vertical flow, data uncertain.
(d) Strong downward vertical flow, data highly uncertain.

Table 5.4. Hydraulic Properties from Slug and Constant Rate Pumping Tests and Calculated Horizontal Flow Velocities at New Wells at Waste Management Area T

Well	Hydraulic[a,b] Conductivity (m/d)	Hydraulic[a,c] Conductivity (m/d)	Transmissivity[a,c] (m^2/d)	Specific[a,c] Yield	Calculated Flow Velocity (m/d)
299-W10-23	1.62 – 2.35	ND	ND	ND	0.024[e]
299-W10-24	1.04 – 1.68	1.22	66	0.11	0.023[f]
299-W10-28	27.9[g]	ND	ND	ND	0.23[e]
299-W11-39	1.31 – 1.69	0.85	44	0.1	0.017[d]
299-W11-40	3.56 – 4.58	2.02	103	0.1	0.046[d]
299-W11-41	7.57 – 7.78	ND	ND	ND	0.078[e]
299-W11-42	28.1[g]	ND	ND	ND	0.28[e]

(a) Data from Spane et al. (2001a,b, 2002, and 2003).
(b) Slug test data.
(c) Constant rate pumping test data.
(d) Estimated using maximum hydraulic conductivity value, a gradient of 0.001, and specific yield from this Table. Specific yield was used because downward flow in the well resulted in uncertain effective porosity.
(e) Estimated using maximum hydraulic conductivity value, a gradient of 0.001 and effective porosity values of 0.1.
(f) Estimated using maximum hydraulic conductivity value, a gradient of 0.001, and effective porosity value from Table 3.2.
(g) Indicates average hydraulic conductivity obtained from high-permeability, non-linear type-curve analysis method.
ND = Not determined.

Taken as a whole, the geologist's logs, geophysical logs, development pumping data, and the hydrologic testing data all indicate heterogeneity in the aquifer properties within the screened intervals of several individual wells and among wells at WMA T. No widespread trends have been identified.

The hydrographs in Figure 5.6 show that water levels have declined by about 6.5 meters since 1991 beneath the T tank farm. This decline, resulting from decreasing effluent discharge in the 200 West Area, became much steeper in 1995 with the effective cessation of discharge to all non-permitted facilities in this area. Between 1998 and 2004 the average rate of water table decline has been between about 0.3 and 0.4 meter per year in all monitoring wells at WMA T. The rapid decrease in water levels after 1995 has resulted in monitoring wells going dry more quickly than previously predicted and has necessitated the drilling of 7 new monitoring wells since 1999.

The pre-Manhattan Project water table was estimated at approximately 123 to 125 meters above sea level in the area of T tank farms by Kipp and Mudd (1974). More recently, Bergeron and Wurstner (2000) modeled the elevation of the water table beneath the Hanford Site for the Immobilized Low-Activity Waste Performance Assessment. Their results predict a post-Hanford Site influenced water table elevation of about 130 to 132 meters above sea level in the T tank farm area. The difference between these two estimates may be due, in part, to the back extrapolation of very few data points by Kipp and Mudd (1974). However, the model results of Bergeron and Wurstner incorporated the increase

in recharge due to increased irrigation in the Cold Creek Valley which would results in a higher water table. The model results probably better represent the future condition and suggest that the elevation of the current water table will continue to decrease another 5 to 7 meters in the T tank farm area.

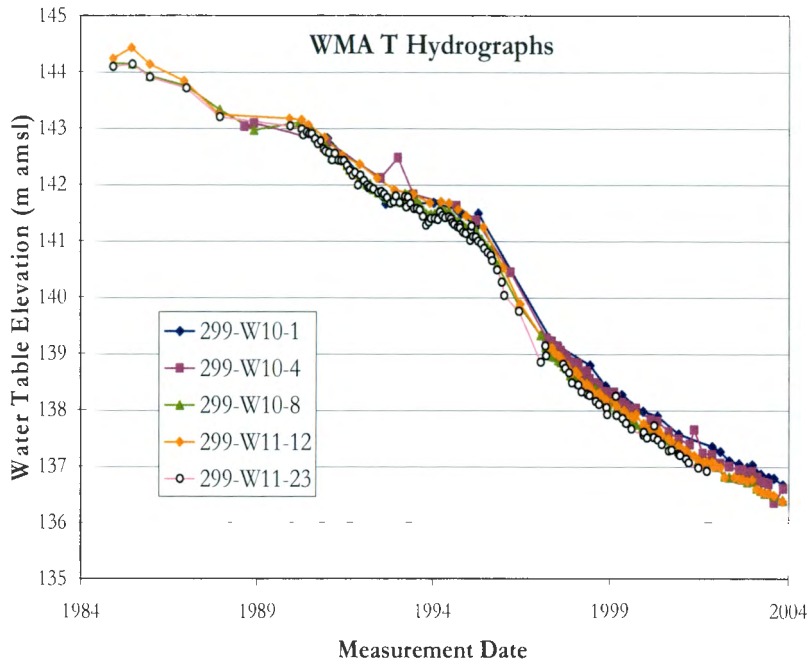

Figure 5.6. Historic Water Table Elevations in Selected Wells at WMA T. *Well 299-W11-23 is now dry.*

5.2 Existing Groundwater Contamination

This section discusses the current and historical groundwater contamination at WMA T. The evaluation of contamination includes descriptions of the types and concentrations of contaminants in the groundwater, the depth distribution of contaminants in the aquifer, and the areal extent of contamination in the area.

Monitoring results from new and existing wells, results of depth sampling during and after installation of new monitoring wells, and comparison of groundwater chemistry in old wells and their adjacent replacement wells, provide new insights into the occurrence and nature of groundwater contamination in the T tank farm area. The information given in this section is taken largely from Horton et al. (2002) and is updated with more current groundwater data.

Groundwater at the T tank farm contains elevated concentrations of carbon tetrachloride, chromium, nitrate, technetium-99, and tritium. This contamination is a result of mixing of wastes from a number of past waste-disposal activities, including: 1) the disposal of process water and steam condensate at nearby ponds, cribs, and trenches, 2) the disposal of plutonium processing waste at cribs and trenches associated with the Plutonium Finishing Plant, and 3) leaks from single-shell tanks and transfer lines within the T tank farm.

5.2.1 Extent of Contamination – Depth Distribution

Determining the vertical extent of contaminants within the uppermost aquifer is part of the RCRA groundwater quality assessments currently underway at WMA T. A variety of data sources including discrete depth sampling during drilling, comparison of adjacent wells that sample different parts of the aquifer, and detailed specific conductance profiling provide important information about the depth distribution of contaminants.

5.2.1.1 Specific Conductance Profiling

In September 2002, specific conductance measurements were taken at 0.5 to 1 meter intervals throughout the screened intervals of four groundwater monitoring wells around the T tank farm. Significant differences in specific conductance with depth were found in three of these wells. The remaining well (299-W10-24) showed no variation of specific conductance with depth.

Figure 5.7 shows a plot of specific conductance versus depth in well 299-W10-28, an upgradient well at WMA T. The specific conductance data show a marked increase with increasing depth through the upper 4 meters of the screened interval below which specific conductance remains unchanged. In general, specific conductance reflects nitrate (and sodium and calcium) concentration in the T tank farm area. At well 299-W10-28, the data suggest that the nitrate concentration increases from the water table to about 4 meters depth within the aquifer. Also shown on the figure are the values of specific conductance measured after purging the well for the four routine quarterly groundwater samples taken prior to the specific conductance profile. The red squares to the left of the curve, representing the pumped values, are at the depth of the pump intake. The pumped values are all less than the measured ambient values and appear to be an average of the low conductance water at the water table surface and the relatively high conductance water deeper in the screened interval.

A specific conductance profile measured in well 299-W11-39, a downgradient well at WMA T, has a shape very similar to that of well 299-W10-28, in Figure 5.7, although the absolute values of the specific conductance are much smaller and the magnitude of the change is much less for well 299-W11-39. A specific conductance profile measured in well 299-W11-42 (Figure 5.8), another downgradient well at WMA T, also looks similar to that of well 299-W10-28 except that the increase in specific conductance occurs between 6 and 9 meters below the water table and, again, the magnitude of the change is much less than that shown for well 299-W10-28. The data from well 299-W11-42 allow for a continued increase in specific conductance below the screened interval.

Comparison of nitrate concentrations in well 299-W11-28 (now dry) with replacement well 299-W11-42 indicate that the nitrate concentration is relatively low at the water table and increases at some depth in the aquifer (see Section 5.2.1.3, "Sampling During Drilling"). The specific conductance profile in well 299-W11-42 supports the interpretation of the nitrate data. These data also are interpreted to reflect the regional nitrate trend found in the WMA T area and suggest that the main part of the regional plume is located at some depth below the water table.

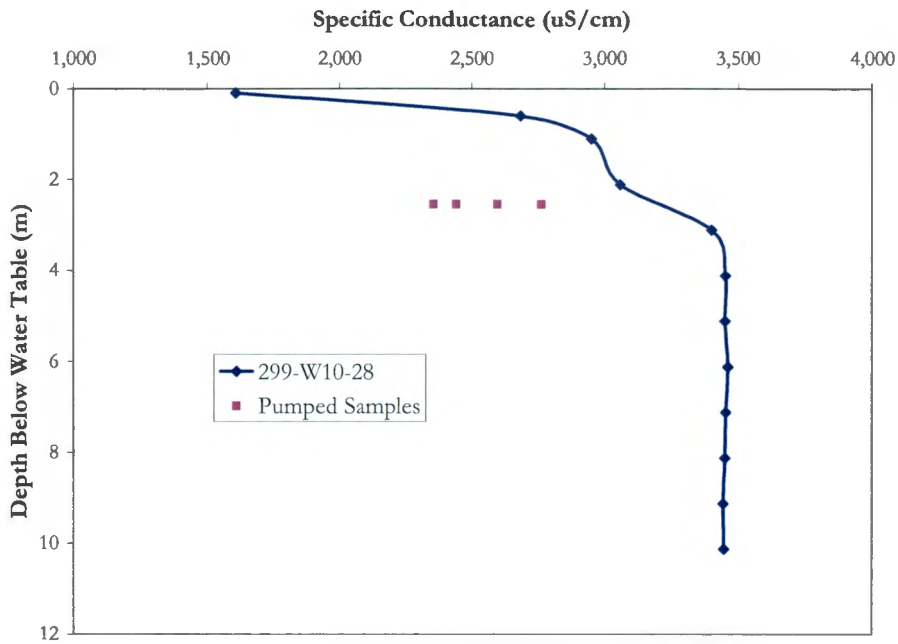

Figure 5.7. Specific Conductance versus Depth Below the Water Table in Well 299-W10-28. *The red squares to the left of the curve are at the depth of the pump intake.*

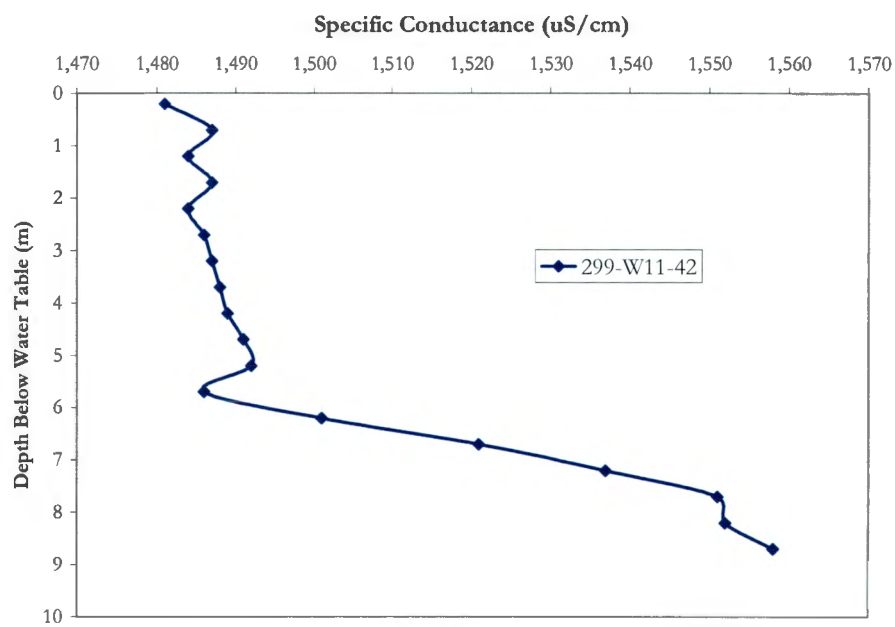

Figure 5.8. Specific Conductance versus Depth Below the Water Table in Well 299-W11-42

5.2.1.2 Comparison of Chemical Data From New and Replaced Wells

Replacement wells, when located immediately adjacent to the older wells, offer an opportunity to look for vertical variation within the upper part of the aquifer. Three well pairs at T tank farm show variable vertical stratification of contaminants in the upper part of the aquifer.

In each case, the old well and its replacement well are separated by only a few meters. In addition, in each case, the older well was last sampled when there was a fraction of a meter of water within the screened interval and the replacement well was sampled with a pump placed at least 3 meters below the water table within a 10.7-meter screened interval. Thus, the last samples from the old well represent the top of the aquifer and the samples from the replacement well represent a composite of water pumped from the length of the screened interval that includes both the water table and deeper parts of the aquifer.

Wells 299-W11-27 and 299-W10-24 are about 3 meters apart and are located near the northeastern corner of WMA T. Well 299-W10-24 is the replacement well for well 299-W11-27 that went dry in early 1999. The last sampling of well 299-W11-27 took place in March 1999 and sampling of replacement well 299-W10-24 started in December 1998, allowing a sampling overlap between the two adjacent wells. The last samples collected from well 299-W11-27 represent the top of the aquifer. The samples collected from well 299-W10-24 represent water throughout the screened interval, which extends from the water table to 10 meters below the water table. The sample pump was at 5.0 meters below the water table when sampling began.

Well 299-W11-27 reached a peak technetium-99 concentration of 21,700 pCi/L in February 1997 and dropped to 6,000 pCi/L for the last sampling in March 1999 before going dry. This sample represented the technetium-99 concentration at the top of the aquifer. The first analysis of technetium-99, from the December 1998 sampling of replacement well 299-W10-24, contained 2,090 pCi/L technetium-99, about 4,000 pCi/L less than the older, dry well (Figure 5.9). The sample from well 299-W10-24 represented the technetium-99 concentration throughout the upper 10 meters of the aquifer after ambient water was purged from the well. The interpretation is that, in early 1999, the technetium concentration at the water table at the northeast corner of T tank farm was 6,000 pCi/L and the concentration decreased with depth in the aquifer.

Well 299-W11-39 is the replacement well for now dry well 299-W11-23; both are located near the northeast corner of the T tank farm. Comparison of technetium-99 concentration in the two wells indicates essentially no difference between the last samples from well 299-W11-23 and the first samples from 299-W11-39 (Figure 5.9). The situation here, however, is complicated by the downward in-well flow and very tight formation at the bottom of the well screen in well 299-W11-39. One possibility is that there are no vertical technetium-99 concentration gradients at these wells. A second possibility is that the tight formation near the bottom of well 299-W11-39 does not contribute sufficient water to the pumped sample to effectively dilute a high technetium-99 concentration in water from near the water table. Because other evidence suggests a technetium-99 concentration gradient in the area, the second possibility is preferred.

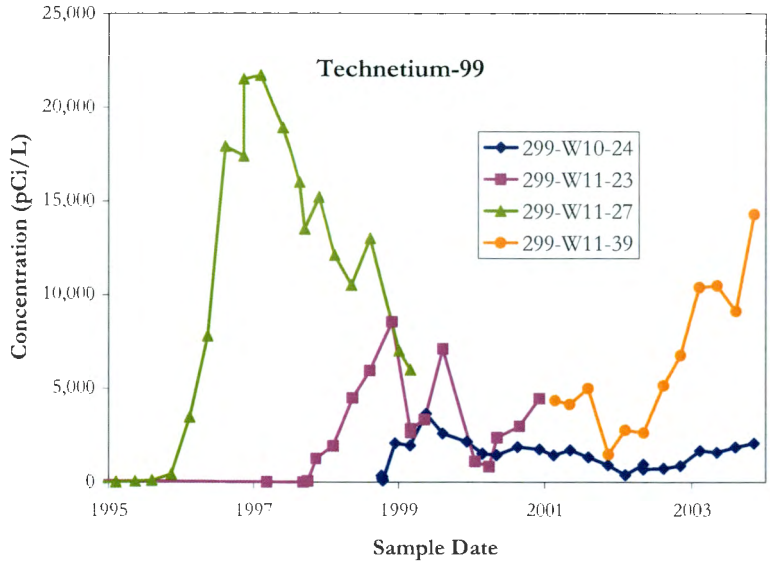

Figure 5.9. Technetium-99 Concentrations in Two Well Pairs at the Northeast Corner of T Tank Farm

Figure 5.10 shows the concentration of nitrate versus time for two well pairs at T tank farm. The well pair 299-W11-28 and 299-W11-42 is located near the center of the downgradient side of WMA T. Well 299-W11-42 is the replacement well for now dry well 299-W11-28. For both well pairs in the figure, the replacement well, which samples the upper 10 meters of the aquifer, has higher concentrations of nitrate than did the older well as it went dry. These data suggest that nitrate concentration in groundwater beneath WMA T is relatively low at the water table and increases with depth in the aquifer. This is consistent with the specific conductance profiles.

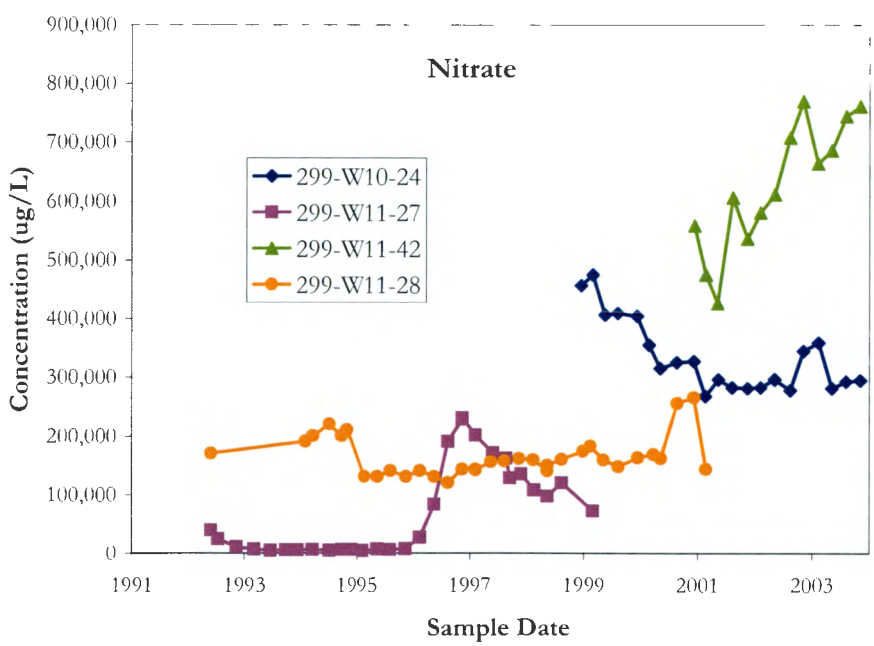

Figure 5.10. Nitrate Concentration in Two Well Pairs Downgradient of WMA T

Figure 5.11 shows the chromium concentration versus time for two well pairs at the T tank farm. These data indicate that the chromium concentrations in the area are relatively low at the water table and higher at some depth in the aquifer. The well pair 299-W11-23 and 299-W11-39 shows essentially the same trend although the older well, 299-W11-23, had a carbon steel casing so that some of the chromium data may be questionable.

Finally, the same kind of information is shown in Figure 5.12 for fluoride. Like chromium, the fluoride concentration appears to be larger at some depth below the water table than it is at the water table. As will be discussed later (Section 5.2.2, "Extent of Contamination"), both chromium and fluoride appear to have a source in one or more of the upgradient cribs at WMA T.

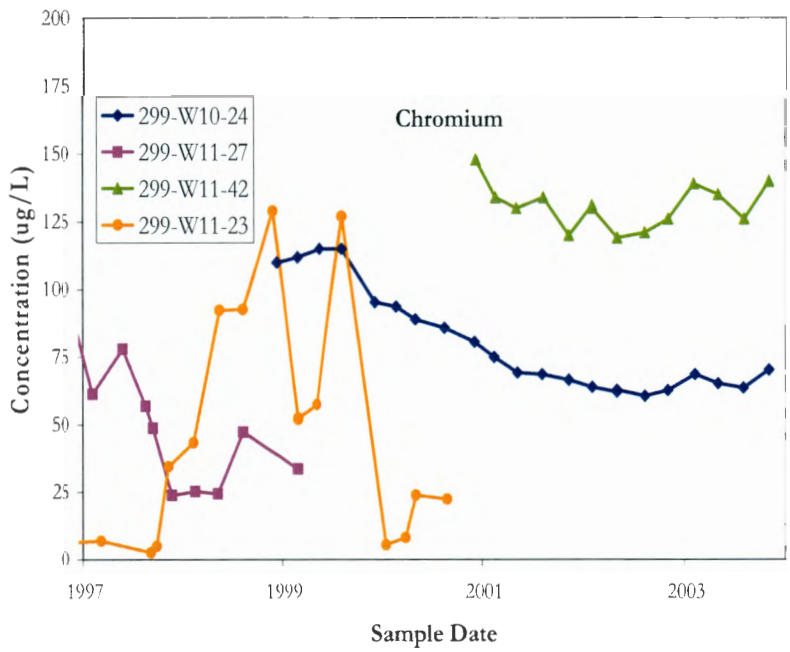

Figure 5.11. Concentrations of Chromium in Filtered Samples from Two Downgradient Well Pairs Near the T Tank Farm

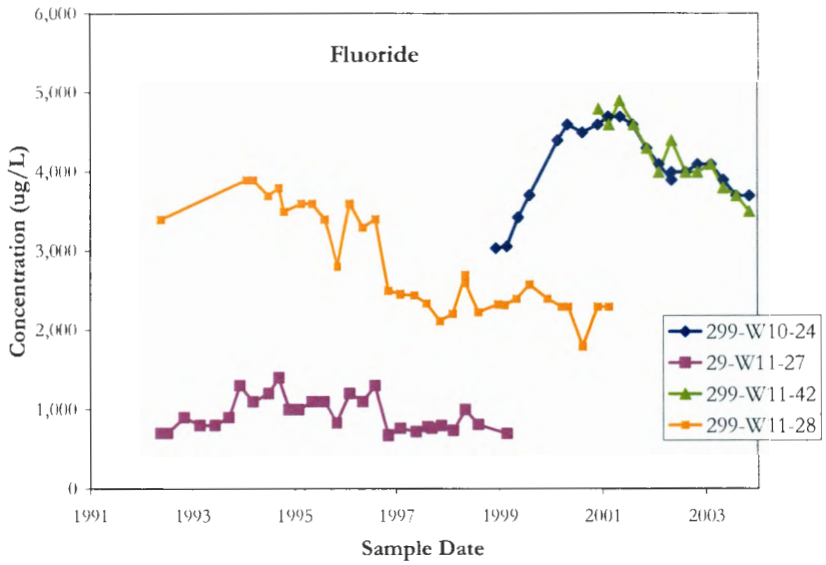

Figure 5.12. Concentrations of Fluoride in Two Downgradient Well Pairs Near the T Tank Farm

5.2.1.3 Sampling During Drilling

Groundwater and saturated sediments brought to the surface during drilling can give an indication of vertical chemical variations within the aquifer. New well 299-W10-24 was sampled in this way in 1998. Well 299-W10-24 was drilled at the northeast corner of T tank farm and through the lower mud unit of the Ringold Formation (hydrogeologic unit 8) prior to being completed as a top-of-the-aquifer monitoring well. The well was sampled with a pump-and-packer assembly at 5 depths in the aquifer (Horton et al. 2002).

The results from the pump-and-packer samples are shown in Figure 5.13. The maximum technetium-99 concentration occurs at the water table, whereas the maximum concentrations of tritium, nitrate, and carbon tetrachloride were found at about 20 meters or greater below the water table. The Ringold formation lower mud unit (hydrogeologic unit 8), a local aquitard, occurs between 52 and 53 meters below the water table in well 299-W10-24. Concentrations of all four key contaminants in Figure 5.13 decrease across the lower mud unit.

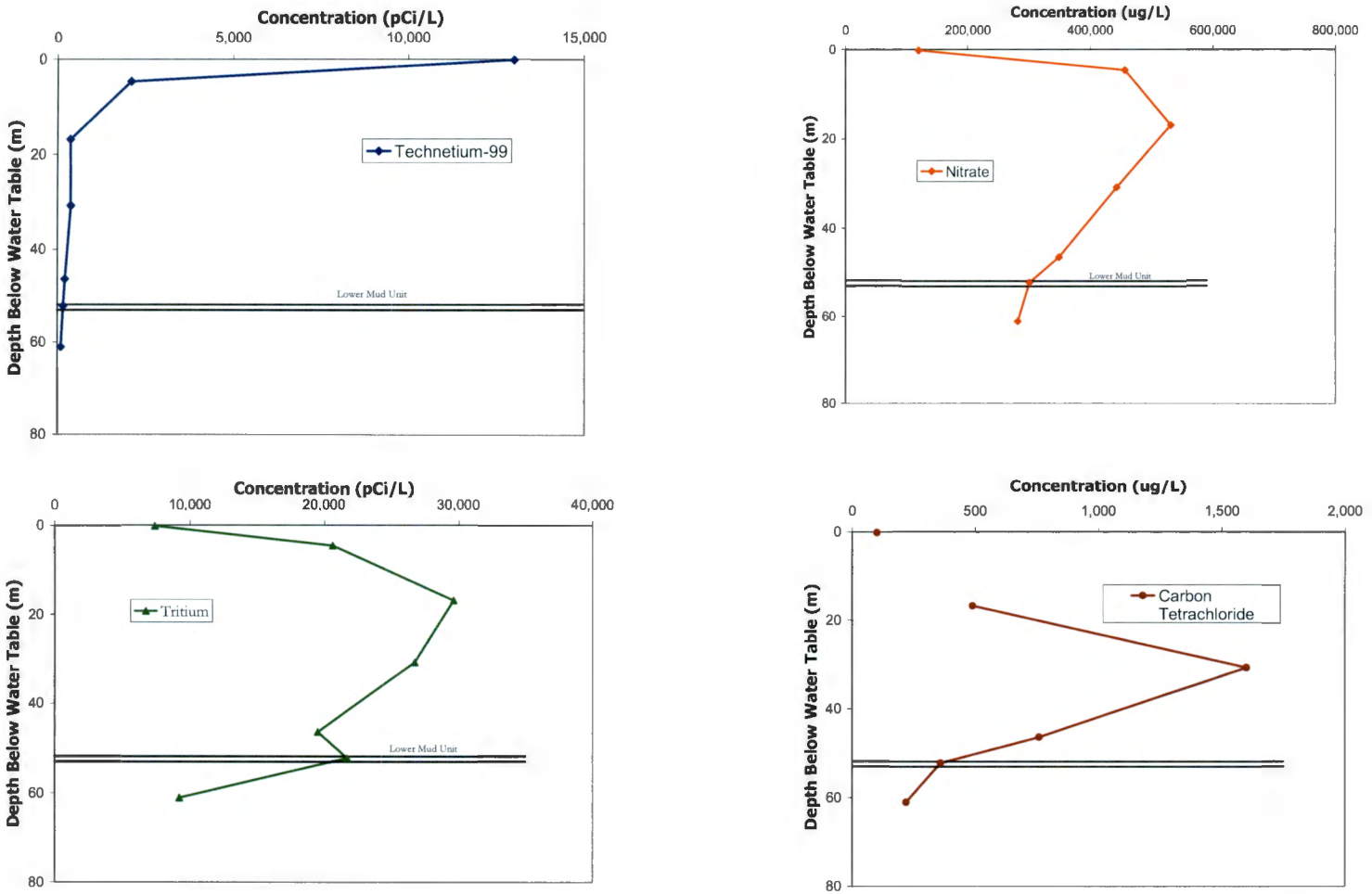

Figure 5.13. Depth Distribution of Key Contaminants in Well 299-W10-24. *The sample at the water table was collected with a Kabis from well 299-W11-27; the sample at about 5 meters depth is a pumped sample from the screened interval after well completion.*

A few other samples were collected from two wells at WMA T during drilling and analyzed for a limited suite of constituents. Selected results are shown in Table 5.5. The data from well 299-W11-42 (downgradient well) in Table 5.5 are consistent with other data suggesting that specific conductance and nitrate increase with increasing depth to some distance below the water table. The data from well 299-W10-28 (upgradient well) do not reflect this trend. The nitrate concentration in well 299-W10-28 was the highest on the Hanford Site in 2003, second only to another upgradient well at WMA T, 299-W10-4 (Hartman et al. 2004). The high nitrate values upgradient of WMA T probably are due to contamination from nearby cribs that may not have had a chance to disperse in the aquifer. The downgradient, and deeper, nitrate contamination is most likely part of the regional nitrate plume in the 200 West Area.

Table 5.5. Nitrate and Specific Conductance in Samples Collected During Drilling at WMA T

Depth Below the Water Table (m)	Nitrate Concentration (μg/L)	Specific Conductance (μS/cm)
299-W10-28[1]		
8.2	562,420	1,381
16.8	274,700	784
299-W11-42[2]		
0.6	Not Measured	580
2.1	Not Measured	688
3.6	Not Measured	660
5.2	302,000	758
8.2	Not Measured	1392
9.8	Not Measured	1419
11.3	Not Measured	1420
12.8	576,000	1400

1. = Laboratory Analyses (Horton 2002)
2. = Field Analyses (Horton and Hodges 2001)

5.2.2 Extent of Contamination – Geographic Distribution

This section summarizes the areal distribution of contaminants in groundwater at WMA T. The contaminants of concern for WMA T are nitrate, fluoride, chromium, carbon tetrachloride, trichloroethene, technetium-99, and tritium. Spatial variation in contaminant concentrations may provide some clues about source areas. Because concentrations change over time, a time-period must be chosen to examine spatial distribution patterns. For this purpose, the most recent data (average of fiscal year 2003 sampling events) were chosen. The data are tabulated in Table 5.6. Data were then plotted and

inspected for distribution patterns or groupings. Contour maps of contaminant concentrations were drawn to identify spatial patterns that might be indicative of source areas. The maps are shown in the series of Figures 5.14 through 5.20.

Table 5.6. Average Concentration of Mobile Contaminants in Groundwater in the Vicinity of Waste Management Areas T for Fiscal Year 2003[a]

Wells	NO_3 (µg/L)	F (µg/L)	Cr (µg/L)	CCl_4 (µg/L)	Trichloroethene (µg/L)	Tc-99 (pCi/L)	Tritium (pCi/L)
299-W10-1[b]	131,000	395	21	540	5	67	1,360
299-W10-4[c]	1,985,000	2,400	327	1,550	10	574	8,285
299-W10-8	170,500	3,700	45	NA	NA	66	6,412
299-W10-22[d]	168,000	700	60	810	6	150	11,200
299-W10-23[b]	312,750	4,150	81	1,500	10	189	12,050
299-W10-24	319,500	3,950	65	NA	NA	1,519	5,525
299-W10-28	1,835,000	1,375	133	NA	NA	176	4,232
299-W11-7[d]	164,000	840	11	1,400	8	404	19,650
299-W11-12	145,000	510	47	NA	NA	226	52,100
299-W11-39	89,000	1,650	70	NA	NA	9,208	2,918
299-W11-40[e]	281,000	2,780	66	NA	NA	513	17,040
299-W11-41	579,600	2,720	140	NA	NA	1,934	21,940
299-W11-42	716,000	3,900	132	NA	NA	1,314	8,230

(a) Average concentration of four, quarterly samples unless specified otherwise.
(b) One analysis for organics.
(c) Average of two analyses for organics.
(d) Average of two analyses for all constituents.
(e) Average of five analyses.
NA = Not analyzed.

Carbon tetrachloride is present in the unconfined aquifer beneath most of the 200 West Area (Figure 5.14). The highest carbon tetrachloride concentration near WMA T in fiscal year 2003 was 1,550 µg/L in well 299-W10-4, south of the waste management area. High concentrations were also found north (299-W10-23) and east (299-W11-7) of the waste management area. The carbon tetrachloride is believed to be from pre-1973 waste from the Plutonium Finishing Plant and not from the WMA T area.

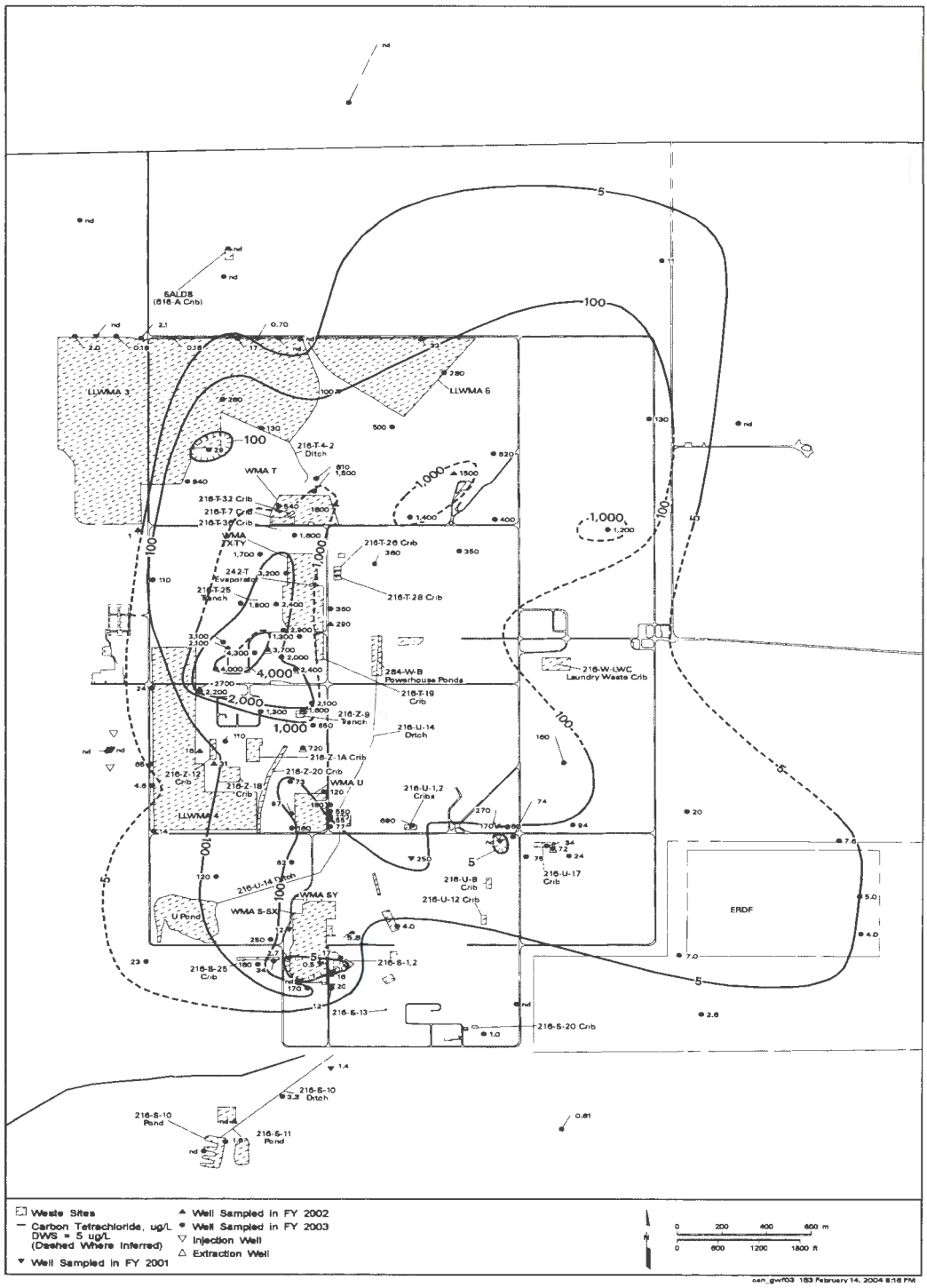

Figure 5.14. Average Concentrations of Carbon Tetrachloride in the 200 West Area, Top of the Unconfined Aquifer (from Hartman et al. 2003)

The major sources for trichloroethene are disposal sites associated with the Plutonium Finishing Plant. A second potential source is disposal near T Plant (Hartman et al. 2003). The maximum trichloroethene concentration found near WMA T in 2003 was 10 µg/L both north (well 299-W10-23) and south (well 299-W10-4) of the WMA. The waste management area is not considered a source for trichloroethene. Figure 5.15 shows the average concentrations of trichloroethene in the north part of the 200 West Area.

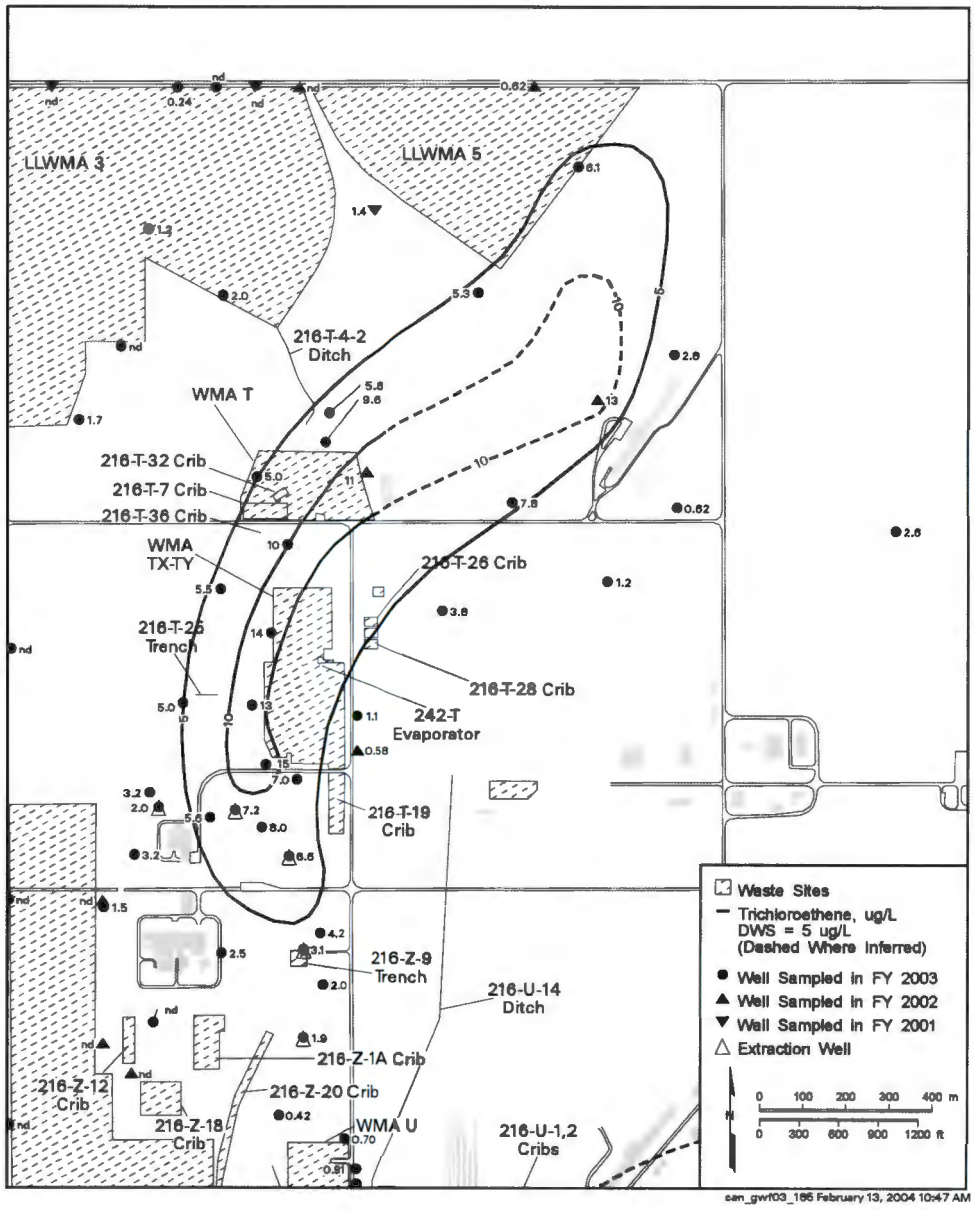

Figure 5.15. Average Concentrations of Trichloroethene in the North Part of the 200 West Area, Top of the Unconfined Aquifer (from Hartman et al. 2003)

A tritium plume lies beneath much of the north half of the 200 West Area (Figure 5.16). The plume geometry suggests that the major tritium source is near the 242-T evaporator, the TY tank farm, and nearby cribs (Hartman et al. 2003). Other contributing sources are likely present in the vicinity of the T tank farm and include associated cribs and trenches and, potentially, tank leaks.

The highest tritium concentration near WMA T in 2003 was 52,100 pCi/L in well 299-W11-12, located at the southeast corner of the waste management area. Waste Management Area T is not thought to be a major contributor of tritium to groundwater in the area.

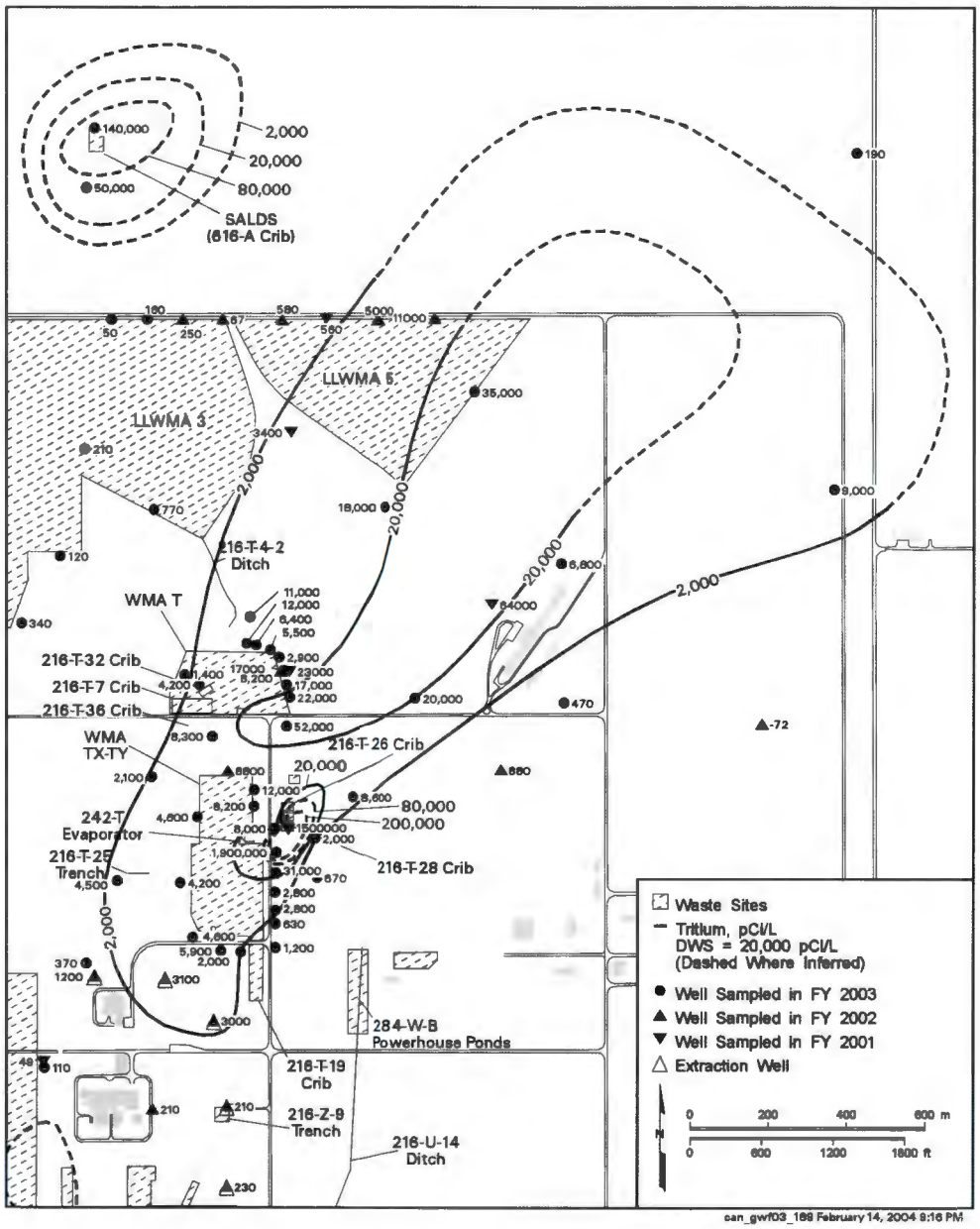

Figure 5.16. Average Concentrations of Tritium in the North Part of 200 West Area, Top of the Unconfined Aquifer (from Hartman et al. 2003)

A regional nitrate plume underlies WMA T and much of the north part of the 200 West Area (Figure 5.17). However, unlike carbon tetrachloride, trichloroethene, and tritium, there also appears to be a source of nitrate local and upgradient to Waste Management Area T. All monitoring wells in the WMA T monitoring network have nitrate concentrations in excess of the 45,000 µg/L maximum contaminant level. The highest nitrate concentrations at the Hanford Site in fiscal year 2003 were from two upgradient wells at WMA T: 1,985,000 µg/L in well 299-W10-4 and 1,835,000 µg/L in well 299-W10-28. The nitrate concentration began to increase in well 299-W10-4 in about 1997 when the groundwater flow direction changed from northerly to easterly (Figure 5.18). Concentrations continued to rise until just recently. Since it was drilled in 2001, the nitrate concentration in well 299-W10-28 has always been high and parallel to concentrations in well 299-W10-4. The most likely source for the nitrate in this area is one or more of the past-practice liquid disposal facilities up gradient of the T tank farm (Table 5.7).

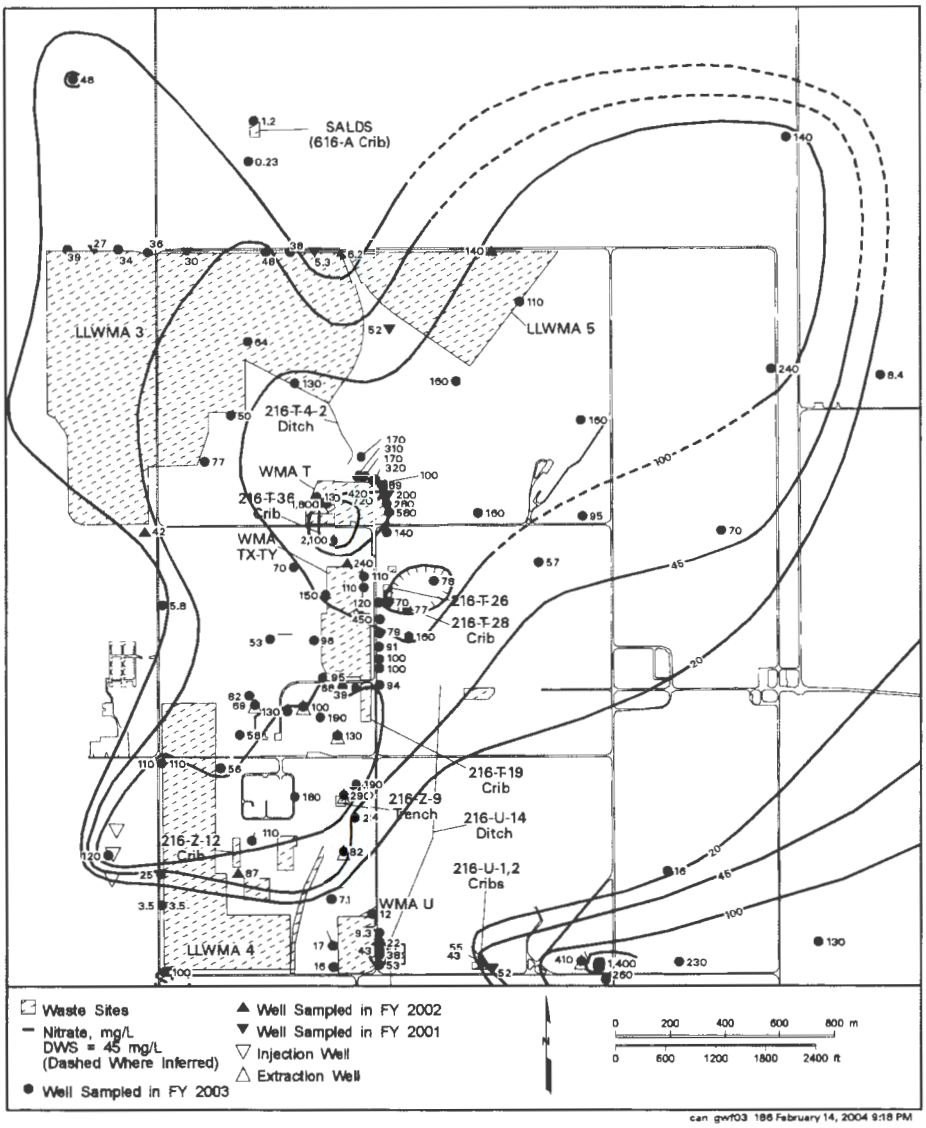

Figure 5.17. Average Concentrations of Nitrate in the North Part of 200 West Area, Top of the Unconfined Aquifer (from Hartman et al. 2003)

Table 5.7. Partial Inventories for Past-Practice Facilities Upgradient of WMA T

Facility	Date of Operation	Effluent Volume (L)[1]	Nitrate (Kg)[2]	Fluoride (Kg)[3]	Chromium (Kg)[3]
216-T-5 crib	1955	2,600,000	140,000	573	220
216-T-7 crib and tile field	1948 - 1955	110,000,000	2,300,000	19,900	3,920
216-T-32 crib	1946 - 1952	29,000,000	1,200,000	16,000	2,490
216-T-36	1966 - 1967	522,000 decontamination waste and condensate	Not Available	Not Available	Not Available

1. Data from Williams 2000.
2. Data from DOE/RL-91-61.
3. Data from Simpson et al. 2001.

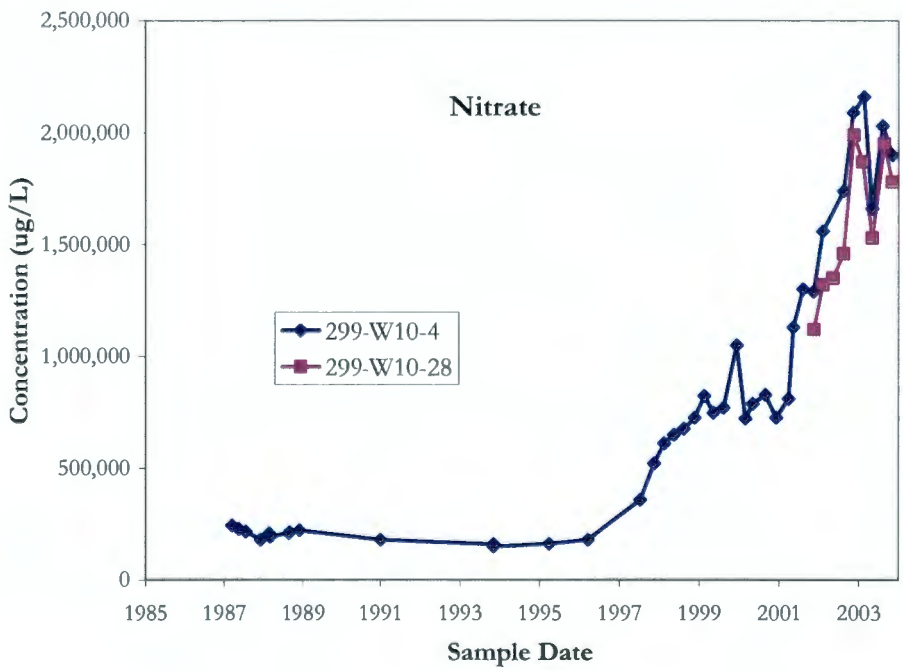

Figure 5.18. Nitrate Concentration versus Time in Upgradient Wells at WMA T

A plume map depicting the fiscal year 2003 average chromium concentration in wells near WMA T is shown in Figure 5.19. The highest chromium concentrations are in upgradient wells 299-W10-28 and 299-W10-4 where chromium reached 215 and 347 µg/L respectively in 2003. Figure 5.20 shows trend

plots for chromium in those wells. (Chromium was also elevated in well 299-W10-3, located inside the tank farm fence between the 216-T-7 crib and tile field and the 216-T-32 crib and upgradient of the tank farm. This well was sampled only in 2000 during its decommissioning when the chromium concentration was 257 μg/L.) Prior to about 1997 when groundwater flow direction was toward the north, several wells on the north (then downgradient) side of the waste management area had relatively high chromium concentrations. Also, prior to 1997, well 299-W10-1, which was parallel to the tank farm with respect to groundwater flow direction but downgradient of the 216-T-5 trench, the 216-T-7 crib and tile field, and the 216-T-32 crib, had chromium concentrations exceeding 200 μg/L. After the flow direction changed toward the east in about 1997, chromium concentrations dropped to <40 μg/L in well 299-W10-1, decreased in all of the northern wells (Figure 5.21), and began increasing in well 299-W10-4. The most likely source for the chromium west and north of Waste Management Area T is one or more of the disposal facilities upgradient of the WMA (Table 5.7). Chromium from these facilities would have been moving north across well 299-W10-1 prior to 1997 and then east across the northern wells and the rest of the waste management area after 1997.

Finally, since December 2000, chromium has exceeded the maximum contaminant level in two downgradient wells, 299-W11-41 (average for fiscal year 2003, 141 μg/L) and 299-W11-42 (average for fiscal year 2003, 132 μg/L). These wells are located downgradient of the disposal facilities east of WMA T but appear to be too far away for chromium to have migrated from west of the WMA to the wells since the 1996 change in groundwater flow direction, given a flow rate of 0.025 meter per day.

Fluoride concentrations exceeded the drinking water standard of 4,000 μg/L in three wells at Waste Management Area T in 2003 and exceeded the secondary drinking water standard of 2,000 μg/L in four additional wells. Currently, the highest concentrations are in downgradient wells (Figure 5.22) but historically, the highest fluoride concentration was in upgradient well 299-W10-4 in late 1999 (5,250 μg/L). A fluoride plume appears to have passed well 299-W10-4 between mid-1997 and late 2000. Although a tank farm source for the fluoride contamination has not been ruled out, one or more of the nearby cribs are believed to be a more likely source for two reasons. The first reason is the high concentrations of fluoride in upgradient wells located near potential fluoride sources (see Table 5.7). Second, the fluoride/technetium-99 ratios vary from well to well at WMA T and with time in some wells (see Figure 5.23 for example). If the technetium-99 has a source within the waste management area, as suggested below, the fluoride/technetium-99 ratios suggest a different source for the fluoride. The most likely source or sources are past practice facilities located upgradient of the waste management area.

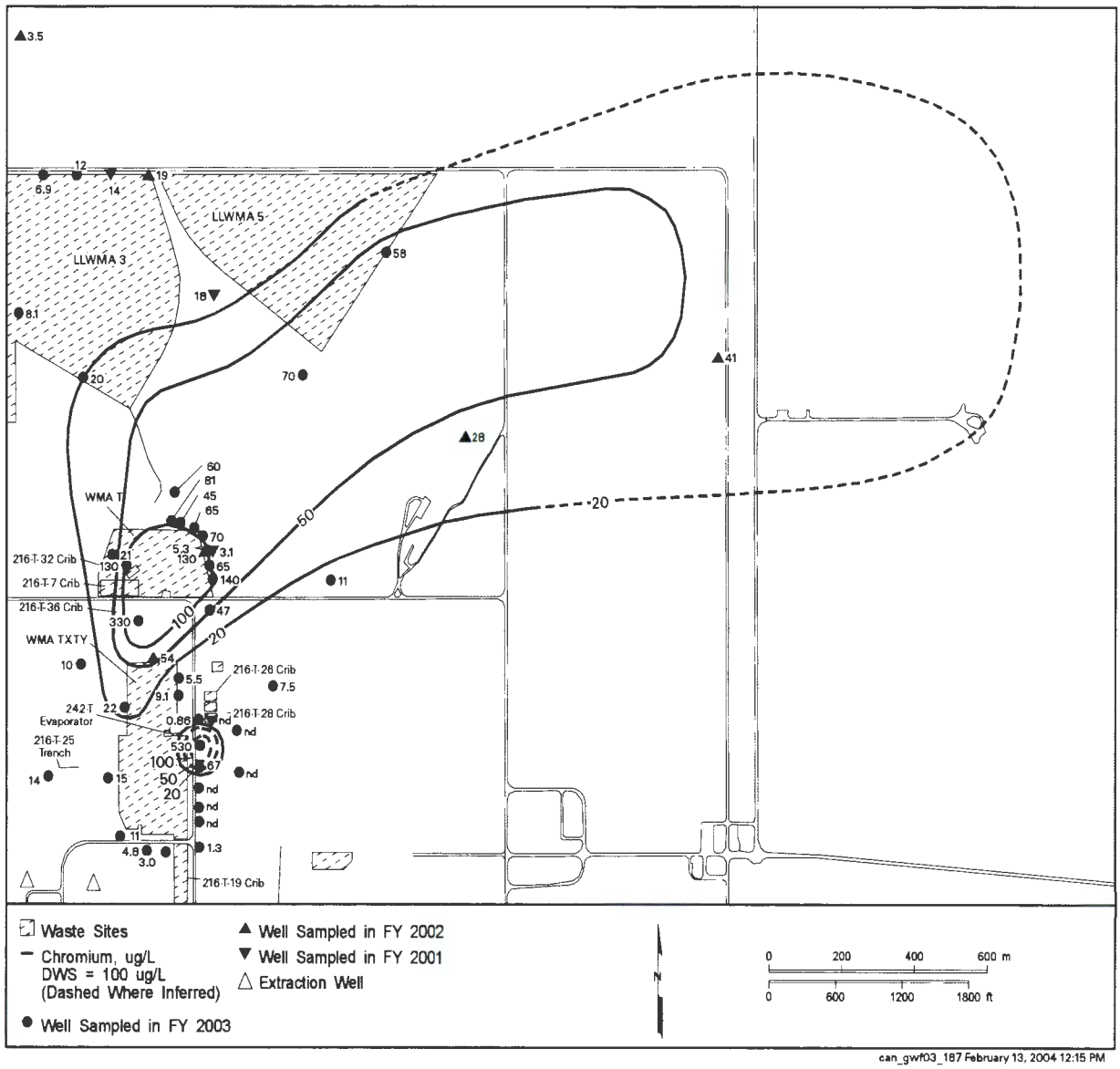

Figure 5.19. Average Concentrations of Chromium in the Area of Waste Management Area T, Top of the Unconfined Aquifer (from Hartman et al. 2003)

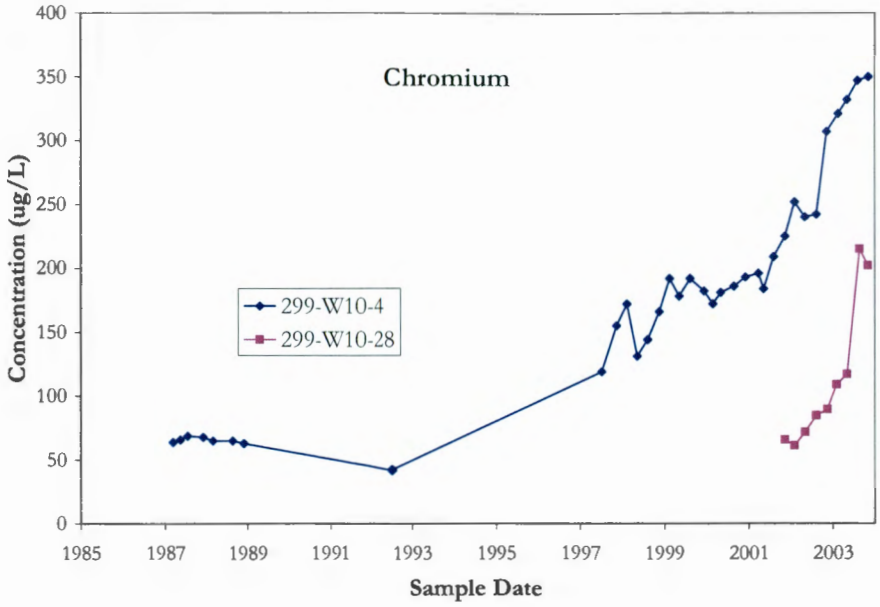

Figure 5.20. Chromium Concentration versus Time for Selected Upgradient Wells at Waste Management Area T

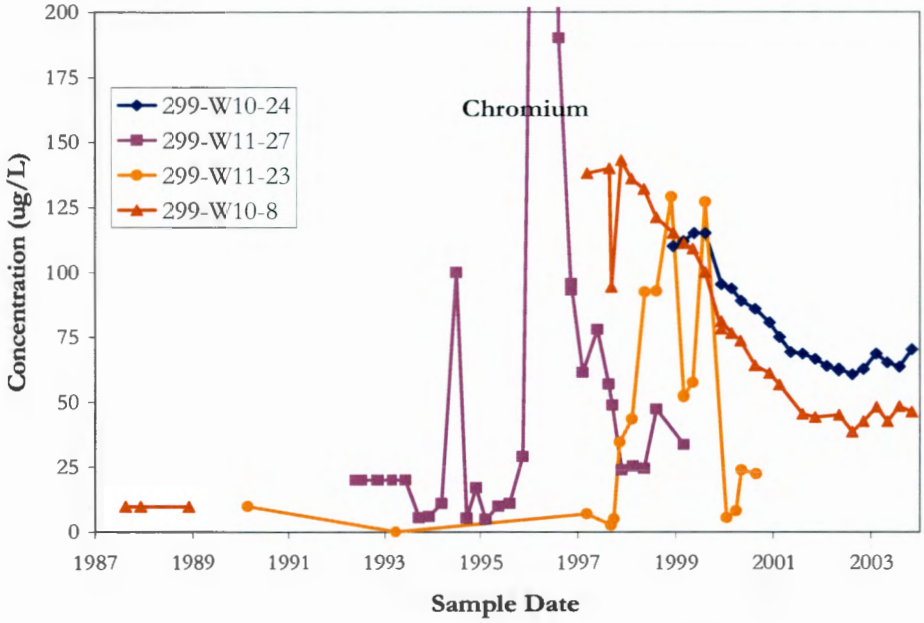

Figure 5.21. Chromium Concentration versus Time for Selected Wells North of Waste Management Area T

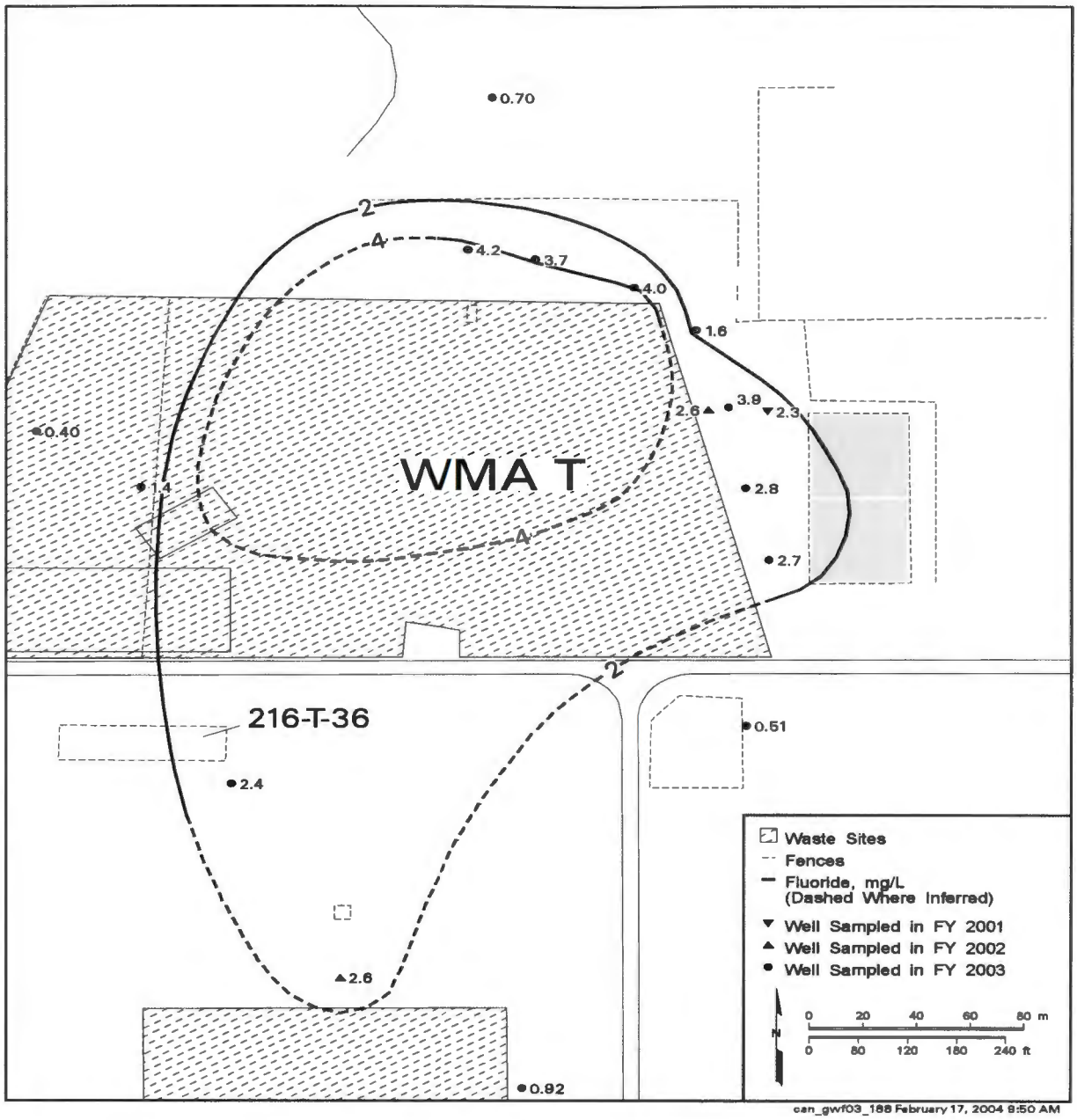

Figure 5.22. Average Concentrations of Fluoride in the Area of Waste Management Area T, Top of the Unconfined Aquifer (from Hartman et al. 2003)

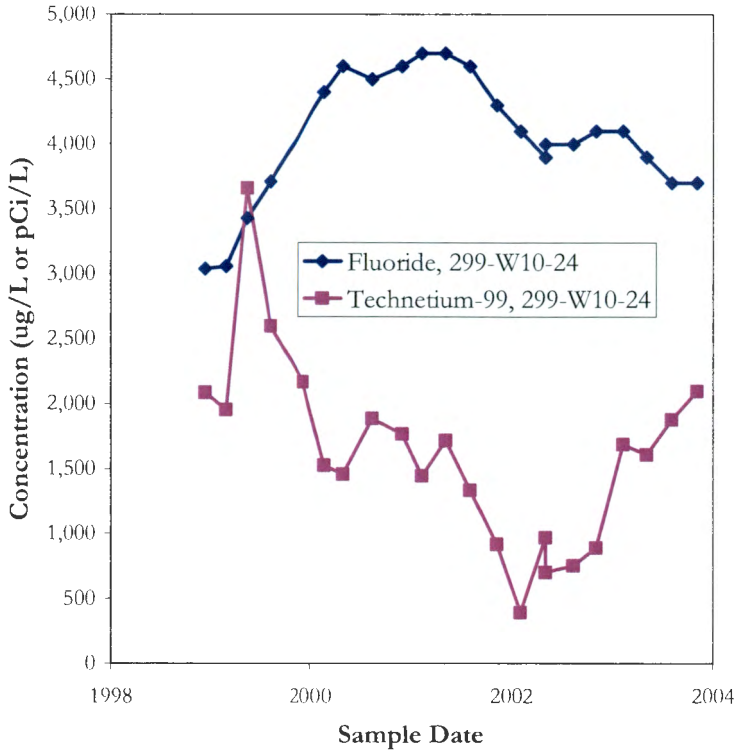

Figure 5.23. Technetium-99 and Fluoride Concentrations in Downgradient Well 299-W-10-24

A technetium-99 groundwater plume exists northeast and east of Waste Management Area T (Figure 5.24). The highest technetium-99 concentration in fiscal year 2003 was 9,200 pCi/L in downgradient well 299-W11-39. The most probable source for the technetium-99 is the waste management area.

Technetium-99 began to increase in well 299-W11-27, located at the northeast corner of 241-T tank farm, in late 1995, coincident with the cessation of surface water disposal in the 200 West Area. Concentrations reached a maximum of 21,700 pCi/L in February 1997 (see Figure 5.9). Technetium-99 concentrations in well 299-W11-27 subsequently decreased to 6,000 pCi/L in March 1999. Hodges (1998) suggested that technetium-99 had arrived at well 299-W11-27 by the early 1990s, but was masked by dilution with water from a leaking water line located immediately adjacent to the well. The water line carried cooling and ventilation steam condensate, process cooling water, and evaporator condensate from the 207-T retention basin to the 216-T-4-2 ditch (DOE/RL-91-61) until 1995. The subsequent decrease in technetium-99 in well 299-W11-27 since 1997 may have been a result of changing groundwater flow direction.

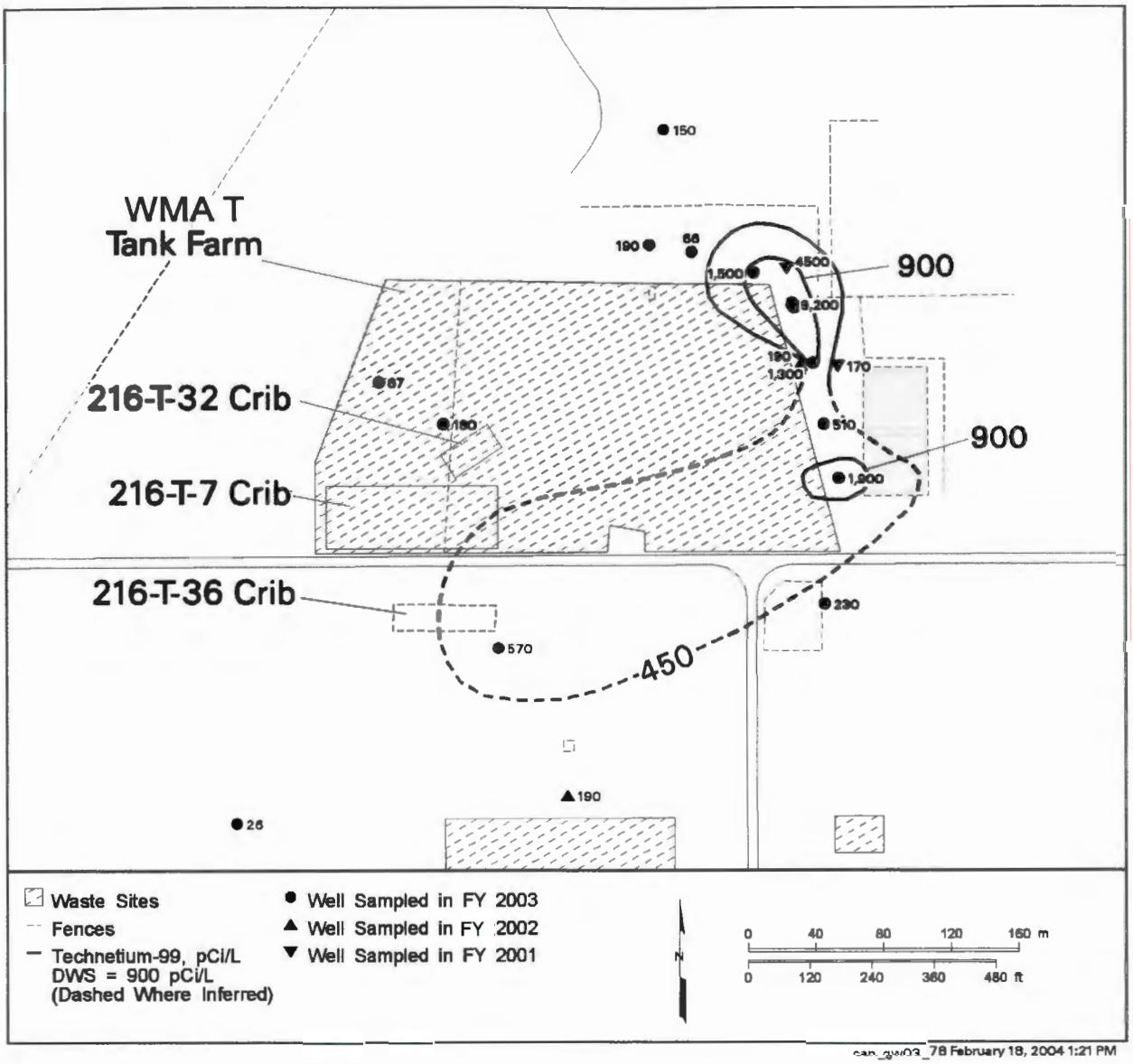

Figure 5.24. Average Concentrations of Technetium-99 in the Area of Waste Management Area T, Top of the Unconfined Aquifer (from Hartman et al. 2003)

Technetium-99 began to increase in well 299-W11-23, located east of well 299-W11-27, in November 1997 coincident with the change in groundwater flow to a more easterly direction. It increased to a high of 8,540 pCi/L in November 1998 (see Figure 5.9). Subsequently, technetium-99 values have fluctuated between 7,110 and 840 pCi/L. The last sample from this well, taken in December 2000, indicated a technetium-99 concentration of 4,470 pCi/L. The most plausible explanation for the 1997 arrival of the contaminant plume at well 299-W11-23 is the change in groundwater flow direction. If this is the case, a narrow contaminant plume initially moved northeast across well 299-W11-27 but not across well 299-W11-23. Changing groundwater flow direction caused this plume to drift east across well 299-W11-23. Sampling of replacement well 299-W11-39 in 2001 detected technetium-99 concentrations

between 4,160 and 5,010 pCi/L, indicating contamination of the upper portion of the aquifer at this well. Subsequently, the technetium-99 concentration rose to a high of 10,400 pCi/L in February 2003 and began a small decline in August 2003.

In early 2002, technetium-99 concentrations began to increase in well 299-W11-42, south of well 299-W11-39 and, in early 2003, technetium-99 began to increase in well 299-11-41, south of 299-W11-42. Apparently, the technetium-99 contamination that was detected in the northeast corner of 241-T tank farm is spreading southward along the east and downgradient side of the WMA. As shown in Section 5.2.1.3 ("Sampling During Drilling"), the highest recent technetium-99 concentrations are at or near the water table and concentrations decrease rapidly with increasing depth in the aquifer. This points to a nearby source for the technetium-99 because the contaminant has not traveled far enough to disperse vertically in the aquifer. The apparent nearness of the technetium-99 source suggests that WMA T is the most likely origin for the technetium-99.

Also, Hodges (1998) explains that even though most tank waste is a multi-molar sodium nitrate brine, calcium is the first cation to increase in concentration when tank waste enters groundwater. This is because 1) tank leaks and tank pipeline leaks are relatively small in volume (relative to the releases sent to cribs and tile fields) and 2) the sodium in the leaked fluids replaces the exchangeable calcium and magnesium in the vadose zone sediment. This results in a high calcium porewater that is pushed ahead of the sodium to the groundwater (see discussions in Serne et al. 2002b, 2002c, 2002d, 2002e and 2004). Figures 4.18 and 4.46 in this report show this phenomenon in the vadose zone sediments and Figure 5.25 illustrates it in the groundwater at the T tank farm.

Figure 5.25 is a series of modified Stiff diagrams for groundwater samples from well 299-W11-27 in which technetium-99 was found in early 1996. (Nitrate has been added to the traditional Stiff diagram because nitrate is a major component in the groundwater beneath the 200 West Area.) The diagrams show that calcium, and not sodium, increases in the groundwater at the time technetium-99 is detected. Also, nitrate begins to increase at the same time as the increase in calcium. This argues for a relatively small, nearby source for the technetium-99 contamination in the area because a large volume source would have saturated the exchange sites in the vadose zone, and breakthrough of sodium to groundwater would have been detected.

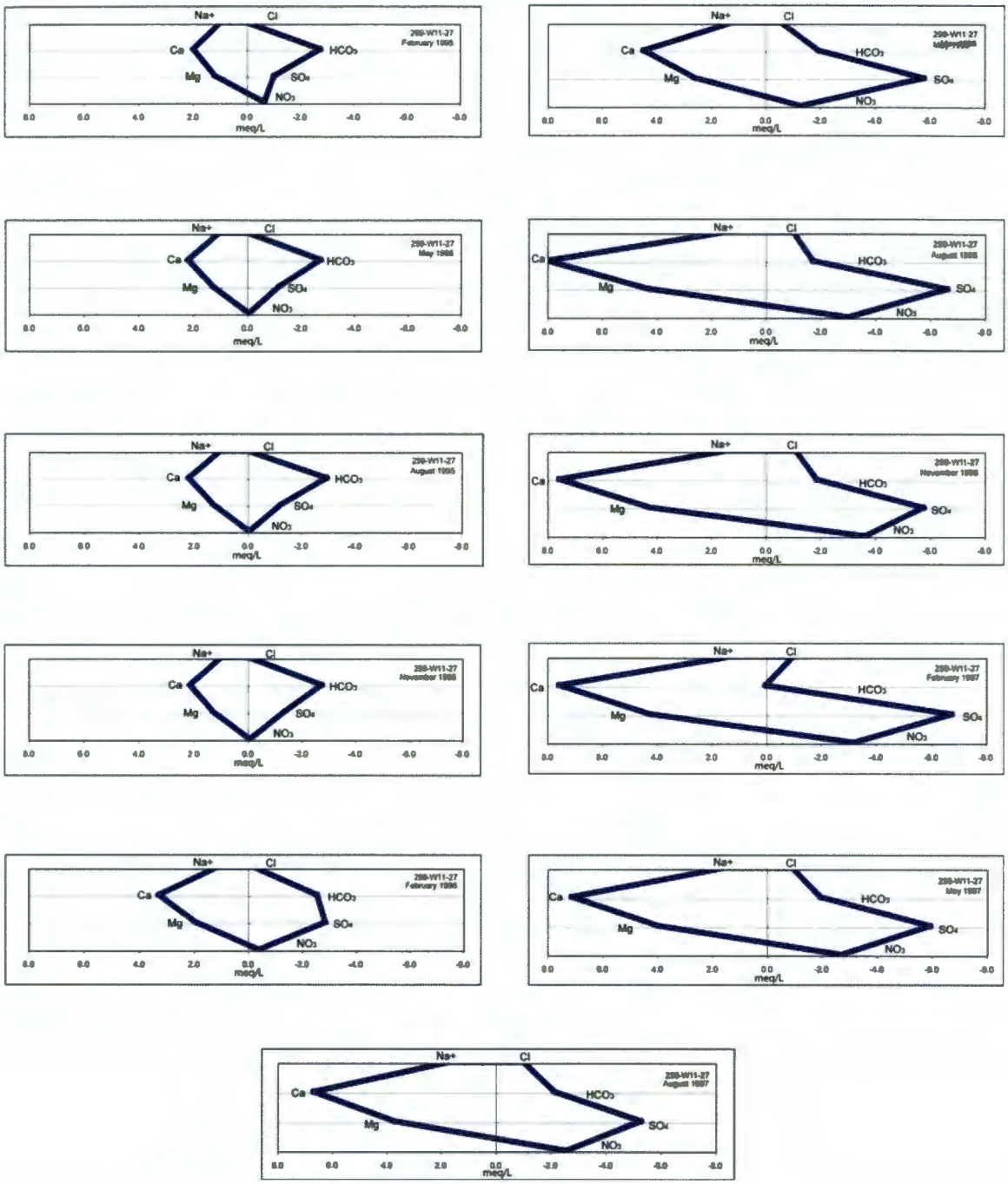

Figure 5.25. Time Series Stiff Diagrams Showing Breakthrough of Calcium and Nitrate to Groundwater at Well 299-W11-27

5.3 Comparison of Groundwater, Vadose Zone Porewater, and Tank Leak Compositions

The previous section discussed the geographic distribution of contaminants and related the distribution to potential contaminant sources. This section compares the chemical composition of groundwater with the composition of the vadose zone porewater and with the composition of tank leaks and discharges to nearby cribs in an attempt to more accurately pinpoint specific sources for the contamination in the groundwater at WMA T.

The earliest evidence of groundwater contamination around WMA T as found in the HEIS[(a)] database is high levels of gross beta in wells located at the cribs and trenches west of WMA T. By 1955 and 1956 levels of gross beta had reached values in excess of 1,000,000 pCi/L in well 299-W10-2, located about 20 meters south of the 216-T-7 tile field (Figure 5.26). The gross beta contamination was accompanied by nitrate levels in excess of 3,000,000 μg/L in the general area and up to 6,900,000 μg/L in well 299-W10-2. It is possible that gross beta and nitrate groundwater contamination pre-dates 1955, but there are no available analyses.

The oldest available analysis for cobalt-60 in groundwater in the area is from well 299-W10-4 in 1957; it showed that the cobalt-60 concentration was 2000 pCi/L at that time. Cobalt-60 was later found in well 299-W10-2 in 1969 at a concentration of 680 pCi/L. Finally, ruthenium-106 was first noted in groundwater in 1972 at wells 299-W10-2 and 299-W10-4 at concentrations of 140 pCi/L and 400 pCi/L, respectively.

Two things should be remembered about these early analyses. First, they are the oldest available analyses and do not represent the first arrival of contamination in groundwater in the area. Second, the concentrations should be considered approximate since detection limits and analytical accuracies have improved through the years.

This early groundwater contamination pre-dates any reported tank leak from the 241-T tank farm. The most likely source for this contamination is either the 216-T-7 crib and tile field, which operated between 1947 and 1955 and received 110,000,000 L of effluent, or the 216-T-32 crib, which operated between 1946 and 1952 and received 29,000,000 L of waste. Groundwater at that time was flowing toward the south from the disposal facilities toward the contaminated wells (Figure 5.4).

Groundwater contamination was first noted north of WMA T in well 299-W10-8 in October 1973, when ruthenium-106 was found at a concentration of 430 pCi/L and quickly increased to 1,100 pCi/L in March 1974. Cobalt-60 was first noted in the well in early 1974 at 20 pCi/L. Groundwater had shifted flow direction from southerly to northeasterly in about 1957. This direction places well 299-W10-8 downgradient of the 216-T-7 tile field and 216-T-32 crib. Well 299-W10-8 is about 150 meters northeast of 216-T-32 crib and 180 meters northeast of the 216-T-7 tile field. Given a typical groundwater flow

---

(a) HEIS is the Hanford Environmental Information System. A URL is located at http://www.hanford.gov/docs/rl-93-69/rl-93-69.pdf. *This link is to DOE/RL-93-69, Revision 4, Tri-Party Agreement Databases, Access Mechanism and Procedures*. It may be accessed by anyone.

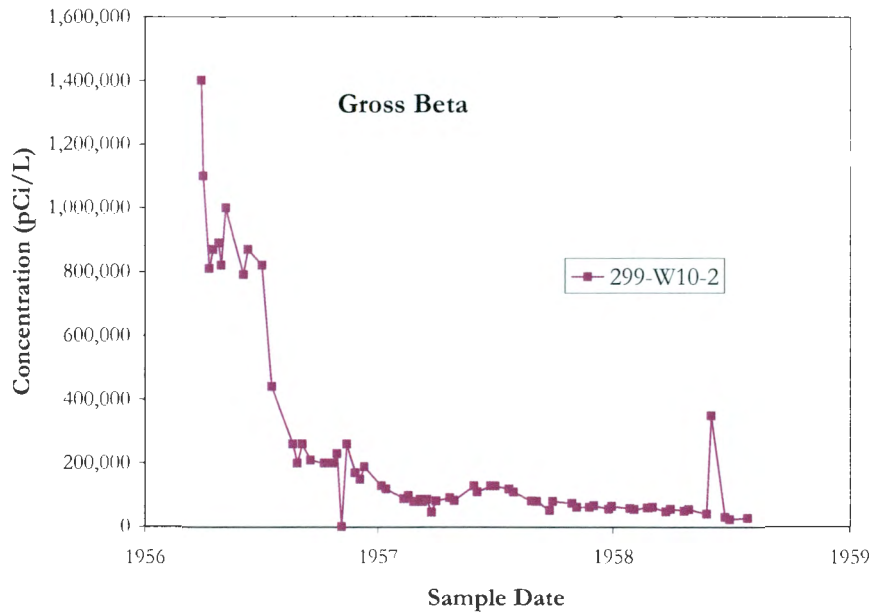

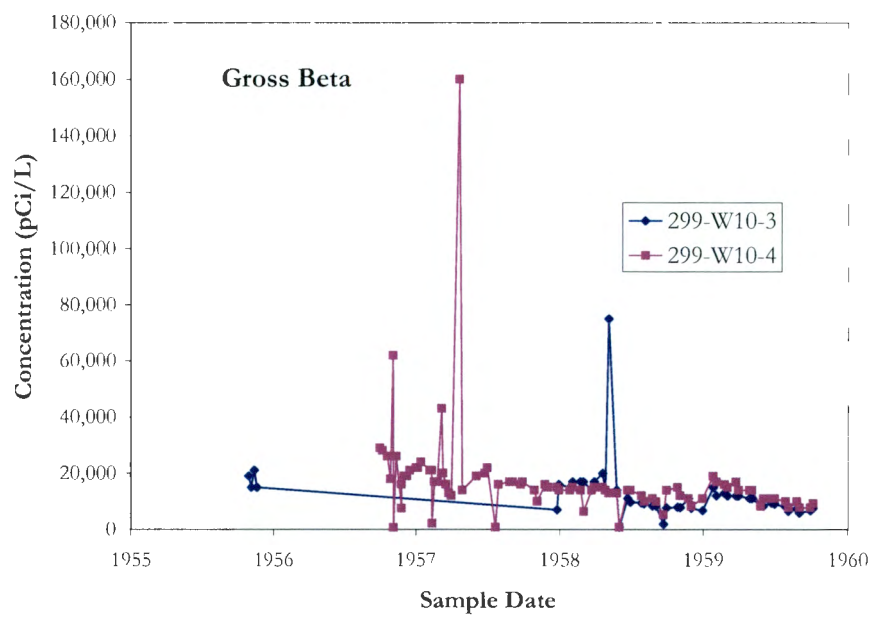

Figure 5.26. Gross Beta Contamination in Wells West and Southwest of WMA T

rate of 0.02 meter per day, contamination could have traveled about 130 meters from the disposal facilities between January 1956 and October 1973. It is possible that the groundwater flow rate was greater than 0.02 m/d in the 1960s driven by the groundwater mound under U pond. A groundwater velocity of 0.03 m/d would allow for transport of contaminants from the 216-T-7 tile field well beyond well 299-W10-8 by late 1973 (assuming no contaminant retardation). Clearly, however, a groundwater flow rate of 0.03 m/d is not sufficient to drive contaminants from the vicinity of tank T-106 to well 299-

W10-8, a distance of about 105 meters, in the 4 month time period between the reported tank leak in June 1973 and the first detection of ruthenium-106 at the well.

To determine whether tank leak T-106 has impacted groundwater quality, one or more components of the leak need to be detected in groundwater. Estimates of the leak composition are available (Jones et al. 2000) but, unfortunately, the major, mobile components in the tank leak for which we have groundwater data, are also major, mobile components disposed in the nearby cribs and trenches.

Hodges (1998) used tritium/technetium-99 and nitrate/technetium-99 ratios from analyses of wells at WMA T to distinguish waste disposed of to cribs, trenches and tile fields in the area from evaporator condensate wastes and waste discharged from the Plutonium Finishing Plant. This section attempts to use the same ratios, and others, to distinguish tank leaks from wastes disposed to cribs and trenches west of WMA T.

Table 5.8 gives the estimated concentration of selected components found in two tank leaks at WMA T and in effluent disposed to three disposal facilities located west of WMA T. The constituents listed in Table 5.8 were dictated by the available analytes from groundwater analyses that also might be in tank and crib wastes. The data in Table 5.8 show that there are significant differences (2 or more orders of magnitude) in the concentrations of chromium, fluoride, tritium, cobalt-60, technetium-99, and ruthenium-106 between tank leaks and the waste streams of interest. Using these components plus nitrate, eight ratios (pairs of constituents) were examined: technetium-99/fluoride, technetium-99/nitrate, technetium-99/chromium, technetium-99/tritium, technetium-99/cobalt-60, cobalt-60/ruthenium-106, ruthenium-106/technetium-99, and chromium/cobalt-60.

Analyses for cobalt-60 and ruthenium-106 were common in the 1950s through 1970s but much less so in the 1980s and 1990s, mostly because these two radionuclides have short half-lives and decayed quickly. Analyses for metals (chromium), anions (fluoride), and technetium-99 are rare or non existent in the 1950s through 1970s but become more common in the 1980s and are abundant in the 1990s. Therefore, insufficient data were available for the analyte pairs of ruthenium-106 and cobalt-60 with technetium-99 or chromium. Some potentially useful information could be obtained from all other analyte pairs.

5.3.1 Technetium-99 – Chromium

The relative groundwater concentrations for technetium-99 and chromium behave quite differently at different wells within WMA T (Figure 5.27). The concentrations of both constituents track each (both increase with time since 1997) other through time in upgradient wells at the WMA (Figure 5.27 A). The same relationship holds for wells north of the WMA; however, the concentrations are dropping with time (Figure 5.27 B). The technetium-99 – chromium concentration relationship is different in wells located at the northeast corner (Figure 5.27 C) and east of the WMA (Figure 5.27 D) where the concentration of the two constituents do not track each other.

Table 5.8. Estimated Compositions for Tank Leaks and Waste Streams Associated with WMA T

Component	T-101[a]	T-106[a]	216-T-5 Trench[b]	216-T-7 Crib and Tile Field[b]	216-T-32 Crib[b]
Sodium (μg/L)	6.99E+07	9.98E+07	2.92E+07	1.19E+07	7.37E+06
Chromium (μg/L)	6.29E+05	2.22E+06	8.46E+04	3.56E+04	2.26E+04
Calcium (μg/L)	3.16E+05	3.67E+05	3.88E+05	6.71E+04	9.18E+03
Nitrate (μg/L)	5.74E+07	7.75E+07	4.27E+07	1.95E+07	1.30E+07
Sulfate (μg/L)	1.36E+06	8.54E+06	2.59E+06	5.11E+05	1.23E+05
Fluoride (μg/L)	6.71E+02	1.03E+05	2.20E+06	1.81E+06	1.45E+06
Chloride (μg/)	8.51E+05	2.54E+06	6.04E+05	3.08E+05	2.15E+05
Tritium (pCi/L)	2.36E+07	1.08E+08	1.14E+06	3.33E+05	6.03E+05
Cobalt-60 (pCi/L)	1.14E+06	2.25E+07	3.60E+03	7.45E+02	6.00E+02
Technetium-99 (pCi/L)	1.01E+07	1.38E+08	9.19E+04	1.85E+04	1.30E+04
Ruthenium-106 (pCi/L)	2.61E+02	3.78E+03	1.81E-03	4.15E-04	4.48E-04
Volume (L)	3.8E+4	4.35E+5	2.60E+06	1.10E+08	2.90E+07

(a) Data from Jones et al. 2000 converted to μg/L or pCi/L. Radionuclides decayed to 1/1/1994.

(b) Data from Simpson et al. 2001 converted or μg/L or pCi/L. Radionuclides decayed to 1/1/1994.

Figure 5.28 shows the technetium-99/chromium groundwater concentration ratios versus time for samples from selected wells at WMA T. The figure also shows the concentration ratios expected in the leaked tank waste from tanks T-101 and T-106 (Jones et al. 2000) and waste disposed to the cribs and trenches located west of WMA T (Simpson et al. 2000). The data plotted in Figure 5.28A show that the technetium-99/chromium ratio in samples from upgradient wells have a signature similar to the upgradient crib and trench disposal sites. Figure 5.28B shows that samples from wells north of WMA T have a similar composition as those from upgradient wells. This information, and the information in Figures 5.28A and B, suggest that the contamination detected in wells north of WMA T is very similar to that found upgradient of the WMA and is dominated by crib waste.

Figure 5.28C suggests a different source for the contamination at the northeast corner of WMA T. A technetium-99, chromium, nitrate, and tritium plume was first detected in this area in well 299-W11-27 in early 1996. Since that time, the technetium-99/chromium composition of the groundwater in that well has evolved toward tank waste compositions. Three other wells in the area support this hypothesis. The technetium-99/chromium compositions greater than the estimated tank waste compositions are in agreement with the data from vadose zone porewaters from boreholes C4104 and C4105 (Section 4 of this report) and probably reflect the slight retardation of chromium relative to technetium-99 as discussed in Section 6.6 (see Table 6.5 for in situ desorption K_d values).

Since monitoring began in 1997, the technetium-99 to Cr ratio for groundwater from wells east of WMA T are intermediate between those from wells upgradient (west and north of the WMA) and those northeast of the WMA. Samples from these wells indicate that the tank waste initially identified at the northeast corner of the WMA is migrating south along the eastern edge of the WMA and is mixing with the crib waste that was initially sampled in the eastern wells.

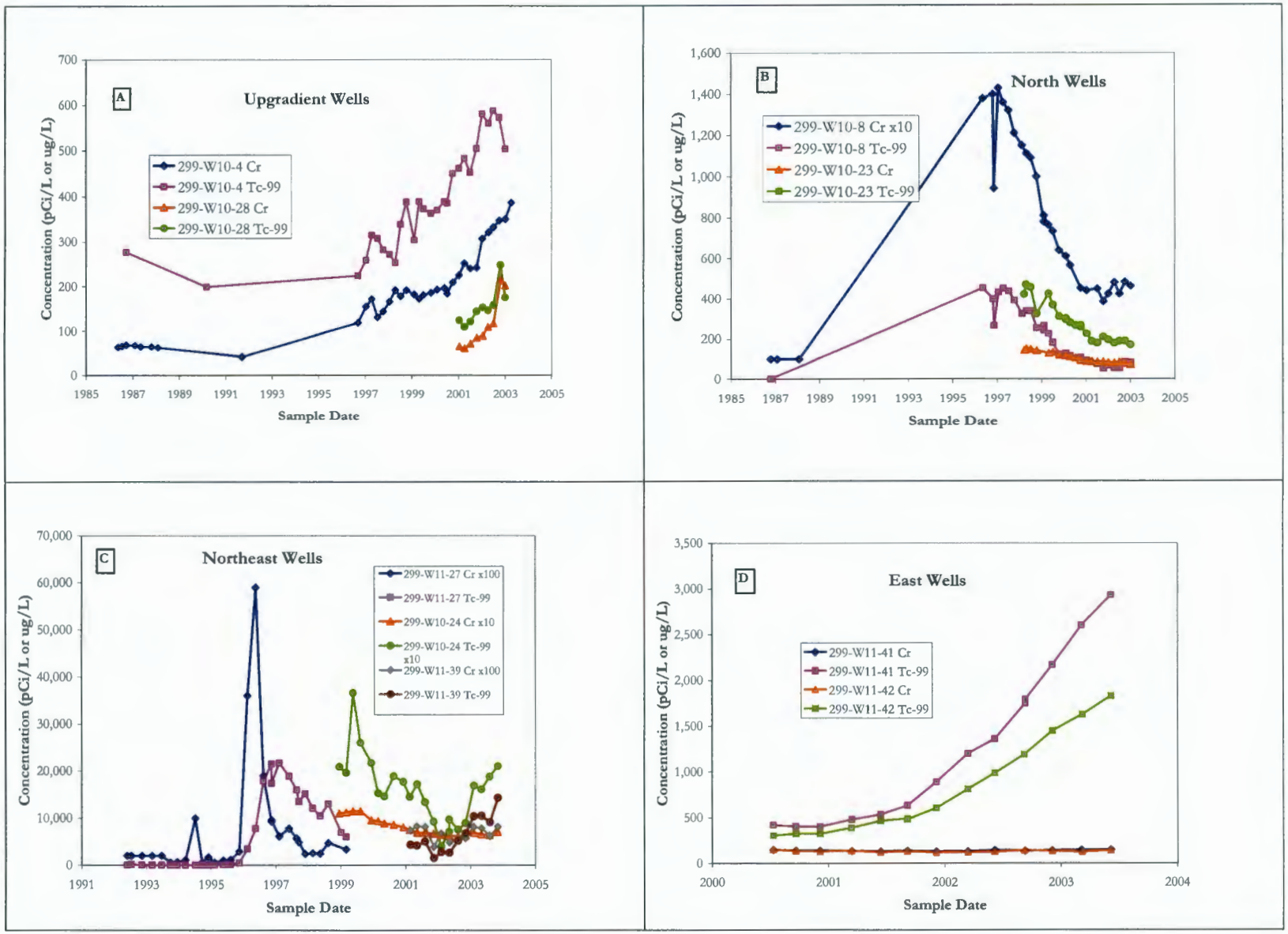

Figure 5.27. Technetium-99 and Chromium Concentrations in Selected Wells at WMA T

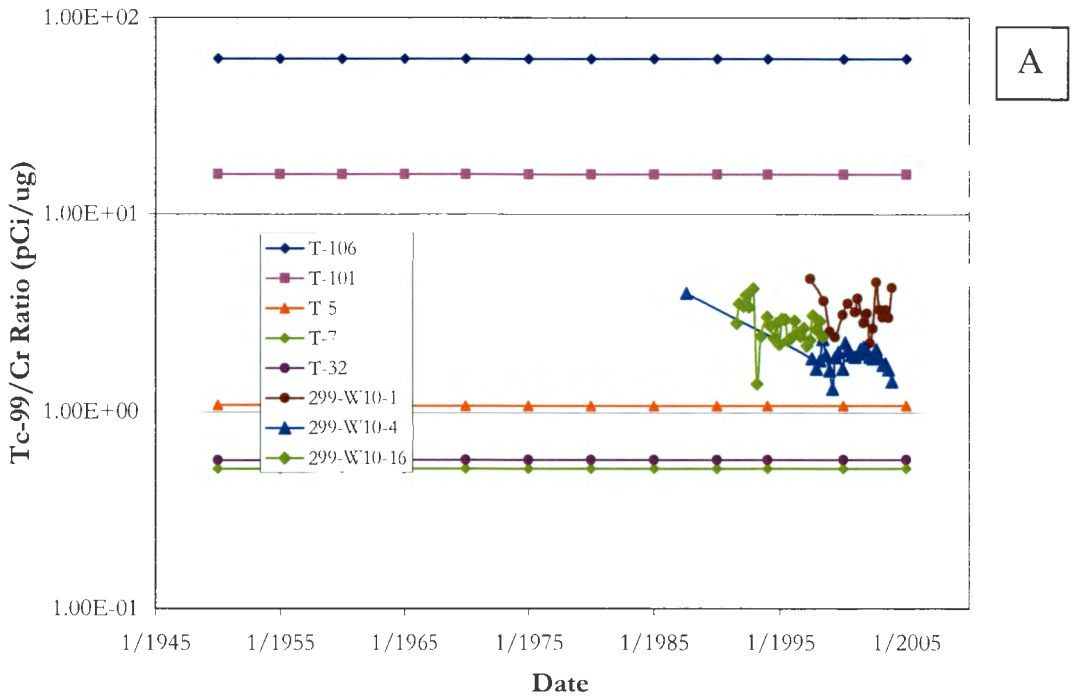

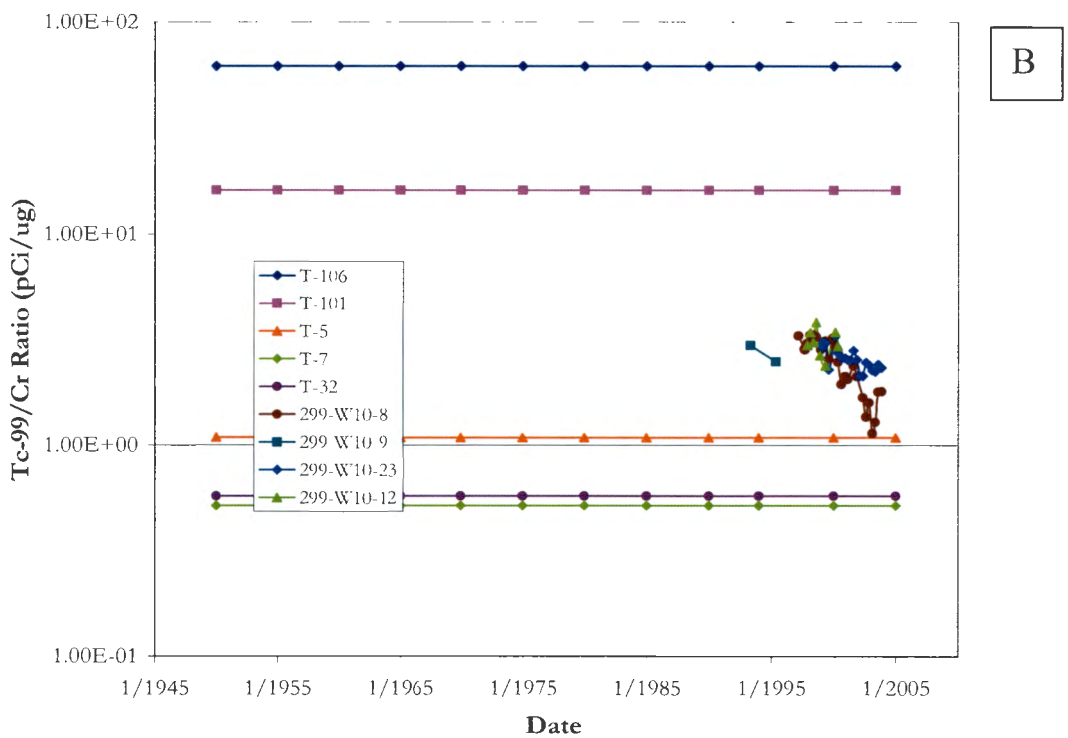

Figure 5.28. Technetium-99/Chromium Concentration Ratios in Samples from Selected Wells at WMA T. A=Upgradient (West) Wells; B=Northern Wells.

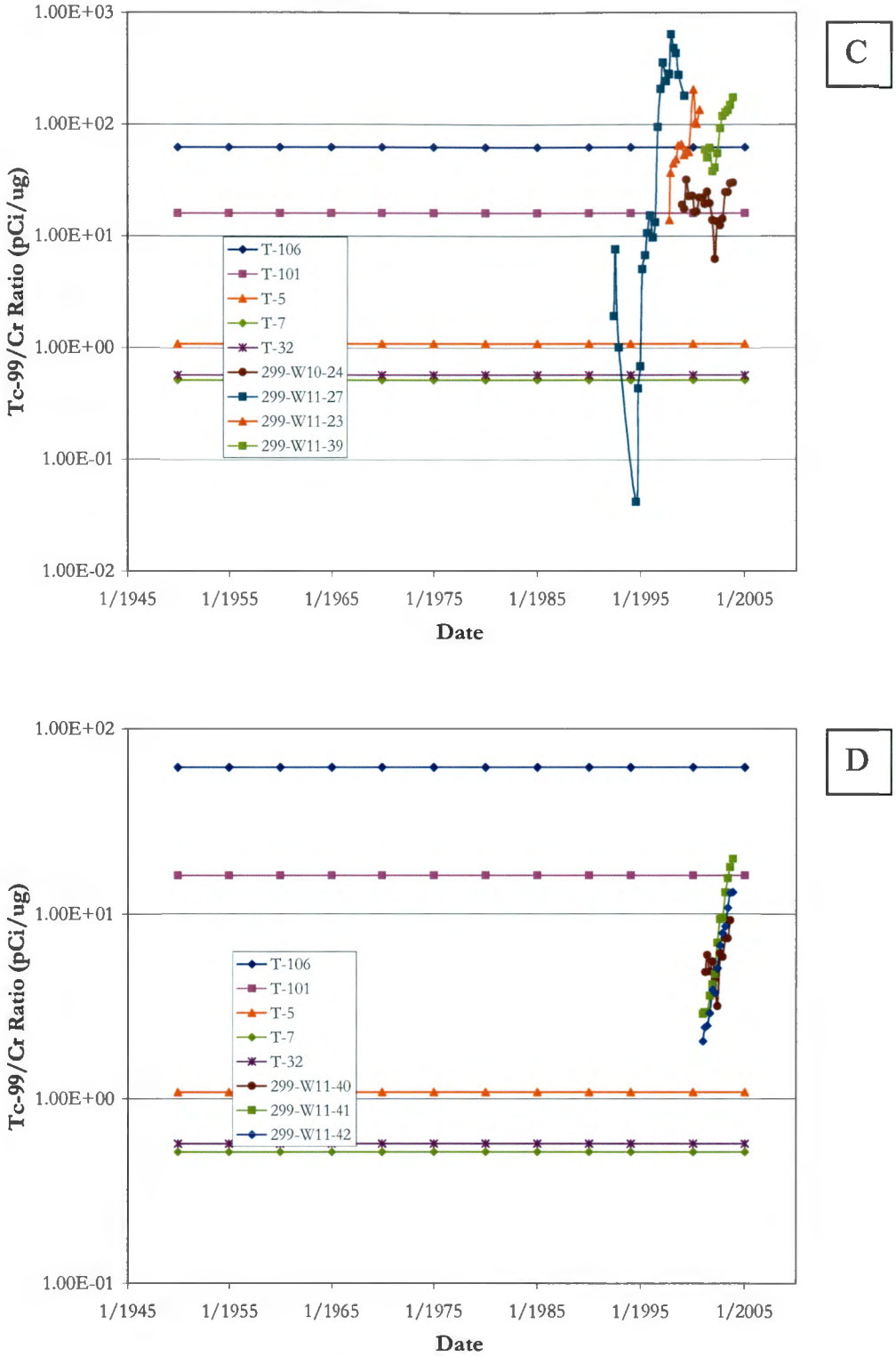

Figure 5.28. Technetium-99/Chromium Concentration Ratios in Samples from Selected Wells at WMA T. C = Northeastern wells, D = Eastern wells

5.3.2 Technetium-99 – Nitrate

The compositional relationship between technetium-99 and nitrate at WMA T is complicated by the regional nitrate plume in the area. Unlike technetium-99 and chromium concentrations, the concentrations of technetium-99 and nitrate track each other through time in all monitoring wells at WMA T although there are about 3 orders of magnitude difference in the technetium-99/nitrate groundwater concentration ratios across the WMA (Figure 5.29). However, when plotted against time and compared to crib and tank waste compositions, the technetium-99/nitrate concentration ratios suggest the same conclusions reached with the technetium-99/chromium ratios (Figure 5.30).

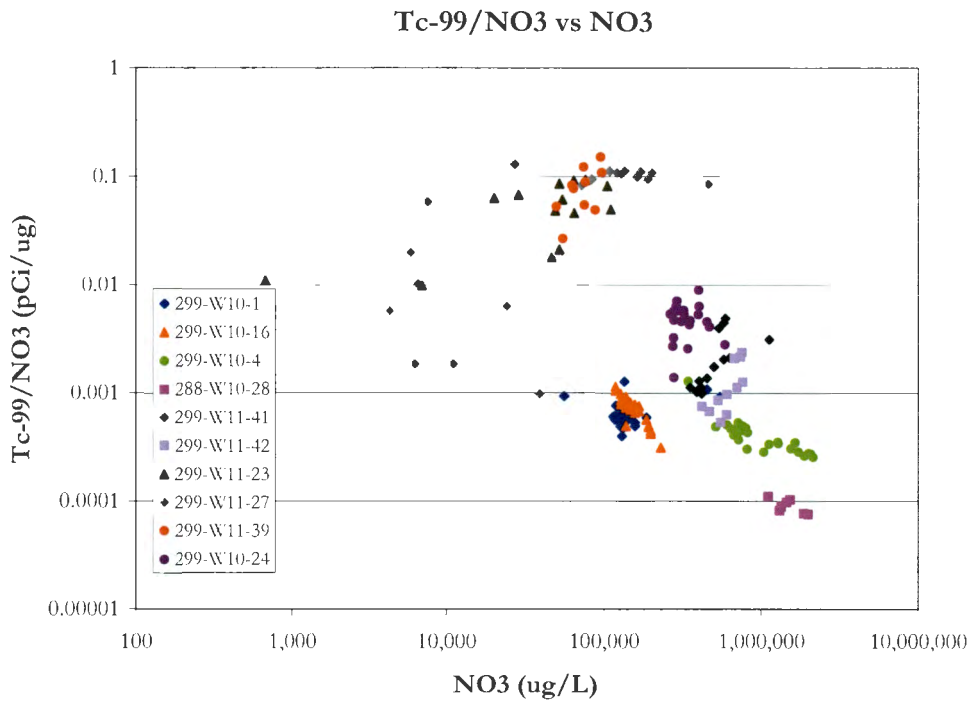

Figure 5.29. Technetium-99 and Nitrate Concentrations in Samples from Selected Wells at WMA T

Figure 5.30A shows the technetium-99/nitrate concentration ratios in samples from upgradient wells at WMA T and compares the ratios to those expected for tank and crib wastes. The figure shows that the groundwater from the upgradient wells has a strong crib waste component. Figure 5.30B shows the same relationship as in Figure 5.30A for the monitoring wells located on the north side of the WMA. Groundwater sampled from the northern wells is essentially indistinguishable, with respect to technetium-99/nitrate composition ratios, from groundwater in the upgradient wells.

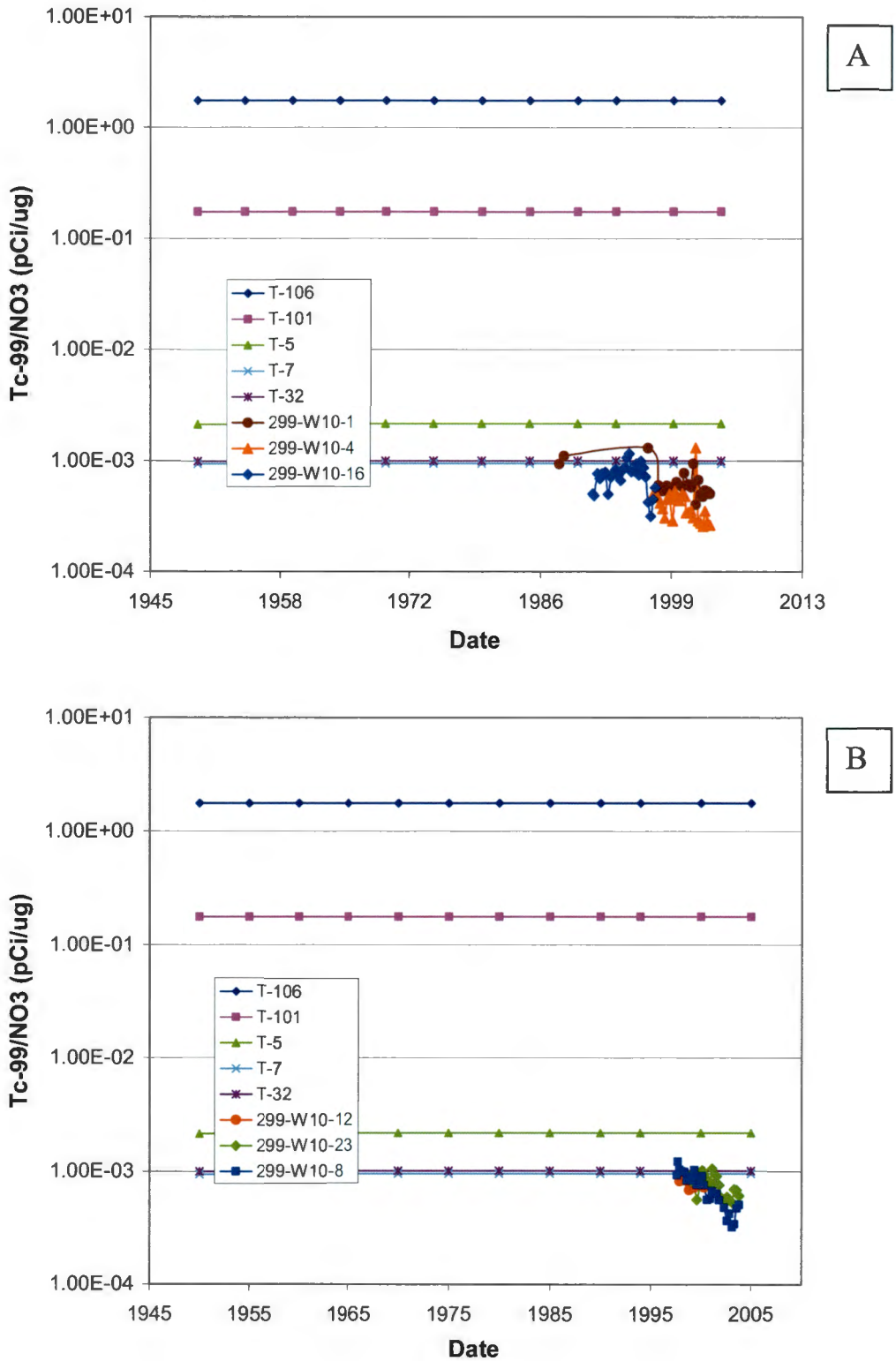

Figure 5.30. Technetium-99/Nitrate Concentration Ratios in Samples from Selected Wells at WMA T. A = Upgradient (west) wells, B = Northern wells.

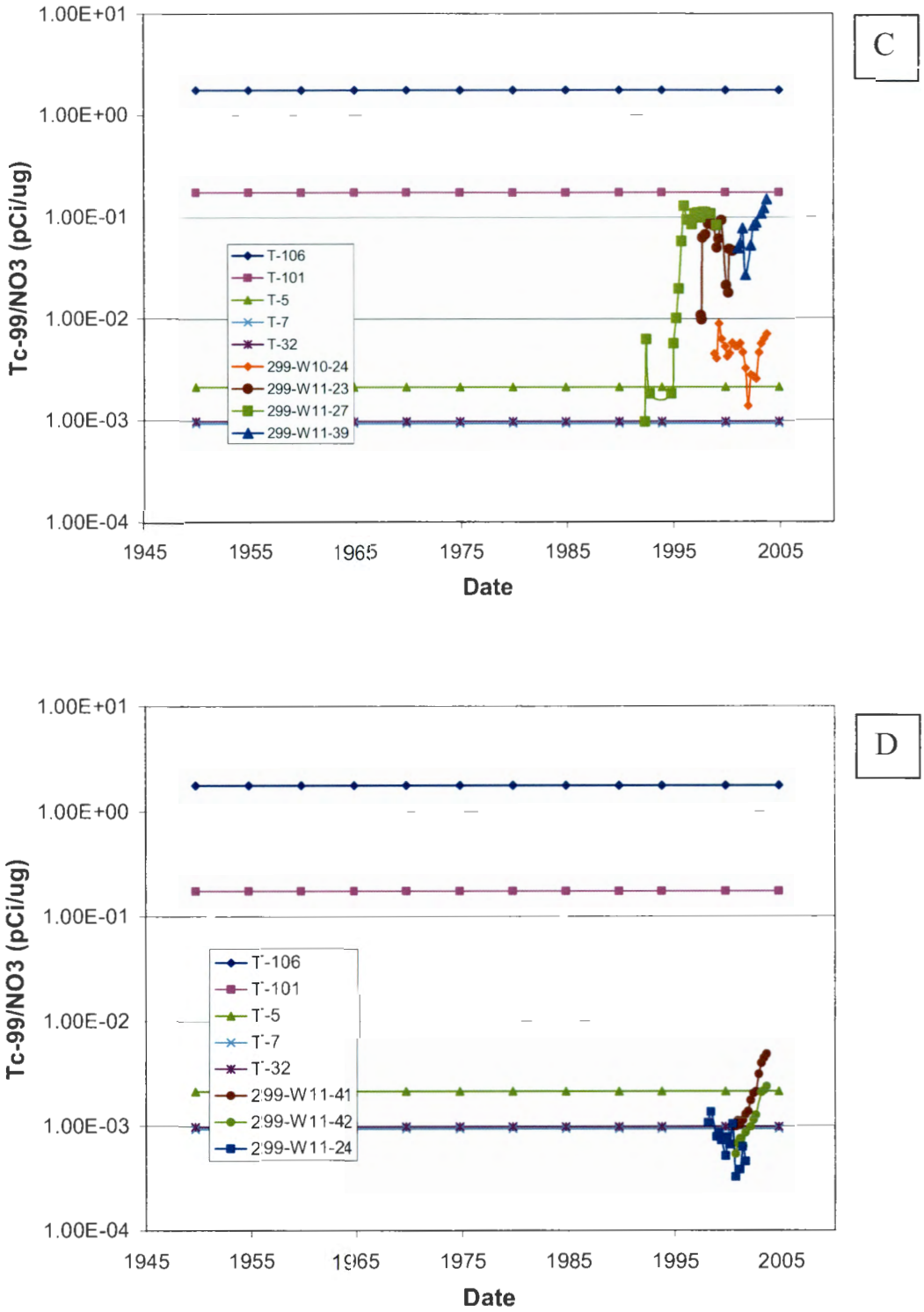

Figure 5.30. Technetium-99/Nitrate Concentration Ratios in Samples from Selected Wells at WMA T. C = Northeastern wells, D = Eastern wells

Water sampled from wells located in the northeast corner of WMA T has a very different technetium-99/nitrate signature than water from the upgradient and northern wells. Groundwater in the northeast corner of the WMA tends toward the technetium-99/nitrate ratios that are indicative of tank waste (Figure 5.30C). Well 299-W10-24 appears to be an exception. However, well 299-W10-24 has a technetium-99 concentration near 2000 pCi/L, which is an order of magnitude greater than that in western (upgradient) or northern wells and samples a deeper part of the aquifer than did wells 299-W11-23 and 299-W11-27. (Both wells 299-W11-23 and 299-W11-27 are now dry and the last, high technetium-99 samples from those wells were collected from near the water table.) Horton et al. (2001) showed that nitrate concentration in the aquifer at well 299-W10-24 increases with depth to about 20 meters below the water table. Thus, the relatively low technetium-99/nitrate ratios from samples from well 299-W10-24 are a mixture of the relatively high technetium-99, low nitrate water near the water table surface with the low technetium-99, high nitrate water from deeper in the aquifer. Although less distinct, the same relationship can be seen for chromium (Figure 5.28C) and for tritium (Figure 5.31C). The nitrate, tritium, and chromium are more regional plumes dispersed deeper in the aquifer beneath WMA T.

Finally, Figure 5.30D shows the technetium-99/nitrate ratios from samples from wells located east of the WMA. As was the case for technetium-99/chromium concentrations, the technetium-99/nitrate concentrations from the eastern wells have a strong crib signature for the first samples collected from the wells in 1997 and then evolve toward tank waste compositions with subsequent samples, especially after 2001.

Figure 5.29 showed the technetium-99/nitrate concentration ratio versus nitrate concentration for several wells at WMA T. The figure shows that water sampled from upgradient wells is distinct with respect to technetium-99 and nitrate from water sampled from wells at the northeast corner of the T tank farm. Water sampled from the eastern wells (and well 299-W10-24) is a mixture of the two.

5.3.3 Technetium-99 – Tritium

Technetium-99 and tritium serve as a final example. Figure 5.31 shows the compositional relationship between technetium-99 and tritium at WMA T. As for nitrate, the tritium and technetium-99 relationship is complicated by a regional tritium plume in the area. However, the technetium-99/tritium ratios lead to the same conclusions as do the technetium-99/chromium and technetium-99/nitrate ratios. That is, groundwater from wells in the west (upgradient) and north sides of WMA T appear to be highly influenced by wastes disposed to the cribs and trenches on the west side of the WMA (Figures 5.31A and B). Groundwater from wells at the northeast corner and the east side of the WMA appears to be evolving towards tank waste from T-101 or T-106 characteristics (Figures 5.31C and D).

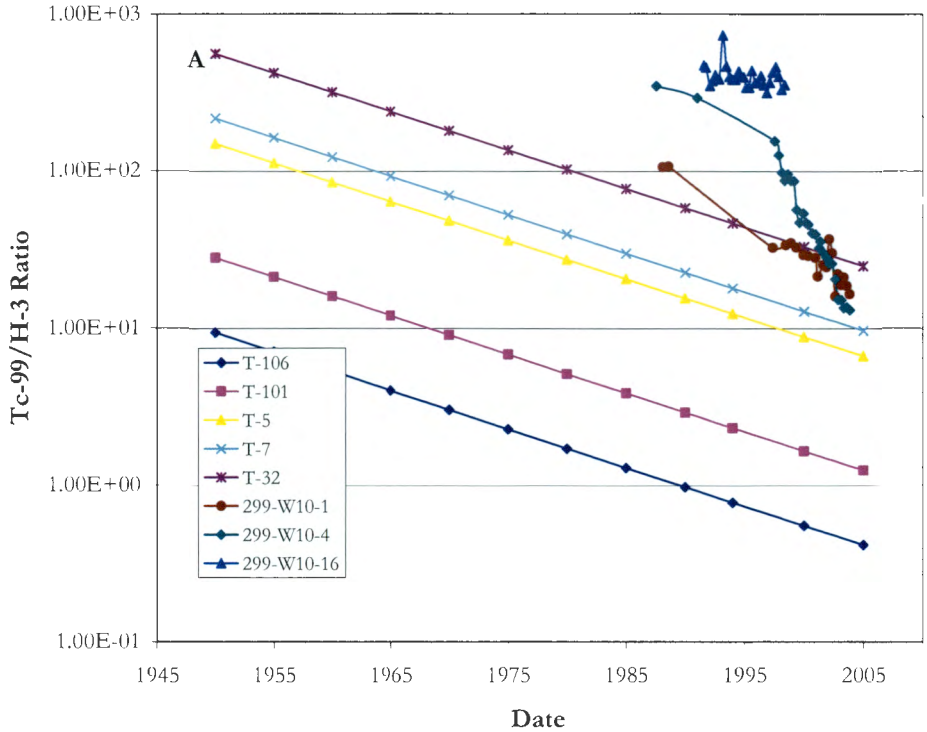

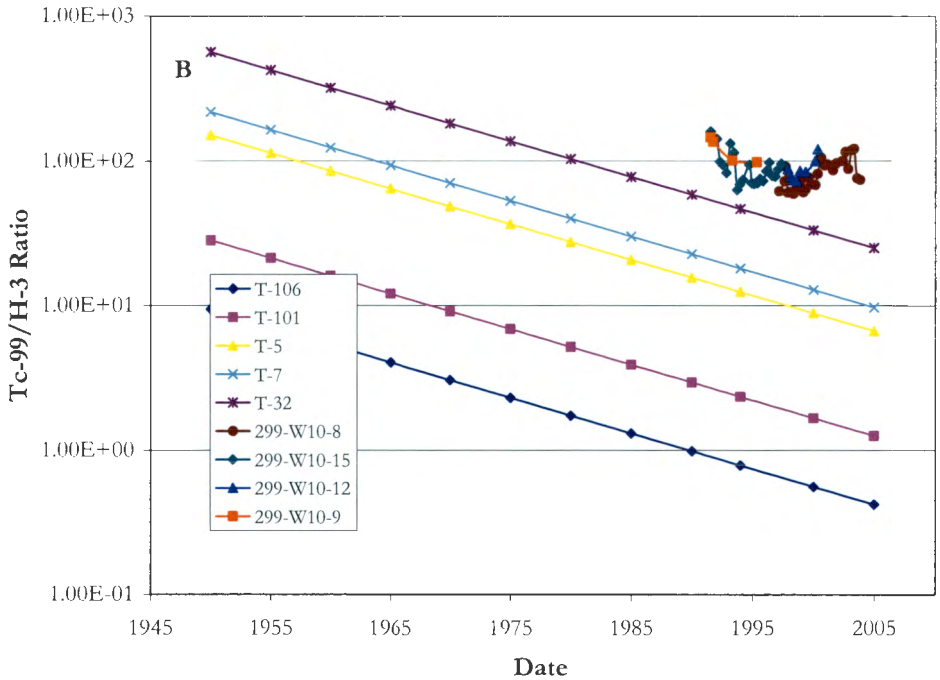

Figure 5.31. Technetium-99/Tritium Concentration Ratios in Samples from Selected Wells at WMA T. A = Upgradient (west) wells, B = Northern wells

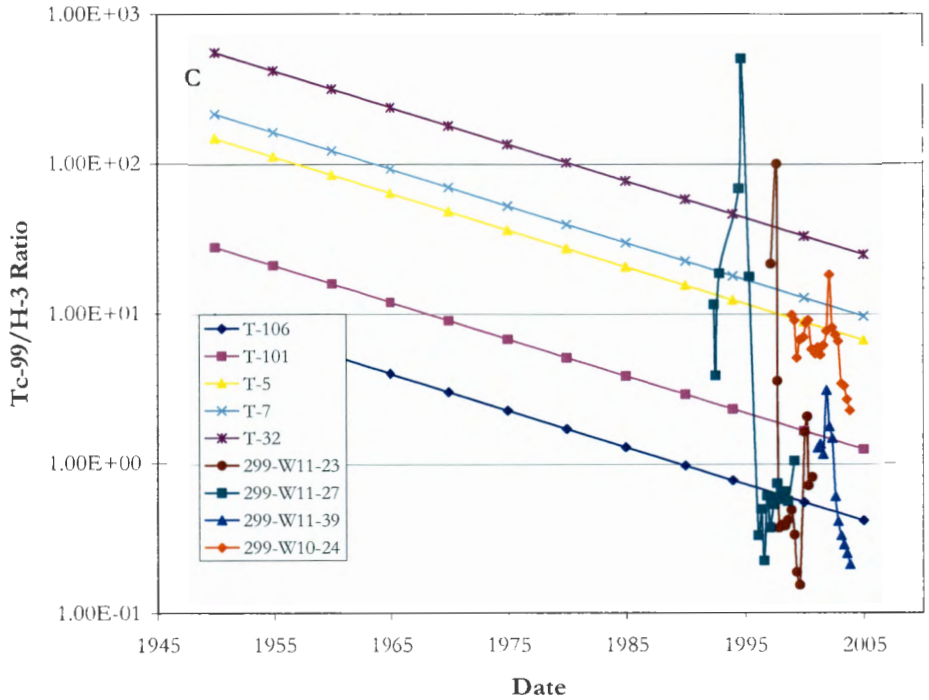

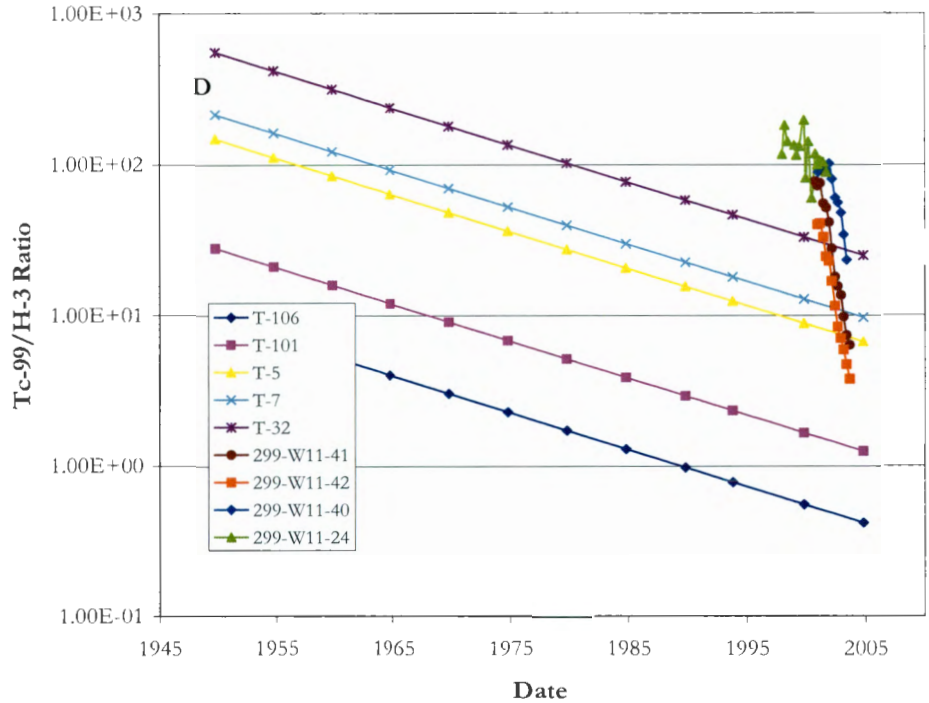

Figure 5.31. Technetium-99/Tritium Concentration Ratios in Samples from Selected Wells at WMA T. C = Northeastern wells, D = Eastern wells

6.0 Summary and Conclusions

In this section, we present summary information on our interpretation of the T Tank Farm borehole sediment characterization data. Conclusions are included to aid in making decisions on what interim actions and future studies are needed to make sound waste-management decisions at the T tank farm.

6.1 Drilling and Sampling Summary at the T Tank Farm

Three boreholes were recently drilled and sampled within or near the T Tank Farm. Two of these holes (C4104 and C4105) were drilled via the closed-end probe method between tanks 241-T-106 and T-109 for the specific purpose of collecting core samples for physical, chemical, and radiological characterization. Locations for the boreholes were selected to evaluate changes in contaminant distributions in the vadose zone since the 1993 study (Freeman-Pollard et al. 1994) and to evaluate the migration of mobile contaminants from the 1973 leak at single-shell tank T-106 in the downgradient direction, respectively. Intermittent core samples, 1.25-ft long by 2.5-in. diameter, were collected at predetermined intervals within the C4104 and C4105 holes.

In addition, almost continuous core samples were collected in well 299-W11-39 (C3117) from 20 to 94 ft bgs. Well 299-W11-39 was installed as a RCRA groundwater monitoring well located along the northeast boundary of the T Tank Farm. Sediments from this well were characterized to determine the background or uncontaminated attributes of T Tank Farm vadose zone sediments, however as discussed in Section 4 the water extract data suggest that sediments from the Hanford formation appear to contain chemicals suggestive of process water. Thus, the sediments from the clean borehole at the TX Tank Farm (299-W10-27) were used as the baseline to compare data from the contaminated boreholes at the T Tank Farm.

Borehole 299-W11-39 (C3117) was drilled using cable-tool methods between November 10 and December 6, 2000. Total depth of the borehole is 282.31 ft (86 m) bgs; the hole terminated within fluvial gravels of the Ringold Formation member of Wooded Island (Unit E), about 40 ft (12.2 m) below the groundwater table. 29 splitspoon cores, 2.5-ft long by 4-in. diameter, were collected from this interval. Two 1.0-ft long plastic (i.e., lexan) core liners were collected for each 2.5-ft core run. The extra 0.5 ft collected in the shoe of the splitspoon was used for geologic description in the field geologist's log. Accounting for the loss of the 0.5-ft shoe samples and slough atop many of the cores, the total recovery for the 20 to 93.5 ft interval is estimated at 66.6%.

Borehole C4104 was drilled and sampled using a driven-probe technique between April 4 and May 22, 2003. The borehole lies between single-shell tanks 241-T-105, -106, -108, and -109 within the 241-T Tank Farm. It is closest to tank 241-T-106, where it lies 18.94 ft (5.77 m) to the southeast. Total depth of the borehole was 127.46 ft (38.8 m) bgs; the hole was terminated when refusal was encountered approximately 5 ft into cemented gravels of the Wooded Island member of the Ringold Formation. Decommissioning of probe hole C4104 was completed on June 9, 2003 by back-pulling the casing while filling the annulus with dry bentonite. During drilling, a total of 23, 1.25-ft long, splitspoon core samples were collected intermittently starting at a depth of 15 ft bgs. A total of 44 characterization samples were collected from this hole. In all, about 30 ft of core was obtained from C4104, or about 24% of the total length of the hole. No samples or drill cuttings were collected between core runs because the hole was

advanced in a closed configuration using a solid, removable tip. Thus no near-continuous geologic field log is available for this hole, unlike the background hole (299-W11-39).

Borehole C4105 was drilled and sampled using the driven-probe technique between January 8 and March 12, 2003. The borehole is closest to single-shell tank 241-T-106, where it lies approximately 28.1 ft (8.6 m) southwest. The borehole is only slightly farther (36 ft [11 m]) from tank 241-T-109, located to the southeast. Borehole C4105 is 87.7 ft west of borehole C4104 in the downgradient direction for most of the vadose zone beds that show dip. Total depth of the borehole was 130.9 ft (39.9 m) bgs; the hole terminated within the vadose zone about 100 ft (30 m) above the groundwater table. During drilling, a total of 22, 1.25-ft-long splitspoon core samples were collected intermittently starting at a depth of about 14 ft bgs. All samples were overdriven beyond the 1.25 ft length of the splitspoon, which resulted in over-compaction of most samples. In all, 30 ft of core was drilled in C4105, which accounts for about 23% of the total length of the hole. No samples or drill cuttings were collected between the 22 core runs because the hole was advanced in a closed configuration using a solid, removable tip. Probe hole C4105 was decommissioned between March 14-18, 2003, by back-pulling the casing while filling the annulus with dry bentonite. A total of 42 samples were collected for physical, chemical, and radiological characterization from C4105. The geology between core runs is inferred and interpreted based on available geophysical logs data, other nearby borehole geologic descriptions, core photographs, laboratory measured gravimetric moisture, and blow-count data.

Each of the 6-in.-long liners from all three boreholes were opened in the chemistry lab and geologically described during the sub-sampling process to obtain aliquots used in the various characterization activities. The geology between core samples was inferred and interpreted based on the geophysical log and blow-count data.

Borehole 299-W10-196 was drilled to 179.6 ft in late 1992 to early 1993 to investigate the vadose-zone contaminant distribution in the vicinity of Tank 241-T-106 (Freeman-Pollard et al. 1994). Borehole 299-W10-196 is included in this report because it is another boring that has produced representative splitspoon samples for physical, chemical, and radiological characterization from T Tank Farm. A total of 43 splitspoon sediment samples were collected and analyzed back in 1993. Spectral-gamma geophysical logging was also performed. During sampling, two overlapping zones of radioactive contamination were encountered; one at 34.5 to 70 ft and the other to 115 ft bgs. The location of 299-W10-196 lies 12.99 feet north and 1.94 ft west of borehole C4104, described previously. Thus the two boreholes are 13.13 ft apart. A main objective was to quantitate the differences in contaminant vertical distribution between these two boreholes to evaluate the extent of movement of species over the 10 year span between these two sampling campaigns.

6.2 Conceptual Model for T Tank Farm Geology

The geology of the vadose zone underlying the 241-T Tank Farm (T Tank Farm) forms the framework through which contaminants that leaked from single-shell tanks or their ancillary piping and junction boxes move, and is fundamental to the understanding of migration and distribution of the contamination in the vadose zone. Of particular interest are the interrelationships between the coarser and finer-grained facies, and the degree of contrast in their physical, chemical, and radiological properties.

Four primary stratigraphic units were encountered in each of the three boreholes: 1) backfill material, 2) the Hanford formation, 3) the Cold Creek unit, and 4) the Ringold Formation. Table 6.1 summarizes

the contacts between the various stratigraphic units in the two new contaminated boreholes, the "clean" borehole (299-W11-39) and the 1993 contaminated borehole 299-W10-196. Below the backfill in the three contaminated boreholes lies the Hanford formation, which is divided into three informal units (H1, H2, and H3). However, the H1 unit was completely removed during excavation and then later used as backfill. Further, at the three boreholes there is no indication that H3 unit materials are present above the contact with Cold Creek units. Therefore, below the T tanks, the Hanford formation H2 unit predominates the stratigraphy. Individual geologic description summaries for each of the new boreholes follow.

The limited sampling at 299-W11-39 led to the following conclusions. Zones of elevated moisture occur within the Hanford formation H2 unit between 75-79 ft bgs, as well as sporadically within the CCU and R_{tf} units. Moisture ranged from as low as 2.8 wt% in pebbly sands of the Hanford formation H1 unit up to 22.8 wt% in the upper CCU subunit. Because coring stopped above the lower CCU subunit, there were no CCU_l or Ringold Formation samples available for laboratory characterization in 299-W11-39. Based on the neutron-moisture log, moisture content is highly variable within the lower CCU subunit [CCU_l], a reflection of the high degree of internal heterogeneity within this unit.

The backfill in C4104 extends from the ground surface to a depth of 40 ft (12.2 m) where it lies in contact with the Hanford formation. Backfill material consists of poorly to moderately sorted, massive, gravelly sand to slightly gravelly sand with variable amounts of silt. Colors range from grayish-brown to olive and yellowish-brown. Backfill materials are unconsolidated and weakly to strongly calcareous. The overall moisture content for backfill materials is relatively low, averaging about 7.9 +/-1.5 wt%. This unit appears to be rather homogeneous and lacks lithologic variation, except at the base.

Pleistocene cataclysmic flood deposits of the Hanford formation underlie backfill materials to a depth of 24.6 m (80.7 ft) in probe hole C4104. Only the sand-dominated Hanford formation H2 unit is represented; all of the coarse-grained Hanford formation H1 unit was removed during tank-farm construction, to be used later as backfill around the tanks. The Hanford formation H2 unit is present between 40 to 80.7 ft (12.2 to 24.6 m) bgs. The H2 unit consists of predominantly fine-to-coarse-grained, gray to brownish-gray "salt and pepper" sand. The H2 unit is weakly to strongly calcareous and occasionally shows weak horizontal laminations. Dispersed within the Hanford formation H2 unit are at least two separate, relatively thin ($\leq$ 0.5 ft), light olive-brown, compact, moderately to well-sorted, silty fine sand beds. These occur at depths starting at 58.6 and 63.5 ft bgs. Other additional fine-grained beds may also be present between cored intervals. The base of the H2 unit, consisting of medium sand, lies in sharp contact with the underlying silty fine sand of the upper CCU at 80.7 ft bgs. Moisture within cores from the H2 unit ranged from dry to slightly moist. One higher moisture zone at about 74 ft bgs, near the base of the H2 unit, is indicated by a spike in the neutron moisture log. This higher moisture interval is probably associated with a fine-grained lens within the H2 unit. Most of the samples from the H2 unit consisted of medium- to coarse-grained sand; two of the samples (S03072-07A and S03072-08B) contained some silty fine sand.

Below the Hanford formation lies the Cold Creek unit, which is 27.3-ft thick at the C4104 borehole. The top of the CCU lies at 80.7 ft (24.6 m) bgs and the bottom lies at about 108 ft (32.9 m). The unit is divided into two distinct subunits, CCU_u and CCU_l, designating upper and lower, respectively. Both the upper and lower contacts of the CCU_u were intersected during coring; the true thickness of the subunit is well established at 11.8-ft thick (80.7 to 92.5 ft bgs). Sediments from this subunit consist of compacted and well-sorted silt to fine sand, which range from moderately to strongly calcareous. All the cores

collected from the upper CCU in C4104 showed horizontal laminations, indicating the calcium carbonate is primarily of detrital origin and not the result of soil development, as is the case with calcic soils of the underlying lower CCU. The structure of upper CCU in this borehole indicates a probable fluvial overbank origin and not a paleosol, as suggested in Reynolds (2003a), because any primary sedimentary structures (e.g., laminae) would have been destroyed during soil development. Moisture in the CCU_u core samples ranged from slightly moist to moist.

Table 6.1. Stratigraphic Units and Contacts (ft bgs)

		Well ID			
		299-W11-39	C4104	C4105	299-W10-196
Surface Elevation ft (amsl)		688.6	675.3	675.0	675.4
Depth (ft) bgs	Backfill	0	0	0	0
	H1	5	NP	NP	NP
	H2	33.5	40	40.6	38.9
	CCU_u	89.9	80.7	85.5	81
	CCU_l	98.0	92.5	92	91.8
	R_{tf}	120.0	108	111	105
	R_{wi}	130	120.9	122	121.3
Thickness (ft)	Backfill	5	40	40.6	38.9
	H1	28.5	NP	NP	NP
	H2	55.4	40.7	44.9	42.1
	CCU_u	8.1	11.8	6.5	10.8
	CCU_l	22	15.5	19	13.2
	R_{tf}	10	12.9	11	16.3
	R_{wi}	ND	ND	ND	ND
Elevation at top of unit (ft above msl)	Backfill	688.6	675.3	675.0	675.4
	H1	683.6	NP	NP	NP
	H2	655.1	635.3	634.4	636.5
	CCU_u	598.7	594.6	589.5	594.4
	CCU_l	590.6	582.8	583.0	583.6
	R_{tf}	568.6	567.3	564.0	570.4
	R_{wi}	558.6	554.4	553.0	554.1

Amsl = above mean sea level
ND = not determined
NP = not present

The contact between the laminated silty sediments of the upper CCU and the calcic paleosol sequence of the lower CCU lies at 92.5 ft (28.2 m) bgs. Sediments from the CCU_l unit consist of mostly poorly sorted, massive mixtures of weathered, pale yellow sand, mud, and gravel, variably cemented with whitish pedogenic calcium carbonate. Some weak secondary pedogenic banding may also be apparent. The base of the lower CCU is defined by the depth of pedogenic weathering and calcic soil development and occurs at 108 ft bgs. Moisture in the CCU_l core samples ranged from slightly moist to moist. Judging from the blow-count data, it appears that the middle portion of the CCU_l is the most strongly cemented.

Almost 20 ft of Ringold Formation sediments were penetrated within C4104 before the probe hole met refusal and was terminated at 127.46 ft bgs. The Ringold Formation member of Taylor Flat in probe hole C4104 extends from 108 to 120.9 ft bgs and is 12.9 ft thick. The R_{tf} unit consists of mostly compacted, well-laminated, well-sorted, olive-brown to yellowish-brown sandy silt with lesser amounts of sand to slightly gravelly sand. The concentration of calcium carbonate appears to decrease with depth and distance from the overlying Cold Creek unit. Observed moisture in R_{tf} core samples was slightly moist to moist and samples measured in the laboratory had the highest moisture of all the stratigraphic units measured with an average of 14.9 +/- 5.5 wt% water. The contact between fine-grained R_{tf} unit with the underlying coarse-grained R_{wi} unit lies at 120.9 ft bgs. The borehole advanced only 6.6 ft into the R_{wi} unit before the borehole was abandoned. Based on core samples alone, all that can be said about the R_{wi} unit is that it consists of a multi-lithologic sandy gravel. During drilling, much pulverization naturally occurred when trying to drive the splitspoon into clast-supported gravels that are larger than the diameter of the splitspoon. As a result, the drilling destroyed the original structure and fabric of the material while adding fines and producing abundant angular rock fragments to the mix.

Based on past studies using other, less-destructive drilling methods as well as outcrop investigations, undisturbed Ringold Formation member of Wooded Island (Unit E) is described as a fluvial, clast-supported, bimodal, pebble to cobble gravel, with well-rounded clasts of basalt, quartzite, porphyritic volcanics, and greenstone, in a well-sorted matrix of quartzo-feldspathic sand (Lindsey 1995). The colors of most facies of the Ringold Formation are shades of brown due to a pervasive iron-oxide film, a weathering product that coats most sand and gravel clasts within the Ringold Formation to varying degrees.

The backfill at C4105 extends from the ground surface to a depth of about 40.6 ft (12.4 m) where it lies in contact with the Hanford formation H2 unit. The exact depth of the base of the backfill is uncertain but tank construction is known to have occurred to a depth of about 37-40 ft. Core run #4, composed of a silty gravelly sand, is identical to samples of backfill above; the contact apparently lies below, but not much below, the 40.53 ft depth. The contact is thus estimated at 40.6 ft bgs. The backfill material consist of predominantly gray to grayish-brown, poorly to very poorly sorted, silty gravelly sand to sandy gravel, which is unconsolidated and weakly to moderately calcareous. The gravimetric moisture content was relatively low, averaging 4.8 +/- 1.7 wt% water, in the backfill material from C4105.

About 45 ft of Pleistocene cataclysmic flood deposits of the Hanford formation underlie backfill materials in C4105. Only the sand-dominated Hanford formation H2 is represented; all of the coarser-grained Hanford formation H1unit was removed during tank-farm construction and later used as backfill around the tanks. The Hanford formation H2 unit is present between 40.6 to 85.5 ft bgs in C4105. The Hanford formation H2 sediments consist of mostly fine- to coarse-grained sand with occasional layers of gravelly sand or silty fine sand. The fine to coarse sand beds are loose, massive to

laminated, brownish gray to olive-brown, moderately to well-sorted, and weakly to moderately calcareous. There appear to be at least two fine-grained layers within the Hanford formation H2 unit in C4105, which could cause lateral spreading of vadose zone moisture. One of these fine-grained layers was encountered at a depth of ~ 56.5 ft bgs. There is also a spike in the neutron-moisture log associated with this depth. Another fine-grained layer is suspected at a depth of ~ 75 ft bgs based on a second spike in the neutron-moisture log for the Hanford formation H2 unit.

The upper and lower contacts of the Cold Creek unit in C4105 are 85.5 ft and 111 ft bgs, respectively. The total thickness of the CCU in probe hole C4105 is 25.5 ft, slightly greater than that observed in companion hole C4104. While both subunits of the Cold Creek unit are clearly present and discernable, the relative thickness of the upper versus lower subunits is very different for the two probe holes. The upper:lower thickness ratio for C4104 is close to 1.0, while this ratio in C4105 is 0.3. This is a remarkable difference considering the holes are only 87.7 ft apart, but serves to illustrate the highly heterogeneous nature of the Cold Creek unit. Sediments from the CCU_u subunit are mostly compacted, laminated, well-sorted, olive-brown, fine sandy silt to silty fine sand. Thin lenses, as coarse as medium-grained sand, were also observed. The subunit is moderately to strongly calcareous, apparently due to a high concentration of detrital calcium-carbonate grains derived from the reworking of the underlying caliche-rich lower CCU. The CCU_u in C4105 is relatively thin (only 6.5-ft thick) compared to adjacent boreholes. This may reflect more erosional scouring of the upper CCU during Ice-Age flooding. Gravimetric moisture content in CCU_u samples shows relatively high water content, which averaged 15.0 +/- 3.9 wt%.

The top of the calcic paleosol sequence of the lower CCU, CCU_l, lies at a depth of about 92 ft, based on a slight increase in penetration resistance and neutron moisture, and sudden decrease in potassium-40 activity in the geophysical logs. The lower CCU in C4105 is relatively thick (19 ft) with an extremely high degree of internal heterogeneity, especially with respect to grain-size distribution and degree of weathering and pedogenesis. Grain sizes within the CCU_l subunit range from pebble gravel (mostly basalt) floating in a poorly sorted mixture of sand, silt, and/or clay to moderately to well-sorted sand and/or mud (i.e., silt and clay). As mentioned, the upper:lower subunit thickness ratio for C4104 is close to 1.0, while this ratio in C4105 is 0.3, illustrating the highly heterogeneous nature of the Cold Creek unit.

Multiple episodes of soil development occur internally within the CCU_l subunit, with tightly cemented, calcic, pedogenic horizons separated by relatively unweathered zones displaying only a few stringers or nodules of secondary calcium carbonate, some of which retain original sedimentary structures. This indicates long periods of land-surface stability and soil development separated by intermittent pulses of sediment accumulation during lower CCU time. Strongly calcic horizons are whitish to pale brown or grayish-brown in color; less pedogenically altered horizons are generally olive-brown. Interpretation of the KUT logs from the T Tank Farm dry wells (Sobczyk 2001) suggests at least two cemented caliche horizons are present, separated by less pedogenically altered sediments. The hardness of the lower CCU is quite variable, as indicated for the log of blow counts. One especially hard, thin cemented zone occurs about half way through the CCU_l at a depth of about 101 ft bgs; this appears to be associated with the lower caliche horizon of Sobczyk (2001). The gravimetric moisture content of the CCU_l averaged 11.3 +/- 4.6 wt% water.

A total of 18 ft of Ringold Formation sediments were penetrated within C4105 before the probe hole met refusal and was terminated at 130.9 ft (39.9 m). The Ringold Formation member of Taylor Flat in probe hole C4105 extends from 111 to 122 ft bgs and is about 11-ft thick. The R_{tf} unit is composed of

interbedded layers of sand, silt, and clay. The strata are mostly fine-grained, compacted and cohesive, well-laminated, and well-sorted, in various shades of brown (gray, olive, and yellow). The concentration of calcium carbonate generally decreases with depth and distance from the overlying Cold Creek unit. Gravimetric moisture contents for the R_{tf} sediments are highly variable – two are relatively high while the other two are low. The average gravimetric moisture was 14.7 +/- 10.7 wt% water. The contact between fine-grained R_{tf} unit and the underlying coarse-grained R_{wi} unit lies at 122 ft bgs. The borehole advanced only ~9 ft into the R_{wi} unit before the borehole was abandoned at 130.9 ft bgs. The gravimetric moisture measured in the R_{wi} samples averaged about 9.1 +/- 7.6 wt% water.

6.3 Stratigraphy and Moisture Content

In general, heterogeneities including fine-grained thin lenses in the Hanford formation and the relatively thick Cold Creek unit likely cause anisotropy in water flow. Increased moisture was found to correlate with each of the fine-grained thin lens intercepted by the coring; other fine-grained lens are inferred to be present in the Hanford formation H2 unit based on the field neutron logging profiles. Recall that only about 25% of the profiles in the boreholes were cored. Several findings and hypotheses on the relationship between moisture content and water and contaminant flow that are gleaned from the characterization efforts reported herein include:

- The highest concentrations of moisture in the vadose zone at T Tank Farm appear to lie within the Cold Creek unit and Ringold Formation member of Taylor Flat (R_{tf}). Moisture is naturally high in these strata and not necessarily from tank leaks.

- Occasional, thin fine-grained lenses within the Hanford formation H2 unit also display higher moisture content.

- Relatively low moisture contents are found in gravelly facies, which include backfill materials, Hanford formation H1 unit, and the Ringold Formation member of Wooded Island.

- Sand-dominated facies of the Hanford formation (H2 unit) are also relatively low in moisture content.

- Average moisture content for the Hanford formation H2 unit and the upper CCU is about the same in the background hole as in the probe holes (C4104 and C4105) within the T Tank farm. This suggests movement of water under both artificial and natural recharge is transient in nature and may be difficult to distinguish with depth in the vadose zone.

6.4 Vertical Extent of Contamination

The following paragraphs describe measurements of various parameters that help us determine the extent of vertical migration of tank or ancillary equipment leaks. We used several parameters including moisture content, pH, electrical conductivity, nitrate, technetium-99 (and other mobile fission products [i.e., ruthenium and molybdenum]), sodium, and uranium concentrations in water and acid extract for our main indicators to determine the leading edge of the plume. The concentrations of water-extractable (for mobile constituents) and acid-extractable or directly measured constituents in the sediment (for sorbing constituents) were used to delineate the total inventory of constituents within the plume. For technetium-99, the water-extractable data were judged to be a more accurate indication of past tank leaks

than acid-extractable concentrations. In this section, we discuss all of the parameters measured except uranium and sodium. The uranium data suggest that only small quantities were present in the leaked fluid and the sodium data set shows obvious ion exchange interactions with the sediments that retard its migration in comparison to the most mobile constituents in the leaked fluids.

Based on evaluating all these measurements, we conclude that the borehole data do not establish the vertical extent of tank contamination, especially in boreholes C4104 and C4105, because contamination was found at the bottom of these boreholes, which met refusal before contamination could be shown to be absent.

The first parameter, moisture content, is a direct measure of the mass of water in the vadose zone sediment. One would logically assume that wetter than normal conditions would represent the existence of leaked tank liquor but, as found at most of the boreholes studied to date, the moisture content in the T boreholes is indicative mainly of grain size.

The second parameter measured was the pH of water extracts of the vadose zone sediment. Based on the assumption that tank fluids are generally caustic and, often, very caustic (>1 M free hydroxide), elevated pH profiles should be indicative of the zones impacted by leaked fluids. The pH profiles for sediments from the two new boreholes (C4104 and C4105) show consistently elevated pH (pH values range from 8.6 to almost 10) in only borehole C4104 from 47 to 92.6 ft bgs. But the pH data at all other depths in borehole C4104 and at all depths in borehole C4105 show no indication of significantly elevated pH values. Based on observations at other tank farms (SX and BX) where it is certain that caustic wastes are in the vadose zone, yet water extract pH values never exceed 10, we have concluded that pH is not a very sensitive parameter to use for evaluating the extent of plume migration in the vadose zone. A recent paper that provides a technically based conceptualization of the evolution of pH in sediments in contact with caustic fluids is Wan et al. (2004).

The third parameter that was assessed to estimate the vertical extent of the leaked plume was dilution-corrected water extract electrical conductivity (EC). The EC depth profiles for the two new T Tank Farm boreholes (C4104 and C4105) do show elevated EC in comparison to the background sediments from borehole 299-W10-27. We also found that the background borehole for the T Tank Farm, 299-W11-39, had suspiciously elevated EC values in the Hanford formation H2 unit above 78 ft bgs so that we used the background borehole from the TX Tank Farm as a more appropriate background well. There is elevated EC in the C4104 borehole sediments from 47 ft bgs to the bottom of the borehole near 127 ft bgs. At 46 ft bgs, EC of the C4104 water extracts and actual porewaters are 6 times higher than background values and differences reach values of ~ 40 times larger than background at 116 ft bgs. The dilution-corrected (calculated) porewaters are also quite elevated between 59 and 76 ft bgs. These data show that tank liquors from the T-106 leak are present in the sediments from C4104. The highest values of dilution-corrected porewater EC found at C4104 (33.4 mS/cm at 116 ft bgs) are equivalent to a pore solution of 0.21 M KCl, the salt solution used to calibrate the conductivity probe.

There is also evidence of elevated EC starting at 86.7.3 ft bgs to the bottom of the C4105 borehole. The EC values for 1:1 water extracts from the Cold Creek units' sediments at C4105 range from 1.2 to 3.1 mS/cm, which is about 10 to 30 times higher than found in dilution-corrected porewaters from nearby background sediments. The six actual porewater EC values are quite similar to the dilution-corrected (derived) porewater conductivities. The highest values of dilution-corrected porewater EC in borehole C4105 occur in two zones, between 87 to 110 ft bgs and at 123 ft bgs. The dilution-corrected EC and

actual porewater values for these two zones are equivalent to a pore solution of 0.10 to 0.175 M KCl. Although dilution-corrected EC values peak slightly higher at C4104 both of the peak values for the two T boreholes are lower than the dilution-corrected EC maximum at borehole C3831 near Tank TX-107, which peaked between 60-61 ft bgs with a value equivalent to a pore solution of 0.4 M KCl.

Because the two new T Tank Farm boreholes could not be pushed through the Ringold Formation Wooded Island member beyond ~ 130 ft bgs, it is difficult to judge whether the vadose zone plumes of saline fluids stopped before reaching the water table. However, the earlier borehole (299-W10-196) that reached almost 180 ft bgs suggests that contamination did stop percolating deeper into the vadose zone profile near the depth where refusal was met at C4104 and C4105. Unlike at SX Tank Farm where contamination appears to stop at the caliche layer (see Serne et al. 2002b and 2002c), contamination near T-106 has penetrated into the Ringold deeper than the upper fine-grained Taylor Flat member and into the upper portion of the coarse grained Wooded Island member.

Despite the evidence that elevated EC values may be present in both new boreholes to their depth of refusal, the concentrations are not large. For example, the maximum dilution-corrected EC at borehole C4104 is 33.41 mS/cm at 116 ft bgs, and at borehole C4105 the maximum is 18.98 mS/cm at 123.9 ft bgs. In both cases the peak EC is not at the very bottom of the borehole but there is no clear indication that the vertical distribution is tailing off dramatically towards background levels, which would indicate that the entire plume had been delineated.

The leaks near the SX108-109 and BX-102 tanks had peak vadose zone porewater concentrations that were equivalent to much more concentrated waste fluids, 524 to 1774 and 77 mS/cm, respectively. At 299-E33-46 near tank B-110 the dilution-corrected EC was 15.1 mS/cm, and at 299-W23-19 near tank SX-115, which contained dilute waste, the dilution-corrected EC was 33 mS/cm. At the TX tank farm maximum dilution-corrected EC values were 6.27 mS/cm (C3830), 12.5 mS/cm (C3832) and 43.3 mS/cm (C3831).

The fourth parameter evaluated to define the vertical extent of contamination was nitrate. The nitrate water extract values for borehole C4104 are elevated from 64 ft bgs to the bottom of the borehole. Starting at 64 ft bgs the water-extractable nitrate is 10 times larger than background, at 87 ft bgs the nitrate values exceed 100 times background, and at 111 ft bgs the water-extractable nitrate is greater than 250 times values found in background sediments. At 116 ft bgs, water-extractable nitrate peaks at 1000 times background sediment values. The water-extractable nitrate data for borehole C4105 sediments show slightly elevated values in comparison to background sediments in the deeper portion of the Hanford formation H2 unit and significantly higher concentrations (>1000 x) than background in both Cold Creek subunits. The nitrate concentrations in C4105 sediments within the Ringold Formation (both subunits) are also elevated versus background by factors of 500 and 100 in R_{tf} and R_{wi}, respectively.

The comparison of the nitrate concentrations in the two contaminated boreholes suggests that in the Hanford formation tank leak fluid percolated into the sediments near C4104, intercept C4104 borehole starting at about 80 ft bgs but did not flow horizontally in the Hanford formation all the way to C4105. However, in the Cold Creek upper subunit, the nitrate concentrations at C4105 exceed the concentrations at C4104 by a factor of 10, thus suggesting a large component of horizontal spreading in the Cold Creek Formation strata. In the CCU_l subunit there is somewhat larger concentrations of nitrate in C4105 sediments, suggesting perhaps some vertical penetration of high nitrate concentrations that originally spread horizontally in the overlying CCU_u stratum. There is more nitrate (factor of 1 to 5 x) in the C4105

sediments in the R_{tf} stratum than at C4104, but in the deepest stratum penetrated, the top of Ringold Formation Wooded Island member, the nitrate concentrations in both contaminated boreholes are similar (several hundred μg/g). The nitrate distribution with depth at these two boreholes support a flow conceptual model that suggests vertical percolation through the Hanford formation H2 unit near tank T-106 and then a strong horizontal spreading within the CCU_u unit followed by more slow vertical percolation, perhaps via diffusion, into the deeper strata.

It is certain at the T-106 region that the plume of leaked fluid was not successfully stopped at the caliche layer (CCU_l) as was inferred from boreholes at the SX tank farm. Around the T-106 tank, leaked tank fluids are found as deep as 130 ft bgs in the Ringold Formation Wooden Island member. The nitrate profile at the 299-W10-196 borehole drilled in 1992 using a different technique reached 180 ft bgs and both its and the C4104 vertical profiles of nitrate appear to show the leading edge of the bulk of the plume resides near 116 ft bgs in the Ringold Formation Taylor Flat member. However, to the southwest at C4105 the high nitrate plume shows three maxima in the vertical profile: at 88, 107, and 124 ft bgs with nitrate concentrations of ~8630, 5400, and 7880 mg/L, respectively. Again, this suggests significant horizontal migration of plume fluids.

The sampling frequency for the nitrate at 299-W10-196 is very sparse in the zone of interest. Further, neither C4104 or 299-W10-196 boreholes have frequent enough sampling to identify the exact depth of maximum concentration. Available data suggest that the maximum concentration in C4104 might be about 6 ft deeper than at 299-W10-196, so perhaps there is some evidence of vertical migration in the ten years between drilling of the boreholes. The concentrations of nitrate found in the sediments vary some with peak concentrations of 4,400 and 2,600 μg/g, in 299-W10-196 and C4104, respectively.

The fifth indicator species often used to define the vertical extent of contamination is technetium-99 in water extract samples. Water-leachable technetium-99 is present in the C4104 sediment from 40 ft bgs to the bottom of the borehole. The bulk of the technetium plume resides between the depths of 115 and 121 ft bgs in the Ringold Taylor Flats unit. The maximum water-leachable technetium in this zone ranges from 500 to 1160 pCi/g. This range is larger than values found at contaminated boreholes in the TX (20 to 130 pCi/g), BX and B tank farms (5 to 20 pCi/g), and higher than the values found at the 299-W23-19 borehole near SX-115 (100 to 500 pCi/g) but lower than the water leachable technetium-99 found in boreholes near the SX-108 and SX-109 tanks (1,000 to 10,000 pCi/g) as described in Serne et al. (2002b, 2000c, 2000d, 2000e, 2000f) and Serne et al. (2004). The maximum concentrations of technetium-99 at C4105 are found between 86.7 and 93.3 ft bgs in the Cold Creek Formation upper subunit (the fine-grained sediment), although significant concentrations are found all the way down to the bottom of the R_{tf} unit. The water-extractable technetium-99 concentrations in the sediments from C4105 are greater than the concentrations in sediments from C4104 in the two Cold Creek units by factors of four to thirty. Deeper in the two Ringold Formation units, the sediments at C4104 contain more water-soluble technetium-99 than the sediments from C4105 by factors of 1 to 10.

We interpret the technetium-99 distributions between the two boreholes to reflect the rapid horizontal migration of the tank T-106 leak plume in the Cold Creek units and a rapid vertical migration of some of the tank fluids near the tank. Slow flushing by enhanced recharge appears to lead to more horizontal movement of the tank fluids downgradient towards C4105. The C4104 to 299-W10-196 comparison data show that technetium-99 present between the depths of 95 to 105 ft bgs in the Cold Creek lower subunit in borehole 299-W10-196 in 1993 is not present in borehole C4104 at similar depths in 2004.

Unfortunately, the sampling and technetium-99 measurement frequency in 1993 for borehole 299-W10-196 was too coarse to adequately complete a profile of the shape of the technetium-99 plume. Depending upon what the technetium-99 concentration was in the peak of the plume (between 105 and 115 ft bgs; the zone where data are missing) in borehole 299-W10-196, the masses of technetium-99 in the two boreholes appears to be quite similar. The sediments below 120 ft bgs in both boreholes are drier and coarser-grained Ringold Formation Wooded Island member. This stratum may be acting as a hydrologic barrier to the migration of unsaturated fluids that have accumulated in the finer-grained R_{tf} strata. One plausible explanation of the differences in the shape (vertical distribution) of the technetium-99 plume between the observed profiles (299-W10-196 versus C4104) is that since 1993, the upper portion of the technetium-99 plume has vertically migrated from the Cold Creek Formation lower subunit into the moist and fine-grained Ringold Formation Taylor Flat member during the ten years that have elapsed since the 299-W10-196 borehole was drilled and measurements performed.

In summary, the moisture content, pH, electrical conductivity, nitrate, and technetium-99 profiles versus depth in the three contaminated boreholes around T-106 do not clearly identify the leading edge of the plume. The profiles do collectively suggest that bulk of tank-related fluids (center of mass) still resides in Ringold Formation Taylor Flats member fine-grained sediments.

6.5 Detailed Characterization to Elucidate Controlling Geochemical Processes

The more detailed characterization activities of the cores from 299-W11-39 and the three contaminated boreholes added some insight on the processes that control the observed vertical distribution of contaminants and on the migration potential of key contaminants in the future.

The porewaters, either calculated by dilution correction of the 1:1 water extracts, or directly obtained by ultracentrifugation, had the following composition. Two regions of the C4104 vadose profile contain high total dissolved salts — 59 to 76 and 116 ft bgs. The uncharged-balanced porewater at these two depth zones is approximated by the following compositions that are based on the actual porewaters, which were obtained by ultracentrifugation. The shallow (between 59 and 76 ft bgs; Hanford formation H2 unit) porewater is dominated by sodium and carbonate/bicarbonate alkalinity with the approximate composition of sodium ~ (150 meq/L), calcium (0.7 meq/L), magnesium (0.6 meq/L), potassium (1.2 meq/L), alkalinity (~220 meq/L), nitrate (9.2 meq/L), fluoride (6.4 meq/L), sulfate (5.6 meq/L), chloride (3.0 meq/L) and phosphate (1.8 meq/L), respectively.

The deeper saline porewater in the C4104 Ringold Formation member of Taylor Flat sediment is dominated by the divalent cations calcium and magnesium and the anions nitrate and nitrite, and represents tank liquor in the ion exchange front that is pushing the divalent cations off sediment exchange sites. The deep porewater has a chemical composition of calcium (190 meq/L), magnesium (125 meq/L), sodium (110 meq/L), and potassium (1.7 meq/L) and nitrate (212 meq/L), nitrite (40 meq/L), sulfate (37 meq/L), chloride (5 meq/L), and bicarbonate alkalinity of 6 meq/L.

These two C4104 porewaters are very dilute compared to the vadose zone porewaters found at the SX and BX tank farms where the total ionic strength of the porewaters were as high as 7,000 to 17,000 and 1,000 meq/L, respectively. At the borehole emplaced near tank B-110, the most saline porewater was 150

to 160 meq/L. At the TX tank farm, the most saline porewater was found in borehole C3831, near tank TX-107, with a total ionic strength of 850 meq/L, about 350 meq/L greater than the concentrations in C4104 sediments.

The porewater in the C4105 borehole Cold Creek upper subunit has a total concentration of ~ 185 meq/L each of cations and anions consisting of 44 meq/L magnesium, 120 meq/L calcium, 18 meq/L sodium, 1.2 meq/L potassium, 5 meq/L chlorine, 30 meq/L bicarbonate, 130 meq/L nitrate, and 20 meq/L sulfate. The saline porewater in C4105 borehole's Cold Creek lower subunit contains ~ 175 meq/L each of cations and anions consisting of 55 meq/L magnesium, 77 meq/L calcium, 40 meq/L sodium, 3 meq/L potassium, 0.3 meq/L fluoride, 3 meq/L chloride, 85 meq/L nitrate, 62 meq/L sulfate and 25 meq/L bicarbonate. The actual porewaters from caliche bearing sediments, obtained from ultracentrifugation, show that 1:1 sediment:water extracts inflate the calculated bicarbonate porewater concentration significantly from dissolution of the caliche. The porewaters from C4105 in the Cold Creek upper subunit are slightly more saline than comparable porewaters at C4104 (depths slightly more shallow and including the deep Hanford formation H2 unit) that contain ~150 meq/L cations and anions that are predominately sodium bicarbonate. The chemical composition in the CCU_u unit at C4105 shows more divalent cations from the ion exchange reactions and more nitrate and sulfate likely from the tank fluids than porewaters within the C4104 sediments from the same strata.

The C4105 porewater in the Cold Creek lower unit is more dilute (~175 vs. 425 meq/L) than the porewater from the same strata in borehole C4104. Both contain a mix of divalent cations (from ion exchange and naturally from caliche) and sodium (from the tank leak) and a mix of nitrate-nitrite and sulfate (from the tank leak) and bicarbonate (from the sediment and reactions with the caustic tank fluids). The porewater chemical compositions at C4104 and C4105 are consistent with a plume migration model that has the tank fluid quickly penetrating vertically right below T-106 through the Hanford formation H2 unit into the Cold Creek formations with additional fluid migrating horizontally in the two Cold Creek units downgradient towards C4105. With time, dilute recharge water has pushed the mobile nitrate out of the shallow C4104 sediments down to the Cold Creek strata where the mobile tank species are transported horizontally towards C4105.

The most concentrated porewaters found in boreholes C4104 and C4105 are shown in Table 6.2 in units of meq/L. Also included in the table for comparison are the maximum porewater concentrations found in other characterization work previously reported for the BX, B, SX, and TX Tank Farms.

As shown in Table 6.2, the calculated porewaters in the T boreholes are much less concentrated than porewaters found in the vadose zone sediments from both the BX and SX WMAs and slightly less than those from the most saline porewater found in the TX tank farm.

Table 6.2. Maximum Pore Water Concentrations in Sediments from Contaminated Sediments in Various Tank Farms

	Closest SST and Borehole Number									
Tank	**TX-107**	**T-106**		**T-106**		**BX-102**	**B-110**	**SX-115**	**SX-109**	**SX-108**
Borehole/ Strata	**C3831-H2**	**C4104-H2**	**C4104-Rtf**	**C4105-CCUu**	**C4105-CCUl**	**E33-45**	**E33-46**	**W23-19**	**41-09-39**	**Slant**
Na	418.5	150	110	18	40	525	150	35.6	6066	16900
Ca	1.2	0.7	190*	120	77	114	4	280.9	619	90
Mg	0.2	0.6	125*	44	55	62	2.5	94.6	24	10
K	4.7	1.2	1.7	1.2	3	13	0.5	3.6	42	92
Sr	0	0	0	0	0	0	0	1.5	4.4	1
UO_2	0	0	0	0	0	2	0	0	0	0
Total Cations	424	152.5	426.7*	183.2	175	716	157	416.2	6755.4	17093
NO_3	202.4	9.2	212	130	85	100	3	420	6710	15677
NO_2	0	0	40	0	0	0	0	0	28	32
SO_4	15.2	5.6	37	20	62	570	14	3.3	95	500
CrO_4	0	0	0.0	0	0	0	0	100	0	0
PO_4	8.4	1.8	0	0	0	0	0	0	0	0
Cl	6.4	3.0	5	5	3	5	0	6	119	147
F	0.8	6.4	0	0	0.3	1	10	0	0	0
HCO_3	191.2	220*	6	30	25	40	130	7	0	666
Total Anions	424	246*	300	185	175.3	716	157	536.3	6952	17022
Dilution-corrected EC (mS/cm)	43.26	24.3	33.4	15.6	18.1	76.8	15.1	33.1	524	1772

Yellow shaded cells signify some round off to give electrical charge balance between the cations and anions.

* Suspect data poor charge balance

The water-extractable major cations' distributions in borehole C4104 and C4105 sediments suggest that an ion-exchange process dominates the porewater/sediment interactions where tank fluid passed by or currently exists. The distribution of water-leachable divalent-alkaline-earth cations (magnesium, calcium, and strontium and to some extent barium) at C4104 shows low quantities between 40 and 93 ft bgs. Conversely, the distribution of water-extractable sodium is higher than the mass that is water-leachable from uncontaminated sediments in the profile from 23 to 116 ft bgs. These trends suggest that tank fluids that are high in sodium and nitrate did seep into the vadose zone near C4104 borehole. The sodium pushed the natural divalent cations off the sediment cation exchange sites in the C4104 sediments between 40 and 93 ft bgs. At and right below the leading edge of the sodium plume, one finds elevated levels of the divalent cations that were displaced. We observe the high levels of divalent cations in the samples between 115 ft bgs to the bottom of the borehole at 127 ft bgs. The water-extractable sodium concentration approaches background levels below 116 ft bgs. The maximum penetration of the cation-exchange front is located between 116 and 120 ft. No samples were obtained between these two depths to locate the exact penetration depth of the cation exchange interactions.

The water-leachable cation distribution in C4105 sediments agrees with the hydrologic conceptual model wherein the T-106 tank leak with high soluble sodium percolates both vertically below tank T-106 into the sediments near borehole C4104 and also horizontally towards borehole C4105 in the Cold Creek upper subunit. As the T-106 tank fluids migrated, the sodium displaced the natural divalent cations and some of the natural potassium off the sediment cation exchange sites in the sediments between boreholes C4104 and C4105. The displaced divalent cations migrated horizontally into the area of borehole C4105 mainly in both Cold Creek units and the upper portion of R_{tf}. Similarly near C4104, some of the divalent cations were pushed vertically into the lower portion of the R_{tf} and somewhat into the R_{wi} unit. The water-leachable anions and cations data for the two boreholes near Tank T-106 show that horizontal plume migration can be as significant as vertical percolation. Borehole C4105 is about 88 ft due west of C4104; thus, the ion exchange front has traveled horizontally as far as the ion exchange front penetrated vertically at C4104.

6.6 Estimates of Contaminant Inventory and Sorption-Desorption Values

In this section, we discuss our measurements and data synthesis used to quantify the inventory of key risk contaminants and our estimates of their adsorption-desorption tendencies. We did perform site-specific desorption studies for cobalt-60 on sediments from C4104 using deionized water as the leachant and the results are discussed below. Further, by combining the data from the dilution-corrected 1:1 water extracts, which represent the porewater, with the concentrations measured on the sediment, we can estimate the desorption K_d values for the contaminants of interest. For a contaminant that has very little water-soluble mass such as cesium-137, the in situ desorption K_d can be approximated as the mass in the total sample per gram of dry sediment divided by the mass in the porewater per milliliter. For a contaminant that is quite soluble in the water extract (this is approximately equivalent to stating that the contaminant resides mainly in the porewater within the sediment), one needs to subtract the amount that was present in the porewater from the total amount present in the moist sediment sample to obtain a value for the amount that would remain on the solid at equilibrium with the pore fluid.

We will first describe our inventory estimates and then address the mobility status of contaminants presently found in the T vadose zone sediments. Tables 6.3 and 6.4 provide our best estimate of the inventory of potentially mobile contaminants found in each of the two new boreholes near tank T-106.

Potential contaminants of concern that have been selected for discussion include technetium-99, uranium, cobalt-60, chromium(VI), and nitrate. For the technetium-99 inventory, we suggest that the water extract data is most accurate and should be used to estimate technetium-99 inventory versus depth. However, we do present the technetium-99 acid extract data as the worst-case maximum inventory estimate. We assume that all technetium is water soluble in the sediments, as found during our characterization studies at SX and the BX WMAs (Serne et al. 2002b, 2002c, 2002d, and 2002e), and that the acid-extract data are biased high and are generally of lesser quality.

For uranium and chromium we have found that one must separate the natural background concentrations from the "Hanford added material" in discussing risk potential. The natural uranium and chromium are almost entirely resistant to water leaching and to becoming mobile, whereas the material added by Hanford activities is somewhat mobile. We thus recommend using the water-extractable uranium and chromium data as representative of the concentrations that could migrate to the water table for future risk calculations. However, we present the acid-extractable chromium and uranium inventories to allow very conservative risk calculations to be performed that assume all acid-extractable masses could ultimately become released to percolating recharge waters. For the cobalt-60, we present the total activity present in the sediments.

For nitrate, as for technetium-99, we assume that the water extract concentrations represent the total inventory. We have no other method to measure nitrate besides the water extract method. We use 8 M nitric acid to measure the total amount of a constituent that is acid leachable. Thus, the nitric acid leachant overwhelms any nitrate present in the sediment. We have also designated in the tables, using yellow shading, samples that may contain Hanford-related wastes as opposed to samples that are likely uncontaminated natural sediments.

Semi-quantitative estimates of desorption K_d values for the potential contaminants, identified in Table 6.5 for C4104 and C4105 vadose zone sediments, can be calculated using the inventory estimates (mass or activity per gram of sediment) divided by the estimated porewater concentration of the constituent. These values are found in Tables 4.30, 4.45, 4.60 (acid extract or direct measure; cobalt-60) and 4.27, 4.42, 4.57 (porewaters) and 4.34 (cobalt-60 in water extracts), respectively. In Table 6.5, the K_d values for sediment samples where the bulk of the contamination is present are highlighted in yellow and in bold red type. The faint blue (lighter) shading in Table 6.5 designates data that are more dominated by natural constituents or impacted by low precision analytical values. From the table one can see two trends. First, where there are significant concentrations of contaminants in the sediments (between 46.33 and 125 ft bgs for C4104 and 70 to 130 ft bgs for C4105), the K_d values for uranium and chromium are smaller than their values at shallower and deeper depths. This is caused both by there being more saline porewaters (competing ions) and higher contributions of Hanford waste species for chromium and uranium being present, which are generally more water leachable than naturally present species.

Table 6.3. Inventory Estimates for Potential Contaminants of Concern in Borehole C4104 Sediments

Depth (ft bgs)	Strat. Unit	Nitrate	Tc-99	U-238	Cr	Tc-99	U-238	Cr
Extract			Water				Acid	
Units		µg/g	pCi/g	µg/g	µg/g	pCi/g	µg/g	µg/g
16.18	Bckfl	2.34	<1.70E-01	2.05E-03	(3.60E-04)	(9.86E-01)[a]	4.35E-01	8.56E+00
22.69	Bckfl	2.72	<1.70E-01	2.40E-03	(4.28E-04)	(1.46E+00)	3.84E-01	6.03E+00
30.74	Bckfl	1.77	<1.70E-01	2.98E-03	(2.03E-03)	(1.22E+00)	4.09E-01	1.97E+01
36.88	Bckfl	0.79	(6.78E-02)[a]	1.60E-03	(1.41E-03)	(1.34E+00)	3.96E-01	8.77E+00
37.4	Bckfl	0.77	1.02E-01	3.99E-03	(1.23E-04)	(1.12E+01)	4.17E-01	1.43E+01
40.01	Bckfl	2.05	2.12E-01	8.49E-03	(6.47E-04)	(1.61E+01)	4.97E-01	2.17E+01
40.01	Bckfl	1.05	0.00E+00	3.95E-03	(3.27E-03)	(1.38E+00)	4.68E-01	1.09E+01
46.33	H2	<0.43	5.53E+00	6.13E-02	4.14E-03	(4.03E+01)	1.07E+00	1.36E+01
46.98	H2	3.47	2.02E+00	3.89E-02	5.28E-03	(2.26E+01)	7.56E-01	9.91E+00
58.39	H2	4.08	1.52E+01	8.34E-01	1.61E-02	(7.96E+01)	2.51E+00	5.40E+01
58.39	H2	5.6	1.38E+01	1.06E+00	3.26E-02	NS[c]	NS[c]	NS[c]
59.09	H2	7.71	2.19E+00	4.74E-01	3.03E-02	(1.41E+01)	1.18E+00	9.24E+00
63.38	H2	<0.44	1.32E+01	7.18E-01	5.30E-02	(4.12E+01)	1.20E+00	1.71E+01
64.03	H2	17.85	4.28E+00	1.12E-01	4.29E-01	(1.97E+01)	6.35E-01	1.42E+01
64.03	H2	20.6	4.51E+00	1.15E-01	3.04E-01	(1.97E+01)	5.21E-01	1.48E+01
76.03	H2	24.71	2.01E+00	9.08E-01	5.31E-01	(2.56E+01)	2.46E+00	1.24E+01
81.04	CCU_u	78.22	5.73E+00	9.46E-01	1.47E+00	(3.28E+01)	2.30E+00	2.57E+01
87.35	CCU_u	168.18	4.43E+01	2.07E-01	3.11E+00	5.56E+01	1.69E+00	5.73E+01
87.35	CCU_u	196.66	4.06E+01	2.29E-01	2.74E+00	5.19E+01	1.63E+00	5.74E+01
92.61	CCU_l	220.37	5.27E+01	4.69E-01	1.83E+00	2.55E+02	2.42E+00	1.92E+01
93.56	CCU_l	510.87	2.95E+02	7.64E-03	6.72E+00	5.88E+02	1.48E+00	2.37E+01
94.67	CCU_l	528.93	1.04E+02	6.81E-03	2.17E+00	2.60E+02	7.39E-01	2.63E+01
99.7	CCU_l	179.76	1.76E+02	1.04E-02	5.70E-01	7.87E+02	6.07E-01	1.87E+01

Table 6.3. (contd)

Depth (ft bgs)	Strat. Unit	Nitrate	Tc-99	U-238	Cr	Tc-99	U-238	Cr
Extract			Water				Acid	
Units		µg/g	pCi/g	µg/g	µg/g	pCi/g	µg/g	µg/g
100.37	CCU_l	276.47	6.32E+01	7.75E-03	6.75E-01	1.01E+03	7.08E-01	1.72E+01
101.33	CCU_l	138.24	1.03E+02	2.79E-02	2.43E+00	1.65E+02	2.61E+00	2.57E+01
101.98	CCU_l	239.88	1.18E+02	2.38E-02	2.83E+00	1.58E+02	3.14E+00	1.43E+01
105.39	CCU_l	177.97	1.78E+02	1.04E-02	5.54E-01	1.92E+02	9.18E-01	1.64E+01
106.09	CCU_l	192.71	2.07E+02	7.38E-03	9.32E-01	2.99E+02	5.48E-01	1.06E+01
107.42	CCU_l	87.41	9.80E+01	2.66E-03	6.25E-01	1.25E+02	4.12E-01	9.12E+00
110.98	R_{tf}	548.12	2.45E+02	6.91E-03	2.45E+00	2.70E+02	4.55E-01	2.47E+01
110.98	R_{tf}	477.37	2.28E+02	6.50E-03	2.19E+00	1.67E+02	4.04E-01	1.86E+01
115.25	R_{tf}	1305.59	1.16E+03	4.46E-03	3.67E-01	2.90E+03	6.95E-01	2.57E+01
116.02	R_{tf}	2565.63	6.11E+03	4.70E-03	8.66E-01	4.67E+03	6.63E-01	1.79E+01
120.3	R_{tf}	562.95	5.06E+02	8.79E-04	(6.39E-04)	6.45E+02	5.64E-01	1.50E+01
120.97	R_{wi}	718.61	5.72E+02	7.41E-04	(1.78E-03)	1.34E+03	3.87E-01	1.13E+01
123.32	R_{wi}	111.65	1.13E+02	7.13E-04	(3.75E-04)	2.38E+02	3.86E-01	2.28E+01
124.05	R_{wi}	245.03	2.64E+02	1.45E-04	(6.25E-04)	2.53E+02	3.15E-01	5.04E+00
127.13	R_{wi}	140.55	6.13E+01	2.69E-04	(9.55E-04)	2.34E+02	3.45E-01	4.45E+00

( ) = Data below quantification values but deemed qualitatively useful.

NS = no sample generated.

Yellow shading represents samples that do or may indicate some Hanford waste fluids are present.

Table 6.4. Inventory Estimates for Potential Contaminants of Concern in Borehole C4105 Sediments

Depth (ft bgs)	Strat. Unit	Nitrate	Tc-99	U-238	Cr	Tc-99	U-238	Cr
Extract		Water				Acid		
Units		µg/g	pCi/g	µg/g	µg/g	pCi/g	µg/g	µg/g
15.3	Bkfl	1.59	(0.00)	1.99E-03	(1.52E-04)	(0.00E+00)[a]	4.76E-01	1.18E+01
22.7	Bkfl	0.77	(0.00)	1.32E-03	(1.63E-04)	<4.68E+01	4.16E-01	3.39E+01
36.8	Bkfl	0.5	(0.02)	2.89E-03	1.24E-03	0.00E+00	4.21E-01	2.54E+01
40.2	Bkfl	1.4	(0.05)	4.02E-03	1.03E-03	0.00E+00	4.46E-01	2.67E+01
48.4	H2	1.5	<0.170	5.23E-04	(1.07E-04)	<4.28E+01	4.38E-01	1.14E+01
56.1	H2	2.17	(0.10)	4.23E-04	9.15E-03	(9.00E-01)	4.04E-01	8.34E+00
70.1	H2	15.44	9.04E+00	1.38E-03	1.09E-01	(1.10E+01)	3.68E-01	1.27E+01
81.2	H2	9.37	6.04E+00	1.31E-03	7.19E-02	(8.56E+00)	5.14E-01	1.26E+01
86.7	CCU_u	1033.64	1.05E+03	1.29E-03	4.15E+00	1.06E+03	6.79E-01	2.45E+01
88.2	CCU_u	1612.98	1.65E+03	1.22E-03	4.24E+00	7.34E+02	7.17E-01	2.34E+01
88.2	CCU_u	1410.42	1.41E+03	1.22E-03	3.40E+00	1.87E+03	6.60E-01	2.52E+01
93.3	CCU_l	1066.31	8.12E+02	3.27E-03	1.28E+00	1.38E+03	8.49E-01	1.50E+01
97.1	CCU_l	768.82	4.97E+02	1.67E-03	3.76E-02	5.41E+02	8.42E-01	1.56E+01
100.3	CCU_l	458.07	4.07E+02	2.02E-03	1.49E-02	6.13E+02	7.04E-01	1.28E+01
102.0	CCU_l	625.18	8.21E+02	3.82E-03	2.15E+00	5.57E+02	1.93E+00	1.07E+01
103.2	CCU_l	609.71	7.83E+02	3.99E-03	2.52E+00	7.64E+02	1.69E+00	1.40E+01
106.9	CCU_l	949.66	3.94E+02	3.40E-03	4.25E+00	8.17E+02	1.02E+00	3.20E+01
110.0	CCU_l	432.34	5.12E+02	8.35E-04	3.59E-01	5.75E+02	4.93E-01	1.55E+01
110.0	CCU_l	425.27	5.44E+02	8.26E-04	9.33E-02	4.48E+02	3.78E-01	1.63E+01
116.0	R_{tf}	402.24	1.94E+02	1.26E-03	(5.15E-04)	9.59E+01	8.16E-01	1.65E+01
120.9	R_{tf}	599.23	6.34E+02	7.49E-04	8.46E-03	5.73E+02	8.76E-01	1.89E+01
123.9	R_{wi}	261.34	2.07E+02	3.68E-04	(6.78E-04)	5.44E+02	7.51E-01	2.14E+01
129.8	R_{wi}	194.83	1.23E+02	1.03E-04	(7.97E-04)	4.44E+02	3.56E-01	1.09E+01

( ) = Data below quantification values but deemed qualitatively useful.
Bright yellow shading represents samples that do indicate some Hanford waste fluids are present. Light yellow shading represents Samples that may contain some Hanford waste fluids.

Table 6.5. Desorption K_d Values (mL/g) for Potential Contaminants of Concern

C4104		Tc-99	U	Cr	Co-60	C4105		Tc-99	U	Cr
Depth (ft bgs)	Strat. Unit	mL/g	mL/g	mL/g	mL/g	Depth (ft bgs)	Strat. Unit	mL/g	mL/g	mL/g
16.18	Bkfl	0.324	1.42E+01	1.60E+03	NA	15.3	Bkfl	ND	7.89E+00	2.57E+03
22.69	Bkfl	0.498	1.04E+01	9.23E+02	NA	22.7	Bkfl	ND	1.32E+01	8.76E+03
30.74	Bkfl	0.587	1.29E+01	9.20E+02	NA	36.8	Bkfl	-5.36E-02[(a)]	7.76E+00	1.09E+03
36.88	Bkfl	1.969	2.59E+01	6.54E+02	NA	40.2	Bkfl	-7.62E-02	8.39E+00	1.98E+03
37.4	Bkfl	18.285	1.75E+01	1.97E+04	NA	48.4	H2	ND	3.12E+01	3.97E+03
40.01	Bkfl	3.118	2.38E+00	1.40E+03	-0.02	56.1	H2	3.39E-01	4.13E+01	3.95E+01
40.01	Bkfl	ND	7.55E+00	2.14E+02	NA	70.1	H2	-9.87E-03	6.43E+01	2.29E+01
46.33	H2	0.210	5.58E-01	1.12E+02	NA	70.1	H2	9.86E-03	1.22E+01	5.29E+00
46.98	H2	0.336	6.08E-01	6.19E+01	0.31	81.2	H2	2.01E-02	1.91E+01	8.52E+00
58.39	H2	0.367	1.81E-01	2.80E+02	NA	86.7	CCU_u	8.05E-04	7.56E+01	7.09E-01
58.39	H2	0.396	1.14E-01	1.38E+02	NA	88.2	CCU_u	-1.14E-01	1.80E+02	1.40E+00
59.09	H2	0.245	6.74E-02	1.37E+01	0.33	88.2	CCU_u	-1.10E-01	1.16E+02	9.00E-01
63.38	H2	0.180	6.24E-02	2.60E+01	NA	88.2	CCU_u	6.22E-02	1.02E+02	1.21E+00
64.03	H2	0.157	1.77E-01	3.88E+00	NA	93.3	CCU_l	1.83E-01	2.18E+02	2.90E+00
64.03	H2	0.179	2.34E-01	1.60E+00	0.23	93.3	CCU_l	9.31E-02	3.44E+01	1.42E+00
64.03	H2	0.186	1.95E-01	2.64E+00	0.14	97.1	CCU_l	1.09E-02	6.09E+01	5.02E+01
76.03	H2	0.599	8.72E-02	1.14E+00	0.22	100.3	CCU_l	3.76E-02	2.58E+01	6.39E+01
81.04	CCU_u	0.615	1.86E-01	2.14E+00	0.21	102	CCU_l	-3.07E-02	4.80E+01	3.80E-01
87.35	CCU_u	-0.001	3.59E+00	4.85E+00	0.17	103.2	CCU_l	-2.36E-03	4.06E+01	4.38E-01
87.35	CCU_u	0.045	1.29E+00	3.13E+00	0.16	106.9	CCU_l	-7.16E-02	9.25E+01	4.79E-01
87.35	CCU_u	0.055	1.20E+00	3.91E+00	0.12	106.9	CCU_l	2.73E-01	7.59E+01	1.65E+00
92.61	CCU_l	0.457	4.95E-01	1.13E+00	0.07	110	CCU_l	8.27E-03	3.94E+01	2.81E+00
93.56	CCU_l	0.383	1.06E+02	1.41E+00	0.14	110	CCU_l	-1.39E-02	3.68E+01	1.36E+01
93.56	CCU_l	0.172	3.32E+01	4.36E-01	0.07	116	R_{tf}	-1.11E-01	1.42E+02	7.05E+03
94.67	CCU_l	0.213	1.53E+01	1.58E+00	0.06	120.9	R_{tf}	7.94E-03	4.25E+02	1.29E+03
99.7	CCU_l	0.306	5.06E+00	2.80E+00	NA	120.9	R_{tf}	-2.48E-02	2.98E+02	5.69E+02
100.37	CCU_l	1.257	7.58E+00	2.06E+00	NA	123.9	R_{wi}	5.57E-03	3.95E+02	5.40E+02

Table 6.5. (contd)

C4104		Tc-99	U	Cr	Co-60
Depth (ft bgs)	Strat. Unit	mL/g	mL/g	mL/g	mL/g
101.33	CCU_l	**0.052**	9.70E+00	**9.92E-01**	**NA**
101.98	CCU_l	**NA**	NA	**NA**	**NA**
101.98	CCU_l	**0.069**	2.71E+01	**8.37E-01**	**NA**
105.39	CCU_l	**-0.012**	7.13E+00	**2.32E+00**	**NA**
106.09	CCU_l	**0.042**	6.98E+00	**9.90E-01**	**NA**
107.42	CCU_l	**0.014**	7.67E+00	**6.80E-01**	**NA**
110.98	R_{tf}	**0.016**	1.05E+01	**1.47E+00**	**NA**
110.98	R_{tf}	**-0.029**	6.57E+00	**8.04E-01**	**NA**
115.25	R_{tf}	**0.309**	3.14E+01	**1.40E+01**	**NA**
116.02	R_{tf}	**-0.052**	1.36E+02	**7.75E+00**	-0.25
116.02	R_{tf}	**-0.058**	3.43E+01	**4.83E+00**	NA
120.3	R_{tf}	**-0.008**	7.57E+01	2.87E+03	NA
120.97	R_{wi}	**0.269**	2.42E+02	5.65E+03	-0.17
120.97	R_{wi}	**0.225**	8.74E+01	1.07E+03	NA
123.32	R_{wi}	**0.011**	1.11E+01	1.25E+03	NA
124.05	R_{wi}	**-0.002**	1.01E+02	3.73E+02	NA
127.13	R_{wi}	**0.147**	6.73E+01	2.44E+02	NA

C4105		Tc-99	U	Cr
Depth (ft bgs)	Strat. Unit	mL/g	mL/g	mL/g
123.9	R_{wi}	**-1.19E-01**	6.75E+01	1.04E+03
129.8	R_{wi}	**1.34E-01**	1.78E+02	7.03E+02

NA = No detectable Co-60/Tc-99 in the sediment or the water extracts; thus can not calculate a K_d. ND = not determined because not enough sample available.

Red (bold) type signifies depths where sediments show obvious signs of some tank related fluids.

Yellow (dark) shading signifies K_d values that are dominated by tank fluids as opposed to a mix of natural and Hanford constituents. Faint blue (light) shading data are likely more dominated by natural constituents (uranium and chromium) or imprecise analytical data (technetium-99 and cobalt-60).

(a) = negative K_d are caused by analytical uncertainties in the measurements of concentrations in the sediment and porewater. For risk analysis assume that negative values are 0 mL/g.

The changes in K_d values for technetium-99 outside the zone of significant contamination are likely more a function of imprecision in the acid versus water extract analytical results. There does not seem to be any difference in the cobalt-60 K_d values in the depths where cobalt-60 is present at measurable concentrations and those zones shallower and deeper where cobalt-60 is not present at readily measurable concentrations. The other trend is that the desorption K_d values for technetium-99 and cobalt-60 in the main portion of the vadose zone plumes are very close to 0 mL/g, while the desorption K_d value for uranium in the main portion of the tank fluid plumes varies between 0.06 and 2 mL/g in borehole C4104 and between 30 and 80 mL/g in borehole C4105 sediments. The desorption K_d values for chromium in the zones where elevated chromium is present vary between 0.5 and 5 mL/g in both borehole vadose zone sediments.

The in situ desorption K_d results suggest that of the potential contaminants, technetium-99 and cobalt-60, are quite mobile, while uranium is considerably less mobile and chromium is the least mobile. For conservative modeling purposes, we recommend using K_d values of 0 mL/g for nitrate, cobalt-60, and technetium-99, a value of 0.1 mL/g for uranium near borehole C4104 and 10 mL/g for uranium at borehole C4105, and 1 mL/g for chromium to represent the entire vadose zone profile from the bottoms of the tanks to the water table. The technetium in situ desorption K_d value of zero is consistent with a wealth of literature that finds essentially no technetium adsorption onto Hanford Site sediment (Kaplan and Serne 1995; Kaplan and Serne 2000 and Cantrell et al. 2003). The cobalt-60 mobility suggests that some complex that perhaps has a net negative charge is altering cobalt's inherent cationic nature. Cobalt-60 has been found in the Hanford groundwater at several places, especially in the 1950s, and can still be measured in a few locations, most notably in the northern 200 East Area (Hartman et al. 2003 and 2004).

6.7 Other Geochemical Characterization Observations

The comparison of the percentage of a constituent that is water extractable versus acid extractable from the contaminated sediment and the total mass that is acid leachable can be used to infer contamination for Hanford tank constituents such as sodium, sulfate, uranium, chromium, and other trace metals that occur naturally in the environment.

For borehole C4104, the acid-extract data for most species suggest that variations in mass leached per gram of sediment versus depth are lithology-related more so than an indication of tank fluid contamination. However, for a few species such as sodium, sulfate, technetium-99, and uranium, chromium, molybdenum and ruthenium at selected depth regions, the acid extract concentrations are elevated and indicative of tank fluids being present. Acid-extractable sodium is elevated from 36 to 102 ft bgs and acid-soluble sulfate is elevated throughout most of the profile indicating that the tank fluids also contained significant quantities of sulfate. The acid-extractable technetium-99 profile in the C4104 borehole sediments is elevated throughout most of the profile and correlates well with the water extract profile although the acid extract values are larger for every sample. The acid extract technetium-99 data are variable and are below our level of quantification. As found in sediments at borehole 299-E33-46 (see Serne et al. 2002f), measuring technetium-99 at low levels by acid extraction yields results that are not as reliable as water extraction data. We thus place more confidence in the water-extract technetium-99 data. The acid-extractable uranium concentrations from the C4104 sediments clearly indicate elevated values between 58 and 94 ft bgs; although natural sediment concentrations in the Cold Creek lower subunit (caliche) often approach the values found in the samples that are considered to be elevated. Thus, the acid-extractable uranium in the CCU_l strata (1 to 2.5 μg/g; [ppm]) is an indication that the tank leak

contained low concentrations of uranium. The acid-extractable chromium and molybdenum in the sample at 58.4 ft bgs is the largest observed for these metals. The rest of the sediment profile does not show atypically high values of acid-extractable chromium but the acid-extractable molybdenum values between 58 and 115 ft bgs do appear to be quite variable and larger than quantities that are acid extractable from background sediment. The acid-extractable ruthenium is also variable and higher than found in background sediments and is likely indicative of fission product-derived material.

The water versus acid extract data for C4104 sediments shows distinct regions where the water to acid extractable percentages are much larger than found for uncontaminated borehole (299-W10-27) sediments. At C4104, there are clear indications of tank fluids present in the vadose zone profile; the following qualitative measure of mobility is inferred: technetium-99 and ruthenium are slightly more mobile than molybdenum, sulfate, and chromium. Zinc and uranium are less mobile than these noted species.

Upon comparing the acid extract data for borehole C4105 with similar lithologies in the uncontaminated borehole 299-W10-27, most of the variation in mass leached per gram of sediment versus depth is found to be lithology related. That is, for most major constituents there are no signs of elevated values of acid-leachable constituents in borehole C4105 sediments, excepting acid-extractable sodium in the backfill, one elevated acid-extractable calcium value at 81.2 ft bgs near the bottom of the Hanford H2 unit, sulfate throughout the profile, and the elevated technetium-99, ruthenium and molybdenum from the tank leak. The high acid-extractable sodium in the shallow background sediments suggests some waste was released on the sediment surface or from pipelines, the elevated calcium near the bottom of the Hanford H2 unit may indicate that the ion exchange front from the tank waste plume has reached C4105 borehole via horizontal flow. For the mobile fission products technetium-99, molybdenum and ruthenium, the C4105 acid extracts show elevated concentrations from 86.7 to the bottom of the borehole ~130, 93.3 to 110, and 86.7 to 110 ft bgs, respectively. The comparison of water to acid extracts for borehole C4105 sediments suggests that there are unnaturally high percentages (technetium-99: 50 to 100%; molybdenum: 3 to 50%; ruthenium: 30 to 85%) of water-leachable technetium-99, molybdenum, and ruthenium between the stated depths.

The acid-extractable concentrations of major cations in the sediments at C4105 show significantly less sodium than the sediments at C4104 as would be expected if the tank leak fluids were interacting with the sediments and having sodium get incorporated into or onto the sediments in a form that readily dissolves in strong acid. Both ion exchangeable and sodium-rich secondary minerals would dissolve in the strong acid. There also appears to be less acid-soluble phosphate in the C4105 sediments than the C4104 sediments suggesting that phosphate present in the T-106 tank fluid that leaked deposited measurable amounts in the vicinity of C4104 but not in the vicinity of C4105.

These comparisons suggest that truly mobile constituents such as technetium-99 descended deep into the sediment profile from the tank T-106 bottom near C4104 as well as spreading out horizontally all the way to the C4105 sediments. Other water-extract data suggests that the Cold Creek Formation upper subunit was the stratum that promoted most of the horizontal migration. The water- to acid-extractable uranium percentages for the C4105 sediments do not show any high values (all are <1%) such that we do not believe there are measurable quantities of tank-derived uranium in the C4105 sediments. Uranium must be interacting quite significantly with the vadose sediments because it is not observed at elevated

concentrations at C4105. Some interaction is also indicated for chromium and molybdenum because acid extractable concentrations at C4105 are lower than at C4104 in contrast to technetium-99, which is higher in sediments from borehole C4105.

As part of our characterization strategy for contaminated sediments, other parameters that can control contaminant migration were measured. For the T tank farm characterization, only calcium carbonate content and the particle size and bulk sediment and clay-sized fraction mineralogy of selected samples from C4105 borehole were measured. Photographs provided in Appendix A and the field moisture log, blow counts, and laboratory moisture contents identify that several fine-grained thin lenses are present within the Hanford formation H2 unit that can promote lateral spreading of leaked fluids. The upper, and to some extent, lower portions of the Cold Creek unit also contain a high percentage of fines that can lead to perched conditions and/or lateral spreading of percolating fluids. The Ringold Formation Taylor Flat member is also relatively fine-grained. XRD patterns for selected sediment samples from borehole C4105 are shown in Appendix C. Briefly, XRD analysis of C4105 borehole samples, excluding the Cold Creek lower subunit (caliche), shows the sediments are mineralogically quite similar. The sediments are dominated by quartz and feldspar (both plagioclase and alkali-feldspar), with lesser amounts of clay, calcite, and amphibole. For the non-caliche bearing samples characterized, quartz concentrations range from 27 to 54 wt%,) with an average quartz concentration of 38 ± 10 wt%. Plagioclase feldspar is present at concentrations between 12 to 43 wt% and potassium feldspar concentrations are between 4 to 15 wt%. Plagioclase feldspar was more abundant than potassium feldspar in all C4105 samples. The amphibole phase comprised <5 wt%. Calcite concentrations measured 55 wt% in caliche sample, with all other samples having <4 wt%. Clay minerals consist primarily of chlorite, smectite) and mica and they make up between 8 and 32 wt% of the bulk sediment samples.

The clay-sized fraction of the caliche-free sediment is dominated by four clay minerals: smectite, chlorite, illite, and kaolinite with minor amounts of quartz and feldspar. Smectite concentrations range from 26 to 56 wt%. Illite concentration varies from 33 to 50 wt% with an average concentration of 42 wt%. Chlorite and kaolinite are the least abundant of the clay minerals identified in the samples with concentrations equal to or less than 20 and 7 wt%, respectively.

Based on the distribution of tank T-106 constituents, potentially mobile tank constituents (nitrate, technetium-99, cobalt-60, uranium, and chromium(VI), and the ion exchange fronts for sodium replacing the native calcium and magnesium), it appears that there is a large horizontal component to the path that the leaked fluids took from the T-106 tank as it percolated into the vadose zone sediments at the three boreholes described in this report (C4104, 299-W10-196, and C4105). That is, the fine-grained sediments in the Cold Creek Formation and Ringold Taylor Flat Member have acted as a barrier to significant vertical percolation of contaminants below tank T-106 at least in the region probed by the three boreholes. As discussed in more detail in Chapter 3 of the T-TX-TY field investigation report,[(a)] based on gross- and spectral- gamma field logging, it also appears that some of the horizontal migration of contaminants in the southwesterly direction (towards borehole C4105) from the two boreholes just south of T-106 tank occurred several years after the 1973 leak event. It is speculated that the large snow-melt event in February 1979 may have provided the driving force for this post-tank leak horizontal migration of T-106 tank constituents.

(a) *Field Investigation Report for Waste Management Areas T and TX-TY*, by FJ Anderson (CH2M HILL Hanford Group, Inc., Richland, Washington), under preparation.

There are highly calcareous zones associated with the lower Cold Creek subunit in both boreholes (CCU_l was not cored in the background borehole at T Tank Farm) at depths that range from 92.6 to 102, and 93.3 to 103 ft bgs at C4104 and C4105, respectively. The caliche content in the samples characterized varies from 16 to 60% by weight in the two boreholes. The wide range in calcium-carbonate contents reflects the variability in weathering processes and time for paleosol horizon development. The caliche at borehole C4105 corresponds quite well to the high values (quantity) and depth of occurrence as the data from borehole C4104. This suggests that the caliche lenses are fairly continuous between these two boreholes. The sediment in the shallow Hanford formation H2 unit for the two contaminated and background borehole contains relatively low calcium carbonate (<2 wt%) and organic carbon. At depth, the H2 unit shows slightly more calcium carbonate (~ 4 wt%). The fine-grained CCU_u samples contain up to 3.3 wt% calcium carbonate. These data for the identified stratigraphic units are quite similar to the data for the same units at the TX Tank Farm background borehole (see Serne et al. 2004).

At 299-W11-39, continuous coring was not performed all the way to the water table; thus, the entire matric potential profile is not available. For the core samples available from 299-W11-39, the water potentials are generally much less than the gravity potential from the shallowest core at 50 ft bgs, which means that the water potentials are consistent with a draining profile. For the core samples available from C4104, the measured water potentials are quite erratic and about two-thirds of the datum are generally greater than the gravity potential, especially in the deeper samples. Two of the samples, 8A and 16A, have very high matric potentials (signifies very dry conditions). About one-third of the matric potentials are very low in comparison of the gravity head suggesting a draining profile, but the general trend for the data from C4104 is that the water potentials are erratic and should not be used to infer whether the profile is draining or actively evapotranspiring water. It appears that inadvertent drying occurred in many of the samples during the core processing, sample photographing and aliquoting for geochemical characterization.

6.8 Description of T Upper Unconfined Aquifer

The suprabasalt aquifers below the Hanford Reservation have been impacted by past practice, liquid waste disposal operations and unplanned releases, and in some instances from single-shell tank leaks. In the area of WMA T, large volumes of waste water disposed to ground between the 1940s and 1997 created large artificial groundwater mounds particularly beneath the 216-T pond system, north of WMA T, and beneath the 216-U pond, southwest of WMA T. The disposed liquids contained many of the contaminants that now move through the upper unconfined aquifer.

The base of the uppermost, unconfined aquifer generally is regarded as the basalt surface and, where this is the case, the entire suprabasalt aquifer is unconfined. However, beneath WMA T (and beneath the entire 200 West Area), the silt and clay deposits of the Ringold Formation lower mud unit form a confining layer that separates the suprabasalt aquifer into the uppermost unconfined aquifer and the underlying Ringold confined aquifer (Williams et al. 2002). Thus, the uppermost, unconfined aquifer in the WMA T area extends from the water table down to the top of the lower mud unit. The unconfined aquifer is about 50 meters thick at well 299-W10-24, located at the northeast corner of WMA T, based on the August 2003 water level. The unconfined aquifer consists of sandy gravels and gravelly sands of the Ringold Formation member of Wooded Island. All wells in the WMA T monitoring networks are screened in hydrogeologic unit 5. Currently, the water table at WMA T is 136 to 137 m above sea level.

Water levels in the uppermost unconfined aquifer raised as much as 13.5 meters (above the pre-Hanford natural water table) beneath WMA T because of artificial recharge from liquid waste disposal operations active since the mid 1940s. The largest volumes of discharge were to the 216-T pond system and the 216-U-10 pond. The 216-T pond system is estimated to have received approximately 424 billion liters of effluent and the 216-U pond to have received about 158 billion liters of effluent. The large-volume disposals to the ponds (and, lesser volumes to cribs and ditches) artificially recharged the uppermost unconfined aquifer creating these large water-table mounds. The increase in water-table elevation was most rapid from 1949 to 1956 and was somewhat stabilized between the late 1960s and the late 1980s. Water levels began to decline in the late 1980s beneath WMA T when wastewater discharges in the 200 West Area were reduced. Hydrographs show that water levels have declined by about 6.5 meters since 1991 beneath the T tank farm. This decline, resulting from decreasing effluent discharge in the 200 West Area, became much steeper in 1995 with the effective cessation of discharge to all non-permitted facilities in this area. Between 1998 and 2004, the average rate of water table decline has been between about 0.3 and 0.4 meter per year in all monitoring wells at WMA T. The rapid decrease in water levels after 1995 has resulted in monitoring wells going dry more quickly than previously predicted and has necessitated the drilling of 7 new monitoring wells since 1999. Recently, Bergeron and Wurstner (2000) modeled the elevation of the water table beneath the Hanford Site. Their results predict a post-Hanford Site influenced water table elevation of about 130 to 132 meters above sea level in the T tank farm area.

Accompanying the changes in water level were changes in groundwater flow direction. Pre-Hanford Site groundwater flow direction was toward the east; groundwater flow changed toward the south in the area by the early 1950s. This shift resulted from the disposal of large volumes of liquid to the 216-T pond system. In 1956, groundwater flow direction changed again and started flowing towards the northeast due to the increasing influence of the groundwater mound under 216-U pond and a decreasing influence of the mound under 216-T pond. Discharges to 216-T pond ended in 1976 but continued at 216-U pond until 1984. As discharges to the 216-U pond declined in the early 1980s, groundwater flow shifted to a more northerly direction as the groundwater mound began to decrease and discharges to the 216-U-14 ditch continued. The slight westerly component to the groundwater flow direction between early 1980s and mid 1990s is probably a result of the discharges to the 216-U-14 ditch, located southwest of WMA T. All non-permitted discharges to the ground ceased and the influence of the 216-U pond mound on the groundwater beneath the T tank farm diminished in 1995. Consequently, the flow direction changed again in about 1996 and began to return toward an easterly direction.

These large shifts in groundwater flow direction have large implications for contaminant distribution in the uppermost aquifer beneath WMA T. In the late 1940s and early 1950s, contamination was spread south in the aquifer. Then, in the late 1950s and until the mid-1990s, that same contamination returned to the north along with any new contamination that entered the aquifer after the 1950s. Today, groundwater contamination beneath the WMA and surrounding area is generally migrating east.

Recent more detailed characterization of monitoring wells found vertical flow gradients detected in some wells, especially along the current downgradient edge of WMA T [eastern edge] that may have an impact on contaminant distribution patterns in the area. Other hydrologic test data suggest higher or lower hydraulic conductivity zones occur at certain depths within the screened interval of some wells relative to other depths. For example, tracer tests indicate that the upper 3 to 4 meters of the screened interval of well 299-W10-24 is less permeable than the lower part of the screened interval. However, a tracer test in nearby well, 299-W11-39, indicated that the lower 3 meters of the screened interval are

relatively impermeable compared to the rest of the screened interval. Thus, apparent differences in permeability do not appear to correlate from well to well. However, there is nothing in the geologist's logs or the geophysical logs to suggest that the formation in the screened interval of these wells is significantly different than the formation at nearby wells.

Taken as a whole, the geologist's logs, geophysical logs, well-development pumping data, and the hydrologic testing data all indicate heterogeneity in aquifer properties within the screened intervals of several individual wells and among wells at WMA T.

6.9 Historical Groundwater Contamination

The earliest evidence of groundwater contamination around WMA T as found in the Hanford Environmental Information System (HEIS)[a] database is high levels of gross beta and nitrate in wells located near the cribs and trenches west of WMA T. By 1955 and 1956, levels of gross beta and nitrate had reached values in excess of 1,000,000 pCi/L and 3,000 mg/L, respectively, in well 299-W10-2 located about 20 meters south of the 216-T-7 tile field. The oldest available analysis for cobalt-60 in groundwater in the area is from well 299-W10-4 in 1957 and showed that the cobalt-60 concentration was 2000 pCi/L at that time. Cobalt-60 was later found in well 299-W10-2 in 1969 at a concentration of 680 pCi/L. Finally, ruthenium-106 was first noted in groundwater in 1972 at wells 299-W10-2 and 299-W10-4. These data are the oldest available analyses and may not represent the first arrival of contamination in groundwater in the area. The most likely source for this contamination is either the 216-T-7 crib/tile field, which operated between 1947 and 1955 and received 110,000,000 L of effluent, or the 216-T-32 crib, which operated between 1946 and 1952 and received 29,000,000 L of waste. Groundwater at that time was flowing toward the south from the disposal facilities toward the wells in which the contamination was observed in 1955 through 1972. The known and suspected T tank leaks occurred later and at locations that are too far away to have reached these wells at the cited dates. On the other hand given slightly increased groundwater velocities caused the mounding under the T WMA, both 216-T-7 and 216-T-32 contaminants could have readily reached the two wells by 1955.

6.10 Existing Groundwater Contamination

Groundwater at the T tank farm contains elevated concentrations of carbon tetrachloride, trichloroethene, chromium, nitrate, fluoride, technetium-99, and tritium. This contamination is a result of mixing of wastes from a number of past waste-disposal activities, including the disposal of process water and steam condensate at nearby ponds, cribs, and trenches; disposal of plutonium processing waste at cribs and trenches associated with the Plutonium Finishing Plant; and leaks from single-shell tanks and transfer lines within the T tank farm. Because concentrations change over time, a time-period must be chosen to examine spatial distribution patterns. For this purpose, the most recent data (average of fiscal year 2003 sampling events) were chosen.

Carbon tetrachloride is present in the unconfined aquifer beneath most of the 200 West Area. The highest carbon tetrachloride concentration near WMA T in fiscal year 2003 was 1,550 μg/L in well 299-W10-4, south of the waste management area. High concentrations were also found north

---

(a) The Hanford Environmental Information System (HEIS) is a Hanford Site resource owned by the Department of Energy and operated by Fluor Hanford.

(299-W10-23) and east (299-W11-7) of the waste management area. The carbon tetrachloride is believed to be from pre-1973 waste from the Plutonium Finishing Plant and not from the WMA T farm.

The major sources for trichloroethene are disposal sites associated with the Plutonium Finishing Plant. A second potential source is disposal near T Plant. The maximum trichloroethene concentration found near WMA T in 2003 was 10 μg/L both north (well 299-W10-23) and south (well 299-W10-4). The T tank farm waste management area is not considered a source for trichloroethene.

The highest chromium concentrations are in upgradient wells 299-W10-28 and 299-W10-4 where chromium reached 215 and 347 μg/L, respectively, in 2003. Chromium was also elevated in well 299-W10-3, located inside the tank farm fence between the 216-T-7 crib and tile field and the 216-T-32 crib and upgradient of the current groundwater flow direction at T tank farm. This well was sampled only in 2000 during its decommissioning when the chromium concentration was 257 μg/L. Prior to about 1997 when groundwater flow direction was toward the north, several wells on the north (then downgradient) side of the waste management area had relatively high chromium concentrations. Also, prior to 1997, well 299-W10-1, which was parallel to the tank farm with respect to groundwater flow direction but downgradient of the 216-T-5 trench, the 216-T-7 crib and tile field, and the 216-T32 crib, had chromium concentrations exceeding 200 μg/L. After flow direction changed toward the east in about 1997, chromium concentrations dropped to <40 μg/L in well 299-W10-1, decreased in all of the northern wells, and began increasing in well 299-W10-4.

The most likely source for the chromium west and north of Waste Management Area T is one or more of the disposal cribs and tile fields upgradient of the T tank farm WMA. Chromium from these facilities would have been moving north across well 299-W10-1 prior to 1997 and then east across the northern wells and the rest of the waste management area after 1997. Finally, since December 2000, chromium has exceeded the maximum contaminant level in two downgradient wells, 299-W11-41 (average for fiscal year 2003, 141 μg/L) and 299-W11-42 (average for fiscal year 2003, 132 μg/L). These wells are located downgradient of the disposal facilities east of WMA T but appear to be too far away for chromium to have migrated from west of the WMA to the wells since the 1996 change in groundwater flow direction, given a flow rate of 0.025 meter per day.

A regional nitrate plume underlies WMA T and much of the north part of the 200 West Area. However, unlike, carbon tetrachloride, trichloroethene, and tritium, there also appears to be a source of nitrate local, and upgradient, to Waste Management Area T. All monitoring wells in the WMA T monitoring network have nitrate concentrations in excess of the 45,000 μg/L maximum contaminant level. The highest nitrate concentrations at the Hanford Site in fiscal year 2003 were from two upgradient wells at WMA T: 1,985,000 μg/L in well 299-W10-4 and 1,835,000 μg/L in well 299-W10-28. The nitrate concentration began to increase in well 299-W10-4 in about 1997 when the groundwater flow direction changed from northerly to easterly. Concentrations continued to rise until just recently. Since it was drilled in 2001, nitrate concentration in well 299-W10-28 has always been high and parallel to concentrations in well 299-W10-4. The most likely source for the nitrate in this area is one or more of the past-practice liquid disposal facilities upgradient of the T tank farm.

Fluoride concentrations exceeded the drinking water standard (4,000 μg/L) in three wells at Waste Management Area T in 2003. Currently, the highest concentrations are in downgradient wells but historically, the highest fluoride concentration was in upgradient well 299-W10-4 in late 1999

(5,250 μg/L). A fluoride plume appears to have passed well 299-W10-4 between mid-1997 and late 2000. Although it is possible that there is a tank farm source for the fluoride contamination, one or more of the nearby cribs are believed to be a more likely source.

A technetium-99 groundwater plume exists northeast and east of Waste Management Area T. The highest technetium-99 concentration in fiscal year 2003 was 9,200 pCi/L in downgradient well 299-W11-39. The most probable source for the technetium-99 is the T tank farm waste management area. Technetium-99 began to increase in well 299-W11-27, located at the northeast corner of the 241-T tank farm in late 1995, coincident with the cessation of surface water disposal in the 200 West Area. Concentrations reached a maximum of 21,700 pCi/L in February 1997. Technetium-99 concentrations in well 299-W11-27 subsequently decreased to 6,000 pCi/L in March 1999. Hodges (1998) suggested that technetium-99 had arrived at well 299-W11-27 by the early 1990s, but was masked by dilution with water from a leaking water line located immediately adjacent to the well. The water line carried cooling and ventilation steam condensate, process cooling water, and evaporator condensate from the 207-T retention basin to the 216-T-4-2 ditch until 1995. The subsequent decrease in technetium-99 in well 299-W11-27 since 1997 may be a result of changing groundwater flow direction. In November 1997, technetium-99 began to increase in well 299-W11-23, located east of well 299-W11-27, coincident with the change in groundwater flow to a more easterly direction. It increased to a high of 8,540 pCi/L in November 1998; subsequently, technetium-99 values fluctuated between 7,110 and 840 pCi/L before the well went dry.

The most plausible explanation for the 1997 arrival of the contaminant plume at well 299-W11-23 is the change in groundwater flow direction. If this is the case, a narrow contaminant plume initially moved northeast across well 299-W11-27 but not across well 299-W11-23. Changing groundwater flow direction caused this plume to drift east across well 299-W11-23. Sampling of replacement well 299-W11-39 in 2001 detected technetium-99 concentrations between 4,160 and 5,010 pCi/L, indicating contamination of the upper portion of the aquifer at this well. Subsequently, technetium-99 concentration rose to a high of 10,400 pCi/L in February 2003 and began a small decline in August 2003.

In early 2002, technetium-99 concentrations began to increase in well 299-W11-42, south of well 299-W11-39 and, in early 2003, technetium-99 began to increase in well 299-11-41, south of 299-W11-42. Apparently, the technetium-99 contamination that was detected in the northeast corner of 241-T tank farm is spreading southward along the east and downgradient side of the WMA. The highest recent technetium-99 concentrations are at or near the water table and concentrations decrease rapidly with increasing depth in the aquifer. This points to a nearby source for the technetium-99 because the contaminant has not traveled far enough to descend vertically into the aquifer. The apparent nearness of the technetium-99 source suggests that the T tank farm is the most likely origin for the technetium-99.

A tritium plume lies beneath much of the north half of the 200 West Area. The plume geometry suggests that the major tritium source is near the 242-T evaporator, the TY tank farm, and nearby cribs. Other contributing sources are likely present in the vicinity of the T tank farm and include associated cribs and trenches and potentially leaks from T farm tanks. The highest tritium concentration near WMA T in 2003 was 52,100 pCi/L in well 299-W11-12, located at the southeast corner of the waste management area. Waste Management Area T is not thought to be a major contributor of tritium to groundwater in the area.

6.11 Complexities in Groundwater Data (Vertical and Temporal Variations)

The groundwater data are complicated by signs that vertical stratification in contaminant and common solutes is present in many wells. Significant differences in specific conductance, technetium-99, chromium, nitrate, and tritium with depth were found in some monitoring wells. After purging some T wells, the pumped samples do not appear to be representative of ambient water because purging the well causes mixing of strata with different contaminant concentrations. Thus, interpreting the contaminant distribution in such wells is very difficult because groundwater at the well contains high concentrations of several contaminants that show different vertical concentration profiles and probably come from several sources in the area.

6.12 Vadose Zone Porewater and Groundwater Chemical Ratio Comparisons

To determine whether T tank leaks (T-106 or T-101) or the mentioned cribs and tile fields have impacted groundwater quality, one or more components of the leak need to be detected in groundwater. Estimates of the leak composition are available (Jones et al. 2000); unfortunately, the major, mobile components in the tank leak for which we have groundwater data are also major, mobile components disposed of to the nearby cribs and trenches.

The relative concentrations of technetium-99 and chromium behave quite differently at different parts of WMA T. The technetium-99/chromium concentration ratios versus time for samples from upgradient wells and wells to the north of the WMA T have a signature similar to the upgradient crib and trench disposal sites. This information suggests that the contamination detected in wells upgradient and north of WMA T is dominated by crib waste. The technetium-99 – chromium concentration relationship is different in wells located at the northeast corner and east of the WMA where the concentrations of the two constituents do not track each other and suggest a different source for the contamination. Since early 1996, the technetium-99/chromium composition of the groundwater in four wells in the northeast corner of WMA T have evolved toward tank waste compositions. Technetium-99/chromium ratios greater than the estimated tank waste compositions are in agreement with the data from vadose zone porewaters from boreholes C4104 and C4105 (see Section 4 of this report) and probably reflect the slight retardation of chromium relative to technetium-99 as discussed in Section 6.6 (see Table 6.5 for in situ desorption K_d values). Since monitoring began in 1996, the technetium-99 to Cr ratio for groundwater from wells east of WMA T are intermediate between those from wells upgradient (west and north of the WMA) and northeast of the WMA. Samples from the wells to the east of the WMA indicate that the tank waste initially identified at the northeast corner of the WMA is migrating south along the eastern edge of the WMA and is mixing with the crib waste that was initially sampled in the eastern wells.

The compositional relationship between technetium-99 and nitrate at WMA T is complicated by the regional nitrate plume in the area. Unlike technetium-99 and chromium concentrations, the concentrations of technetium-99 and nitrate track each other through time in all monitoring wells at WMA T although there are about 3 orders of magnitude difference in the technetium-99/nitrate groundwater concentration ratios across the WMA. However, when plotted against time and compared to crib and tank waste compositions, the technetium-99/nitrate concentration ratios suggest the same conclusions reached with the technetium-99/chromium ratios. That is, the groundwater from the upgradient wells and wells to the north of WMA T have a strong crib waste component. Water sampled from wells located in the northeast corner of WMA T has a very different technetium-99/nitrate signature

than does water from the upgradient and northern wells. Groundwater in the northeast corner of the WMA tends toward technetium-99/nitrate ratios indicative of tank waste.

The technetium-99/tritium ratios lead to the same conclusions as do the technetium-99/chromium and technetium-99/nitrate ratios. That is, groundwater from wells in the west (upgradient) and north of WMA T appear to be highly influenced by wastes disposed to the cribs and trenches on the west side of the WMA. Groundwater from wells at the northeast corner and the east side of the WMA appears to be evolving towards tank waste that has leaked from tank T-101 or T-106.

7.0 References

Alexander, DJ, SD Evelo, VG Johnson, and MD Sweeney. 1995. *Groundwater Impact Assessment Report for the 216-T-4-2 Ditch.* WHC-EP-0815, Westinghouse Hanford Company, Richland, Washington.

ARHCO 1973. *241-T-106 Tank Leak Investigation,* Atlantic Richfield Hanford Company, Richland, Washington.

American Society of Agronomy (ASA). 1986a. "Hydrometer Method." Chapter 15-5 in *Methods of Soil Analysis-Part 1*, 2nd Edition of Physical and Mineralogical Methods, SSSA Book Series No. 5, ed. A Klute, pp. 404-408. Soil Science Society of America, Madison, Wisconsin.

American Society of Agronomy (ASA). 1986b. "Pynchnometer Method." Chapter 14-3 In *Methods of Soil Analysis-Part 1*, 2nd Edition of Physical and Mineralogical Methods, SSSA Book Series No. 5, ed. A Klute, pp. 378-379. Soil Science Society of America, Madison, Wisconsin.

American Society of Agronomy (ASA). 1996a. *Methods of Soil Analysis-Part 3, Chemical Methods*, SSSA Book Series 5, ed. DL Sparks, Soil Science Society of America, Madison, Wisconsin.

American Society of Agronomy (ASA). 1996b. "Elemental Analysis by XRF Spectroscopy." Chapter 7 in *Methods of Soil Analysis-Part 3, Chemical Methods*, SSSA Book Series 5, ed. DL Sparks, pp. 161-223. Soil Science Society of America, Madison, Wisconsin.

American Society for Testing and Materials (ASTM) D4129-88. 1988. "Standard Test Method for Total and Organic Carbon in Water by High Temperature Oxidation and by Coulometric Detection." American Society for Testing and Materials, West Conshohocken, Pennsylvania.

American Society for Testing and Materials (ASTM) D2488-93. 1993. "Standard Practice for Description and Identification of Soils (Visual-Manual Procedure)." American Society for Testing and Materials, West Conshohocken, Pennsylvania.

American Society for Testing and Materials (ASTM) D2216-98. 1998. "Test Method for Laboratory Determination of Water (Moisture) Content of Soil and Rock." American Society for Testing and Materials, West Conshohocken, Pennsylvania.

American Society for Testing and Materials (ASTM) D-5298-94. 2002. "Test Method for Measurement of Soil Potential (Suction) Using Filter Paper." American Society for Testing and Materials, West Conshohocken, Pennsylvania.

Baker VR, BN Bjornstad, AJ Busacca, KR Fecht, EP Kiver, UL Moody, JG Rigby, DF Stradling, and AM Tallman. 1991. "Quanternary Geology of the Columbia Plateau." In *Quaternary Nonglacial Geology: Conterminous U.S. Geology of North America,* ed. RB Morrison, K-2: 215-250. Geol. Soc. Am., Boulder, Colorado.

Baker, VR and RC Bunker. 1985, "Cataclysmic Late-Pleistocene Flooding from Glacial Lake Missoula: A Review." *Quaternary Science Reviews*, v. 4, pp. 1-41.

Bergeron, MP and SK Wurstner. 2000. *Groundwater Flow and Transport Calculations Supporting the Immobilized Low-Activity Waste Disposal Facility Performance Assessment*. PNNL-13400, Pacific Northwest National Laboratory, Richland, Washington.

Bjornstad, BN. 1984. *Suprabasalt Stratigraphy Within and Adjacent to the Reference Repository Location*. SD-BWI-DP-039, Rockwell Hanford Operations, Richland, Washington.

Bjornstad, BN. 1990. *Geohydrology of the 218-W-5 Burial Ground*. PNL-7336, Pacific Northwest Laboratory, Richland, Washington.

Bjornstad BN, KR Fecht, and CJ Pluhar. 2001. "Long History of Pre-Wisconsin, Ice-Age, Cataclysmic Floods: Evidence from Southeastern Washington State." *J. of Geology*. Volume 109, p. 695-713.

Bjornstad, BN, GV Last, SP Reidel, DG Horton, KR Fecht, GA Smith, and KA Lindsey. 2002. "Characterization and Proposed Formalization (Hanford formation) for Ice Age Flood Deposits Within the Pacific Northwest," In *Geological Society of America, Abstracts with Programs*, p. A-24, Geological Society of America, Boulder, Colorado.

Bjornstad BN, GV Last, and DG Horton. 2003. *Hydrogeology of the Hanford Site Vadose Zone*. 4th Symposium on the Hydrogeology of Washington State, Abstracts with Programs, p. 61. Available online at URL: http://www.ecy.wa.gov/events/hg/abstracts2003.pdf, as accessed on June 10, 2004.

Black, RF. 1979. *Clastic Dikes of the Pasco Basin, Southeastern Washington*. RHO-BWI-C-64, Rockwell Hanford Operations, Richland, Washington.

Brindley, GW, and G Brown (eds.). 1980. "Crystal Structures of Clay Minerals and Their X-Ray Identification." *Monograph No. 5,* Mineralogical Society, London, England.

Brown, DJ. 1959. *Subsurface Geology of the Hanford Separation Areas*. HW-61780, General Electric Company, Richland, Washington.

Brown, DJ. 1960. *An Eolian Deposit Beneath the 200 West Area*. HW-67549, General Electric Company, Richland, Washington.

Brown, DJ, RC Routson, WH Price, and KR Fecht. 1979. *Status of Liquid Waste Leaked from the 241-T-106 Tank*, Rockwell Hanford Operations, Richland, Washington.

Brown, RE. 1970. *Interrelationships of Geologic Formations and Processes Affecting Ecology as Exposed at Rattlesnake Springs*. BNWL-B-29, Battelle Northwest Laboratory, Richland, Washington.

Caggiano, JA and SM Goodwin. 1991. *Interim Status Groundwater Monitoring Plan for the Single-Shell Tanks*. WHC-SD-EN-AP-012, Westinghouse Hanford Company, Richland, Washington.

Cantrell, KJ, RJ Serne, and GV Last. 2003. *Hanford Contaminant Distribution Coefficient Database and Users Guide*. PNNL-13895, Rev. 1, Pacific Northwest National Laboratory, Richland, Washington.

Connelly, MP, BH Ford, and JV Borghese. 1992a. *Hydrogeologic Model for the 200 West Groundwater Aggregate Area*. WHC-SD-EN-TI-014, Westinghouse Hanford Company, Richland, Washington.

Connelly, MP, JV Borghese, CD Delaney, BH Ford, JW Lindberg, and SJ Trent. 1992b. *Hydrogeologic Model for the 200 East Groundwater Aggregate Area*. WHC-SD-EN-TI-019, Westinghouse Hanford Company, Richland, Washington.

Crumpler, JD. 2002. *Site Specific SST Phase 1 RFI/CMS Work Plan Addendum for WMAs T and TX-TY*. RPP-7578, Rev. 2, CH2M HILL Hanford Group, Inc., Richland, Washington.

Deka RN, M Wairiu, PW Mtakwa, CE Mullins, EM Veenendaal, and J Towend. 1995. "Use and Accuracy of the Filter Paper Method for Measuring Soil Matric Potential." *European J. of Soil Sci.* 46:233-238.

Delaney, CD, KA Lindsey, and SP Reidel. 1991. *Geology and Hydrology of the Hanford Site: A Standardized Text for Use in Westinghouse Hanford Company Documents and Reports*. WHC-SC-ER-TI-003, Westinghouse Hanford Company, Richland, Washington.

Drever, JI. 1973. "The Preparation of Oriented Clay Mineral Specimens for X-Ray Diffraction Analysis by a Filter-Membrane Peel Technique." *Amer. Minerl.* 58:553-554.

DOE/RL-91-61. 1992a. *T Plant Source Aggregate Area Management Report*. U.S. Department of Energy, Richland Operations Office, Richland, Washington.

DOE/RW-0164. 1988. *Consultation Draft Site Characterization Plan, Reference Repository Location, Hanford Site, Washington*. U.S. Department of Energy, Office of Civilian Radioactive Waste Management, Washington, D.C.

US Department of Energy (DOE). 1984. *Draft Environmental Assessment, Reference Repository Location, Hanford Site, Washington*, DOE/RW-0017, U.S. Department of Energy, Washington, D.C.

US Department of Energy (DOE). 1988. *Consultation Draft Site Characterization Plan, Reference Repository Location, Hanford Site, Washington*. DOE/RW-0164, U. S. Department of Energy, Office of Civilian Radioactive Waste Management, Washington, D.C.

US Department of Energy (DOE). 1992. *T Plant Source Aggregate Area Management Report*. DOE/RL-91-61, U.S. Department of Energy, Richland Operations Office, Richland, Washington.

US Department of Energy (DOE). 1999. *Phase 1 RCRA Facility Investigation/Corrective Measures Study Work Plan for the SST Waste Management Areas*. DOE/RL-99-36, Rev. 0, U.S. Department of Energy, Richland Operations Office, Richland, Washington.

US Department of Energy (DOE). 2002a. *Standardized Stratigraphic Nomenclature for Post-Ringold-Formation Sediments Within the Pasco Basin*. DOE/RL-2002-39, U.S. Department of Energy, Richland Operations Office, Richland, Washington.

DOE/GJO 1997. US Department of Energy, Grand Junction Office. (DOE/GJO). 1997. *Hanford Tank Farms Vadose Zone, TX Tank Farm Report*. GJO-HAN-11, prepared by U.S. Department of Energy Grand Junction Office for U.S. Department of Energy, Richland Operations Office, Richland, Washington.

DOE/GJO 1999a. US Department of Energy, Grand Junction Office. (DOE/GJO). 1999a. *Hanford Tank Farms Vadose Zone, T Tank Farm Report*. GHO-HAN-27, prepared by U.S. Department of Energy Grand Junction Office for U.S. Department of Energy, Richland Operations Office, Richland, Washington.

DOE/GJO 1999b. US Department of Energy, Grand Junction Office (DOE/GJO). 1999b. *Tank Summary Data Report for Tank T-106*, GJ-HAN-120, US Department of Energy, Grand Junction Office, Grand Junction, Colorado. Available on web http://www.gjo.doe.gov/programs/hanf

DOE/GJO 2000. US Department of Energy, Grand Junction Office (DOE/GJO). 2000. *Hanford Tank Farms Vadose Zone, Addendum to the T Tank Farm Report*. GHO-HAN-27, prepared by U.S. Department of Energy Grand Junction Office for U.S. Department of Energy, Richland Operations Office, Richland, Washington.

EPA (US Environmental Protection Agency)

EPA. 1986. *Test Methods for Evaluating Solid Waste: Physical/Chemical Methods*, SW-846, 3rd ed. U.S. Environmental Protection Agency, Office of Solid Waste and Emergency Response, Washington, D.C. [Online manual]. Available URL: http://www.epa.gov/epaoswer/hazwaste/test/sw846.htm

EPA Method 300.0A. 1984. *Test Method for the Determination of Inorganic Anions in Water by Ion Chromatography*. EPA-600/4-84-017, U.S. Environmental Protection Agency, Washington, D.C.

EPA Method 3050B. 2000a. "Acid Digestion of Sediments, Sludges, and Soils." *Test Methods for Evaluating Solid Waste, Physical/Chemical Methods*. EPA Publication SW-846, available online http://www.epa.gov/epaoswer/hazwaste/test/sw846.htm

EPA Method 6010B. 2000b. "Inductively Coupled Plasma-Atomic Emission Spectrometry." *Test Methods for Evaluating Solid Waste, Physical/Chemical Methods*. EPA Publication SW-846, available online http://www.epa.gov/epaoswer/hazwaste/test/sw846.htm

EPA Method 6020. 2000c. "Inductively Coupled Plasma-Mass Spectrometry." *Test Methods for Evaluating Solid Waste, Physical/Chemical Methods*. EPA Publication SW-846, available online http://www.epa.gov/epaoswer/hazwaste/test/sw846.htm

EPA Method (see EPA US Environmental Protection Agency)

Fecht, KR and DC Weekes. 1996. *Geologic Field Inspection of the Sedimentary Sequence at the Environmental Restoration Disposal Facility*. BHI-00230, Bechtel Hanford, Inc., Richland, Washington.

Fecht, KR, BN Bjornstad, DG Horton, GV Last, SP Reidel, and KA Lindsey. 1999. *Clastic Injection Dikes of the Pasco Basin and Vicinity: Geologic Atlas Series*. BHI-01103, Rev. 0. Bechtel Hanford Company, Richland, Washington.

Fecht, KR, GV Last, and KR Price, 1977. *Evaluation of Scintillation Probe Profiles from 200 Are Crib Monitoring Wells, Volume III.* ARH-ST-156, Atlantic Richfield Hanford Company, Richland, Washington.

Flint, RF. 1938. "Origin of the Cheney-Palouse Scabland Tract." *Geological Society of America Bulletin*, v. 49, p. 461-524.

Folk, RL. 1968. *Petrology of Sedimentary Rocks.* Hemphill, Austin, Texas.

Freeman-Pollard, JR, JA Caggiano, and SJ Trent. 1994. *Engineering Evaluation of the GAO-RCED-89-157, Tank 241-T-106 Vadose Zone Investigation.* BHI-00061, Bechtel Hanford, Inc., Richland, Washington.

Gardner, MG, KD Reynolds, and DE Skoglie. 2002a. *Completion Report for Probe Hole C3831 (TX-107) TX Tank Farm 200 West Area.* RPP-12293, Rev. 0, Prepared for the Office of River Protection, CH2M HILL Hanford Group, Inc., Richland, Washington.

Gardner, MG, KD Reynolds, and DE Skoglie. 2002b. *Completion Report for Probe Hole C3832 (TX-104) TX Tank Farm 200 West Area.* RPP-12017, Rev. 0-A, Prepared for the Office of River Protection, CH2M HILL Hanford Group, Inc., Richland, Washington.

Gee, GW. 1987. *Recharge at the Hanford Site. Status Report.* PNL-6403, Pacific Northwest Laboratory, Richland, Washington.

Gee, GW, MJ Fayer, ML Rockhold, and MD Campbell. 1992. "Variations in Recharge at the Hanford Site," *NW Sci.* 66:237-250.

Hartman, MJ, ed. 1999. *Hanford Site Groundwater Monitoring for Fiscal Year 1998.* PNNL-12086, Pacific Northwest National Laboratory, Richland, Washington.

Hartman, MJ, LF Morasch, and WD Webber (eds.). 2003. *Hanford Site Groundwater Monitoring for Fiscal Year 2002.* PNNL-14187, Pacific Northwest National Laboratory, Richland, Washington.

Hartman, MJ, LF Morasch, and WD Weber (eds.). 2004. *Hanford Site Groundwater Monitoring for Fiscal Year 2003.* PNNL-14548, Pacific Northwest National Laboratory, Richland, Washington.

Hodges, FN, 1998. *Results of Phase 1 Groundwater Quality Assessment for Single-Shell Tank Waste Management Areas T and TX-TY at the Hanford Site.* PNNL-11809, Pacific Northwest National Laboratory, Richland, Washington.

Hodges, FN and CJ Chou, 2001. *RCRA Assessment Plan for Single-Shell Tank Waste Management Area TX-TY at the Hanford Site.* PNNL-12072, Pacific Northwest National Laboratory, Richland, Washington.

Horton, DG. 2002. *Borehole Data Package for Calendar Year 2001 RCRA Well Installation at Single-Shell Tank Waste Management Area T.* PNNL-13830, Pacific Northwest National Laboratory, Richland, Washington.

Horton, DG. 2003. *Data Package for Calendar Year 2002 RCRA Groundwater Monitoring Wells at Single-Shell Tank Waste Management Area TX-TY.* PNNL-14249, Pacific Northwest National Laboratory, Richland, Washington.

Horton, DG. and FN Hodges. 2001. *Borehole Data Package for Calendar Year 2000 - 2001 RCRA Wells at Single-Shell Tank Waste Management Area T.* PNNL-13590, Pacific Northwest National Laboratory, Richland, Washington.

Horton, DG, FN Hodges, VG Johnson, and CJ Chou, 2002. *RCRA Groundwater Quality Assessment Report for Single-Shell Tank Waste Management Area T (January 1998 through December 2001).* PNNL-13929, Pacific Northwest National Laboratory, Richland, Washington.

Jackson, ML. 1969. *Soil Chemical Analysis – Advanced Course – 2nd Edition.* Department of Soil Science, University of Wisconsin, Madison, Wisconsin.

Jones, TE, BC Simpson, MI Wood, and RA Corbin. 2000. *Preliminary Inventory Estimates for Single-Shell Tank Leaks in T, TX, and TY Tank Farms.* RPP-7218, Rev. 0, CH2M HILL Hanford Group, Inc., Richland, Washington.

Johnson, VG and CJ Chou, 2001. *RCRA Groundwater Quality Assessment Report for Waste Management Area S-SX (November 1997 through April 2000).* PNNL-13441, Pacific Northwest National Laboratory, Richland, Washington.

Johnson, VG, TE Jones, SP Reidel, and MI Wood. 1999. *Subsurface Physical Conditions of the S-SX Waste Management Area.* HNF-4936, Lockheed Martin Hanford Corporation, Richland, Washington.

Kaplan, DI, and RJ Serne. 1995. *Distribution Coefficient Values Describing Iodine, Neptunium, Selenium, Technetium, and Uranium Sorption to Hanford Sediment.* PNL-10379, Supplement 1, Pacific Northwest Laboratory, Richland, Washington.

Kaplan, DI, and RJ Serne. 2000. *Geochemical Data Package for the Hanford Immobilized Low-Activity Tank Waste Performance Assessment (ILAW-PA).* PNNL-13037, Rev.1, Pacific Northwest National Laboratory, Richland, Washington.

Kincaid, CT, MP Bergeron, CR Cole, MD Freshley, VG Johnson, DI Kaplan, RJ Serne, GP Streile, DL Strenge, PD Thorne, LW Vail, GA Whyatt, and SK Wurstner. 1998. *Composite Analysis for Low-Level Waste Disposal in the 200 Area Plateau of the Hanford Site.* PNNL-11800, Pacific Northwest National Laboratory, Richland, Washington.

Kipp, RL and RD Mudd, 1974. *Selected Water Table Contour Maps and Well Hydrographs for the Hanford Reservation, 1944-1973.* BNWL-B-360, Pacific Northwest Laboratories, Richland, Washington.

Last, GV, ed. 1994. *216-U-10 Pond and 216-Z19 Ditch Characterization Studies.* WHC-EP-0707 (formerly RHO-ST-45), Westinghouse Hanford Company, Richland, Washington.

Last, GV, BN Bjornstad, MP Bergeron, DW Wallace, DR Newcomer, JA Schramke, MA Chamness, CS Cline, SP Airhart, and JS Wilbur. 1989. *Hydrogeology of the 200 Areas Low-Level Burial Grounds - An Interim Report.* PNL-6820, 2 volumes, Pacific Northwest Laboratory, Richland, Washington.

Lindenmeier, CW, RJ Serne, BN Bjornstad, GW Gee, HT Schaef , DC Lanigan, MJ Lindberg, RE Clayton, VL LeGore, IV Kutnyakov, SR Baum, KN Geiszler, KMM Valenta, TS Vickerman, and LJ Royack. 2002. *Characterization of Vadose Zone Sediment: RCRA Borehole 299-E33-338 Located Near the B-BX-BY Waste Management Area*, PNNL-14121, Pacific Northwest National Laboratory, Richland, Washington.

Lindsey, KA. 1995. *Miocene-to Pliocene-Aged Suprabasalt Sediments of the Hanford Site, South Central Washington*, BHI-00184, Bechtel Hanford Inc., Richland, Washington.

Lindsey, KA. 1996. *Miocene-Pliocene Ringold Formation and Associated Deposits of the Ancestral Columbia River System, South-Central Washington and North-Central Oregon.* Department of Natural Resources, Division of Geology and Earth Resources Open-File Report 96-8, Olympia, Washington, 45p.

Lindsey, KA, BN Bjornstad, JW Lindberg, and KM Hoffman. 1992a. *Geologic Setting of the 200 East Area: An Update.* WHC-SD-EN-TI-012, Westinghouse Hanford Company, Richland, Washington.

Lindsey, KA, MP Connelly, and BN Bjornstad. 1992b. *Geologic Setting of the 200 West Area – An Update.* WHC-SD-EN-TI-008, Westinghouse Hanford Company, Richland, Washington.

Lindsey, KA, SP Reidel, KR Fecht, JL Slate, AG Law, and AM Tallman. 1994a. "Geohydrologic Setting of the Hanford Site, South-Central Washington." In *Geologic Field Trips in the Pacific Northwest,* eds. DA Swanson and RA Hagerud, pp. 1C-1 to 1C-16. Geological Society of America Meeting, Geological Society of America, Boulder, Colorado.

Lindsey, KA, JL Slate, GK Jaeger, KJ Swett, and RB Mercer. 1994b. *Geologic Setting of the Low-Level Burial Grounds.* WHC-SD-EN-TI-290, Rev. 0, Westinghouse Hanford Company, Richland, Washington.

Lindsey, KA, SE Kos, and KD Reynolds. 2000. *Vadose Zone Geology of the Boreholes 299-W22-50 and 299-W23-19 S-SX Waste Management Area, Hanford Site, South-Central Washington.* RPP-6149, Rev. 0, prepared for the Office of River Protection, CH2M HILL Hanford Group, Inc., Richland, Washington.

Lindsey, KA, SE Kos, and KD Reynolds. 2001. *Vadose Zone Geology of Boreholes 299-W10-27 and 299-W11-39 T-TX-TY Waste Management Area, Hanford Site, South-Central Washington.* RPP-8531, Rev. 0. prepared for the Office of River Protection, CH2M HILL Hanford Group, Inc., Richland, Washington.

March 8, 2004, Listing of borehole geophysical logs for Well 299W10-27; Available URL: http://boreholelogs.pnl.gov/200WEST/W10027

Maxfield, HL. 1979. *Handbook 200 Areas Waste Sites, Volume II.* RHO-CD-673, Rockwell Hanford Operations, Richland, Washington.

Moody, UL. 1987. *Late Quaternary Stratigraphy of the Channeled Scabland and Adjacent Areas*, Ph.D. Thesis, University of Idaho, Moscow, Idaho.

Myers, CW. and SM Price (eds.). 1979. *Geologic Studies of the Columbia Plateau – A Status Report.* RHO-BWI-ST-4, Rockwell Hanford Operations, Richland, Washington.

O'Connor, JE. 1993. *Hydrology, Hydraulics, and Geomorphology of the Bonneville Flood.* Special Paper #274, Geological Society of America, Boulder, Colorado, 83 p.

Or, D and JM Wraith. 2002. "Soil Water Content and Water Potential Relationships," pp. 49-84. In: *Soil Physics Companion*, ed. AW Warrick, CRC Press, Boca Raton, Florida.

Pacific Northwest Laboratory (PNL). 1990a. *Procedures for Groundwater Investigations.* PNL-MA-567-DO-1, Pacific Northwest Laboratory, Richland, Washington.

Pacific Northwest Laboratory (PNL). 1990b. *Procedures for Groundwater Investigations.* PNL-MA-567-SFA-2, Pacific Northwest Laboratory, Richland, Washington.

Pacific Northwest National Laboratory (PNNL). 1995. *Precipitation Plating of Actinides for High-resolution Alpha Spectrometry.* PNL-ALO-496, Pacific Northwest National Laboratory, Richland, Washington.

Pacific Northwest National Laboratory (PNNL). 1997. *Gamma Energy Analysis Operation and Instrument Verification Using the Genie2000™ Support Software.* PNNL-RRL-01, Pacific Northwest National Laboratory, Richland, Washington.

Pacific Northwest National Laboratory (PNNL). 1998. *Inductively Coupled Plasma Mass Spectrometric (ICP-MS) Analysis.* PNNL-AGG-415, Pacific Northwest National Laboratory, Richland, Washington.

Pacific Northwest National Laboratory (PNNL). 1999. *Visual Description and Classification of Potentially Contaminated Borehole Samples.* PNL Procedure D9T81-99-GVL-1, Pacific Northwest National Laboratory, Richland, Washington, 6 p.

Pacific Northwest National Laboratory (PNNL). 2000a. *Liquid Scintillation Counting and Instrument Verification Using the 1400 DSM™ Support Software.* PNNL-AGG-002, Pacific Northwest National Laboratory, Richland, Washington.

Pacific Northwest National Laboratory (PNNL). 2000b. *Tc99 and Sr90 Analysis Using Eichrom TEVA-spec and Sr-spec Resin.* AGG-RRL-003.2., Pacific Northwest National Laboratory, Richland, Washington.

Price, WH and KR Fecht. 1976. *Geology of the 241-TX Tank Farm.* ARH-LD-136, Atlantic Richfield Hanford Company, Richland, Washington.

Randall, R, R Price, and JA Caggiano. 2000. *Analysis and Summary Report of Historical Dry Well Gamma Logs for the 241-T-Tank Farm – 200 West.* RPP-6088, Rev. 0, CH2M HILL Hanford Group, Inc., Richland, Washington.

Reidel, SP, and KR Fecht. 1994. *Geologic Map of the Priest Rapids 1:100,000 Quadrangle, Washington.* Washington Division of Geology and Earth Resources Open-File Report 94-13, 22 p.

Reidel, SP, KA Lindsey, and KR Fecht. 1992. *Field Trip Guide to the Hanford Site.* WHC-MR-0391, Westinghouse Hanford Company, Richland, Washington.

Reineck, HE, and IB Singh, 1975. *Depositional Sedimentary Environments*. Springer-Verlag, New York, 439p.

Reynolds, KD. 2003a. *Completion Report for Probe Hole C4104 (T-106) T Tank Farm Drilling and Sampling*. RPP-17275, Rev. 0, Prepared for the Office of River Protection, CH2M HILL Hanford Group, Inc., Richland, Washington.

Reynolds, KD. 2003b. *Completion Report for Probe Hole C4105 (T-106) T Tank Farm Drilling and Sampling*. RPP-16340, Rev. 0, Prepared for the Office of River Protection, CH2M HILL Hanford Group, Inc., Richland, Washington.

Rhoades, JD. 1996. "Salinity: Electrical Conductivity and Total Dissolved Solids." In *Methods of Soil Analysis Part 3,* ed. JM Bigham, pp. 417-435. American Society of Agronomy, Madison, Wisconsin.

Routson, RC, G Jansen, and AV Robinson. 1976. "241-Am, 237-Np, and 99-Tc Sorption on Two United States Subsoils from Differing Weathering Intensity Areas." *Health Phys.* 33:311-317.

Routson, RC, WH Price, DJ Brown, and KR Fecht. 1979. *High-Level Waste Leakage from the 241-T-106 Tank at Hanford.* RHO-ST-14, Rockwell Hanford Operations, Richland, Washington.

Salvador, A, ed. 1994. *International Stratigraphic Guide*. International Union of Geological Sciences and the Geological Society of America, Boulder, Colorado, second edition.

Serne, RJ, HT Schaef, BN Bjornstad, BA Williams, DC Lanigan, DG Horton, RE Clayton, VL LeGore, MJ O'Hara, CF Brown, KE Parker, IV Kutnyakov, JN Serne, AV Mitroshkov, GV Last, SC Smith, CW Lindenmeier, JM Zachara, and DS Burke. 2002a. *Characterization of Vadose Zone Sediment: Uncontaminated RCRA Borehole Core Samples and Composite Samples*. PNNL-13757-1, Pacific Northwest National Laboratory, Richland, Washington.

Serne, RJ, HT Schaef, BN Bjornstad, DC Lanigan, GW Gee, CW Lindenmeier, RE Clayton, VL LeGore, MJ O'Hara, CF Brown, RD Orr, GV Last, IV Kutnyakov, DS Burke, TC Wilson, and BA Williams. 2002b. *Characterization of Vadose Zone Sediment: Borehole 299-W23-19 [SX-115] in the S-SX Waste Management Area*. PNNL-13757-2. Pacific Northwest National Laboratory, Richland, Washington.

Serne, RJ, GV Last, GW Gee, HT Schaef, DC Lanigan, CW Lindenmeier, RE Clayton, VL LeGore, RD Orr, MJ O'Hara, CF Brown, DS Burke, AT Owen, IV Kutnyakov, and TC Wilson. 2002c. *Characterization of Vadose Zone Sediment: Borehole 41-09-39 in the S-SX Waste Management Area.* PNNL-13757-3, Pacific Northwest National Laboratory, Richland, Washington.

Serne, RJ, GV Last, HT Schaef, DC Lanigan, CW Lindenmeier, CC Ainsworth, RE Clayton, VL LeGore, MJ O'Hara, CF Brown, RD Orr, IV Kutnyakov, TC Wilson, KB Wagnon, BA Williams, and DB Burke. 2002d. *Characterization of Vadose Zone Sediment, Part 4: Slant Borehole SC-108 in the S-SX Waste Management Area.* PNNL-13757-4, Pacific Northwest National Laboratory, Richland, Washington.

Serne, RJ, GV Last, GW Gee, HT Schaef, DC Lanigan, CW Lindenmeier, MJ Lindberg, RE Clayton, VL LeGore, RD Orr, IV Kutnyakov, SR Baum, KN Geiszler, CF Brown, MM Valenta, and TS Vickerman, 2002e. *Characterization of Vadose Zone Sediment: Borehole 299-E33-45 Near BX-102 in the B-BX-BY Waste Management Area*, PNNL-14083, Pacific Northwest National Laboratory, Richland, Washington.

Serne, RJ, BN Bjornstad, GW Gee, HT Schaef, DC Lanigan, CW Lindenmeier, RD Orr, VL LeGore, RE Clayton, MJ Lindberg, IV Kutnyakov, SR Baum, KN Geiszler, MM Valenta, TS Vickerman, and LJ Royack. 2002f. *Characterization of Vadose Zone Sediment: Borehole 299-E33-46 Near B-110 in the B-BX-BY Waste Management Area*, PNNL-14119, Pacific Northwest National Laboratory, Richland, Washington.

Serne, RJ, BN Bjornstad, DG Horton, DC Lanigan, CW Lindenmeier, MJ Lindberg, RE Clayton, VL LeGore, RD Orr, IV Kutnyakov, SR Baum, KN Geiszler, MM Valenta, and TS Vickerman. 2004. *Characterization of Vadose Zone Sediments Below the TX Tank Farm: Boreholes C3830, C3831, C3832 and RCRA Borehole 299-W10-27.* PNNL-14594, Pacific Northwest National Laboratory, Richland, Washington.

Shaw, J, M Munro-Stasuik, B Sawyer, C Beaney, JE Lesemann, A Musacchio, B Rains, and RR Young. 1999. "The Channeled Scabland: Back to Bretz," *Geology*, v. 27, p. 605-608.

Simpson, BC, RA Corbin, and SF Agnew, 2001. *Hanford Soil Inventory Model.* BHI-01496 Rev. 0, Bechtel Hanford, Inc., Richland, Washington.

Slate, JL. 1996. "Buried Carbonate Paleosols Developed in Pliocene-Pleistocene Deposits of the Pasco Basin, South-Central Washington." *USA: Quaternary International*, Vol. 34-36, pp. 191-196.

Slate, JL. 2000. *Nature and Variability of the Plio-Pleistocene Unit in the 200 West Area of the Hanford Site.* BHI-01203, Rev. 0, Bechtel Hanford, Inc., Richland, Washington.

Smith, GA. 1993. "Missoula Flood Dynamics and Magnitudes Inferred from Sedimentology of Slack-Water Deposits on the Columbia Plateau." *Geological Society of America Bulletin*, v. 195, p. 77-100.

Sobczyk, SM. 2001. *Subsurface Interpretation of the T Tank Farm, Hanford Site, Washington, Based on Gamma-Ray Logging*, Nez Perce Tribe Environmental Restoration Waste Management Program, Lapwai, Idaho.

Spane, FA, Jr., PD Thorne, and DR Newcomer. 2001a. *Results of Detailed Hydrologic Characterization Tests – Fiscal Year 1999.* PNNL-13378, Pacific Northwest National Laboratory, Richland, Washington.

Spane, FA, Jr., PD Thorne, and DR Newcomer. 2001b. *Results of Detailed Hydrologic Characterization Tests – Fiscal Year 2000.* PNNL-13514, Pacific Northwest National Laboratory, Richland, Washington.

Spane, FA, Jr., PD Thorne, and DR Newcomer. 2002. *Results of Detailed Hydrologic Characterization Tests – Fiscal Year 2001.* PNNL-14113, Pacific Northwest National Laboratory, Richland, Washington.

Spane, FA, Jr., PD Thorne, and DR Newcomer. 2003. *Results of Detailed Hydrologic Characterization Tests – Fiscal Year 2002*. PNNL-14186, Pacific Northwest National Laboratory, Richland, Washington.

Tallman, AM, KR Fecht, MC Marratt, and GV Last. 1979. *Geology of the Separations Areas, Hanford Site, South-Central Washington*. RHO-ST-23, Rockwell Hanford Operations, Richland, Washington.

Tallman, AM, JT Lillie, and KR Fecht. 1981. "Suprabasalt Sediment of the Cold Creek Syncline Area," In *Subsurface Geology of the Cold Creek Syncline*, eds. CW Myers and SM Price, RHO-BWI-ST-14, Rockwell Hanford Operations, Richland, Washington.

USGS (United States Geological Survey). 2001. "Alkalinity and Acid Neutralizing Capacity." In: *National Field Manual for the Collection of Water-Quality Data*, 2nd Edition, eds. SA Rounds and FD Wilde. [Online Report Revised 9/2001]. As of March 23, 2004 available URL: http://water.usgs.gov/owq/Field Manual/ Chapter6/section 6.6/html/section6.6htm.

Waldrop, WR and HS Pearson. 2000. *Results of Field Tests with the Electromagnetic Borehole Flowmeter at the Pacific Northwest National Laboratory, Richland, WA*. QEC-T-132, Quantum Engineering Corporation, London, Tennessee.

Wan, J, JT Larsen, TK Tokunaga, and Z Zheng. 2004. "pH Neutralization and Zonation in Alkaline-Saline Tank Waste Plumes." *Environ. Sci. Technol.* Vol. 38, p. 1321-1329.

Ward, AL, GW Gee, and MD White. 1997. *A Comprehensive Analysis of Contaminant Transport in the Vadose Zone Beneath Tank SX-109*. PNNL-11463, Pacific Northwest National Laboratory, Richland, Washington.

Webster, GD, and JW Crosby, 1982, *Stratigraphic Investigation of the Skagit/Hanford Nuclear Project*, S/HNP-PSAR, Appendix 2R, Bellevue, Washington, Puget Sound Power and Light Company, p. 2R-i to 2R-35.

Wentworth, CK. 1922. "A grade scale and class terms for clastic sediments." *Journal of Geology*, Vol. 30, p. 377-392.

WHC 1990. 1990. *Liquid Effluent Study Final Project Report*. WHC-EP-0367, Westinghouse Hanford Company, Richland, Washington.

Williams, JC. 2000. *Historical Vadose Zone Contamination from T, TX, and TY Tank Farm Operations*. RPP-5957, Rev. 0, CH2M HILL Hanford Group,, Inc., Richland, Washington.

Williams, BA, BN Bjornstad, R Schalla, and WD Webber. 2002. *Revised Hydrogeology for the Suprabasalt Aquifer System, 200-West Area and Vicinity*, Hanford Site, Washington. PNNL-13858, Pacific Northwest National Laboratory, Richland, Washington.

Wood, MI, R Schalla, BN Bjornstad, and FN Hodges. 2001. *Subsurface Conditions Description of the T and TX-TY Waste Management Areas*. RPP-7123, Rev. 0, CH2M HILL Hanford Group, Inc., Richland, Washington.

Wood, MI, TE Jones, R Schalla, BN Bjornstad, and FN Hodges. 2001. *Subsurface Conditions Description of the T and TX-TY Waste Management Areas.* RPP-7123, Rev. 0. CH2M HILL Hanford Group, Inc., Richland, Washington.

Zachara, JM, SC Smith, C. Lui, JP McKinley, RJ Serne, and PL Gassman. 2002. "Sorption of Cs^+ to Micaceous Subsurface Sediments from the Hanford Site, USA." *Geochimica et Cosmochimica Acta.* 66: 193-211.

Appendix A. Core Photographs

A.1 C3117 (299-W11-39)

A.2. C4104 (T-106)

A.3. C4105 (T-106)

Appendix A-1

C3117 (299-W11-39)

SPLITSPOON CORE

SAMPLE PHOTOGRAPHS

Contents

Appendix A-1 ..... A-1.1

Figures

A-1.1. Hanford Formation (H1 unit) 23.0 ft – 24.0 ft A-1.1
A-1.2. Hanford Formation (H1 unit) 31.5 ft – 32.5 ft A-1.2
A-1.3. Hanford Formation (H1 unit) 32.5 ft – 33.5 ft A-1.3
A-1.4. Hanford Formation (H2 unit) 34.0 ft – 35.0 ft A-1.4
A-1.5. Hanford Formation (H2 unit) 35.0 ft – 36.0 ft A-1.5
A-1.6. Hanford Formation (H2 unit) 36.5 ft – 37.5 ft A-1.6
A-1.7. Hanford Formation (H2 unit) 37.5 ft – 38.5 ft A-1.7
A-1.8. Hanford Formation (H2 unit) 39.0 ft – 40.0 ft A-1.8
A-1.9. Hanford Formation (H2 unit) 40.0 ft – 41.0 ft A-1.9
A-1.10. Hanford Formation (H2 unit) 41.5 ft – 42.5 ft A-1.10
A-1.11. Hanford Formation (H2 unit) 42.5 ft – 43.5 ft A-1.11
A-1.12. Hanford Formation (H2 unit) 44.0 ft – 45.0 ft A-1.12
A-1.13. Hanford Formation (H2 unit) 45.0 ft – 46.0 ft A-1.13
A-1.14. Hanford Formation (H2 unit) 46.5 ft – 47.5 ft A-1.14
A-1.15. Hanford Formation (H2 unit) 47.5 ft – 48.5 ft A-1.15
A-1.16. Hanford Formation (H2 unit) 49.0 ft – 50.0 ft A-1.16
A-1.17. Hanford Formation (H2 unit) 50.0 ft – 51.0 ft A-1.17
A-1.18. Hanford Formation (H2 unit) 51.5 ft – 52.5 ft A-1.18
A-1.19. Hanford Formation (H2 unit) 52.5 ft – 53.5 ft A-1.19
A-1.20. Hanford Formation (H2 unit) 55.0 ft – 56.0 ft A-1.20
A-1.21. Hanford Formation (H2 unit) 57.5 ft – 58.5 ft A-1.21
A-1.22. Hanford Formation (H2 unit) 59.0 ft – 60.0 ft A-1.22
A-1.23. Hanford Formation (H2 unit) 60.0 ft – 61.0 ft A-1.23
A-1.24. Hanford Formation (H2 unit) 61.5 ft – 62.5 ft A-1.24
A-1.25. Hanford Formation (H2 unit) 62.5 ft – 63.5 ft A-1.25
A-1.26. Hanford Formation (H2 unit) 64.0 ft – 65.0 ft A-1.26
A-1.27. Hanford Formation (H2 unit) 65.0 ft – 66.0 ft A-1.27

A-1.28. Hanford Formation (H2 unit) 67.5 ft – 68.5 ft A-1.28
A-1.29. Hanford Formation (H2 unit) 69.0 ft – 70.0 ft A-1.29
A-1.30. Hanford Formation (H2 unit) 70.0 ft – 71.0 ft A-1.30
A-1.31. Hanford Formation (H2 unit) 71.5 ft – 72.5 ft A-1.31
A-1.32. Hanford Formation (H2 unit) 72.5 ft – 73.5 ft A-1.32
A-1.33. Hanford Formation (H2 unit) 74.0 ft – 75.0 ft A-1.33
A-1.34. Hanford Formation (H2 unit) 75.0 ft – 76.0 ft A-1.34
A-1.35. Hanford Formation (H2 unit) 76.5 ft – 77.5 ft A-1.35
A-1.36. Hanford Formation (H2 unit) 77.5 ft – 78.5 ft A-1.36
A-1.37. Hanford Formation (H2 unit) 79.0 ft – 80.0 ft A-1.37
A-1.38. Hanford Formation (H2 unit) 80.0 ft – 81.0 ft A-1.38
A-1.39. Hanford Formation (H2 unit) 81.5 ft – 82.5 ft A-1.39
A-1.40. Hanford Formation (H2 unit) 82.5 ft – 83.5 ft A-1.40
A-1.41. Hanford Formation (H2 unit) 85.0 ft – 86.0 ft A-1.41
A-1.42. Hanford Formation (H2 unit) 86.5 ft – 87.5 ft A-1.42
A-1.43. Hanford Formation (H2 unit) 87.5 ft – 88.5 ft A-1.43
A-1.44. Hanford Formation (H2 unit) / Cold Creek Unit – Upper (CCU_u) 89.0 ft – 90.0 ft A-1.44
A-1.45. Cold Creek Unit – Uper (CCU_u) 90.0 ft – 91.0 ft A-1.45
A-1.46. Cold Creek Unit – Upper (CCU_u) 91.5 ft – 92.5 ft A-1.46

Figure A-1.1. Hanford Formation (H1 unit) 23.0 ft – 24.0 ft

Figure A-1.2. Hanford Formation (H1 unit) 31.5 ft – 32.5 ft

Figure A-1.3. Hanford Formation (H1 unit) 32.5 ft – 33.5 ft

Figure A-1.4. Hanford Formation (H2 unit) 34.0 ft – 35.0 ft

Figure A-1.5. Hanford Formation (H2 unit) 35.0 ft – 36.0 ft

Figure A-1.6. Hanford Formation (H2 unit) 36.5 ft – 37.5 ft

Figure A-1.7. Hanford Formation (H2 unit) 37.5 ft – 38.5 ft

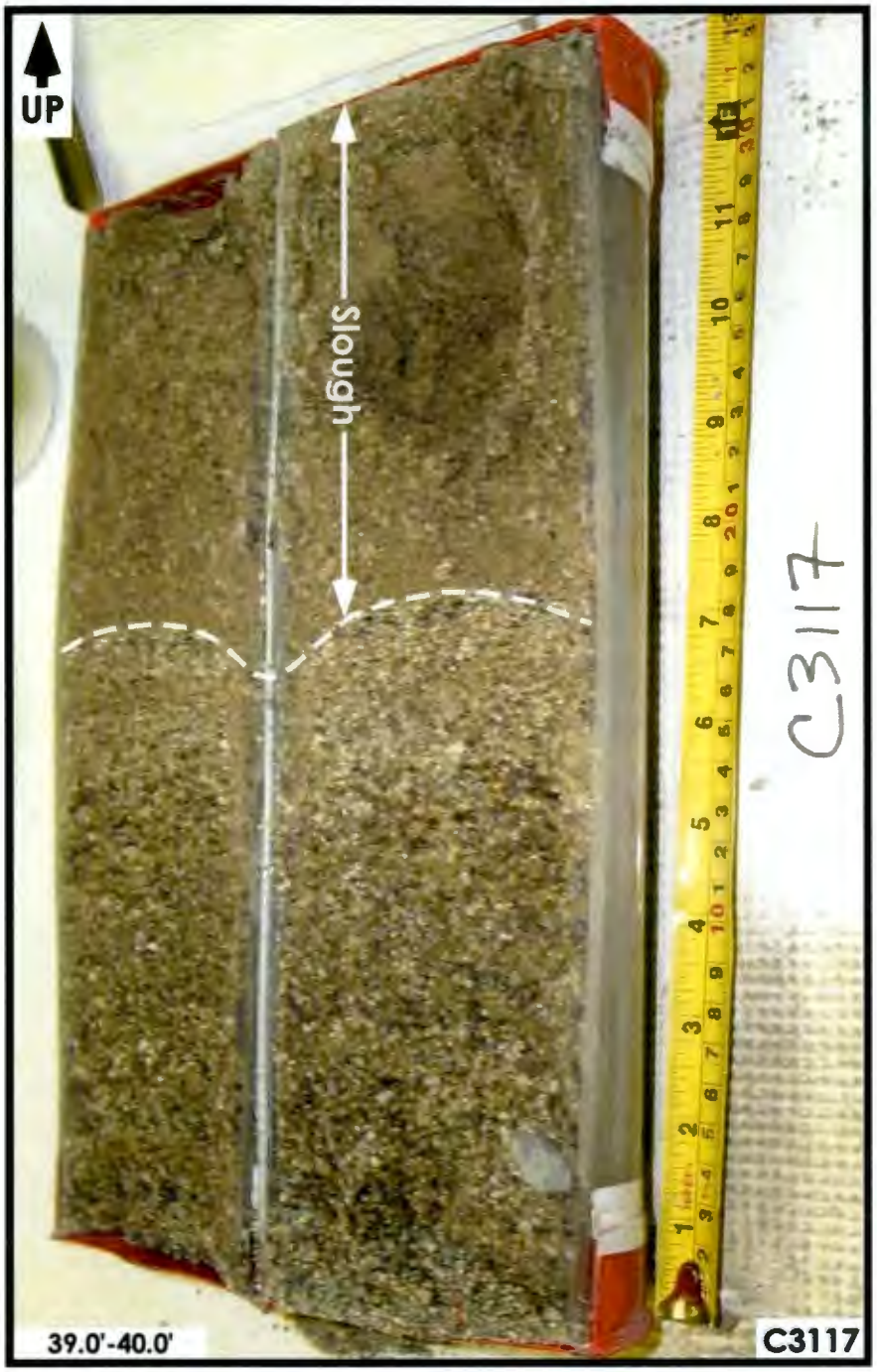

Figure A-1.8. Hanford Formation (H2 unit) 39.0 ft – 40.0 ft

Figure A-1.9. Hanford Formation (H2 unit) 40.0 ft – 41.0 ft

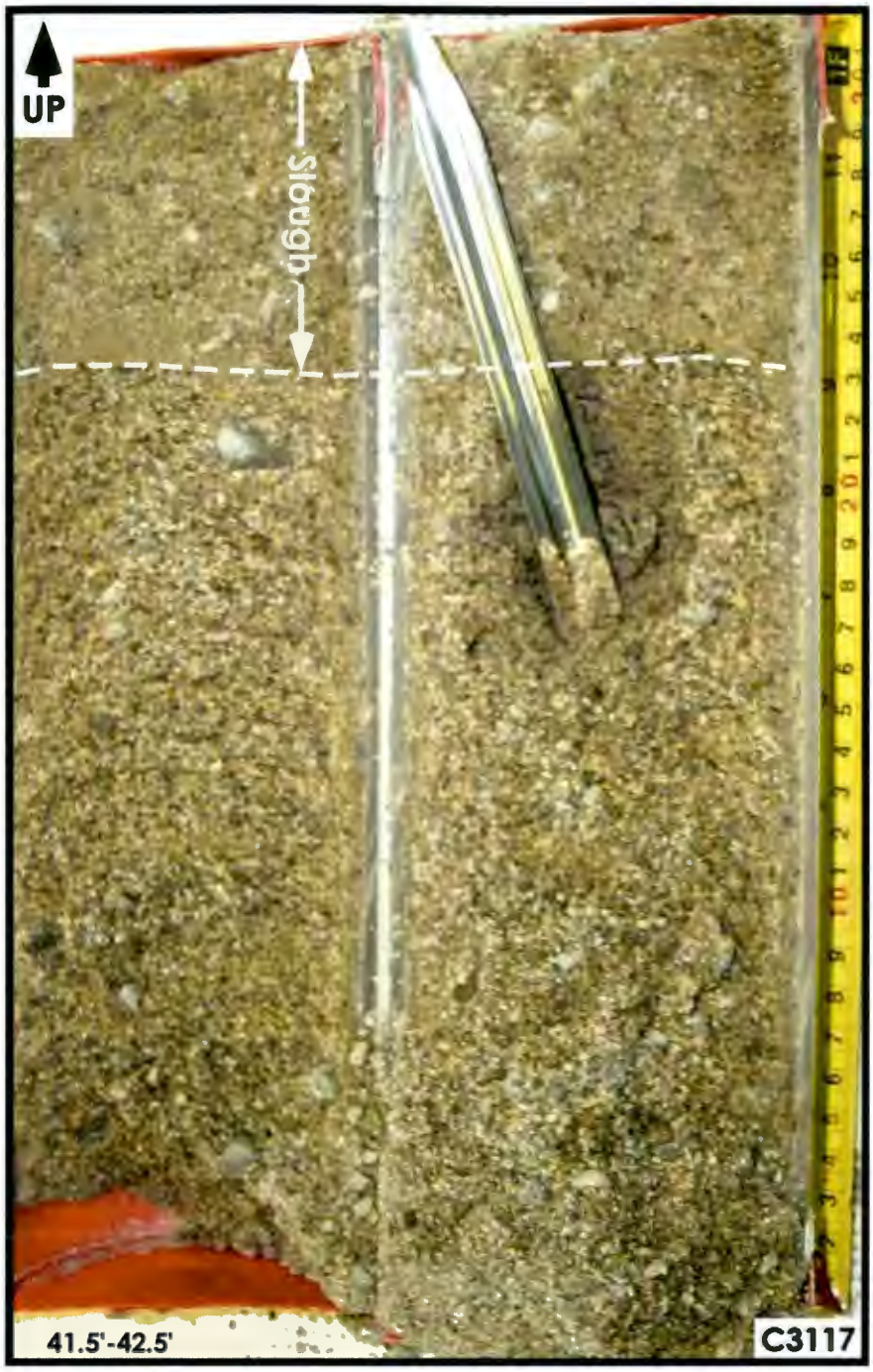

Figure A-1.10. Hanford Formation (H2 unit) 41.5 ft – 42.5 ft

Figure A-1.11. Hanford Formation (H2 unit) 42.5 ft – 43.5 ft

Figure A-1.12. Hanford Formation (H2 unit) 44.0 ft – 45.0 ft

Figure A-1.13. Hanford Formation (H2 unit) 45.0 ft – 46.0 ft

Figure A-1.14. Hanford Formation (H2 unit) 46.5 ft – 47.5 ft

Figure A-1.15. Hanford Formation (H2 unit) 47.5 ft – 48.5 ft

Figure A-1.16. Hanford Formation (H2 unit) 49.0 ft – 50.0 ft

Figure A-1.17. Hanford Formation (H2 unit) 50.0 ft – 51.0 ft

Figure A-1.18. Hanford Formation (H2 unit) 51.5 ft – 52.5 ft

Figure A-1.19. Hanford Formation (H2 unit) 52.5 ft – 53.5 ft

Figure A-1.20. Hanford Formation (H2 unit) 55.0 ft – 56.0 ft

Figure A-1.21. Hanford Formation (H2 unit) 57.5 ft – 58.5 ft

Figure A-1.22. Hanford Formation (H2 unit) 59.0 ft – 60.0 ft

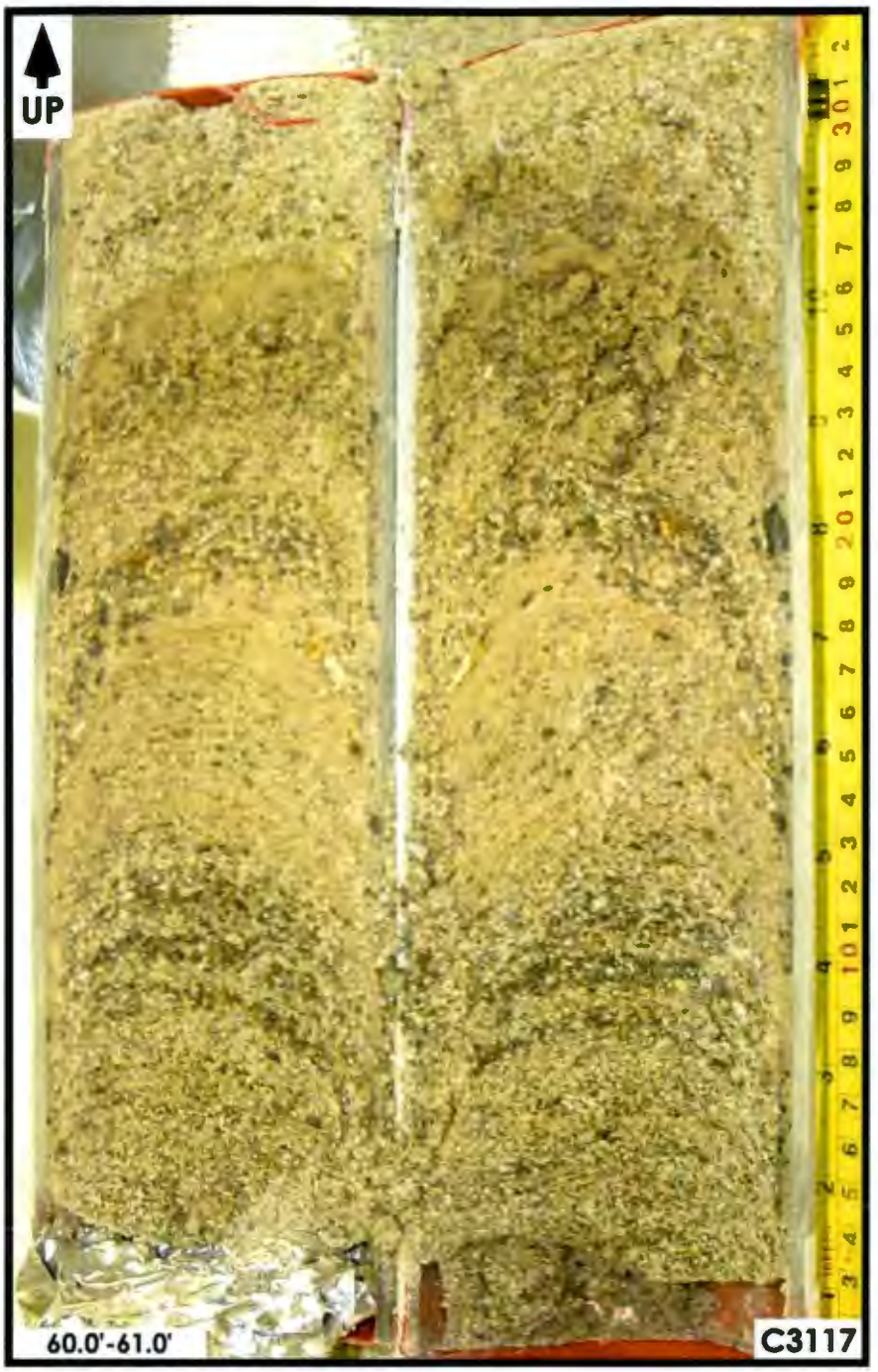

Figure A-1.23. Hanford Formation (H2 unit) 60.0 ft – 61.0 ft

Figure A-1.24. Hanford Formation (H2 unit) 61.5 ft – 62.5 ft

Figure A-1.25. Hanford Formation (H2 unit) 62.5 ft – 63.5 ft

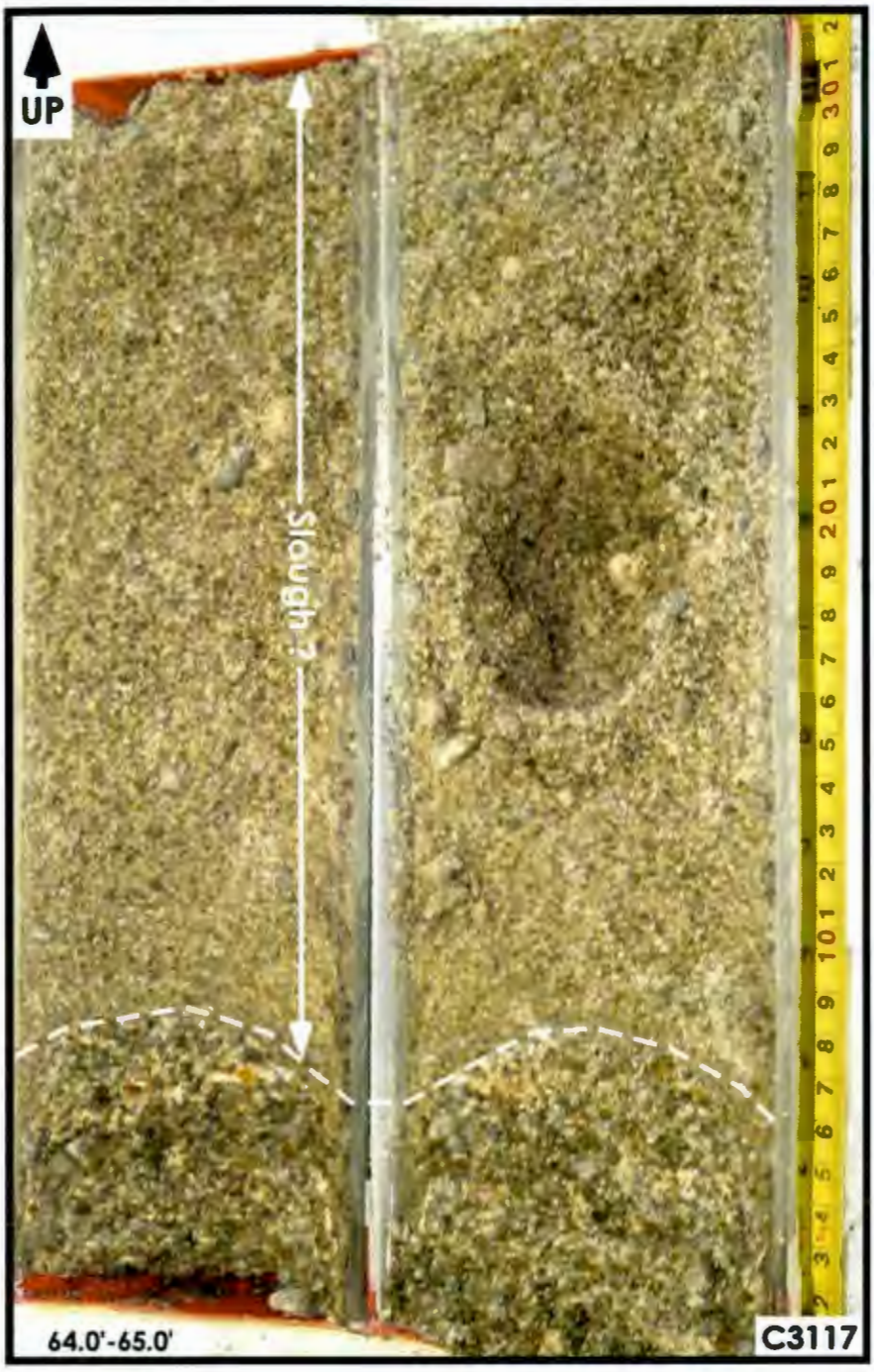

Figure A-1.26. Hanford Formation (H2 unit) 64.0 ft – 65.0 ft

Figure A-1.27. Hanford Formation (H2 unit) 65.0 ft – 66.0 ft

Figure A-1.28. Hanford Formation (H2 unit) 67.5 ft – 68.5 ft

Figure A-1.29. Hanford Formation (H2 unit) 69.0 ft – 70.0 ft

Figure A-1.30. Hanford Formation (H2 unit) 70.0 ft – 71.0 ft

Figure A-1.31. Hanford Formation (H2 unit) 71.5 ft – 72.5 ft

Figure A-1.32. Hanford Formation (H2 unit) 72.5 ft – 73.5 ft

Figure A-1.33. Hanford Formation (H2 unit) 74.0 ft – 75.0 ft

Figure A-1.34. Hanford Formation (H2 unit) 75.0 ft – 76.0 ft

Figure A-1.35. Hanford Formation (H2 unit) 76.5 ft – 77.5 ft

Figure A-1.36. Hanford Formation (H2 unit) 77.5 ft – 78.5 ft

Figure A-1.37. Hanford Formation (H2 unit) 79.0 ft – 80.0 ft

Figure A-1.38. Hanford Formation (H2 unit) 80.0 ft – 81.0 ft

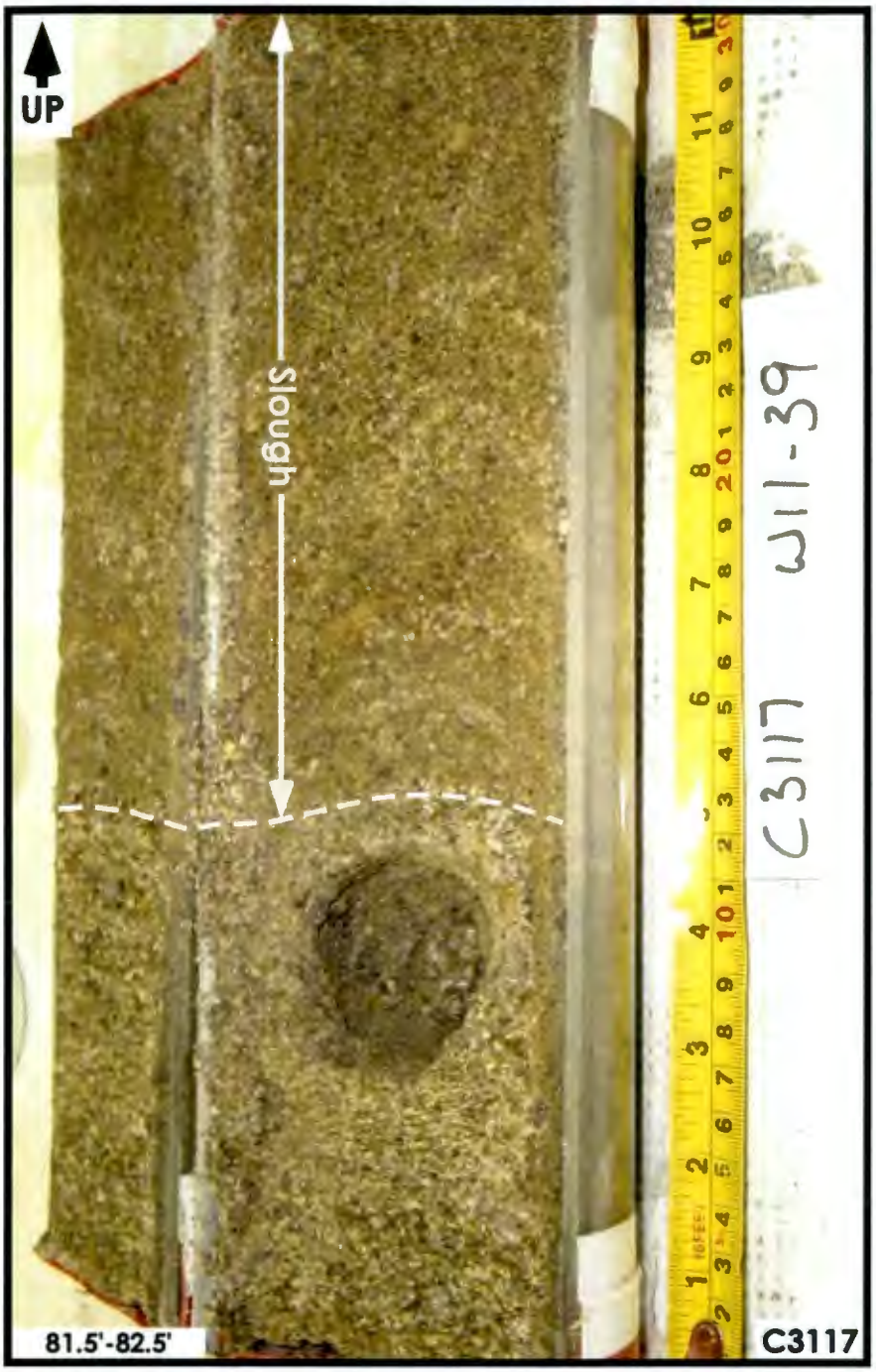

Figure A-1.39. Hanford Formation (H2 unit) 81.5 ft – 82.5 ft

Figure A-1.40. Hanford Formation (H2 unit) 82.5 ft – 83.5 ft

Figure A-1.41. Hanford Formation (H2 unit) 85.0 ft – 86.0 ft

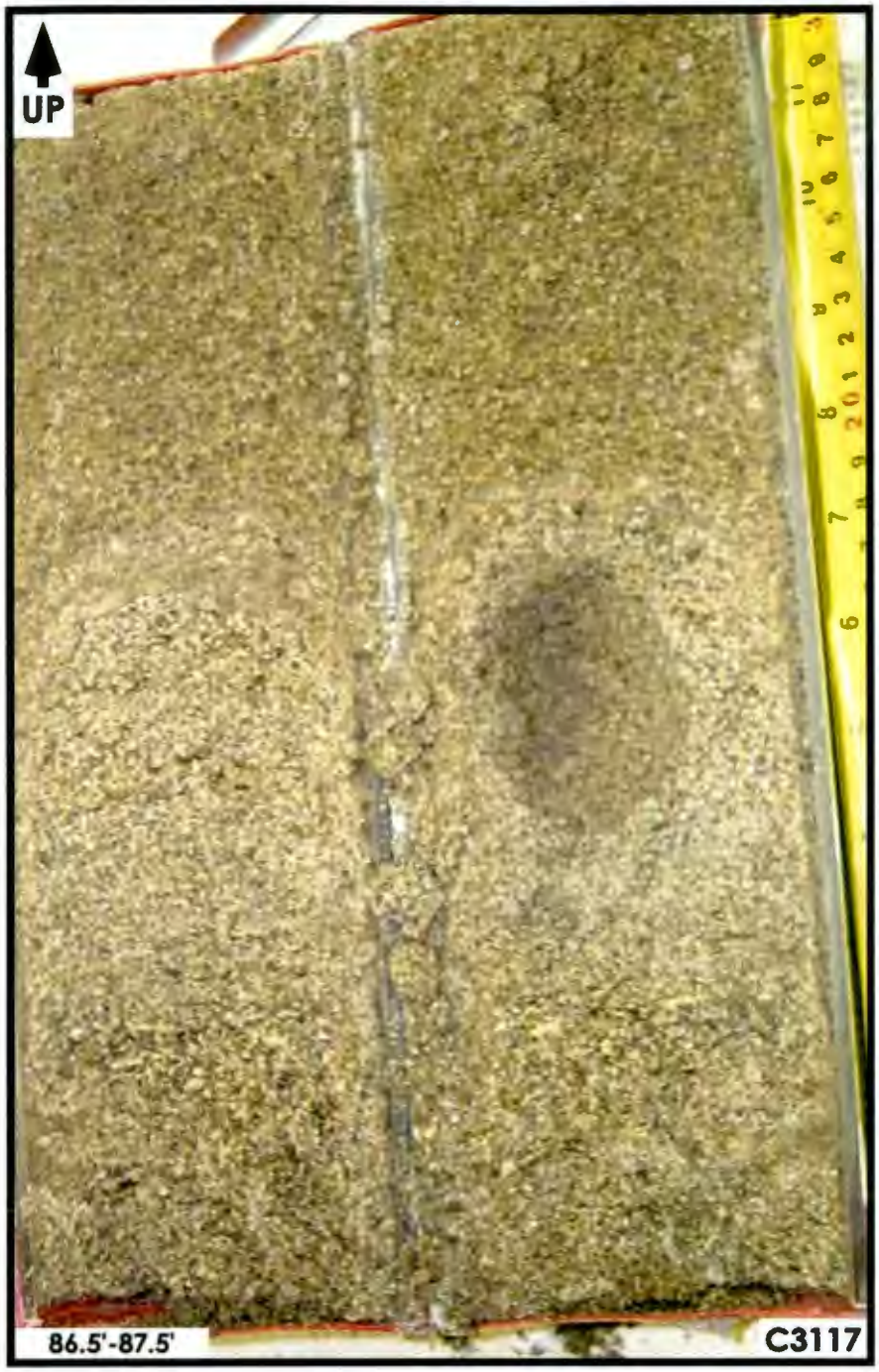

Figure A-1.42. Hanford Formation (H2 unit) 86.5 ft – 87.5 ft

Figure A-1.43. Hanford Formation (H2 unit) 87.5 ft – 88.5 ft

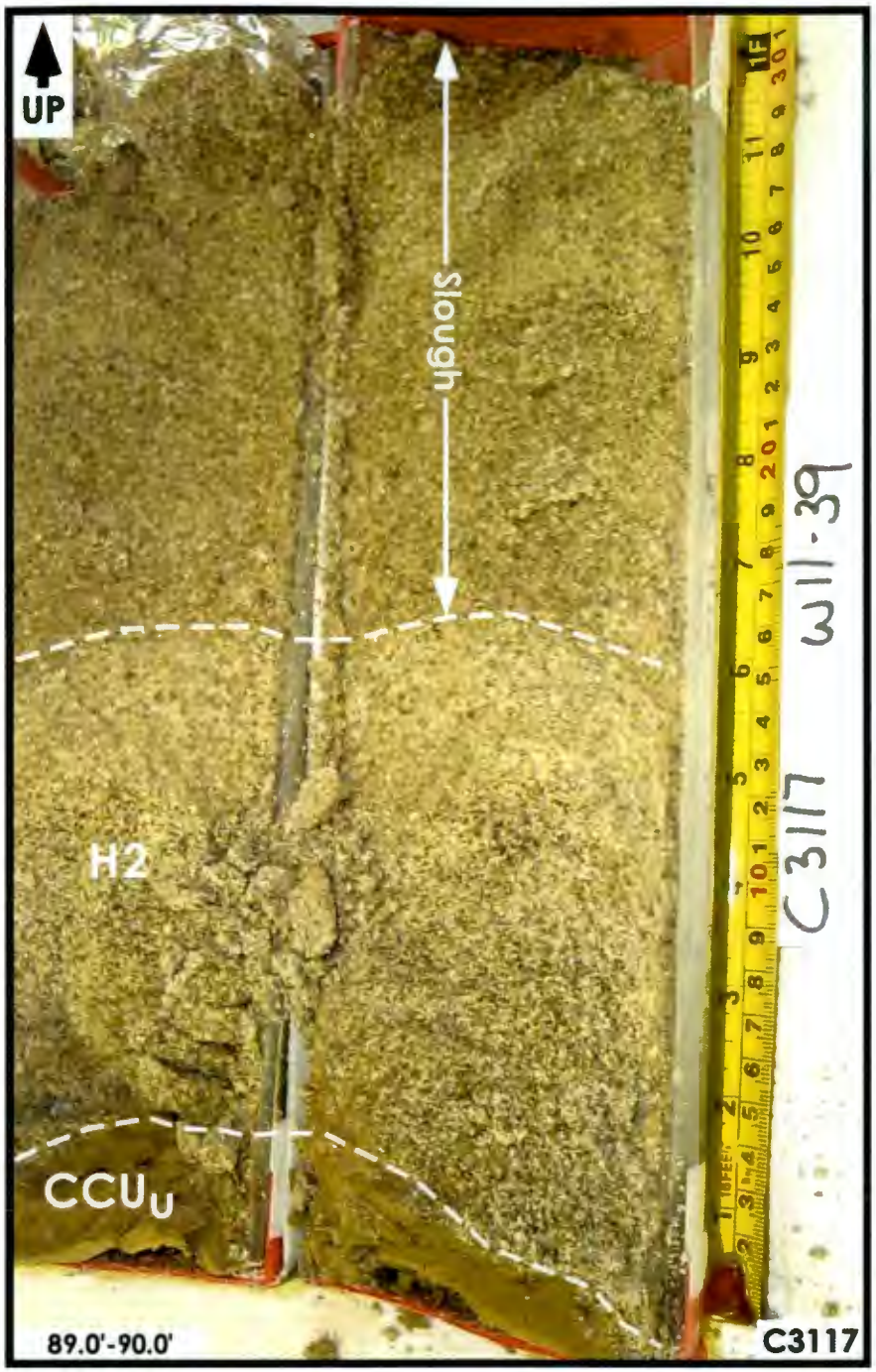

Figure A-1.44. Hanford Formation (H2 unit) / Cold Creek Unit – Upper (CCU$_u$) 89.0 ft – 90.0 ft

Figure A-1.45. Cold Creek Unit – Upper (CCU_u) 90.0 ft – 91.0 ft

Figure A-1.46. Cold CreekUnit – Upper (CCU_u) 91.5 ft – 92.5 ft

Appendix A-2

C4104 (T-106)

SPLITSPOON CORE

SAMPLE PHOTOGRAPHS

Contents

Appendix A-2 ..... A-2.1

Figures

A-2.1. Backfill 14.98 ft – 16.58 ft A-2.1
A-2.2. Backfill 21.68 ft – 23.03 ft A-2.2
A-2.3. Backfill 29.73 ft – 31.08 ft A-2.3
A-2.5. Backfill 39.00 ft – 40.35 ft A-2.5
A-2.6. Hanford Formation (H2 unit) 46.00 ft – 47.30 ft A-2.6
A-2.7. Hanford Formation (H2 unit) 58.04 ft – 59.44 ft A-2.7
A-2.8. Hanford Formation (H2 unit) 63.05 ft – 64.35 ft A-2.8
A-2.9. Hanford Formation (H2 unit) 75.05 ft – 76.35 ft A-2.9
A-2.10. Hanford Formation (H2 unit) / Cold Creek Unit – Upper (CCU_u) 80.05 ft – 81.37 ft A-2.10
A-2.11. Cold Creek Unit – Upper (CCU_u) 86.30 ft – 87.70 ft A-2.11
A-2.13. Cold Creek Unit – Lower (CCU_l) 92.58 ft – 93.88 ft A-2.13
A-2.14. Cold Creek Unit – Lower (CCU_l) 93.73 ft – 95.17 ft A-2.14
A-2.15. Cold Creek Unit – Lower (CCU_l) 99.37 ft – 100.70 ft A-2.15
A-2.16. Cold Creek Unit – Lower (CCU_l) 101.00 ft – 102.30 ft A-2.16
A-2.17. Cold Creek Unit – Lower (CCU_l) 105.04 ft – 106.44 ft A-2.17
A-2.18. Cold Creek Unit – Lower (CCU_l) 106.44 ft – 107.74 ft A-2.18
A-2.19. Ringold Formation – Member of Taylor Flat (R_{tf}) 110.00 ft – 111.30 ft A-2.19
A-2.20. Ringold Formation – Member of Taylor Flat (R_{tf}) 114.86 ft – 116.41 ft A-2.20
A-2.21. Ringold Formation – Member of Taylor Flat (R_{tf}) / Member of Wooded Island (R_{wi}) 119.96 ft – 121.30 ft A-2.21
A-2.22. Ringold Formation – Member of Wooded Island (R_{wi}) 122.96 ft – 124.41 ft A-2.22
A-2.23. Ringold Formation – Member of Wooded Island (R_{wi}) 126.12 ft – 127.46 ft A-2.23

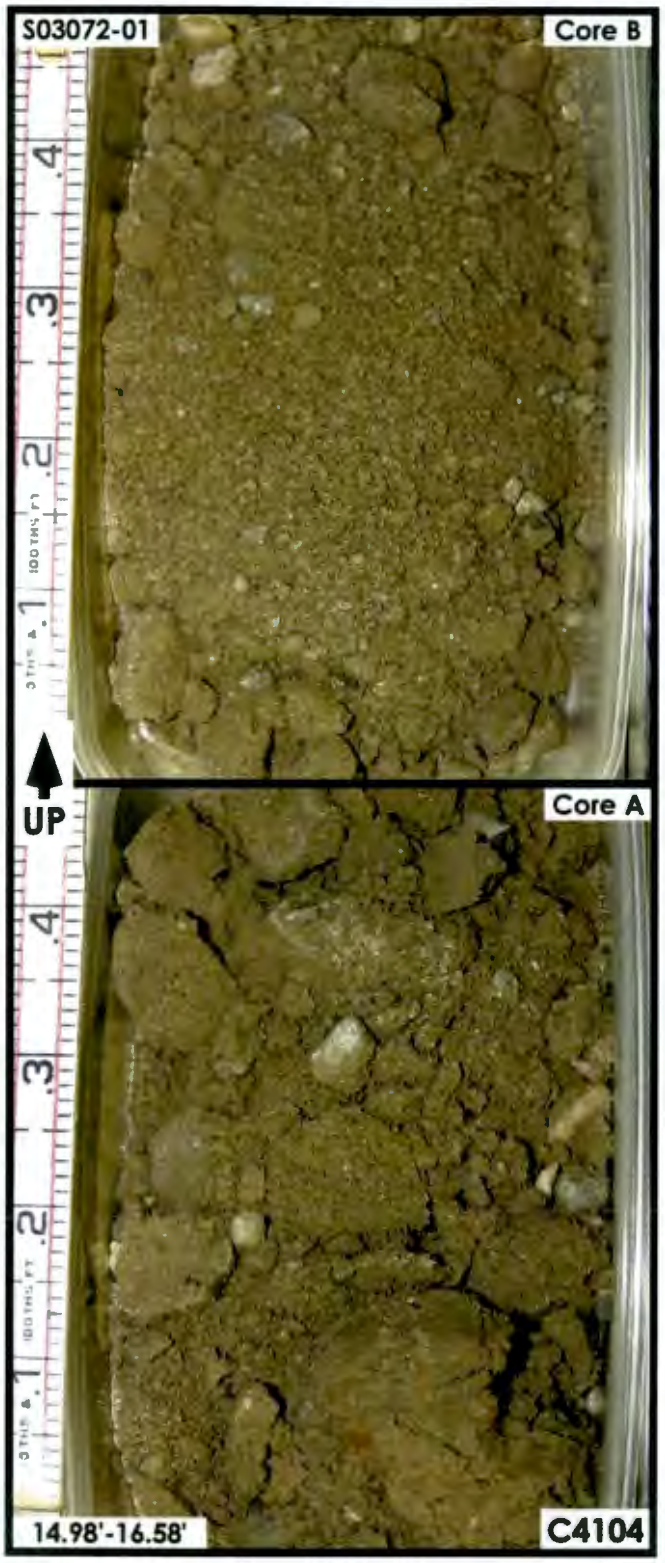

Figure A-2.1. Backfill 14.98 ft – 16.58 ft

Figure A-2.2. Backfill 21.68 ft – 23.03 ft

Figure A-2.3. Backfill 29.73 ft – 31.08 ft

Figure A-2.4. Backfill 35.90 ft – 37.20 ft

Figure A-2.5. Backfill 39.00 ft – 40.35 ft

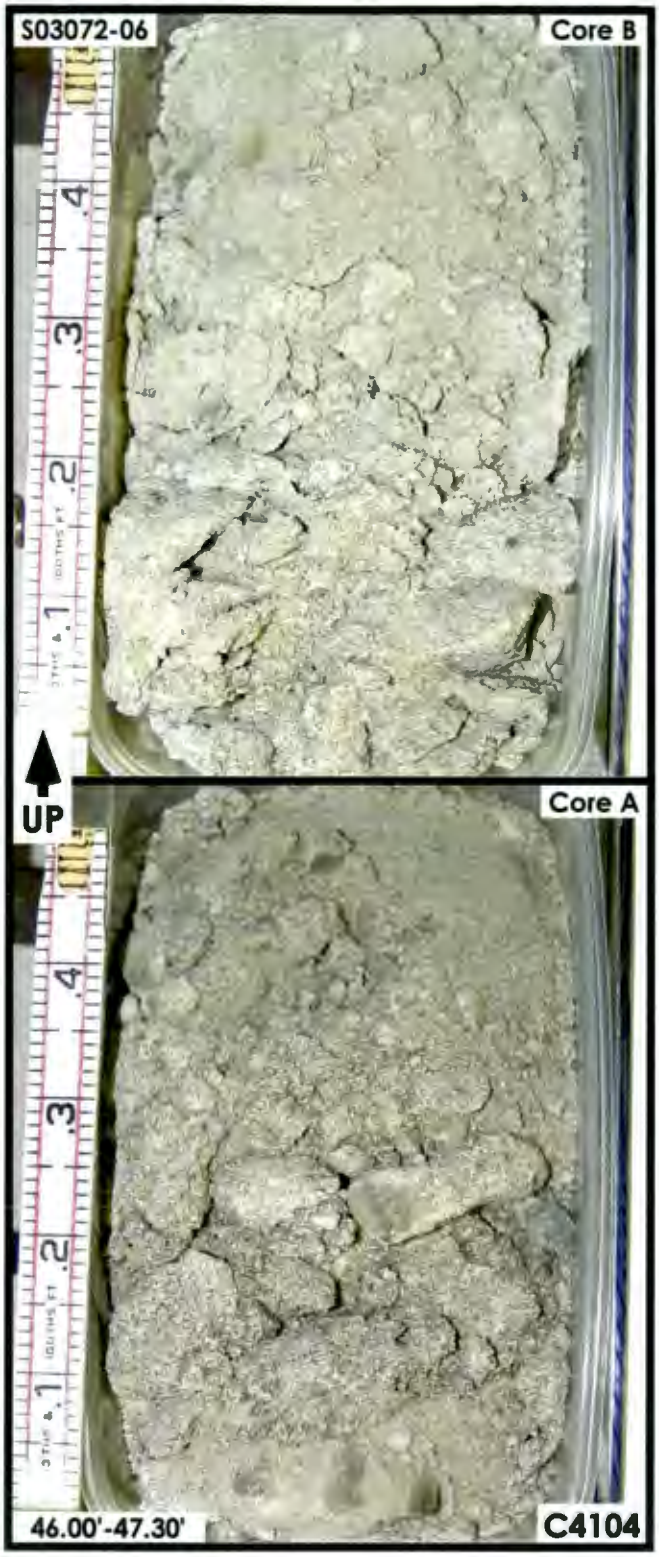

Figure A-2.6. Hanford Formation (H2 unit) 46.00 ft – 47.30 ft

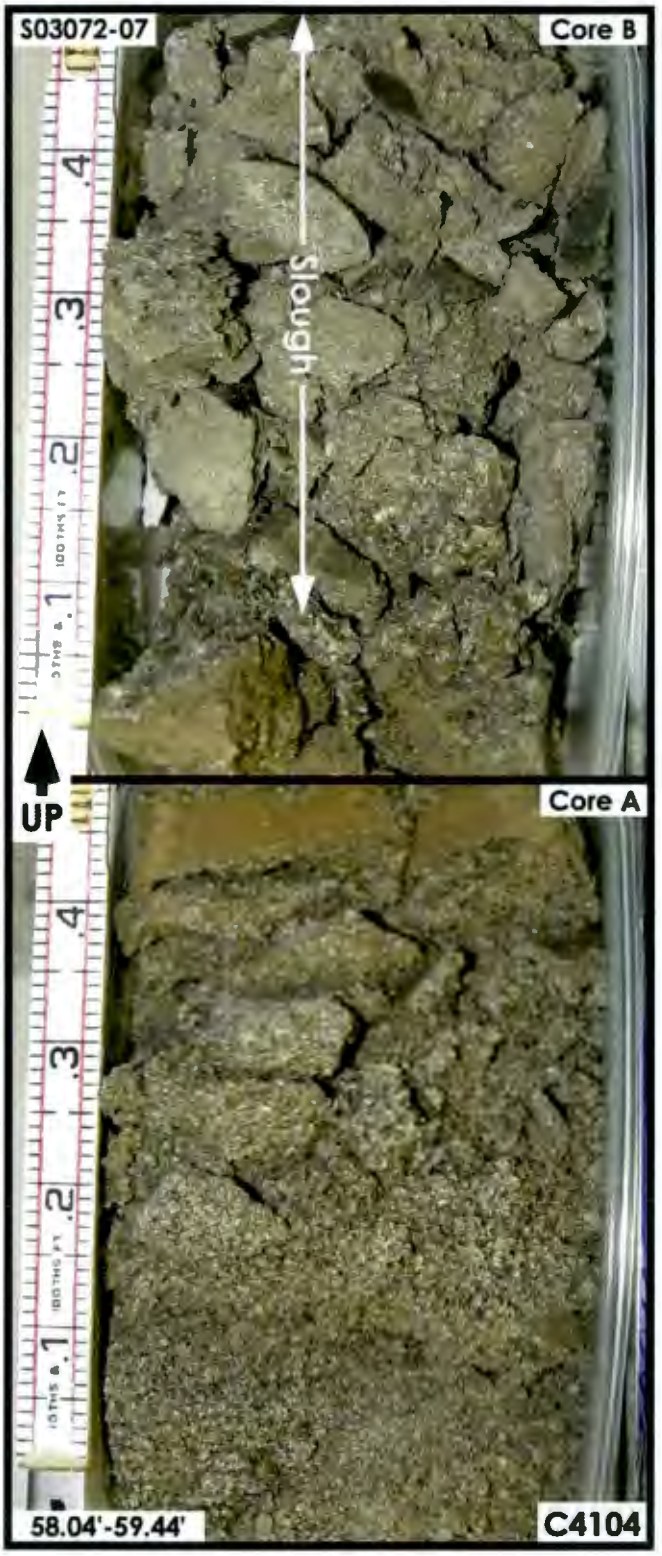

Figure A-2.7. Hanford Formation (H2 unit) 58.04 ft – 59.44 ft

Figure A-2.8. Hanford Formation (H2 unit) 63.05 ft – 64.35 ft

Figure A-2.9. Hanford Formation (H2 unit) 75.05 ft – 76.35 ft

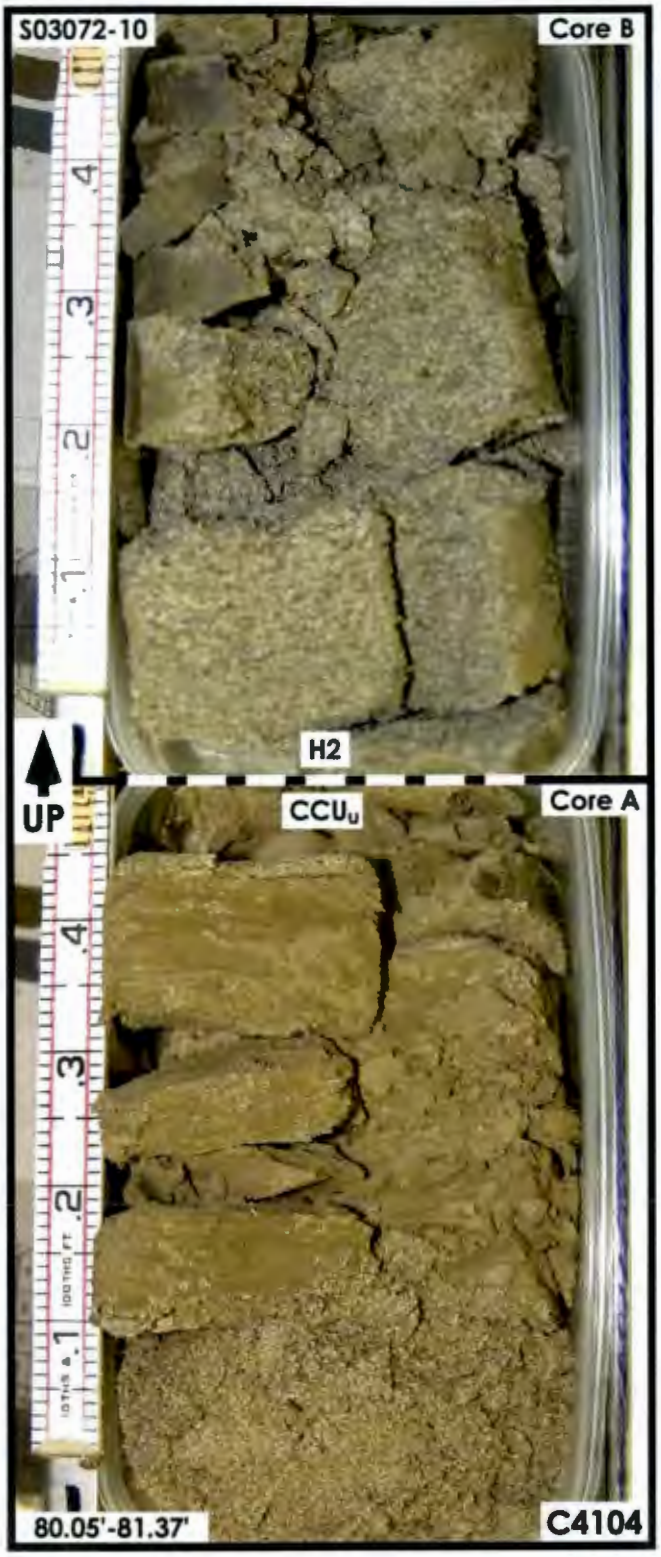

Figure A-2.10. Hanford Formation (H2 unit) / Cold Creek Unit – Upper (CCU_u) 80.05 ft – 81.37 ft

Figure A-2.11. Cold Creek Unit – Upper (CCU_u) 86.30 ft – 87.70 ft

Figure A-2.12. Cold Creek Unit – Upper (CCU$_u$) / Lower (CCUl) 91.63 ft – 92.93 ft

Figure A-2.13. Cold Creek Unit – Lower (CCU_l) 92.58 ft – 93.88 ft

Figure A-2.14. Cold Creek Unit – Lower (CCU_l) 93.73 ft – 95.17 ft

Figure A-2.15. Cold Creek Unit – Lower (CCU_l) 99.37 ft – 100.70 ft

Figure A-2.16. Cold Creek Unit – Lower (CCU_l) 101.00 ft – 102.30 ft

Figure A-2.17. Cold Creek Unit – Lower (CCU_l) 105.04 ft – 106.44 ft

Figure A-2.18. Cold Creek Unit – Lower (CCU_l) 106.44 ft – 107.74 ft

Figure A-2.19. Ringold Formation – Member of Taylor Flat (R_{tf}) 110.00 ft – 111.30 ft

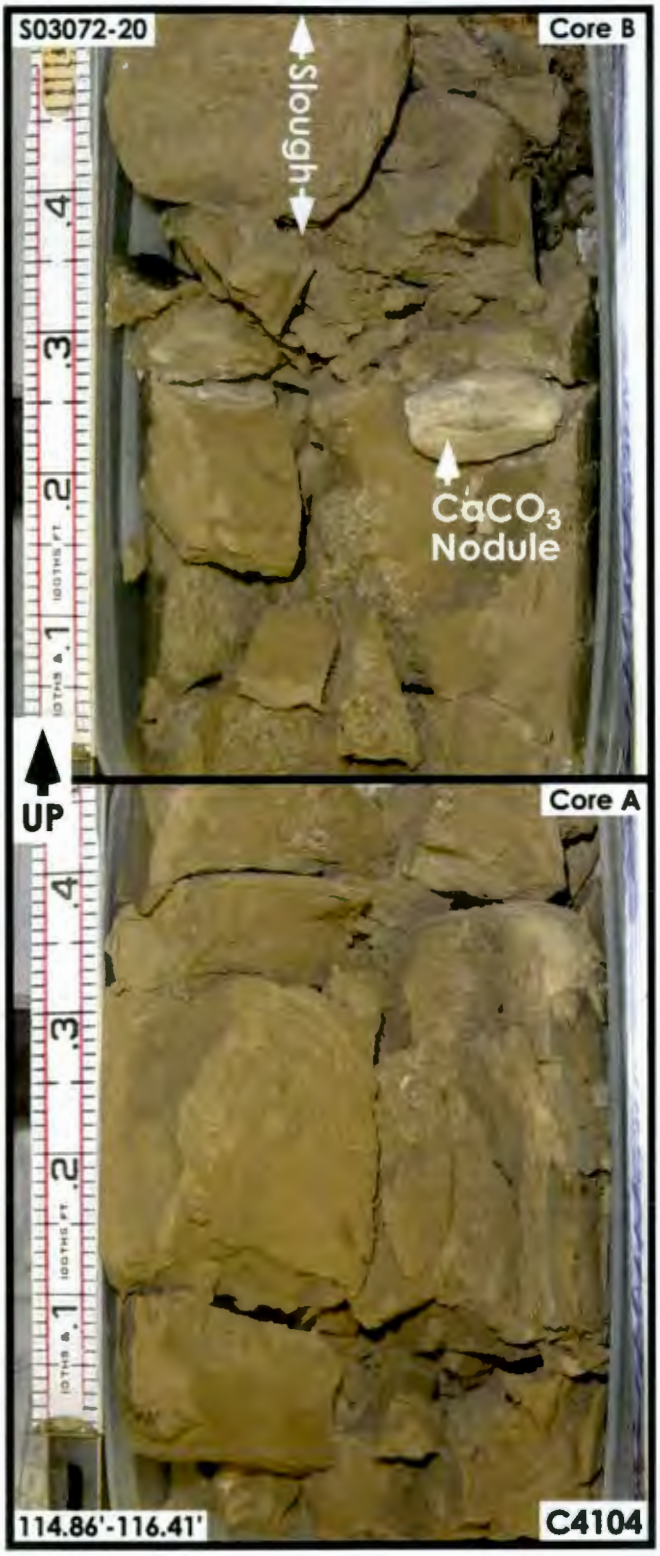

Figure A-2.20. Ringold Formation – Member of Taylor Flat (R_{tf}) 114.86 ft – 116.41 ft

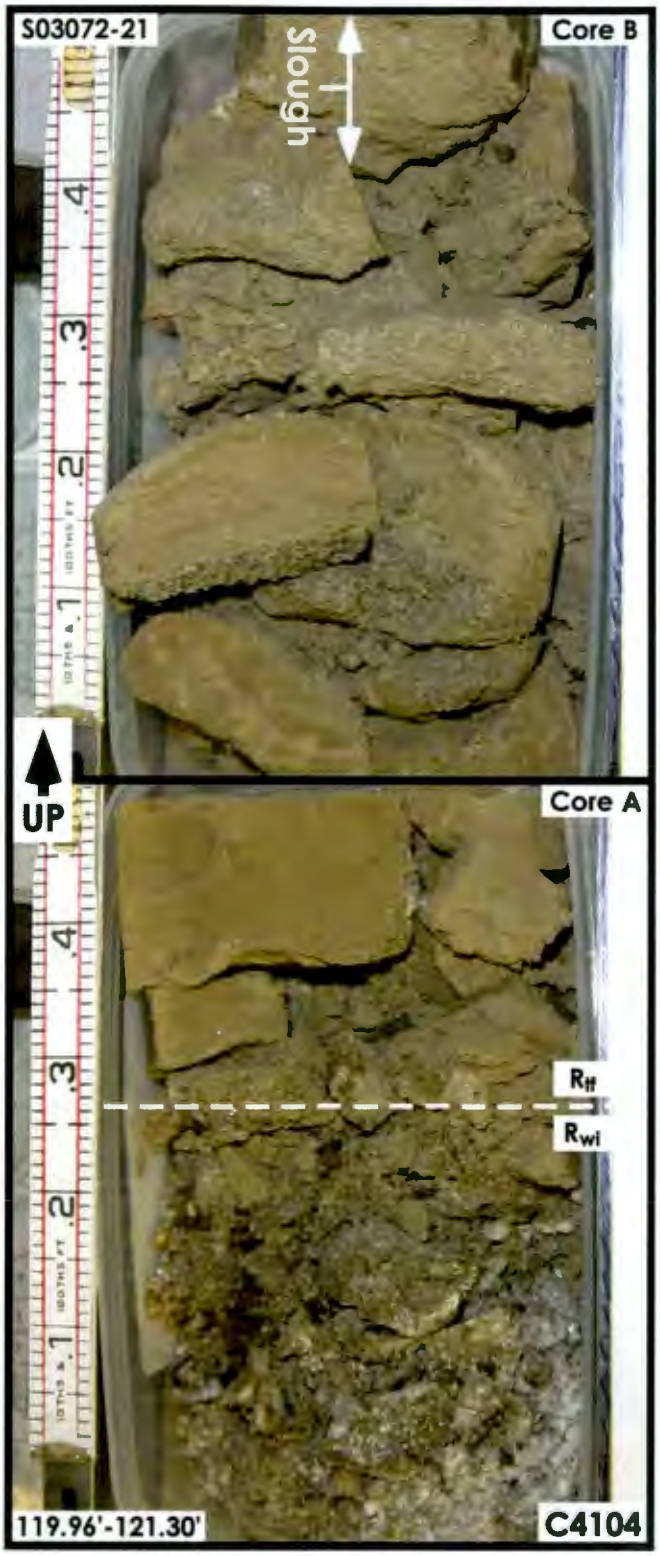

Figure A-2.21. Ringold Formation – Member of Taylor Flat (R_{tf}) / Member of Wooded Island (R_{wi}) 119.96 ft – 121.30 ft

Figure A-2.22. Ringold Formation – Member of Wooded Island (R_{wi}) 122.96 ft – 124.41 ft

Figure A-2.23. Ringold Formation – Member of Wooded Island (R_{wi}) 126.12 ft – 127.46 ft

Appendix A-3

C4105 (T-106)

SPLITSPOON CORE

SAMPLE PHOTOGRAPHS

Contents

Appendix A-3 ..... A-3.1

Figures

A-3.1. Backfill 14.16 ft – 15.66 ft A-3.1
A-3.2. Backfill 21.70 ft – 23.05 ft A-3.2
A-3.3. Backfill 35.74 ft – 37.14 ft A-3.3
A-3.4. Backfill 39.18 ft – 40.53 ft A-3.4
A-3.5. Hanford Formation (H2 unit) 47.30 ft – 48.03 ft A-3.5
A-3.6. Hanford Formation (H2 unit) 54.98 ft – 56.53 ft A-3.6
A-3.7. Hanford Formation (H2 unit) 68.95 ft – 70.45 ft A-3.7
A-3.8. Hanford Formation (H2 unit) 80.18 ft – 81.58 ft A-3.8
A-3.9. Cold Creek Unit – Upper (CCU_u) 85.36 ft – 87.11 ft A-3.9
A-3.10. Cold Creek Unit – Upper (CCU_u) 87.22 ft – 88.52 ft A-3.10
A-3.11. Cold Creek Unit – Lower (CCU_l) 92.24 ft – 93.59 ft A-3.11
A-3.12. Cold Creek Unit –Lower (CCU_l) 96.01 ft – 97.46 ft A-3.12
A-3.13. Cold Creek Unit – Lower (CCU_l) 99.33 ft – 100.68 ft A-3.13
A-3.14. Cold Creek Unit – Lower (CCU_l) 101.02 ft – 102.36 ft A-3.14
A-3.15. Cold Creek Unit – Lower (CCU_l) 102.17 ft – 103.52 ft A-3.15
A-3.16. Cold Creek Unit – Lower (CCU_l) 105.89 ft – 107.24 ft A-3.16
A-3.17. Cold Creek Unit – Lower (CCU_l) 109.07 ft 110.37 ft A-3.17
A-3.18. Ringold Formation – Member of Taylor Flat (R_{tf}) 114.97 ft – 116.30 ft A-3.18
A-3.19. Ringold Formation – Member of Taylor Flat (R_{tf}) 119.85 ft 121.19 ft A-3.19
A-3.20. Ringold Formation – Member of Wooded Island (R_{wi}) 122.90 ft – 124.24 ft A-3.20
A-3.21. Ringold Formation – Member of Wooded Island (R_{wi}) 128.91 ft – 130.12 ft A-3.21
A-3.22. Ringold Formation – Member of Wooded Island (R_{wi}) 128.58 ft – 129.58 ft A-3.22

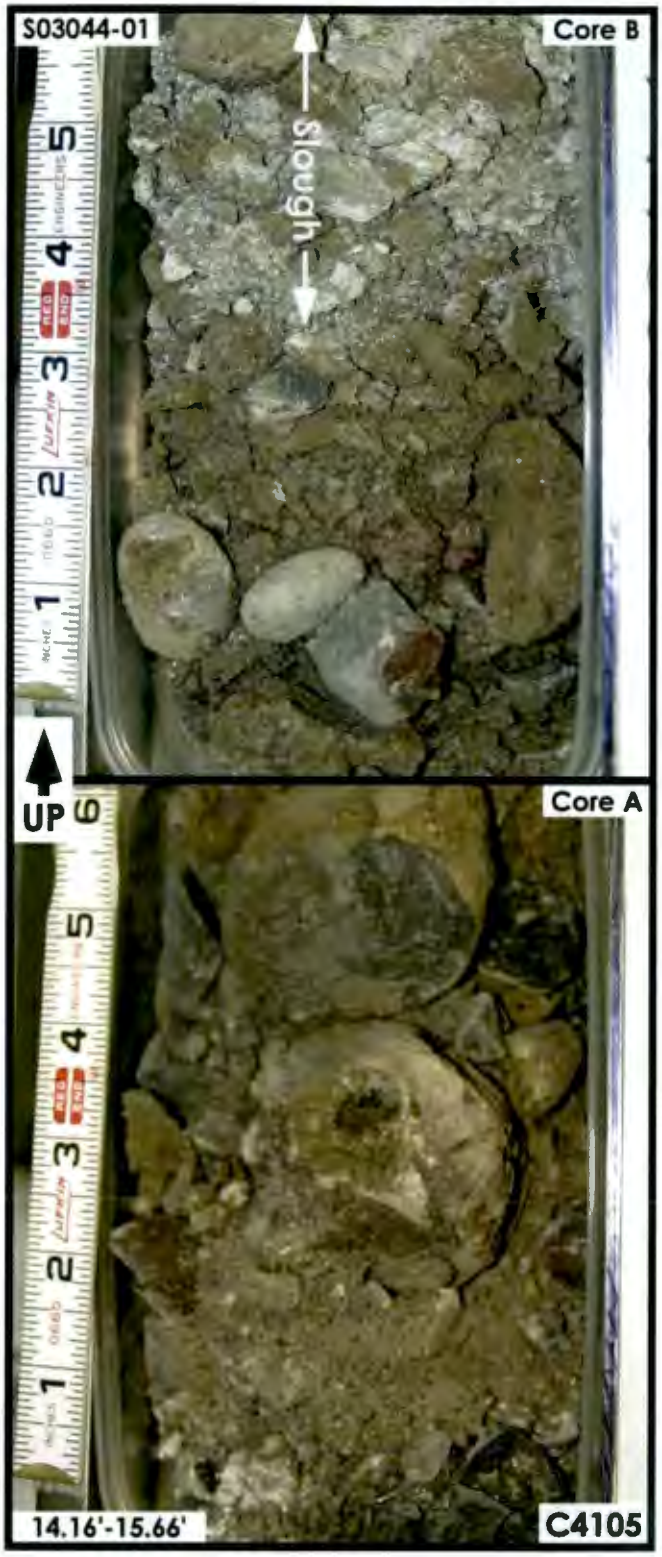

Figure A-3.1. Backfill 14.16 ft – 15.66 ft

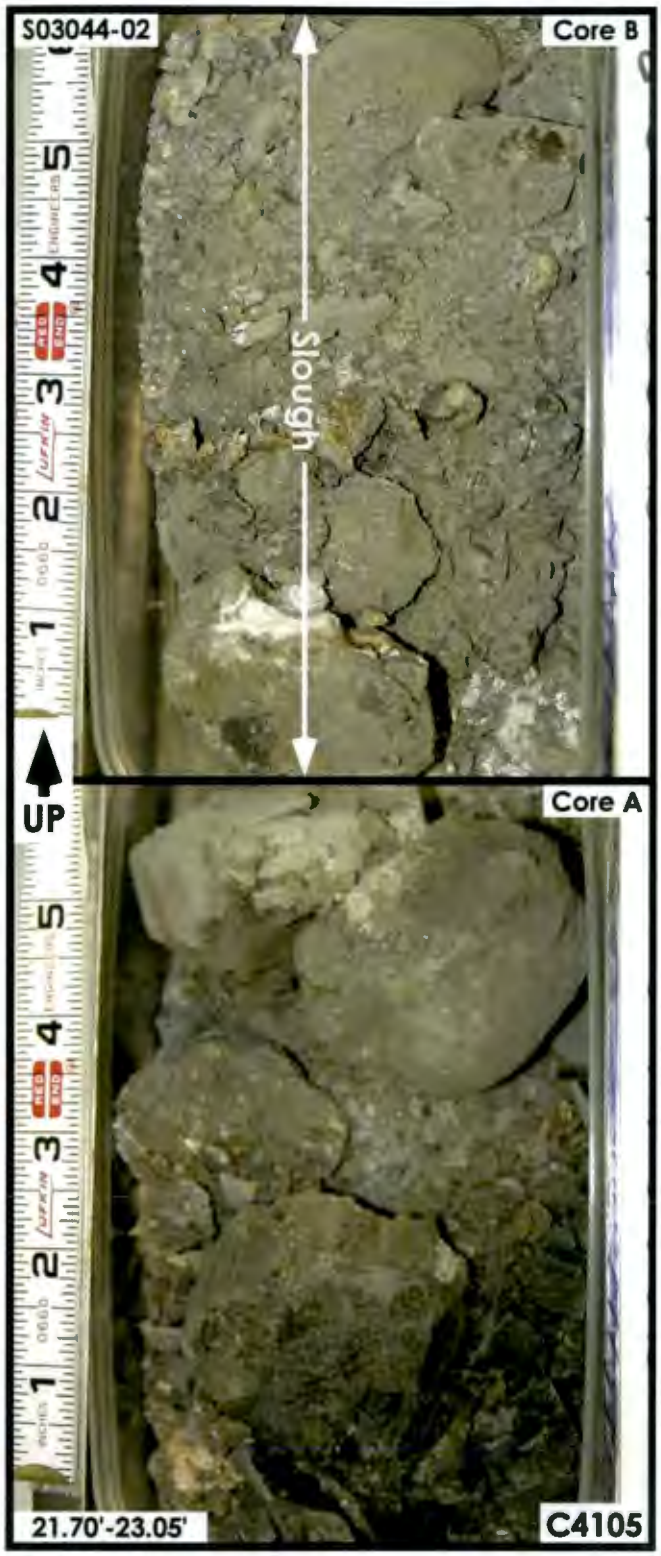

Figure A-3.2. Backfill 21.70 ft – 23.05 ft

Figure A-3.3. Backfill 35.74 ft – 37.14 ft

Figure A-3.4. Backfill 39.18 ft – 40.53 ft

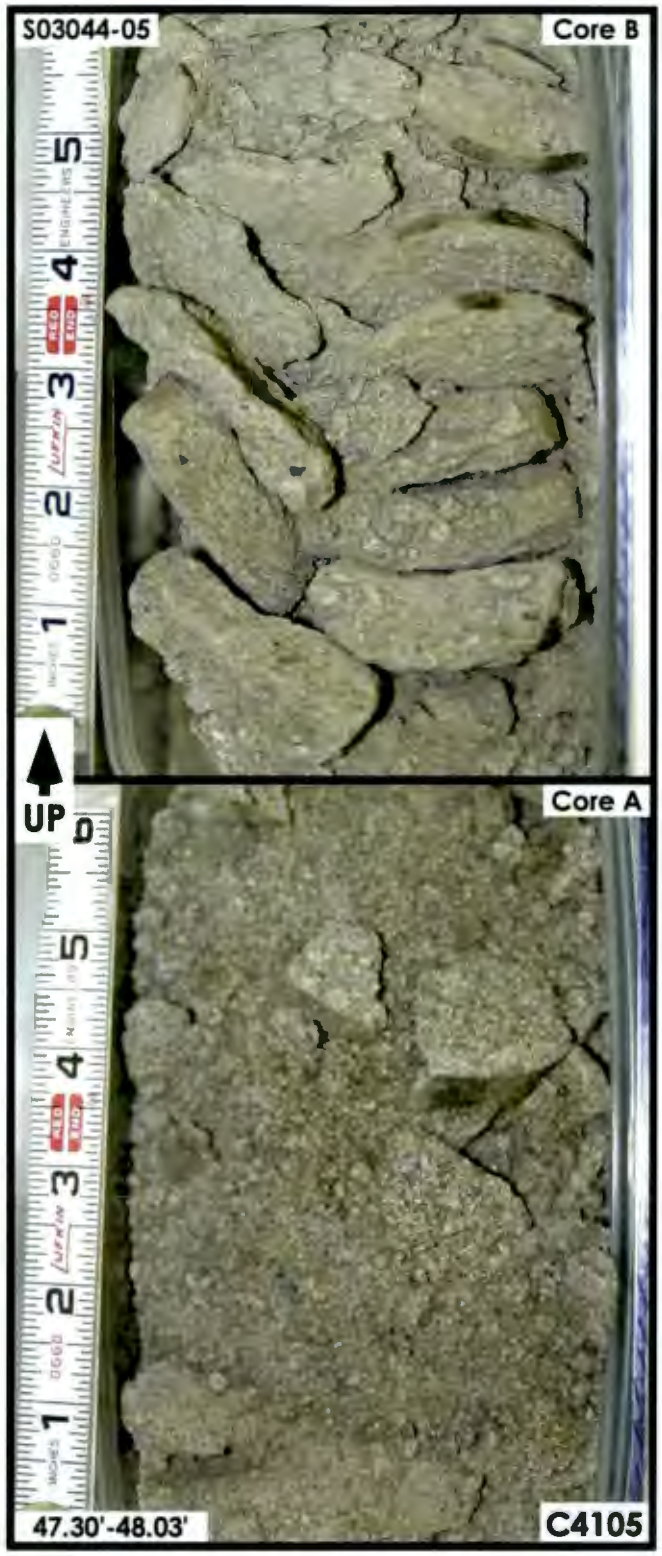

Figure A-3.5. Hanford Formation (H2 unit) 47.30 ft – 48.03 ft

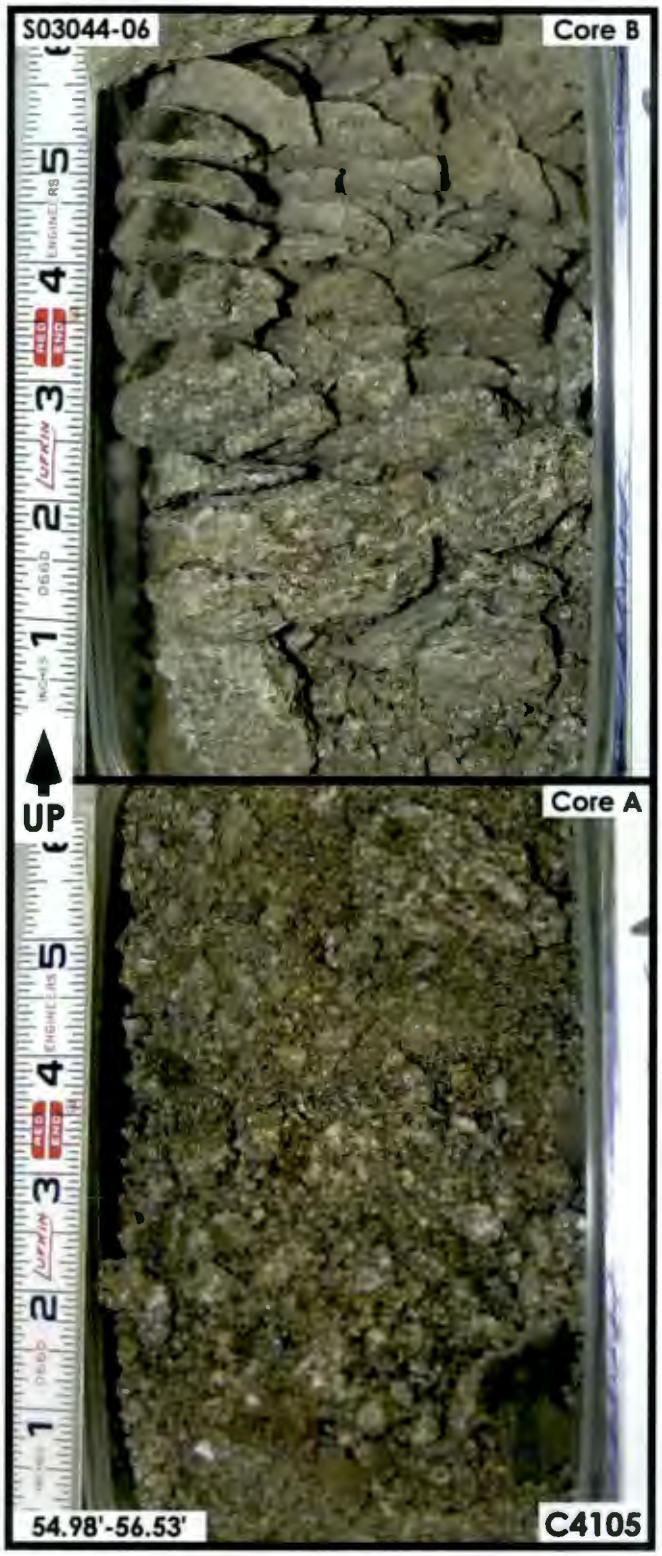

Figure A-3.6. Hanford Formation (H2 unit) 54.98 ft – 56.53 ft

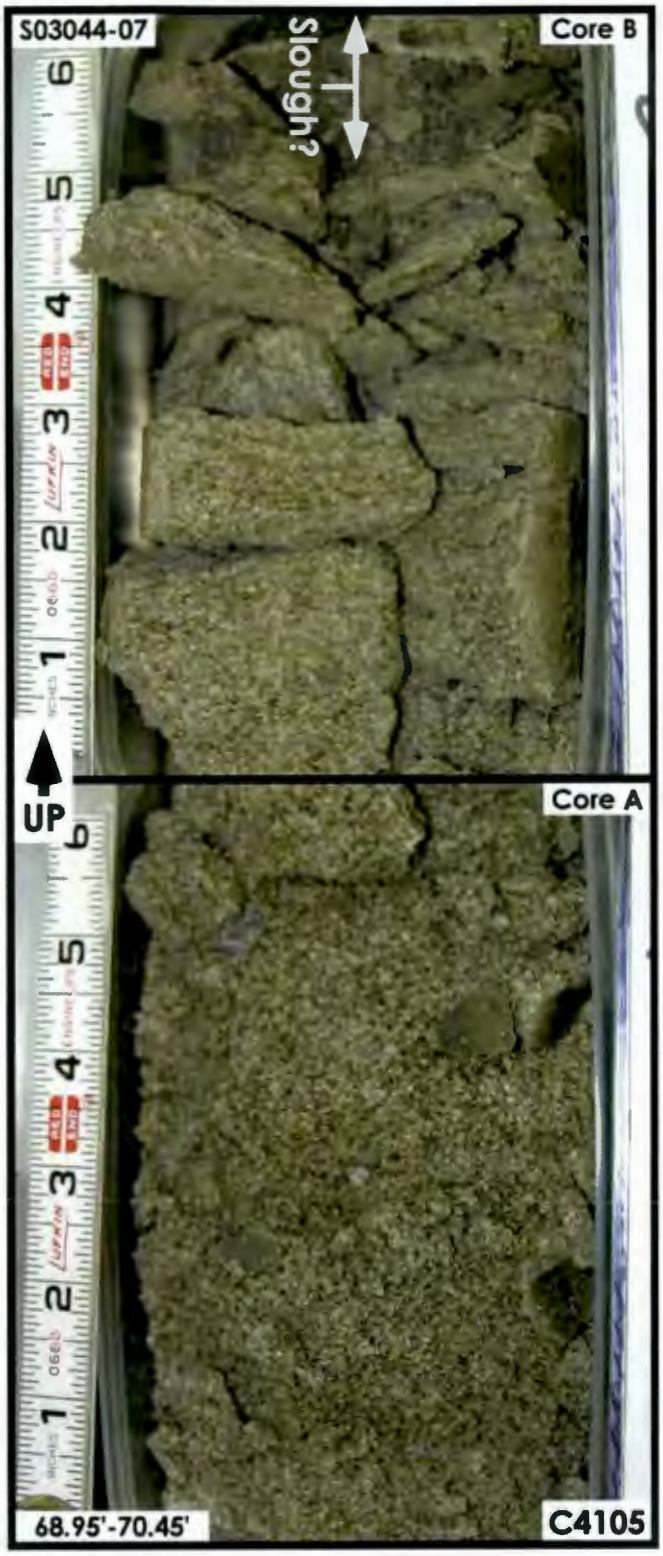

Figure A-3.7. Hanford Formation (H2 unit) 68.95 ft – 70.45 ft

Figure A-3.8. Hanford Formation (H2 unit) 80.18 ft – 81.58 ft

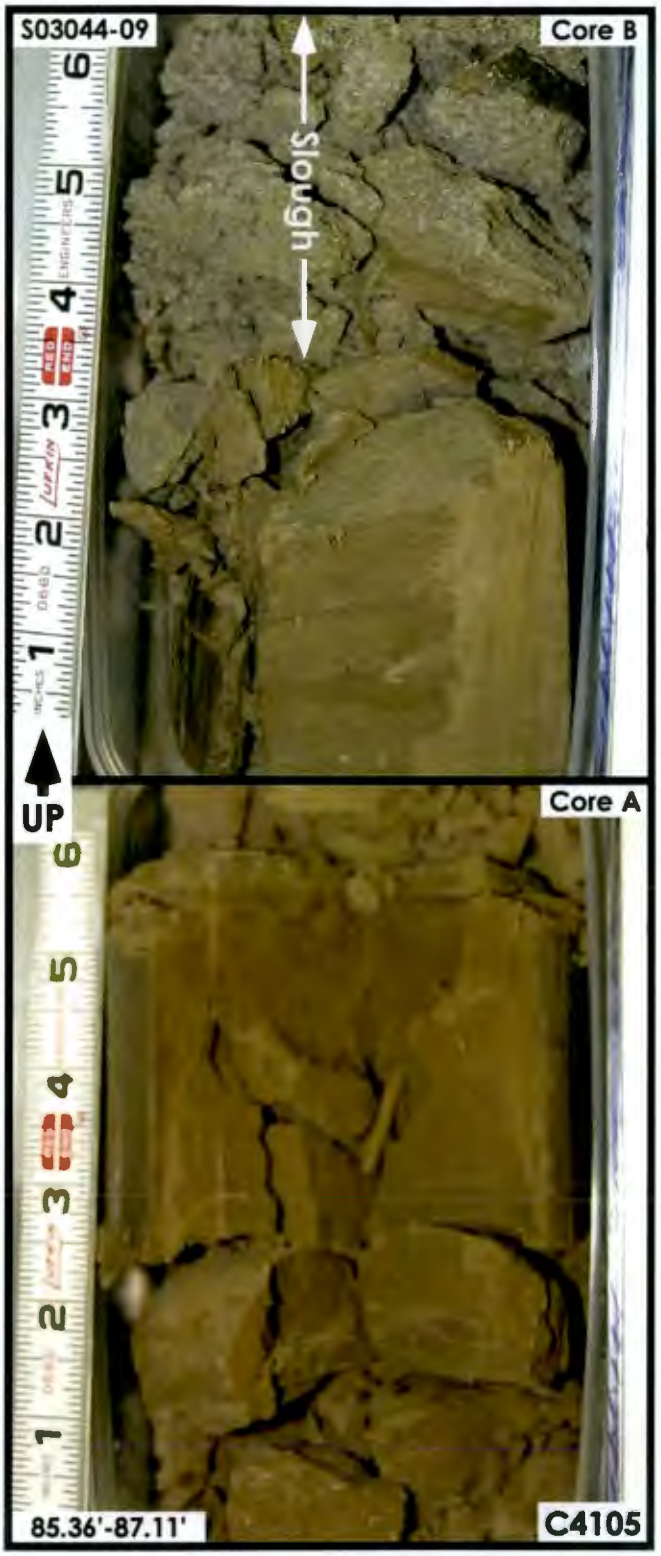

Figure A-3.9. Cold Creek Unit – Upper (CCU_u) 85.36 ft – 87.11 ft

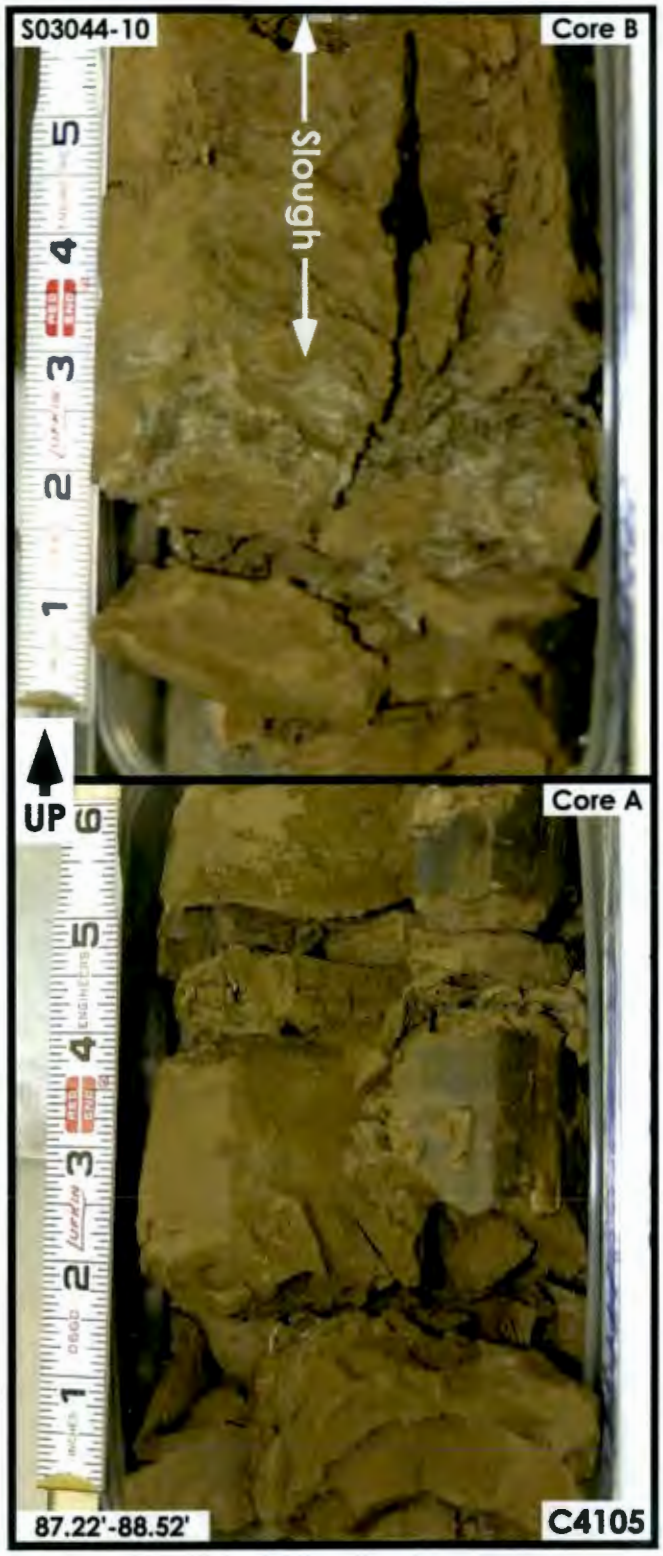

Figure A-3.10. Cold Creek Unit – Upper (CCU_u) 87.22 ft – 88.52 ft

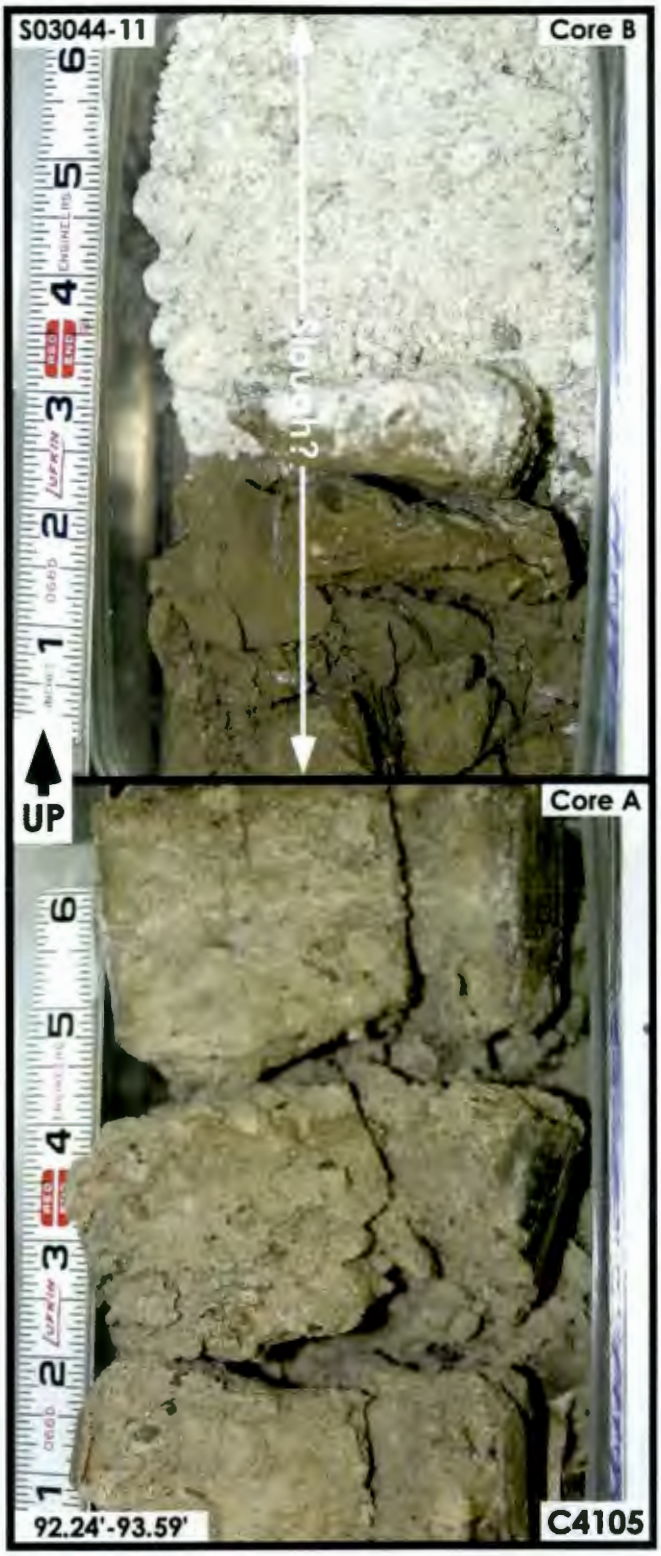

Figure A-3.11. Cold Creek Unit – Lower (CCU_l) 92.24 ft – 93.59 ft

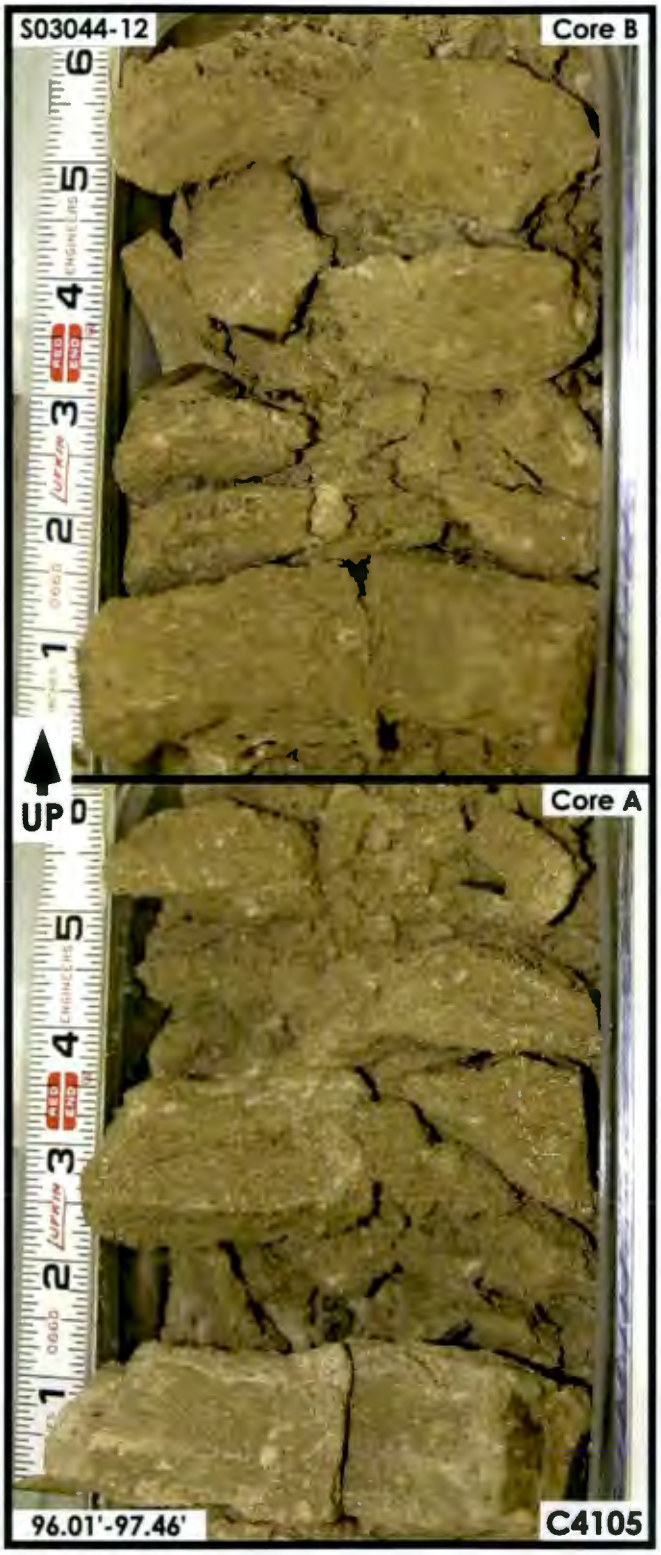

Figure A-3.12. Cold Creek Unit –Lower (CCU_l) 96.01 ft – 97.46 ft

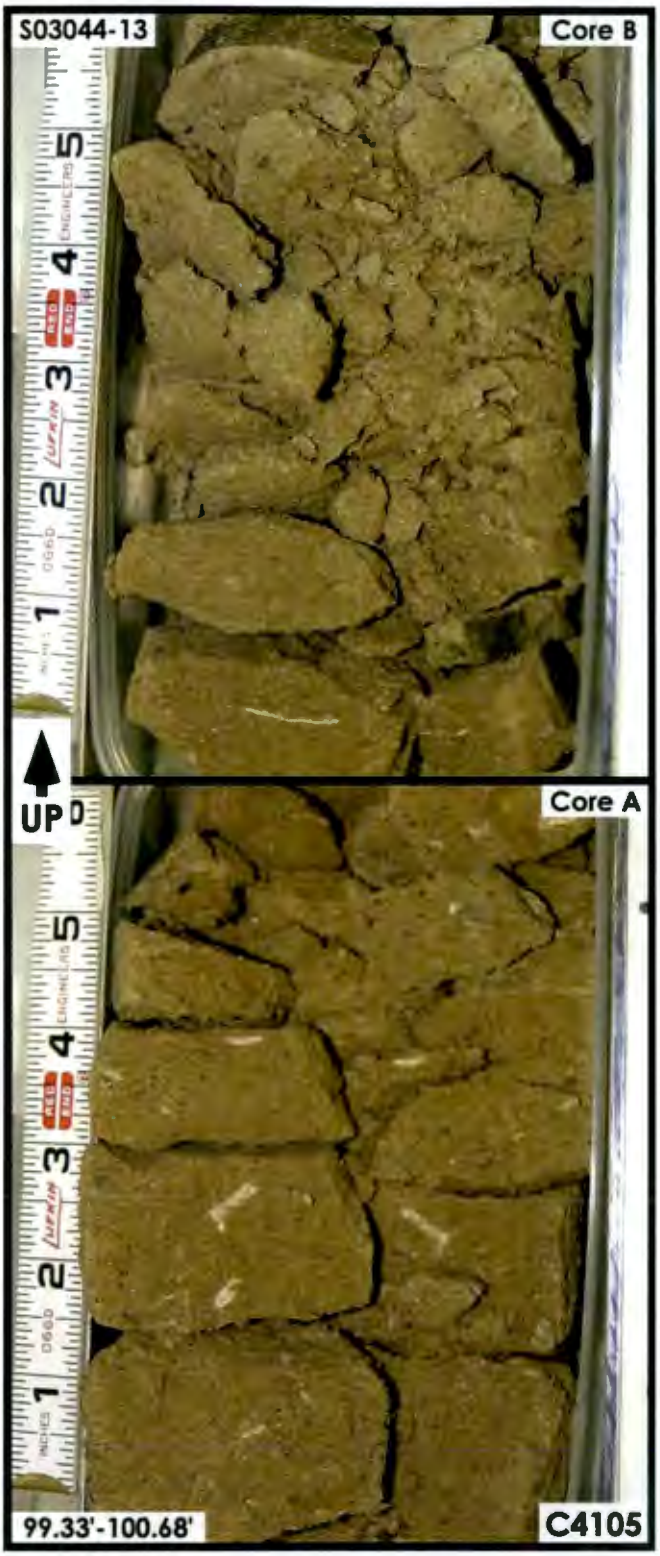

Figure A-3.13. Cold Creek Unit – Lower (CCU_l) 99.33 ft – 100.68 ft

Figure A-3.14. Cold Creek Unit – Lower (CCU_l) 101.02 ft – 102.36 ft

Figure A-3.15. Cold Creek Unit – Lower (CCU_l) 102.17 ft – 103.52 ft

Figure A-3.16. Cold Creek Unit – Lower (CCU_l) 105.89 ft – 107.24 ft

Figure A-3.17. Cold Creek Unit – Lower (CCU_l) 109.07 ft 110.37 ft

Figure A-3.18. Ringold Formation – Member of Taylor Flat (R_{tf}) 114.97 ft – 116.30 ft

Figure A-3.19. Ringold Formation – Member of Taylor Flat (R_{tf}) 119.85 ft 121.19 ft

Figure A-3.20. Ringold Formation – Member of Wooded Island (R_{wi}) 122.90 ft – 124.24 ft

Figure A-3.21. Ringold Formation – Member of Wooded Island (R_{wi}) 128.91 ft – 130.12 ft

Figure A-3.22. Ringold Formation – Member of Wooded Island (R_{wi}) 128.58 ft – 129.58 ft

Appendix B. Core Logs

B.1 C4104 (T-106)

B.2 C4105 (T-106)

Appendix B-1

C4104 (T-106)

GEOLOGIC DESCRIPTION OF CORE

OBTAINED DURING OPENING IN LAB

Contents

Appendix B.1 C4104 (T-106) GEOLOGIC DESCRIPTION OF CORE B-1.1

Pacific Northwest National Laboratory	DAILY BOREHOLE LOG	Boring/Well No C4104	Depth 14.98 - 23.03	Date 5-15-03	Sheet 1 of 9
		Location T-106	Project Vadose Zone		

Logged by BN Bjornstad (Print / Sign) | (Print / Sign)

Reviewed by (Print / Sign) Date

Lithologic Class. Scheme Procedure Rev

Steel Tape/E-Tape / Field Indicator Equip. 1) 2)

Drilling Contractor

Driller

Rig/Method

Depth Control Point

DEPTH ( )	TIME	SAMPLES TYPE	SAMPLES ID NUMBER	CONTAMINATION INSTR.	CONTAMINATION READING	MOISTURE	GRAPHIC LOG C Z S G	LITHOLOGIC DESCRIPTION (particle size distribution, sorting, mineralogy, roundness, color, reaction to HCl, etc.)	H_2O ADDED	CASING	DRILLING COMMENTS (drilling rate, down time, blow counts, water level, drill fluid, etc.)
14.98		GP	503072-1B			SM		gS, 25% G, 15% S, 10% Z			1.6' = drilled length
			↓			↓					GP = geoprobe splitspoon
											66 mm ID
			-1A			M		gS, 30% gravel, 60% sand, 10% Z			Backfill
								max. part. ≈ 2cm, mod rxn			
16.58			↓			↓		w/ HCl 2.5Y 4/4 (olive brn)			
								mod sorted, loose, ~50% broken			
								angular clasts, otherwise			
								subangular to subrounded,			
								g = 80-90% basalt			
21.68		GP	-2B			SM		ZSG 30% G, 40% S, 20% Z			1.35' = drilled length
			↓			↓		max. part size = 15 mm, mod.			
								rxn w/ HCl, poorly sorted,			
			-2A					2.5Y 4/2, sl. compact, mostly broken			
								gravel clasts.			
23.03			↓			↓		lower portion distinctly different			
								color but about same texture,			
								wk-mod rxn w/ HCl 10YR 5/4			
								(yellowish brn)			

W = Wet, M = Moist, D = Dry

1998/DCL/PROC/DBL/001

Pacific Northwest National Laboratory	DAILY BOREHOLE LOG	Boring/Well No C4104	Depth 29.73-40.35	Date 5-15-03	Sheet 2 of 9
		Location T-106	Project Vadose Zone		

Logged by B N Bjornstad (Print / Sign)

Reviewed by _____ (Print / Sign) Date _____

Lithologic Class. Scheme _____ Procedure _____ Rev ____

Steel Tape/E-Tape _____ / _____ Field Indicator Equip. 1) _____ 2) _____

Drilling Contractor _____

Driller _____

Rig/Method _____

Depth Control Point _____

DEPTH ( )	TIME	SAMPLES TYPE	SAMPLES ID NUMBER	CONTAMINATION INSTR.	CONTAMINATION READING	MOISTURE	GRAPHIC LOG C Z S G	LITHOLOGIC DESCRIPTION (particle size distribution, sorting, mineralogy, roundness, color, reaction to HCl, etc.)	H_2O ADDED	CASING	DRILLING COMMENTS (drilling rate, down time, blow counts, water level, drill fluid, etc.)
29.73		GP	503072-3B			SM		zgS, G=25% S=60% Z=15%			1.35' = drilled length
			↓			↓		lgst clast = 30mm, wk-mod rxn			
								w/HCl, 1lg. granite and wthrd			
			-3A					basalt clast, lower part more			
								compact, poorly sorted,			
31.08			↓			↓		2.5Y 4/4			
35.9		GP	-4B								B liner empty
			↓								shielded liner = smaller
											diam = 48mm
			-4A			W		zgS, 30% G, 50% S, 20% Z,			drilled length = 1.3'
								poorly sorted, max part size =			
37.2			↓			↓		15mm, mod rxn w/HCl,			
								2.5Y 4/2, some Feoxide blebs			
								sl compact			
39.0		GP	-5B								drilled length = 1.35'
			↓					max pat size = 10mm			B liner empty
								gS 20% G 70% S 10% Z			shielded liner = smaller
			-5A					loose, 2.5Y 5/2 (grayish brn),			diam = 48mm
						SM		poorly sorted, wk-mod rxn			Backfill?
40.35			↓			↓		w/HCl, G = mostly angular			
								basalt, loose, looks like			
								slough			

W = Wet, M = Moist, D = Dry

1998/DCL/PROC/DBL/001

Pacific Northwest National Laboratory	DAILY BOREHOLE LOG	Boring/Well No C4104	Depth 46.0-64.35	Date 5-15-03	Sheet 3 of 9
		Location T-106	Project Vadose Zone		

Logged by B N Bjornstad (Print / Sign)

Reviewed by _____ (Print / Sign) Date _____

Lithologic Class. Scheme _____ Procedure _____ Rev _____

Steel Tape/E-Tape _____ / _____ Field Indicator Equip. 1) _____ 2) _____

Drilling Contractor _____

Driller _____

Rig/Method _____

Depth Control Point _____

DEPTH ( )	TIME	SAMPLES TYPE	SAMPLES ID NUMBER	CONTAMINATION INSTR.	CONTAMINATION READING	MOISTURE	GRAPHIC LOG C Z S G	LITHOLOGIC DESCRIPTION (particle size distribution, sorting, mineralogy, roundness, color, reaction to HCl, etc.)	H_2O ADDED	CASING	DRILLING COMMENTS (drilling rate, down time, blow counts, water level, drill fluid, etc.)
46.0		GP	S03072-6B			D		S, 90% sand, 10% pebbles,			1.3' = drilled length
			↓			↓		mod. sorted wk rxn w/ HCl			Hanford fm - H2 unit
								max part size = 5-10 mm,			
			-6A			SM		sand mostly med-crs,			
								2.5Y6/2 (lt. grayish brn.)			
47.3			↓			↓		felsic sand (15-25% basalt)			
58.04		GP	-7B			SM		sandy slough, max part size =			Drilled length = 1.4'
			↓					↓ crs sand, poorly sorted,			
								loose			
			-7A					(2.5Y5/4, ZS, laminated, wk rxn			
								w/HCl well sorted, compact			
59.44			↓			↓		80% fn-md sand 20% Z,			
								distinctly more brn, compact			
								S, mostly md-crs 30-40%			
								basalt, max part size = 15mm, 2.5Y4/2			
								wk-mod rxn w/HCl, loose,			
								mod. sorted, single pebble			
63.05		GP	-8B			SM		S, md-v.crs, poorly sorted, loose			1.3' = drilled length
			↓					Z fnS, strong rxn w/HCl, 2.5Y5/4,			
			-8A					mod. sorted, laminated, compact			
								S, md-crs, few sm. pebbles, wk			
64.35			↓			↓		rxn w/HCl, mod. sorted, loose,			
								S = 50-60% basalt, 2.5Y5/2			
								(grayish brn)			

W = Wet, M = Moist, D = Dry

1998/DCL/PROC/DBL/001

Pacific Northwest National Laboratory	DAILY BOREHOLE LOG	Boring/Well No C4104	Depth 75.05-87.7	Date 5-15-03	Sheet 4 of 9
		Location T-106	Project Vadose Zone		

Logged by B N Bjornstad (Print / Sign)

Reviewed by _____ (Print / Sign) Date _____

Lithologic Class. Scheme _____ Procedure _____ Rev _____

Steel Tape/E-Tape _____ / _____ Field Indicator Equip. 1) _____ 2) _____

Drilling Contractor _____

Driller _____

Rig/Method _____

Depth Control Point _____

DEPTH ( )	TIME	SAMPLES TYPE	SAMPLES ID NUMBER	CONTAMINATION INSTR.	CONTAMINATION READING	MOISTURE	GRAPHIC LOG C Z S G	LITHOLOGIC DESCRIPTION (particle size distribution, sorting, mineralogy, roundness, color, reaction to HCl, etc.)	H_2O ADDED	CASING	DRILLING COMMENTS (drilling rate, down time, blow counts, water level, drill fluid, etc.)
75.05		GP	503072-9B			SM		S, mostly md-crs, laminated, 2.5Y5/2, wk-mod. rxn w/ HCl, S = 20-30% basalt, max part size = v. crs. sand lower half = 2.5Y5/4 (lt. olive brn)			1.3' = drilled length
			↓			↓					x = sample location
			-9A								
76.35			↓			↓					
80.05		GP	-10B			SM		S, fn-crs, mostly md wk-mod rxn w/ HCl, max part size = crs. sand, finer at v. bottom ? B liner, 2.5Y5/2 (grayish brn), laminated, 20-30% basalt			1.32' = Drilled length Hanford fm - H2 unit
			↓			↓					80.7' = contact
			-10A			M					Upper Cold Creek unit
81.37			↓			SM		zfnS, mod-strong rxn w/ HCl, well laminated, compact, 2.5Y4/4, well sorted S, fn, well sorted, loose, mod rxn w/ HCl			
86.3		GP	-11B			M		z-zfnS, z in middle is stiff, well laminated, 2.5Y4/4, strong rxn w/ HCl, compact, cohesive, v. well sorted, max part size = fn sand			1.4' = drilled length
			↓			↓					
			-11A								
87.7			↓			↓					

W = Wet. M = Moist. D = Dry

1998/DCL/PROC/DBL/001

Pacific Northwest National Laboratory

DAILY BOREHOLE LOG

Boring/Well No C4104 Depth 91.63-93.88 Date 5-15-03 Sheet 5 of 9

Location T-106 Project Vadose Zone

Logged by B N Bjornstad

Reviewed by _____ Date _____

Lithologic Class. Scheme _____ Procedure _____ Rev _____

Steel Tape/E-Tape _____ / _____ Field Indicator Equip. 1) _____ 2) _____

Drilling Contractor _____

Driller _____

Rig/Method _____

Depth Control Point _____

DEPTH ( )	TIME	SAMPLES TYPE	SAMPLES ID NUMBER	CONTAMINATION INSTR.	CONTAMINATION READING	MOISTURE	GRAPHIC LOG C Z S G	LITHOLOGIC DESCRIPTION (particle size distribution, sorting, mineralogy, roundness, color, reaction to HCl, etc.)	H_2O ADDED	CASING	DRILLING COMMENTS (drilling rate, down time, blow counts, water level, drill fluid, etc.)
91.63		GP	503072-12B			SM		zfuS, 30% Z 70% sand,			1.3' = drilled length
			↓			↓		weakly lam toward center of B liner,			Rubber sheathing at top of B
								mod. sorted, 2.5Y4/2, mod-			liner - fragments
			-12A			M		strong rxn w/ HCl, carbonate			upper CCU
			↓			↓		nodules (1-2cm diam.)			92.5' contact
92.93			↓			↓		gmS, 30% G, 40% M, 40% S			lower CCU - caliche
								max part size = 2cm			caliche indicated with diagonal
								v. poorly sorted, cemented,			line in graphic log
								violent rxn w/ HCl, G = angular			
								to subrounded small pebbles			
								w 30% basalt, M = mixture of			
								silt and clay 2.5Y7/4			
92.58		GP	-13B			M		zfuS - slough w/ sheathing,			1.3' = drilled length
								2.5Y4/4			More sheathing (in slough)
			↓					(g)mS 5% G, 45% M, 45% S,			0.35' overlap with run 12
			-13A					laminated (secondary pedogenic)			
								2.5Y7/4 pale yellow, v. poorly			
93.88			↓			↓		sorted, cemented, compact			
								max part size = 5mm, violent			
								rxn w/ HCl, pinkish banding			
								G = mostly v.sm. pebbles and			
								granules of basalt			

W = Wet, M = Moist, D = Dry

1998/DCL/PROC/DBL/001

Pacific Northwest National Laboratory

DAILY BOREHOLE LOG

Boring/Well No C4104 Depth 93.75-102.3 Date 5-15-03 Sheet 6 of 9

Location T-106 Project Vadose Zone

Logged by B N Bjornstad

Reviewed by Date

Lithologic Class. Scheme Procedure Rev

Steel Tape/E-Tape / Field Indicator Equip. 1) 2)

Drilling Contractor

Driller

Rig/Method

Depth Control Point

DEPTH ( )	TIME	SAMPLES TYPE	SAMPLES ID NUMBER	CONTAMINATION INSTR.	CONTAMINATION READING	MOISTURE	GRAPHIC LOG C Z S G	LITHOLOGIC DESCRIPTION (particle size distribution, sorting, mineralogy, roundness, color, reaction to HCl, etc.)	H_2O ADDED	CASING	DRILLING COMMENTS (drilling rate, down time, blow counts, water level, drill fluid, etc.)
93.75		GP	303072-14B			M		zfnS with CaCO3 nodules			1.42' = drilled length
			↓					2.5Y 4/4, strong rxn w/ HCl, massive			0.13' overlap with run 13
								1 subang. basalt pebble ~ 2cm diam., poorly sorted			
			-14A					gmS, massive, 2.5Y 7/4, v. poorly			
								sorted, violent rxn w/ HCl, CaCO3 nodules			v. sharp contact w/ zS below
95.17			↓			↓		zfnS 2.5Y 5/4, 20% Z, 80% fn sand,			
								well sorted, sl. compact, massive			
								strong rxn w/ HCl, few CaCO3 nodules			
99.37		GP	-15B			SM		(z)S, 10% Z, 90% S, strong rxn w/			1.33' = drilled length
			↓			↓		HCl, massive 2.5Y 6/2 (lt.			liners stuck in core barrel -
						M		brnish gray, mod sorted			have to pound out sample
			-15A					S, fn-md sand, 2.5Y 5/4 (lt.			
								olive brn), wk-mod rxn w/ HCl,			
100.7			↓			↓		max part size = med. sand			
								pure fn sand at bottom, laminated, strong rxn w/ HCl			
101.0		GP	-16B			SM		SM sandy mud, poorly sorted,			1.3' = drilled length
			↓					violent rxn w/ HCl, 2.5Y 7/4			liners stuck - have to pound out
								(pale yellow), massive, compact,			of core barrel
			-16A					bottom more cemented			plastic-rubber sheathing at
											top of B liner
102.3			↓			↓					

W = Wet, M = Moist, D = Dry

1998/DCL/PROC/DBL/001

Pacific Northwest National Laboratory	DAILY BOREHOLE LOG	Boring/Well No C4104	Depth 105.04-111.3	Date 5-26-03	Sheet 7 of 9
		Location T-106	Project Vadose Zone		

Logged by BN Bjornstad

Reviewed by _____ Date _____

Lithologic Class. Scheme _____ Procedure _____ Rev _____

Steel Tape/E-Tape _____ / _____ Field Indicator Equip. 1) _____ 2) _____

Drilling Contractor _____

Driller _____

Rig/Method _____

Depth Control Point _____

DEPTH ( )	TIME	SAMPLES TYPE	SAMPLES ID NUMBER	CONTAMINATION INSTR.	CONTAMINATION READING	MOISTURE	GRAPHIC LOG C Z S G	LITHOLOGIC DESCRIPTION (particle size distribution, sorting, mineralogy, roundness, color, reaction to HCl, etc.)	H_2O ADDED	CASING	DRILLING COMMENTS (drilling rate, down time, blow counts, water level, drill fluid, etc.)
105.04		GP	503072-16			SM		(g)S, sand 85% 5% gravel			Rtf - Ringold member Taylor Flat
								10% silt, few small pebbles, mostly md-crs sand			
			↓			↓		cemented, strng rxn w/ HCl, 20-30% basalt			Drilled length = 1.4'
			-17A			SM		largest clast = 5 mm, wkly			
								laminated 2.5Y5/4 (lt. olive brn)			
106.44			↓			↓		moderately sorted, looser and less calcareous toward bottom, no gravel			
106.44		GP	-18B			SM	S1	(g)S, mostly md sand (slough), mod rxn w/ HCl, pebbles up to 3 cm, rubber sheathing			
								SZ, strng rxn w/ HCl, massive,			Drilled length = 1.3'
			↓			↓		compact, 2.5Y6/4 (lt. yellowish brn)			
			-18A			SM		poorly sorted			
								S, mostly md-crs, well sorted, 2.5Y5/4,			
107.74			↓			↓		loose, wk rxn w/ HCl			
110.0		GP	-19B			M		SZ, 50% v.fn sand, 50% Z,			Drilled length = 1.3'
								laminated, 2.5Y 5/4 (lt. olive			
			↓			↓		brn), compact, no rxn w/ HCl			
			-19A			M		well sorted, sand dikelet			
								filled with well sorted fine sand			
111.3			↓			↓		~5 mm wide in B liner, vertical			

W = Wet, M = Moist, D = Dry

1998/DCL/PROC/DBL/001

Pacific Northwest National Laboratory	DAILY BOREHOLE LOG	Boring/Well No C4104	Depth 114.86-124.41	Date 5-26-03	Sheet 8 of 9
		Location T-106	Project Vadose Zone		

Logged by B N Bjornstad (Print / Sign)

Reviewed by _____ (Print / Sign) Date _____

Lithologic Class. Scheme _____ Procedure _____ Rev _____

Steel Tape/E-Tape _____ / _____ Field Indicator Equip. 1) _____ 2) _____

Drilling Contractor _____

Driller _____

Rig/Method _____

Depth Control Point _____

DEPTH ( )	TIME	SAMPLES TYPE	SAMPLES ID NUMBER	CONTAMINATION INSTR.	CONTAMINATION READING	MOISTURE	GRAPHIC LOG C Z S G	LITHOLOGIC DESCRIPTION (particle size distribution, sorting, mineralogy, roundness, color, reaction to HCl, etc.)	H_2O ADDED	CASING	DRILLING COMMENTS (drilling rate, down time, blow counts, water level, drill fluid, etc.)
114.86		GP	503072-20B			M	S1	mS, msv, 2.5Y5/4			Drilled length = 1.55'
			↓			↓		SZ fn sandy silt, 30% sand, calcareous 70% silt, 2.5Y5/4, laminated, well sorted, compact, no rxn w/HCl except for concretion			concretion ~ 3cm dia toward top.
			-20A			M		fn sand dikelet at bottom of A liner.			
			↓			↓		SZ to ZS, grading between fine sandy silt to silty fn sand, laminated, compact, 2.5Y5/4, well sorted, wk rxn w/HCl			
116.41											
119.96		GP	-21B			SM	S1	silty fn sand to medium sand (ZS to S), interbedded and laminated, sand is loose - rest is compact, 2.5Y6/4 (lt. yellowish brn)			Drilled length = 1.34'
			↓			↓					
						M		mod-well sorted, wk-mod rxn w/HCl			
			-21A			↓					
						SM		SG, 60% G, 30% S, 10% Z, loose, pulverized (most clasts broken)			RWi cont
121.3			↓			↓		2.5Y4/2 (dk grayish brn), no rxn w/HCl, S ≈ 30% basalt, poorly sorted			
								shoe filled with SG also			
122.96		GP	-22B			D		SG, dk gray, v. poorly sorted, mostly angular basalt - pulverized on top, some granitic clasts, no rxn w/HCl, 2.5Y3/0 (v. dk. gray), silt coatings on some gravel clasts, loose, v. poorly sorted			
			↓			↓					
			-22A			SM					
			↓			↓					
124.41											

W = Wet, M = Moist, D = Dry

1998/DCL/PROC/DBL/001

Pacific Northwest National Laboratory	DAILY BOREHOLE LOG	Boring/Well No C4104	Depth 126.12-127.46	Date 5-26-03	Sheet 9 of 9
		Location T-106	Project Vadose Zone		

Logged by BN Bjornstad (Print / Sign) | (Print / Sign)

Reviewed by (Print / Sign) Date

Lithologic Class. Scheme Procedure Rev

Steel Tape/E-Tape / Field Indicator Equip. 1) 2)

Drilling Contractor

Driller

Rig/Method

Depth Control Point

DEPTH ( )	TIME	SAMPLES TYPE	SAMPLES ID NUMBER	CONTAMINATION INSTR.	CONTAMINATION READING	MOISTURE	GRAPHIC LOG C	Z	S	G	LITHOLOGIC DESCRIPTION (particle size distribution, sorting, mineralogy, roundness, color, reaction to HCl, etc.)	H_2O ADDED	CASING	DRILLING COMMENTS (drilling rate, down time, blow counts, water level, drill fluid, etc.)
126.12			-23B			D				SI	(f) S, olive gray, v. poorly sorted, msv			Rw:
			↓			↓					SG, pulverized, some reddish			Drilled length = 1.34'
											weathered basalt, no rxn w/HCl			
			-23A			SM					v. poorly sorted, loose, mostly			
			↓			↓					angular basalt clasts w/ some			
127.46											granitics, multicolored			
											(mostly 10YR 4/1 - dk gray)			

W = Wet, M = Moist, D = Dry

1998/DCL/PROC/DBL/001

Appendix B-2

C4105 (T-106)

GEOLOGIC DESCRIPTION OF CORE OBTAINED

DURING OPENING IN LABORATORY

Contents

Appendix B-2 C4105 (T-106) Geologic Description of Core Obtained During Opening in Laboratory B-2.i

Pacific Northwest National Laboratory	DAILY BOREHOLE LOG	Boring/Well No C4105	Depth 14.16 - 37.14	Date 2-24-03	Sheet 1 of 10
		Location T-106	Project Vadose Zone		

Logged by B N Bjornstad (Print / Sign)

Reviewed by _____ (Print / Sign) Date _____

Lithologic Class. Scheme _____ Procedure _____ Rev _____

Steel Tape/E-Tape _____ / _____ Field Indicator Equip. 1) _____ 2) _____

Drilling Contractor _____

Driller _____

Rig/Method _____

Depth Control Point _____

DEPTH ( )	TIME	SAMPLES TYPE	SAMPLES ID NUMBER	CONTAMINATION INSTR.	CONTAMINATION READING	MOISTURE	GRAPHIC LOG C Z S G	LITHOLOGIC DESCRIPTION (particle size distribution, sorting, mineralogy, roundness, color, reaction to HCl, etc.)	H_2O ADDED	CASING	DRILLING COMMENTS (drilling rate, down time, blow counts, water level, drill fluid, etc.)
14.16		GP	S030441-1B			D		slough pulverized			GP = geoprobe
								mod rxn w/HCl, dk grayish brn			1.5' drilled length
			1A			SM		zsG, silty sandy gravel,			2.75' core diameter
								poorly sorted, broken gravel			Backfill
15.66								clasts loose, 2.5Y5/2 (grayish			
								brown), wk rxn w/ HCl, max			
								part. size = sm. cobble			
21.70			2B			D		zgS, silty gravelly sand, v.			pulverized slough
								poorly sorted, 2.5Y6/1 (gray),			
								wk rxn w/HCl, loose			
23.05			2A			SM		zsG, silty sandy gravel, v.			
								poorly sorted, max part			Backfill
								size = 6cm, loose, 2.5Y4/			
								(dk gray), wk-med rxn w/ HCl			
35.74			3B					zgS - silty gravelly sand			smaller diameter core - no "B"
								2.5Y4/2 (dk grayish brn), v.			liner - empty; 2" OD
								poorly sorted, loose,			1.4' drilled length <50%
			3A			SM		pulverized, max part. size =			recovery
								3cm, v. wk rxn w/ HCl			
37.14											Backfill

W = Wet, M = Moist, D = Dry

1998/DCL/PROC/DBL/001

Pacific Northwest National Laboratory	DAILY BOREHOLE LOG	Boring/Well No C4105	Depth 39.18-48.75	Date 2-24-03	Sheet 2 of 10
		Location T-106	Project Vadose Zone		

Logged by BN Bjornstad

Reviewed by _____ Date _____

Lithologic Class. Scheme _____ Procedure _____ Rev _____

Steel Tape/E-Tape _____ / _____ Field Indicator Equip. 1) _____ 2) _____

Drilling Contractor _____

Driller _____

Rig/Method _____

Depth Control Point _____

DEPTH ( )	TIME	SAMPLES TYPE	SAMPLES ID NUMBER	CONTAMINATION INSTR.	CONTAMINATION READING	MOISTURE	GRAPHIC LOG C	Z	S	G	LITHOLOGIC DESCRIPTION (particle size distribution, sorting, mineralogy, roundness, color, reaction to HCl, etc.)	H_2O ADDED	CASING	DRILLING COMMENTS (drilling rate, down time, blow counts, water level, drill fluid, etc.)
39.18		GP	503044-4B											Small diameter (2") core
			↓				empty							1.35 drilled length
			4A			SM					zgS, silty gravelly sand, mod.			<50% recovery
			↓			↓					sorted, loose, 2.5Y4/2 (dk			Backfill
40.53			↓			↓					grayish brn, max particle			
											size = 3.5 cm, wk-mod rxn			
											w/ HCl			
47.30			5B			D					S, fine-med. sand, well sorted,			1.45 drilled length
			↓			↓					laminated, loose to sl. compact,			standard diam = 2.75"
			↓			↓					max part. size = crs sand,			
			5A			SM					mod rxn w/ HCl, 10-20%			1.45' drilled length
			↓			↓					basalt - remainder qtz + feld.			Hanford fm. H2
48.75			↓			↓					2.5Y6/2 (lt. brnish gray).			
											sand crsens at bottom, max			
											part. = sm pebble; 2.5Y4/2			
											(grayish brn), wk rxn w/ HCl,			
											loose			

W = Wet, M = Moist, D = Dry

1998/DCL/PROC/DBL/001

Pacific Northwest National Laboratory	DAILY BOREHOLE LOG	Boring/Well No C4105	Depth 54.98 – 81.50	Date 2-24-03	Sheet 3 of 10
		Location T-106	Project Vadose Zone		

Logged by BN Bjornstad (First / Sign) | (First / Sign)

Reviewed by (First / Sign) Date

Lithologic Class. Scheme Procedure Rev

Steel Tape/E-Tape / Field Indicator Equip. 1) 2)

Drilling Contractor

Driller

Rig/Method

Depth Control Point

DEPTH ( )	TIME	SAMPLES TYPE	SAMPLES ID NUMBER	CONTAMINATION INSTR.	CONTAMINATION READING	MOISTURE	GRAPHIC LOG C Z S G	LITHOLOGIC DESCRIPTION (particle size distribution, sorting, mineralogy, roundness, color, reaction to HCl, etc.)	H_2O ADDED	CASING	DRILLING COMMENTS (drilling rate, down time, blow counts, water level, drill fluid, etc.)
54.98			S03044-6B			SM		gS, fine-crs sand (upper finer),			
			↓					platy, mod-poorly sorted,			1.55 drilled length
								2.5Y5/2 (grayish brn), coser			
			6A			SM		sand looks pulverized, pebbles			Hanford fm. H2
			↓			↓		in lower part, max part size			
56.53			↓			↓		= 0.5 cm, mod. rxn w/HCl			
								S = 50-60% basalt, 2.5Y4/2			silty sand collected in close core ~~below~~ core liner
								(dk grayish brn) below,			
								wk rxn w/HCl, loose, msv.			
								max part size = 0.1 cm			
68.95			7B			SM	*	S, fn-md sand, mod-well sorted			* = slough? - darker, non lam-
								laminated (upper part msv)			inated
			↓			↓		2.5Y5/2 (grayish brn), mod			1.5' drilled length
			7A			SM		rxn w/HCl, max. part. size =			
			↓			↓		crs. sand, lower half:			
70.45								md-crs sand, 30-40%			
								basalt, few sm. pebbles,			
								max. part size = 0.8 cm			
80.18			8B			SM	S1.	pebbly fn-md sand = slough			1.4' drilled length
								S, fn-md sand, mod sorted, lam.,			
			↓			↓		mod rxn w/HCl, 2.5Y6/2 (lt grayish			Hanford fm. H2
			8A			SM		brn), max part size = crs. sand,			
			↓			↓		S = 20-30% basalt			
81.50											

W = Wet, M = Moist, D = Dry

1998/DCL/PROC/DBL/001

Pacific Northwest National Laboratory

DAILY BOREHOLE LOG

Boring/Well No C4105 Depth 85.36-93.59 Date 2-24-03 Sheet 4 of 10

Location T-106 Project Vadose Zone

Logged by B N Bjornstad (Print / Sign) (Print / Sign)

Reviewed by (Print / Sign) Date

Lithologic Class. Scheme Procedure Rev

Steel Tape/E-Tape / Field Indicator Equip. 1) 2)

Drilling Contractor

Driller

Rig/Method

Depth Control Point

DEPTH ( )	TIME	SAMPLES TYPE	SAMPLES ID NUMBER	CONTAMINATION INSTR.	CONTAMINATION READING	MOISTURE	GRAPHIC LOG C Z S G	LITHOLOGIC DESCRIPTION (particle size distribution, sorting, mineralogy, roundness, color, reaction to HCl, etc.)	H_2O ADDED	CASING	DRILLING COMMENTS (drilling rate, down time, blow counts, water level, drill fluid, etc.)
85.36		GP	50304498			SM	S1	loose fn-md S = slough			
						M		fn S Z, fine sandy silt, well lam.,			1.75 ft drilled length
								compact / cohesive, well sorted,			Cold Creek + upper unit
			9A					mod-strong rxn w/ HCl, 2.5Y5/4			
								(lt. olive brn), mod-strong rxn			
87.11								w/ HCl			
87.22			10B			M	S1				1.3 drilled length
								.1" median sand lens, mottled with			Note: This core was
								adjacent layers,			accidentally processed first
			10A			M		Z fn S, silty fn sand, well sorted,			Mistakingly identified as
								weakly laminated, compact-			Core #1, therefore identified
88.52								cohesive, homogeneous,			as 1A in core photo. Core
								2.5Y5/4 (lt. olive brn), mod-			10B is correctly identified.
								strong rxn w/ HCl			
92.24			11B			SM	S1	Powdery to granular - white, pulverized slough?.			Ground up granitic cobble?
								no rxn w/ HCl, loose			1.35 drilled length
								gmS, pebbly muddy sand, poorly sorted,			
			11A					mod-strong rxn w/ HCl, 2.5Y5/2			Cold Creek - lower unit
								(grayish brn), compact, msv			diagonal line = zone of
93.59								lower half, well cemented,			pedogenic alteration
								max part. size = 5mm, mottled			
								to msv with stringers and nodules of			
								light-colored $CaCO_3$, g = 90-100% basalt			

W = Wet, M = Moist, D = Dry

1996/DCL/PROC/DBL/001

Pacific Northwest National Laboratory	DAILY BOREHOLE LOG	Boring/Well No C4105	Depth 96.01 – 102.36	Date 2-24-03	Sheet 5 of 10
		Location T-106	Project Vadose Zone		

Logged by BN Bjornstad

Reviewed by _____ Date _____

Lithologic Class. Scheme _____ Procedure _____ Rev ____

Steel Tape/E-Tape _____ / _____ Field Indicator Equip. 1) _____ 2) _____

Drilling Contractor _____

Driller _____

Rig/Method _____

Depth Control Point _____

DEPTH ( )	TIME	SAMPLES TYPE	SAMPLES ID NUMBER	CONTAMINATION INSTR.	CONTAMINATION READING	MOISTURE	GRAPHIC LOG C Z S G	LITHOLOGIC DESCRIPTION (particle size distribution, sorting, mineralogy, roundness, color, reaction to HCl, etc.)	H_2O ADDED	CASING	DRILLING COMMENTS (drilling rate, down time, blow counts, water level, drill fluid, etc.)
96.01		GP	S03044-12B			SM		MS, muddy fn-md sand, mod-poorly sorted, compact, $CaCO_3$ nodules and stringers violent rxn w/ HCl, max part size = cb. sand, slightly finer grained toward bottom wk to mod cemented, violent rxn w/ HCl; 2.5Y5/2 (grayish brown) w/ 2.5Y7/2 (lt. gray) stringers and nodules			1.45' drilled length
			12A			SM					Cold Creek - lower unit
97.46											diagonal line = zone of pedogenic alteration
99.33			13B			SM		ZS, silty fn-md sand, mod sorted, sl. compact, msv w/ few white $CaCO_3$ stringers and nodules 2.5Y5/4 (lt. olive brn), mod-strong rxn w/ HCl, more cemented in middle			1.35' drilled length
			13A			SM					
100.68											
101.02			14B			SM		SZ, sandy silt, mod-poorly sorted, 2.5Y7/4 (yellow), violent rxn w/ HCl, $CaCO_3$ nodules, msv, v. cemented lower half			1.34' drilled length
			14A			SM					
102.36											

W = Wet, M = Moist, D = Dry

1998/DCL/PROC/DBL/001

Pacific Northwest National Laboratory	DAILY BOREHOLE LOG	Boring/Well No C4105	Depth 102.17-107.24	Date 2-24-03	Sheet 6 of 10
		Location T-106	Project Vadose Zone		

Logged by B N Bjornstad (Print / Sign) | (Print / Sign)

Reviewed by (Print / Sign) Date

Lithologic Class. Scheme Procedure Rev

Steel Tape/E-Tape / Field Indicator Equip. 1) 2)

Drilling Contractor

Driller

Rig/Method

Depth Control Point

DEPTH ( )	TIME	SAMPLES TYPE	SAMPLES ID NUMBER	CONTAMINATION INSTR.	CONTAMINATION READING	MOISTURE	GRAPHIC LOG C Z S G	LITHOLOGIC DESCRIPTION (particle size distribution, sorting, mineralogy, roundness, color, reaction to HCl, etc.)	H_2O ADDED	CASING	DRILLING COMMENTS (drilling rate, down time, blow counts, water level, drill fluid, etc.)
102.17			503044-15B			SM	s1	gSM, pebbly sandy mud, v.			
								poorly sorted, mod cemented,			1.35' drilled length
								MSV 10YR 7/3 (v. pale brown)			
			15A			SM		violent rxn w/ HCl, basaltic			CCU lower
								granules and sm. pebbles,			
103.52								weakly bedded, stg =			
								80-90% basalt, lighter and			
								darker banding (soil			
								horizonation), gravel			
								subangular to subrounded			
								violent rxn. w/ HCl			
105.89			16B			SM	s1				1.35' drilled depth
								SM, sandy mud, v. poorly sorted,			Had to pound out of liner to
								cemented, violent rxn w/ HCl,			remove, therefore no
			16A			SM		10YR6/3 (pale brn)			structure preserved
107.24								Z, silt, well sorted, compact-			
								cohesive, wk lam., may be			
								some clay also, strong rxn w/			
								HCl, 2.5Y 5/4 (lt. olive brn)			

W = Wet, M = Moist, D = Dry

1998/DCL/PROC/DBL/001

Pacific Northwest National Laboratory

DAILY BOREHOLE LOG

Boring/Well No C4105 | Depth 109.07-116.3 | Date 2-24-03 / 2-25-03 | Sheet 7 of 10

Location T-106 | Project Vadose Zone

Logged by BN Bjornstad

Reviewed by _____ Date _____

Lithologic Class. Scheme _____ Procedure _____ Rev _____

Steel Tape/E-Tape _____ / _____ Field Indicator Equip. 1) _____ 2) _____

Drilling Contractor _____

Driller _____

Rig/Method _____

Depth Control Point _____

DEPTH ( )	TIME	SAMPLES TYPE	SAMPLES ID NUMBER	CONTAMINATION INSTR.	CONTAMINATION READING	MOISTURE	GRAPHIC LOG C Z S G	LITHOLOGIC DESCRIPTION (particle size distribution, sorting, mineralogy, roundness, color, reaction to HCl, etc.)	H_2O ADDED	CASING	DRILLING COMMENTS (drilling rate, down time, blow counts, water level, drill fluid, etc.)
109.07			S0304417B			SM	S1	Poorly sorted, msv			
			↓			↓		Z to fn sZ, laminated, well sorted,			CCU lower
								compact, white $CaCO_3$ stringers			
			17A			SM		sS, slightly fine sand, lam. well sorted,			1.3' drilled length
			↓			↓		loose, mod rxn w/ HCl, 2.5Y5/4			
110.37			↓			M		(lt. olive brn), lamina of md sand			
								Z, silt, well sorted, compact-			
								cohesive, msv., several rounded			
								$CaCO_3$ nodules, 2.5Y5/4			
								(lt. olive brn)			
114.97			18B			M	S1?	S, fn-md sand, 2.5Y5/2 (grayish			Upper Ringold = R+f
			↓			↓		brn), lam, max part size = md sand, mod rxn w/ HCl, well sorted			
								fnsZ, fine sandy silt, lam.			
			18A			M		2.5Y4/2 (olive brn), compact-			1.33 drilled length
								cohesive, mod, rxn w/ HCl, well sorted;			
116.3			↓			↓		alternating beds 2-4" thick			
								of fine sand to fine sandy			
								silt as described above			

W = Wet, M = Moist, D = Dry

1998/DCL/PROC/DBL/001

Pacific Northwest National Laboratory	DAILY BOREHOLE LOG	Boring/Well No C4105	Depth 119.85-124.24	Date 2-25-03	Sheet 8 of 10
		Location T-106	Project Vadose Zone		

Logged by B N Bjornstad

Reviewed by _____ Date _____

Lithologic Class. Scheme _____ Procedure _____ Rev _____

Steel Tape/E-Tape _____ / _____ Field Indicator Equip. 1) _____ 2) _____

Drilling Contractor _____

Driller _____

Rig/Method _____

Depth Control Point _____

DEPTH ( )	TIME	SAMPLES TYPE	SAMPLES ID NUMBER	CONTAMINATION INSTR.	CONTAMINATION READING	MOISTURE	GRAPHIC LOG C Z S G	LITHOLOGIC DESCRIPTION (particle size distribution, sorting, mineralogy, roundness, color, reaction to HCl, etc.)	H_2O ADDED	CASING	DRILLING COMMENTS (drilling rate, down time, blow counts, water level, drill fluid, etc.)
119.85			19B			M		ZfnS interbedded w/ md-crs basaltic sand, loose (like below. ZfnS looks like bottom of core above			Upper Ringold
								S, crs sand, 60-70% basalt, loose, 10YR4/1 (dk gray), no rxn w/ HCl, mod sorted,			1.34' drilled length
			19A			M				x	sharp contact between sand and silt
121.19								cZ clayey silt, msv, compact-cohesive, well sorted, 10YR5/6 (yellowish brn), stiff, mod rxn w/ HCl			
122.9			20B			SM		SG, sandy gravel, highly pulverized angular clasts, loose, v. poorly sorted, max part. size = 3cm, no rxn w/ HCl, G = 40-60% basalt, some granitics, 10YR5/1 (gray), clast-supported?			1.34' drilled length Ringold - Unit E
			20A			M					
124.24								ZG, silty gravel, poorly sorted, silt is cohesive, gravel is matrix supported, 10YR6/4 (lt. yellowish brn), mod rxn w/ HCl			

W = Wet, M = Moist, D = Dry

1999/DCL/PROC/DBL/001

Pacific Northwest National Laboratory	DAILY BOREHOLE LOG	Boring/Well No C4105	Depth 128.91-130.12	Date 2-25-03	Sheet 9 of 10
		Location T-106	Project Vadose Zone		

Logged by BN Bjornstad (Print / Sign) | (Print / Sign)

Reviewed by (Print / Sign) Date

Lithologic Class. Scheme Procedure Rev

Steel Tape/E-Tape / Field Indicator Equip. 1) 2)

Drilling Contractor

Driller

Rig/Method

Depth Control Point

DEPTH ( )	TIME	SAMPLES TYPE	SAMPLES ID NUMBER	CONTAMINATION INSTR.	CONTAMINATION READING	MOISTURE	GRAPHIC LOG C Z S G	LITHOLOGIC DESCRIPTION (particle size distribution, sorting, mineralogy, roundness, color, reaction to HCl, etc.)	H_2O ADDED	CASING	DRILLING COMMENTS (drilling rate, down time, blow counts, water level, drill fluid, etc.)
128.91			21B			SM		≥5G, 100% pulverized angular gravel clasts mixed with silt and sand, loose, v. poorly sorted, max part size = 2cm. 10YR6/2 (lt. brnish gray) no rxn w/ HCl, G = 30-40% basalt, more granitics/felsics than previous smpl, no rxn w/HCl			
			↓			↓					
			21A			SM					
130.12			↓			↓					

W = Wet, M = Moist, D = Dry

1996/DCL/PROC/DBL/001

Pacific Northwest National Laboratory	DAILY BOREHOLE LOG	Boring/Well No C4105	Depth 128.58 - 130.9	Date 3-21-03	Sheet 10 of 10
		Location T-106	Project Vadose Zone		

Logged by B N Bjornstad (Print / Sign) | (Print / Sign)

Reviewed by (Print / Sign) Date

Lithologic Class. Scheme Procedure Rev

Steel Tape/E-Tape / Field Indicator Equip. 1) 2)

Drilling Contractor

Driller

Rig/Method

Depth Control Point

DEPTH ( )	TIME	SAMPLES TYPE	SAMPLES ID NUMBER	CONTAMINATION INSTR.	CONTAMINATION READING	MOISTURE	GRAPHIC LOG C Z S G	LITHOLOGIC DESCRIPTION (particle size distribution, sorting, mineralogy, roundness, color, reaction to HCl, etc.)	H_2O ADDED	CASING	DRILLING COMMENTS (drilling rate, down time, blow counts, water level, drill fluid, etc.)
128.58		GP	503044-22			SM		msG silty sandy Gravel, poorly sorted, 2.5Y 4/2 (dk grayish brn) mod. rxn w/HCl, most gravel clasts are angular (ie. broken) loose, max particle size = 2cm, S = 50% basalt			Redrill of #21?
129.58											
130.55		Amber glass jar				W		MSG silty sandy Gravel, 2.5Y N2/0 (black), no rxn w/ HCl, max part. size = 2cm, v. poorly sorted, reduced chemically?, loose, pulverized gravel clasts subrounded to angular			
130.9		500ml									

W = Wet, M = Moist, D = Dry

1998/DCL/PROC/DBL/001

Appendix C

X-Ray Diffraction Patterns for C4105 (T-106)

Contents

Appendix C. X-Ray Diffraction Patterns for C4105 (T-106) C.1

C.1 X-Ray Diffraction Patterns for Bulk Sediment from C4105 (T-106) C.1

C.2 X-Ray Diffraction Patterns for Clay Separates from C4105 (T-106) (< 2 μm) C.4

Figures

C.1 Bulk Sediment XRD Patterns for Samples 7A and 10A from H2 and CCU_u Units, Respectively C-1

C.2. Bulk Sediment XRD Patterns for Samples 11A and 16A from CCU_l Unit C-2

C.3. Bulk Sediment XRD Patterns for Samples 19A and 20A from R_{tf} and R_{wi} Units, Respectively C-3

C.4. XRD Patterns for Clay Separates -Sample 7A (Standard and Ethylene Glycol Saturated) C-4

C.5. XRD Patterns for Clay Separates -Sample 10A (Standard and Ethylene Glycol Saturated) C-5

C.6. XRD Patterns for Clay Separates -Sample 16A (Standard and Ethylene Glycol Saturated) C-6

C.7. XRD Patterns for Clay Separates -Sample 19A (Standard and Ethylene Glycol Saturated) C-7

C.8. XRD Patterns for Clay Separates -Sample 20A (Standard and Ethylene Glycol Saturated) C-8

Appendix C. X-Ray Diffraction Patterns for C4105 (T-106)

C.1 X-Ray Diffraction Patterns for Bulk Sediment from C4105 (T-106)

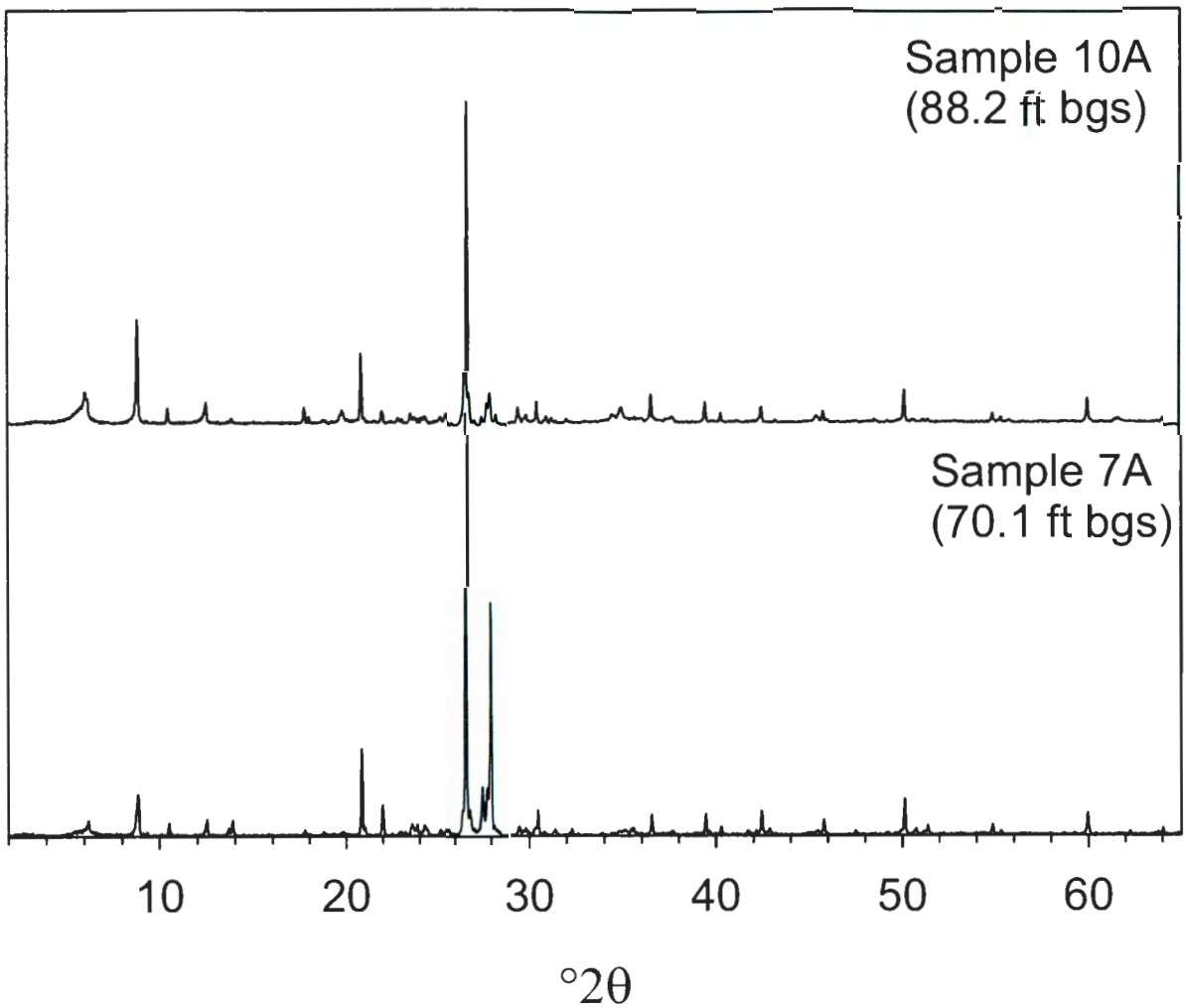

Figure C.1 Bulk Sediment XRD Patterns for Samples 7A and 10A from H2 and CCU_u Units, Respectively

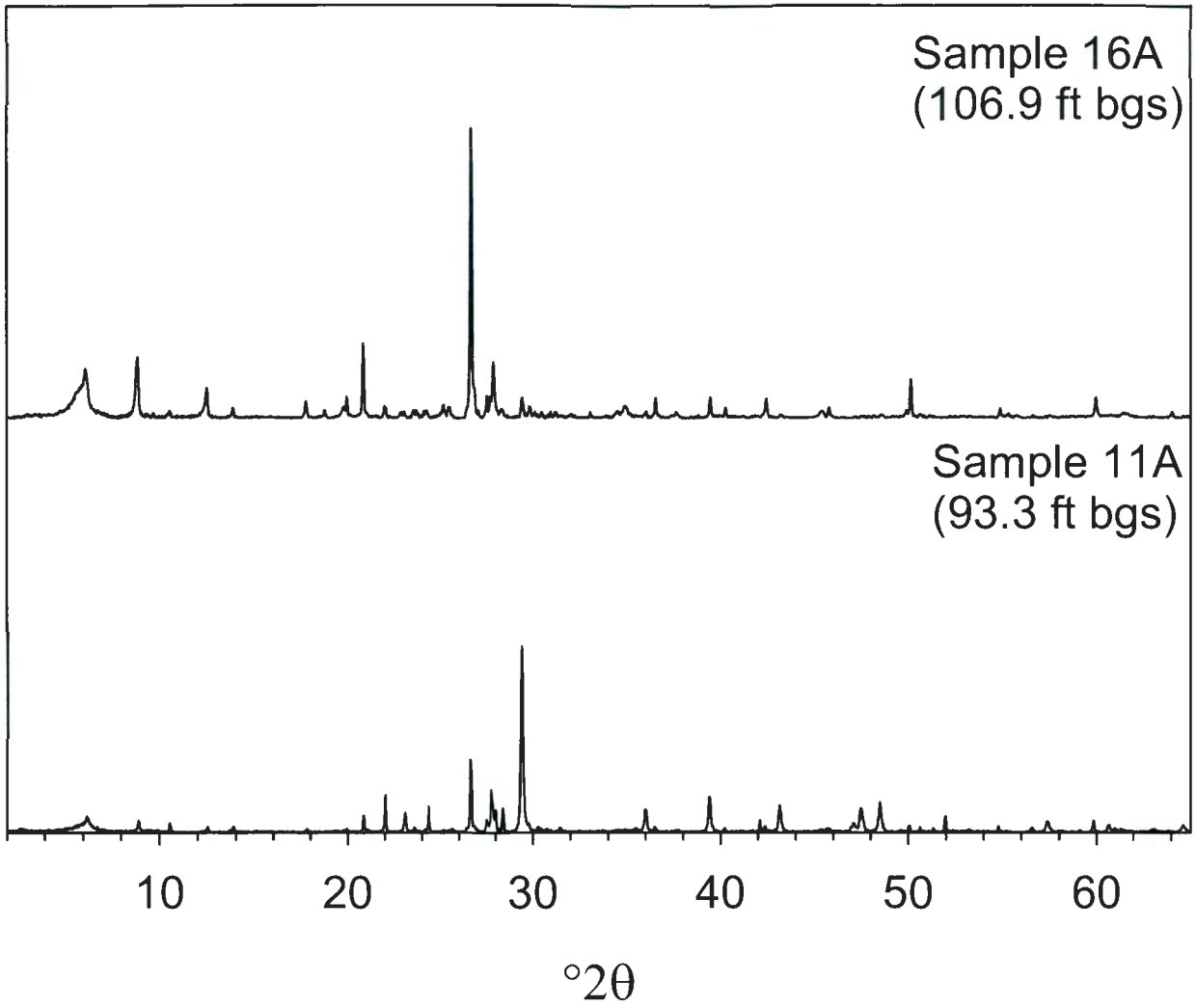

Figure C.2. Bulk Sediment XRD Patterns for Samples 11A and 16A from CCU_1 Unit

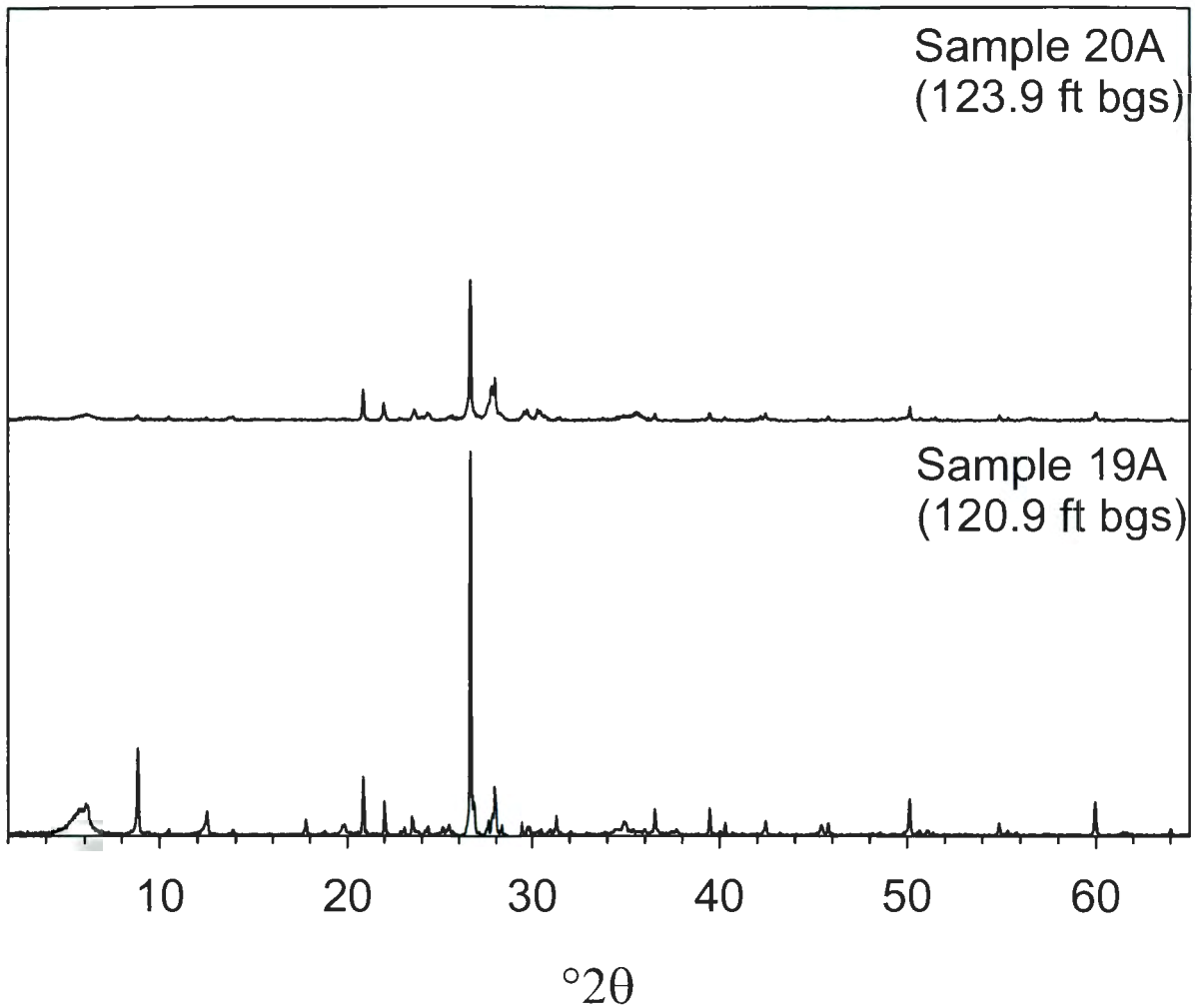

Figure C.3. Bulk Sediment XRD Patterns for Samples 19A and 20A from R_{tf} and R_{wi} Units, Respectively

C.2 X-Ray Diffraction Patterns for Clay Separates from C4105 (T-106) (< 2 µm)

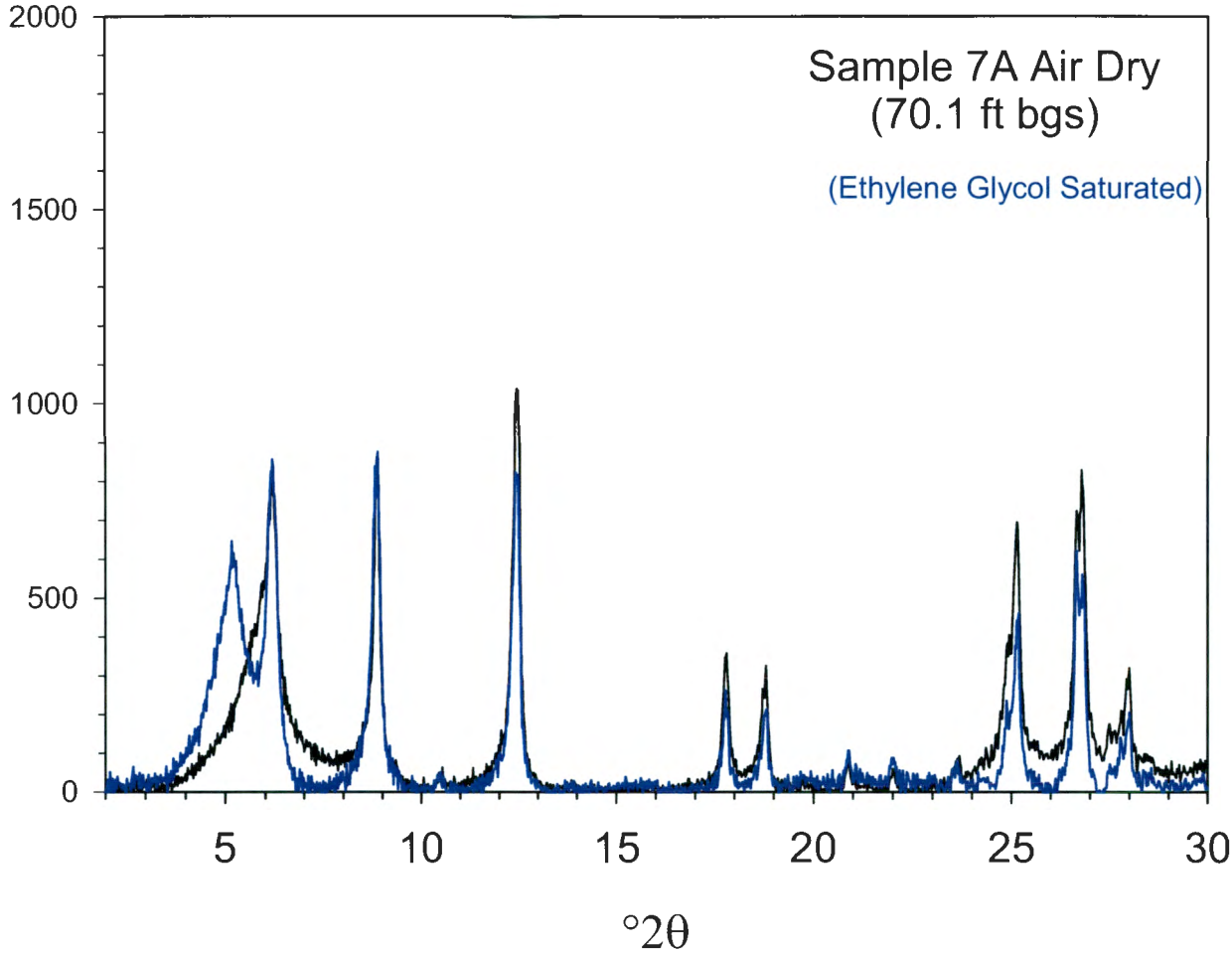

Figure C.4. XRD Patterns for Clay Separates -Sample 7A (Standard and Ethylene Glycol Saturated)

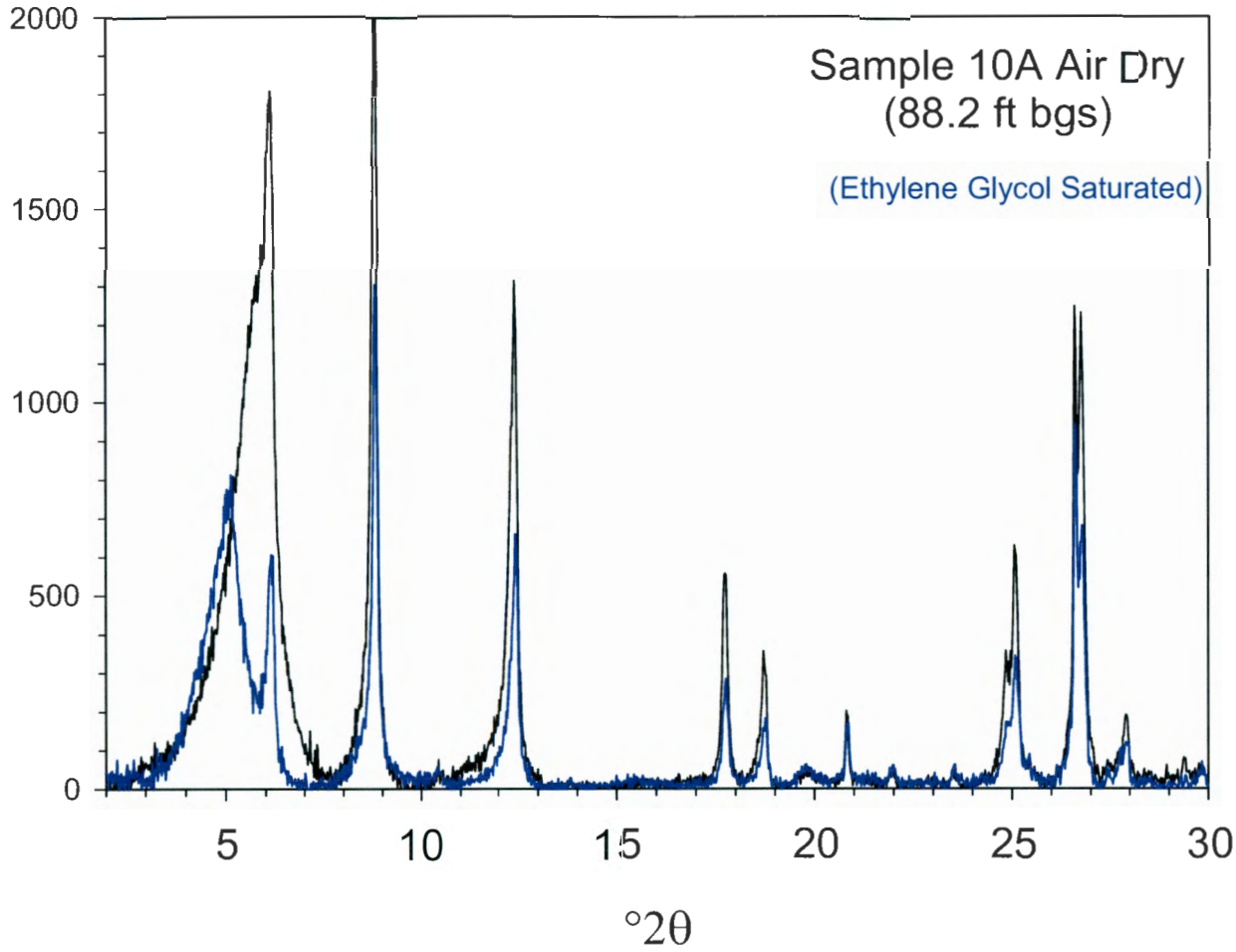

Figure C.5. XRD Patterns for Clay Separates -Sample 10A (Standard and Ethylene Glycol Saturated)

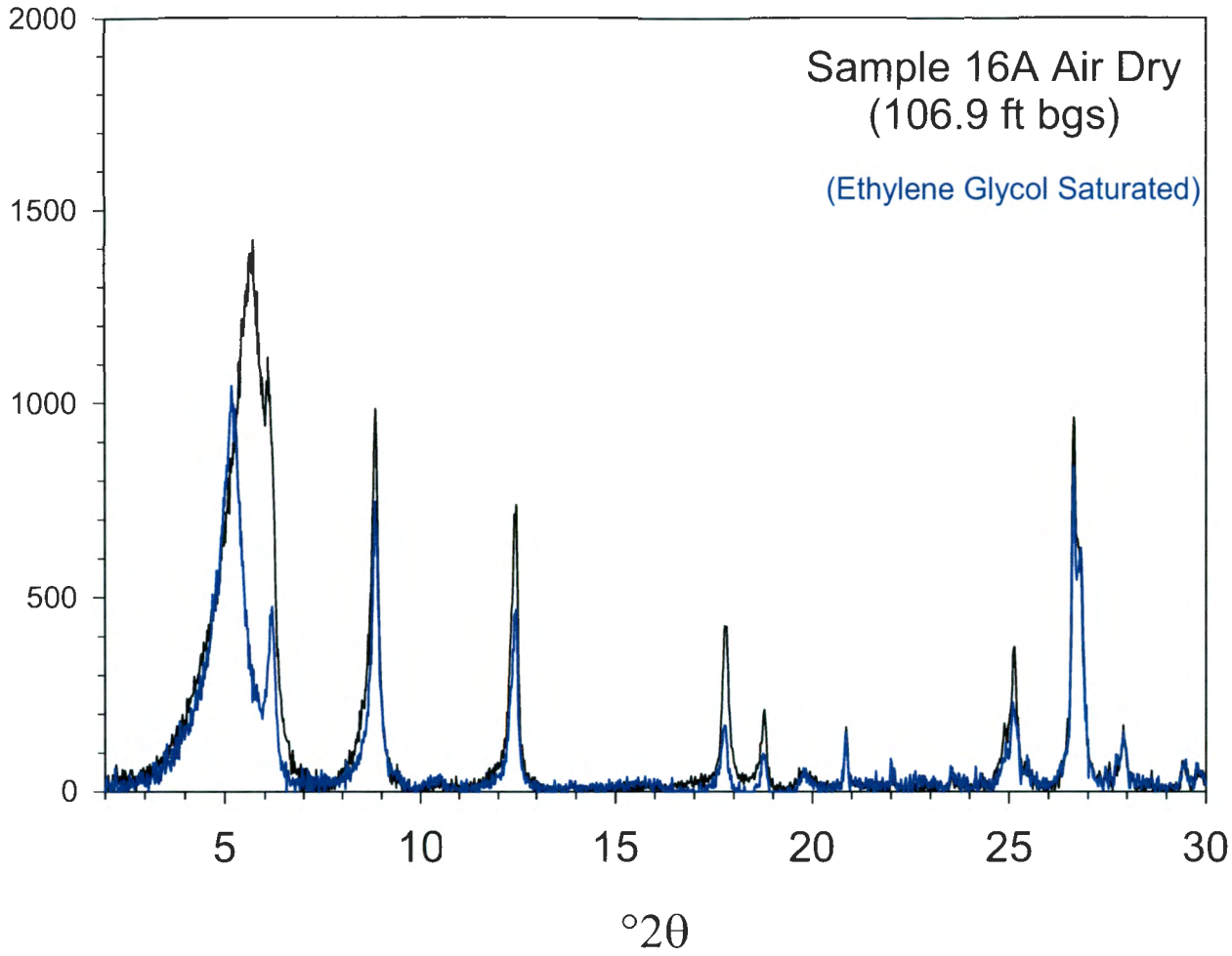

Figure C.6. XRD Patterns for Clay Separates -Sample 16A (Standard and Ethylene Glycol Saturated)

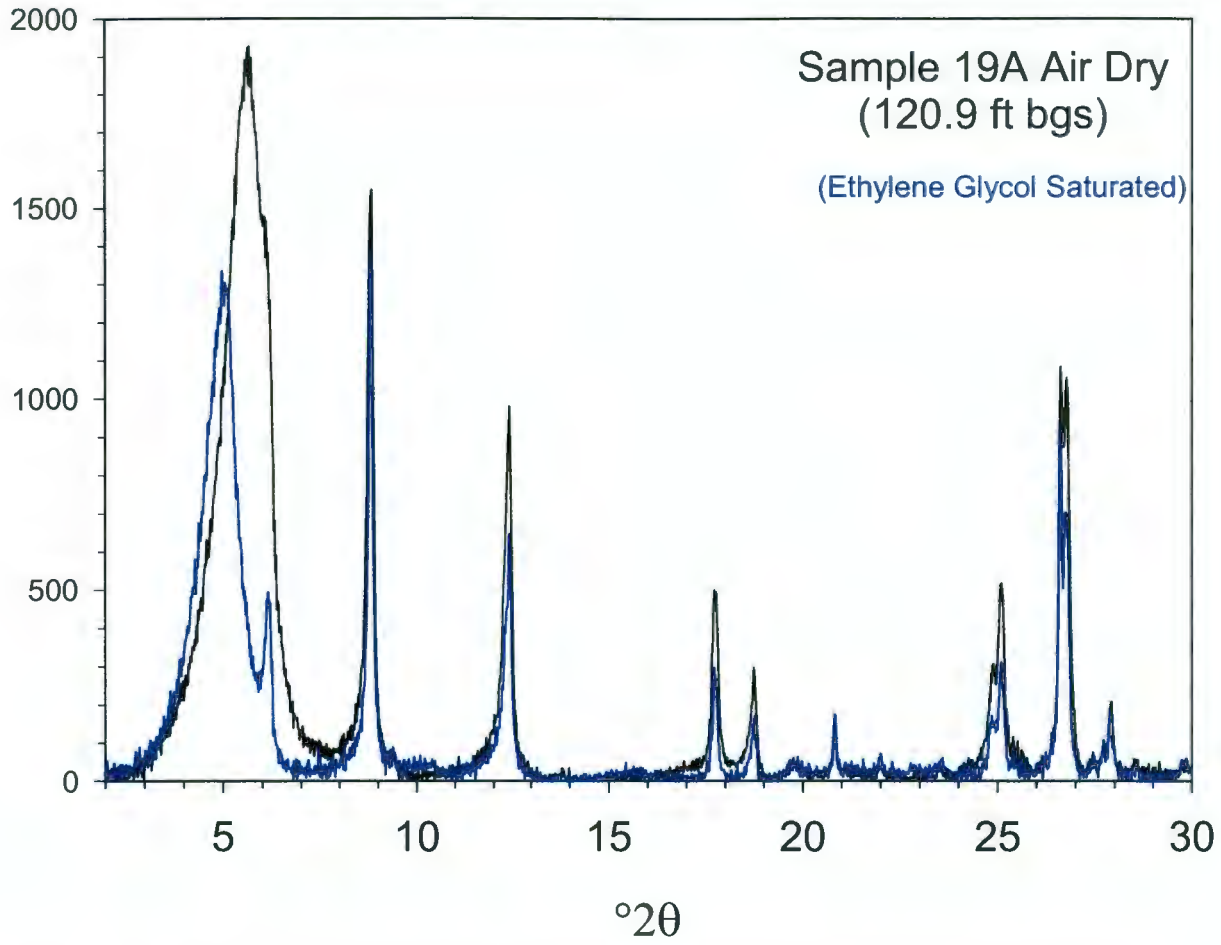

Figure C.7. XRD Patterns for Clay Separates -Sample 19A (Standard and Ethylene Glycol Saturated)

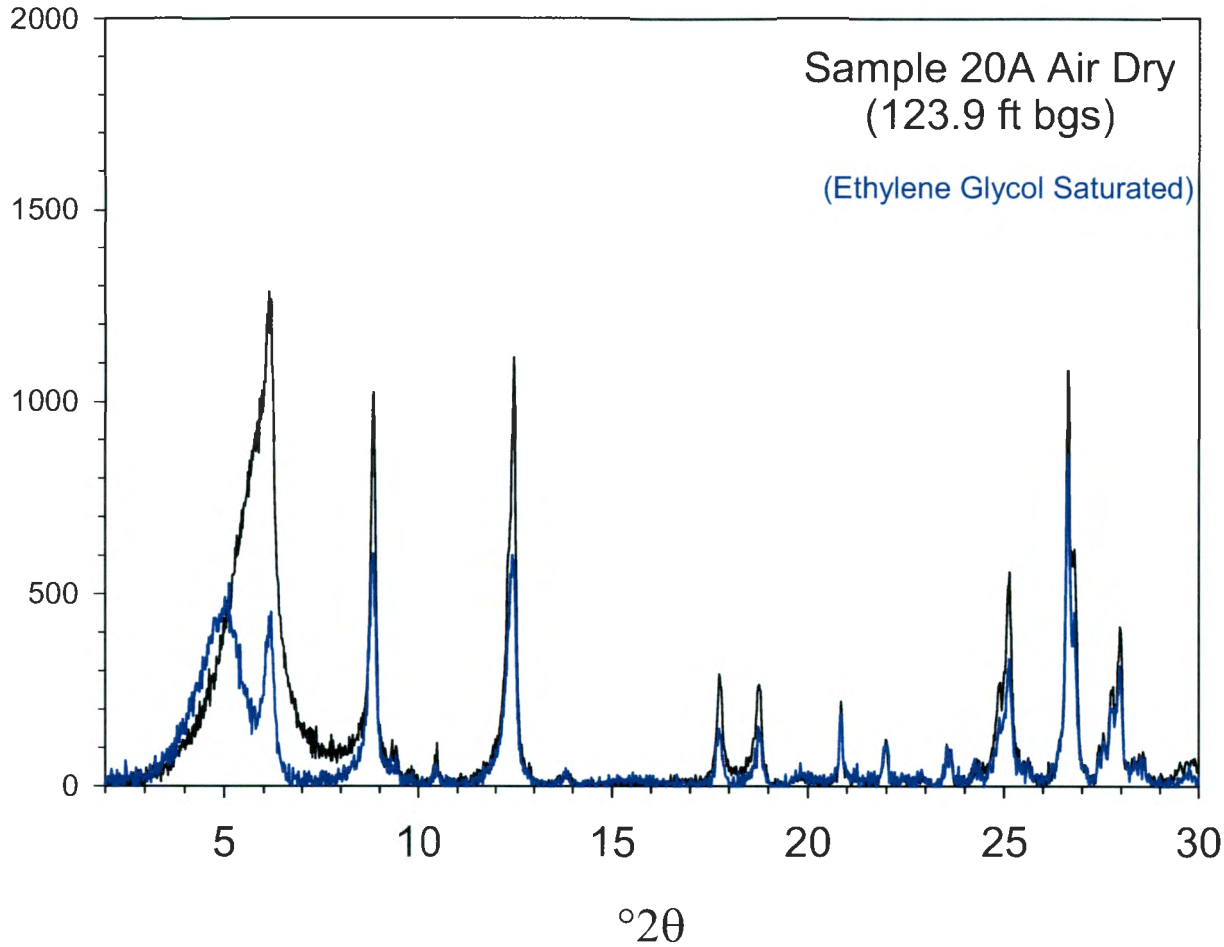

Figure C.8. XRD Patterns for Clay Separates -Sample 20A (Standard and Ethylene Glycol Saturated)

Distribution

No. of Copies

44 OFFSITE

Steve Airhart
Freestone Environmental Services
1933 Jadwin Ave.
Suite 135
Richland, WA 99352

Dr. Harry Babad
2540 Cordoba Court
Richland, WA 99352-1609

Pat Brady
Geochemistry Department, 6118
Sandia National Laboratories
P.O. Box 5800
Albuquerque, New Mexico 87185-0750

Charles R. Bryan
Sandia National Laboratories
4100 National Parks Highway
Carlsbad, N.M. 88220

Susan Carroll
Lawrence Livermore National Laboratory
Mail Stop L-219
Livermore, CA 94550

John N. Christensen
Center for Isotope Geochemistry
Lawrence Berkeley National Laboratory
1 Cyclotron Road Bldg, Mail Stop 70A4418
Berkeley, CA 94720-8179

Jon Chorover
Associate Professor – Environmental Chemistry
Department of Soil, Water and Environmental Science
Shantz 429, Building #38
University of Arizona
Tucson, AZ 85721-0038

No. of Copies

Dave G. Coles
Coles Environmental Consulting
750 South Rosemont Rd
West Linn, OR 97068

Mark Conrad
Department of Earth and Planetary Sciences
University of California Berkeley
Berkeley, CA 94720

Dr. James A. Davis
U.S. Geological Survey
MS-465
345 Middlefield Rd.
Menlo Park, CA 94025

Donald J. DePaolo
Geology & Geophysics Dept., MC4767
University of California
Berkeley, CA 94720-4767

Dirk A. Dunning
Oregon Office of Energy
625 Mariona St. N. E.
Salem, OR 97301-3742

Mark Ewanic
MSE Technology Applications, Inc.
200 Technology Way
Butte, MT 59701

Markus Flury
Department of Crop and Soil Sciences
Washington State University
Pullman, WA 99164

Amy P. Gamerdinger
2122 E. Hawthorne
Tucson, AZ 85719

No. of
Copies

Jim Harsh
Department of Crop & Soil Sciences
Washington State University
Johnson Hall - Room 249
Pullman WA 99164-6420

Victoria Johnson
Kennedy/Jenks Consultants, Inc.
1020 N. Center Parkway, Suite F
Kennewick, WA 99336

Dr. Cliff Johnston
Soil Chemistry and Mineralogy
1150 Lily Hall
Purdue University
West Lafayette, IN 47907-1150

Dr. Daniel I. Kaplan
Westinghouse Savannah River Company
Bldg. 774-43A, Rm 215
Aiken, SC 29808

Dr. Peter C. Lichtner
Los Alamos Natl. Lab
P.O. Box 1663
Los Alamos, NM 87545

Kevin A. Lindsey
Kennedy / Jenks Consultants, Inc.
1020 N. Center Parkway, Suite F
Kennewick, WA 99336

Patrick Longmire
Los Alamos National Laboratory
Mail Stop J534
P.O. Box 1663
Los Alamos, NM 87545

Kate Maher
The Center for Isotope Geochemistry
301 McCone Hall
University of California, Berkeley
Berkeley, CA 94702-4746

No. of
Copies

John M. Matuszek
82 McGuffey Lane
Delmar, NY 12054

Melanie A. Mayes
Environmental Sciences Division
Oak Ridge National Laboratory
P.O. Box 2008
[*Bethel Valley Road for FedEX/UPS delivery*]
Oak Ridge, TN 37831-6038

Jean Moran
Isotopic Tracers and Transport Group
Analytical and Nuclear Chemistry Division
Lawrence Livermore National Laboratory
L-231, P.O. Box 808
Livermore, CA 94550

Dr. Kathryn L. Nagy
Department of Earth and Environmental Sciences
University of Illinois at Chicago (MC-186)
845 West Taylor Street
Chicago, IL 60607-7059

Heino Nitsche
Director, Center for Advanced Environmental and Nuclear Studies
Lawrence Berkeley National Laboratory
1 Cyclotron Road
MS 70A-1150
Berkeley, CA 94720

Phil Reed
U.S. Nuclear Regulatory Commission
Office of Nuclear Regulatory Research
Division of Systems Analysis and Regulatory Effectiveness
Radiation Protection, Env. Risk and Waste Management Branch
Mail Stop: T9-F31
Washington, DC 20555-0001

No. of Copies

Richard J. Reeder
Dept. of Geosciences
State University of New York at
Stony Brook
Stony Brook, NY 11794-2100

Al Robinson
68705, E 715 PRNE
Richland WA, 99352

Phil Rogers
13 Mountain Oak
Littleton, CO 80127

Sherry D. Samson
Research Assistant Professor
Department of Earth and
Environmental Sciences
University of Illinois at Chicago (MC186)
845 W. Taylor St.
Chicago, IL 60607-7059

Dawn A. Shaughnessy
Glenn T. Seaborg Center
Lawrence Berkeley National Laboratory
1 Cyclotron Road
MS 70A-1150
Berkeley, CA 94720

Doug Sherwood
Rivers Edge Environmental
1616 Riverside Drive
West Richland, WA 99353

David K. Shuh
Lawrence Berkeley National Lab
1 Cyclotron Road
Mail Stop 70A-1150
Berkeley, CA 94720

James "Buck" Sisson
Idaho National Engineering and
Environmental Laboratory
P.O. Box 1625, MS-2107
Idaho Falls, ID 83415-2107

No. of Copies

Robert W. Smith, Ph.D.
Professor of Subsurface Science
Adjunct Professor of Geological Sciences
University of Idaho at Idaho Falls
1776 Science Center Drive
Idaho Falls, ID 83402

Stan Sobczyk
242 N. Laurel St.
Genesee, ID 83832-9760

Carl I. Steefel
Earth Sciences Division
Lawrence Berkeley National Laboratory
1 Cyclotron Road, Mail Stop 90R1116
Berkeley, CA 94720

Dr. Samuel J. Traina, Director
Sierra Nevada Research Institute
University of California, Merced
P.O. Box 2039
Merced, CA 95344

Dr. T. T. Chuck Vandergraaf
P.O. Box 857
Pinawa, Manitoba ROE 1LO
Canada

Dr. Jiamin Wan
Lawrence Berkeley National Laboratory
1 Cyclotron Rd. MS 70-0127A
Berkeley, CA 94720

Mr. Ronald G. Wilhelm
Office of Radiation and Indoor Air
401 M Street, S.W.,
Mail Code 6603J
Washington, D.C. 20460

W. Alexander Williams
U.S. Department of Energy
Office of Environmental Restoration
EM-33
19901 Germantown Road
Germantown, MD 20874-1290

No. of Copies		
ONSITE		
4	**DOE Office of River Protection**	
	P. E. LaMont	H6-60
	R. W. Lober	H6-60
	S. A. Wiegman	H6-60
	R. B. Yasek	H6-60
8	**DOE Richland Operations Office**	
	B. L. Foley	A6-38
	J. P. Hanson	A5-13
	R. D. Hildebrand	A6-38
	K. A. Kapsi	A5-13
	J. G. Morse	A6-38
	K. M. Thompson	A6-38
	DOE Public Reading Room (2)	H2-53
	Bechtel Hanford, Inc.	
	K. R. Fecht	H0-02
22	**CH2M HILL Hanford Group, Inc.**	
	A. Amonette Technical Writer's Ink	E6-35
	F. J. Anderson	E6-35
	R. Calmus	H6-05
	M. P. Connelly	E6-35
	J.G. Field	H6-62
	T. E. Jones (2)	E6-35
	A. J. Knepp	H6-60
	S. L. Lambert Lambert Engineering	E6-35
	J. E. Laurenz	H6-62
	F. M. Mann (5)	E6-35
	W. J. McMahon	E6-35
	C. W. Miller	H6-35
	D. A. Myers (3)	E6-35
	G. Parsons	H6-19
	T. L. Sams	H6-05

No. of Copies		
3	**Duratek Federal Services, Inc., Northwest Operations**	
	M. G. Gardner	H1-11
	K. D. Reynolds	H1-11
	D. E. Skoglie	H1-11
2	**Environmental Protection Agency**	
	N. Ceto	B5-01
	D. A. Faulk	B5-01
2	**Fluor Federal Services**	
	R. Khaleel	E6-17
	R. J. Puigh	E6-17
6	**Fluor Hanford, Inc.**	
	M. W. Benecke	E6-35
	T. W. Fogwell	E6-35
	B. H. Ford	E6-35
	J. G. Hogan	H1-11
	V. G. Johnson	E6-35
	M. I. Wood	H8-44
72	**Pacific Northwest National Laboratory**	
	S. R. Baum	P7-22
	B. N. Bjornstad (3)	K6-81
	T. M. Brouns	K9-69
	C. F. Brown	P7-22
	R. W. Bryce	E6-35
	K. J. Cantrell	K6-81
	R.. E. Clayton	P7-22
	W. J. Deutsch	K6-81
	P. E. Dresel	K6-96
	K. M. Geisler	P7-22
	M. J. Fayer	K9-33
	A. R. Felmy	K8-96
	V. L. Freedman	K9-36
	M. D. Freshley	K9-33
	J. S. Fruchter	K6-96
	G. W. Gee	K9-33
	D. G. Horton (3)	K6-81

No. of Copies		
	J. P. Icenhour	K6-81
	C. T. Kincaid	E6-35
	K. M. Krupka	K6-81
	I. V. Kutnyakov	P7-22
	G. V. Last (2)	K6-81
	V. L. LeGore	P7-22
	M. J. Lindberg	P7-22
	C. W. Lindenmeier (2)	P7-22
	W. J. Martin	K6-81
	S. V. Mattigod	K6-81
	B. P. McGrail	K6-81
	P. D. Meyer	BPO
	C. J. Murray	K6-81
	S. M. Narbutovskih	K6-96
	R. D. Orr	K6-81
	E. M. Pierce	K6-81
	Nik Qafoku	K3-61
	S. P. Reidel	K6-81
	R. J. Serne (20)	P7-22
	H. T. Schaef	K6-81
	W. Um	P7-22

No. of Copies		
	M. Valenta	P7-22
	T. S. Vickerman	P7-22
	A. L. Ward	K9-33
	B. A. Williams	K6-81
	S. B. Yabusaki	K9-36
	J. M. Zachara	K8-96
	F. Zhang	K9-33
	Information Release Office (2)	
	S.M. Stoller	
	R. G. McCain	B2-62
6	**Washington State Department of Ecology**	
	S. Dahl-Crumpler	HO-57
	J. A. Caggiano	HO-57
	F. Hodges	HO-57
	A. D. Huckaby	HO-57
	B. Rochette	HO-57
	J. Yokel	HO-57